Thermal hydrolysis of sludge for process intensification and mitigation of oxidative stress of nanoplastics in anaerobic digestion

by

Seyed Mohammad Mirsoleimani Azizi

A thesis submitted in partial fulfilment of the requirements for the degree of

Doctor of Philosophy

in

ENVIRONMENTAL ENGINEERING

Department of Civil and Environmental Engineering

University of Alberta

Abstract

Anaerobic digestion (AD) has been widely implemented for sludge stabilization, resource recovery, pathogens removal, as well as production of methane-rich biogas. The thermal hydrolysis process (THP) is a widely implemented sludge pre-treatment process to boost methane generation and solids reduction in AD. However, several fundamental and engineering bottlenecks are associated with their practical application. Also, microplastics and nanoplastics (MPs/NPs) have been extensively detected in sewage sludge. They inevitably transfer to AD and induce oxidative stress on the anaerobic microbiome. To date, there is limited knowledge about how THP can influence MPs/NPs-induced stress during AD. Given these research gaps, this doctoral thesis focused on exploring various retrofitting schemes of low-temperature THP in AD under batch and semi-continuous conditions and assessing the impact of THP of sludge on MPs/NPs stress during AD.

First, primary sludge (PS) fermentation prior to AD is becoming more common in wastewater treatment plants (WWTPs) for the production and utilization of volatile fatty acids-rich sludge liquor in biological nutrient removal processes. However, the THP for enhancing AD of sludge in WWTPs with PS fermentation has rarely been investigated. This study examined low-temperature THP (50–90°C, 30–90 min) for enhancing co-digestion of fermented primary sludge (FPS) and thickened waste-activated sludge (TWAS). The experiments were conducted under two schemes: scheme-1 (THP of TWAS + FPS) and scheme-2 (THP of TWAS only). Scheme-2 was more effective in solubilizing COD (up to 20.4% increase in SCOD) and various macromolecular compounds (e.g., proteins and carbohydrates). In contrast, scheme-1 was more efficient in VSS solubilization (up to 26.12%). Scheme-1 also resulted in a greater enhancement in methane production over the control (scheme-1: 56.28% at 90°C, 90 min vs. scheme-2: 43.4% at 90°C, 60 min). Thus, these results suggested that low-temperature THP of TWAS alone (scheme-2) would result in solubilization of refractory macromolecular compounds, leading to a relatively lower positive impact on methane yields than scheme-1. The preliminary economic assessment considering THP operating cost, enhancement in energy recovery, and saving in biosolids handling costs indicated that THP at 90°C (90 min) under scheme-1 could provide the highest net saving of $79.55/dry tonne solids compared to the control (AD without THP). These results will provide technical guidance in adopting THP in WWTPs with PS fermentation.

Second, the impact of THP (80 and 160 °C) on AD of sewage sludge exposed to different levels (50–150 μg/L) of polystyrene nanoplastics (PsNPs) was investigated. Compared to the control, higher PsNPs levels of 100 and 150 μg/L decreased methane yields by 17.98 and 29.34%, respectively. Moreover, reactive oxygen species (ROS) levels increased by 17.18 and 34.84%. Our results demonstrated that THP counteracted the suppression of methane production imposed by such PsNPs concentrations, with decreased ROS levels. Also, THP reduced antibiotic resistance gene (ARG) propagation that can be encouraged by PsNPs, thus minimizing the ARG transmission risks of digestate biosolids. These findings suggest that THP holds a high promise to further develop as a remediation method for MPs/NPs in WWTPs.

Third, although few recent reports indicated that the THP could alleviate oxidative stress of MPs/NPs in AD, little is known about how different solids contents of sludge would influence its effectiveness. This study scrutinized how the THP (160 °C, 60 min) affects AD of primary sludge with 4, 8, and 12% total solids (TS) when exposed to PsNPs. The presence of PsNPs (150 μg/L) substantially enhanced ROS levels at lower TS (4 and 8%) compared to a higher TS of 12% (16.20–16.71% vs 8.79%). Consequently, methane production decreased by 7.25–15.07% for 4–8% TS. Nonetheless, applying the THP could effectively mitigate ROS-induced stress and the propagation of most ARGs. Moreover, a positive correlation was observed between the changes in extracellular polymeric substances due to the THP and the impact of PsNPs. These results provide new insights into understanding the significance of the sludge solids content in the THP for coremediation of PsNPs-induced oxidative stress and ARGs propagation in AD.

Fourth, previous research has shown that THP and FPS play a crucial role in improving methane production during the AD process. However, it's essential to consider that the chemistry of continuous or semi-continuous fed digesters may differ significantly from batch tests. For the most accurate representation of industrial AD conditions, this study investigated the impact of THP (at 90 °C for 30 min) on the mixture of FPS+TWAS and TWAS alone, under semi-continuous mode. The digesters were operated at different solid retention times (SRT) of 20, 15, and 10 d. The findings revealed that applying THP to the mixture of FPS+TWAS led to a 34.5%-37.9% increase in methane production compared to the control. Similarly, when TWAS was exposed to THP under the same conditions, it resulted in a methane production enhancement of 25.6%-31.2%. Further, The presence of PsNPs resulted in a higher reactive oxygen species (ROS) production and

a higher abundance of antibiotic resistance genes (ARGs). Additionally, their presence caused a significant inhibition of methane production by 28.2%, 29.3%, and 38.8% for SRTs of 20, 15, and 10 d, respectively. Nevertheless, the application of THP proved to be effective in mitigating ROS-induced stress and curbing the propagation of ARGs during the AD process. These results provide new insights into the semi-continuous AD of pretreated FPS+TWAS and TWAS and the impact of THP on mitigating the negative impact of PsNPs on the AD process.

Preface

A part of chapter 2 of this thesis has been published as S.M. Mirsoleimani-Azizi, F.I. Hai, W. Lu, A. Al-Mamun, B.R. Dhar (2021) "A review of mechanisms underlying the impacts of (nano)microplastics on anaerobic digestion" in *Bioresource Technology*, 329, 124894. .M. Mirsoleimani-Azizi was responsible for the data collection from the literature, writing original draft, review, and editing. F.I. Hai, W. Lu, A. Al-Mamun were responsible for writing - review & editing. B.R. Dhar was responsible for the review, editing, and supervising this work.

Chapter 3 of this thesis has been published as S.M. Mirsoleimani-Azizi, W. Dastyar, M. N. A. Meshref, R. Mall-Bared and B.R. Dhar, (2021) "Low-temperature thermal hydrolysis for anaerobic digestion facility in wastewater treatment plant with primary sludge fermentation" in *Chemical Engineering Journal*, vol. 426, 130485. S.M. Mirsoleimani-Azizi was responsible for conceptualization and experiment design, experiment and data collection, writing original draft, review, and editing. Dastyar, M. N. A. Meshref, and R. Mall-Bared were responsible for the investigation, formal analysis, methodology, writing – review, and editing. B.R. Dhar was responsible for the review, editing, and supervising this work.

Chapter 4 of this thesis has been published as S.M. Mirsoleimani-Azizi, N. Haffiez, B.S. Zakaria, and B.R. Dhar, (2022) "thermal hydrolysis of sludge counteracts polystyrene nanoplastics-induced stress during anaerobic digestion" in *ACS ES& T Engineering*, vol. 7, 1306-1315. S.M. Mirsoleimani-Azizi was responsible for conceptualization and experiment design, experiment and data collection, writing original draft, review, and editing. N. Haffiez, and B.S. Zakaria, were responsible for the investigation, formal analysis, methodology, writing – review, and editing. B.R. Dhar was responsible for the review, editing, and supervising this work.

Chapter 5 of this thesis has been published as S.M. Mirsoleimani-Azizi, B.S. Zakaria, N. Haffiez, and B.R. Dhar, (2022) "sludge thermal hydrolysis for mitigating oxidative stress of polystyrene nanoplastics in anaerobic digestion: significance of the solids content" in *ACS Sustainable Chemistry & Engineering*, vol. 18, 7253-7262. S.M. Mirsoleimani-Azizi was responsible for conceptualization and experiment design, experiment and data collection, writing original draft, review, and editing. N. Haffiez, and B.S. Zakaria, were responsible for the

investigation, formal analysis, methodology, writing – review, and editing. B.R. Dhar was responsible for the review, editing, and supervising this work.

Chapter 6 of this thesis will be submitted as S.M. Mirsoleimani-Azizi and B.R. Dhar, (2023) "low-temperature thermal hydrolysis for boosting the performance of semi-continuous anaerobic digestion of fermented primary sludge and antibiotic resistance genes management" in a peer-reviewed journal. S.M. Mirsoleimani-Azizi was responsible for conceptualization and experiment design, experiment and data collection, writing original draft, review, and editing. B.R. Dhar was responsible for the review, editing, and supervising this work.

Chapter 7 of this thesis will be submitted as S.M. Mirsoleimani-Azizi and B.R. Dhar, (2023) "exploring the potential of thermal hydrolysis to mitigate oxidative stress from polystyrene nanoplastics during semi-continuous anaerobic digestion" in a peer-reviewed journal. S.M. Mirsoleimani-Azizi was responsible for conceptualization and experiment design, experiment and data collection, writing original draft, review, and editing. B.R. Dhar was responsible for the review, editing, and supervising this work.

Dedication

This work is dedicated:

To my beloved parents who have been my source of inspiration and gave me strength, support and encouragement. Words can never tell how much I am grateful to you for your care, love and support.

To my beloved wife, Parisa who I am truly blessed to have her in my life. You are an endless support, love, and inspiration to me.

To my lovely brother, Hamid who is far away but his love and endless support are always with me and I am so grateful to have you in my life.

Acknowledgements

I would like to express my deep appreciation to my supervisor Dr. Bipro Ranjan Dhar, for the patient guidance, constructive criticism, invaluable support and valuable suggestions. I have been extremely lucky to have a supervisor who improved my research and writing skills, always keen to advise and provide me with the guidance to be an independent researcher.

My sincere thanks also go to my Ph.D. supervisory committee (Dr. Tong Yu and Dr. Jeffery Farner), Ph.D. candidacy exam committee (Dr. Tong Yu and Dr. Jeffery Farner, Dr. Hamid Zaman, Dr. Yashar Pourrahimian, and Dr. Samir Mushrif), and PhD defense committee (Dr. …) for their time and valuable critical feedback on my thesis work.

I express my warm thanks to all my past and present colleagues for their valuable support. Thanks to Dr. Basem Zakaria and Dr. Mohamed Meshref for providing me with training on the equipment and Lab techniques. I also thank Mr. Yupeng (David) Zhao for their laboratory-related training. I sincerely appreciate the help from Arlene Oatway, and Kacie Norton and for providing me with training on different microscopic imaging techniques.

I express my gratitude to the donors of the scholarships (Alberta Innovates Graduate Student Scholarship and Alberta Graduate Excellence Scholarship) and awards (Bill Shostak Wildlife Award, Martha Piper Awards, Graduate Student Teaching Assistant Award, Andrew Stewart Memorial Graduate Prize, Dr Donald R Stanley Graduate Scholarship in Environmental Engineering, Gordon R Finch Memorial Graduate Scholarship in Environmental Engineering) that I received during my PhD journey.

I am also thankful to the Discovery Grant from the Natural Sciences and Engineering Research Council of Canada (NSERC), John R. Evans Leaders Fund from the Canada Foundation for Innovation (CFI), and Small Equipment Grant (Research Capacity Program) from the Ministry of Economic Development and Trade, Government of Alberta.

Table of Content

List of Tables

List of Figures

Abbreviations

AD	Anarobic digestion
THP	Thermal hydrolysis process
MPs	Microplastics
NPs	Nanoplastics
WWTPs	Wastewater treatment plants
FPS	Fermented primary sludge
TWAS	Thickened waste-activated sludge
PsNPs	Polystyrene nanoplastics
ROS	Reactive oxygen species
MSW	Municipal solid wastes
OLR	Organic loading rate
VS	Valotile solids
ARG	Antibiotic resistance gene
TS	Total solids
SRT	Solids residence time
CH_4	Methane
BMP	Biochemical methane potential
TSS	Total suspended solids
VSS	Volatile suspended solids
TAN	Total ammonium nitrogen
TCOD	Total chemical oxygen demand
VFA	Volatile fatty acid

TEM	Transmission electron microscope
SEM	Scanning electron microscope
qPCR	Quantitative polymerase chain reaction
EPS	Extracellular polymeric substances
HGT	Horizontal gene transfer
MGE	Mobile genetic elements
SOD	Superoxide dismutase
CAT	Catalase
SDS	Sodium dodecyl sulfate

Chapter 1

Introduction

1.1. Background

The sludge management and disposal costs in typical wastewater treatment plants (WWTPs) have been estimated at 50-70% of the total operating costs (Appels et al., 2008). Thus, efficient and economic sludge management techniques are critical for the wastewater industry to achieve energy-neutral or even energy-positive wastewater treatment. Among various sludge handling/disposal approaches, anaerobic digestion (AD) is most widely used in large-scale WWTPs (Mohammad Mirsoleimani Azizi et al., 2021b). AD is considered as a cost-effective and eco-friendly approach for sludge volume reduction, stabilization, and energy recovery through methane-rich biogas generation (Jianwei Liu et al., 2020).

AD is a complex biochemical process that includes four major steps: hydrolysis, acidogenesis, acetogenesis, and methanogenesis (Appels et al., 2008; Kim et al., 2015). The hydrolysis step is recognized as a rate-limiting step in sludge AD (Nazari et al., 2017). During hydrolysis, insoluble and high-molecular weight macromolecular compounds (e.g., lipids, polysaccharides, and proteins) are degraded into low-molecular weight soluble organics, such as amino acids, sugars, and fatty acids (Appels et al., 2008). Various pre-treatment methods can accelerate sluggish hydrolysis kinetics (Appels et al., 2008). To date, several pre-treatment approaches, such as chemical (alkali, acid, and oxidants) (Li et al., 2012), thermal (conventional and microwave heating) (Appels et al., 2010), mechanical (ultrasonic, high-pressure homogenization, etc.) (Nguyen et al., 2017), biological (enzyme and ensilage) (Liu et al., 2017), and hybrid processes (Nazari et al., 2017) have been investigated for enhancing AD process. Among them, the thermal hydrolysis process (THP) has been mostly implemented in full-scale AD facilities in WWTPs (Jianwei Liu et al., 2020). The key benefits of THP include enhanced energy and heat recovery and increased biosolids acceptability and sludge volume reduction by high solids removal (Jeong et al., 2019).

With growing concerns about reducing nutrients (nitrogen and phosphorous) discharge, many WWTPs adopted PS fermentation to produce sludge fermentation liquor rich in volatile fatty

acids (VFA) that can be utilized as an exogenous readily biodegradable carbon source for biological nutrient removal (e.g., biological phosphorus removal and denitrification) process (Zhou et al., 2021). The remaining solid residue, usually called fermented primary sludge (FPS), is then used as a co-substrate with thickened waste activated sludge (TWAS) for the AD facility (Zhou et al., 2021). However, to date, limited information is available on the effects of different THP conditions for anaerobic co-digestion of FPS and TWAS.

Recently, the presence of microplastics (MPs, a particle size of <5mm) and nanoplastics (NPs, 1 to 1000 nm) in aquatic environments captured widespread attention worldwide(Azizi et al., 2022). MPs/NPs can enter the aquatic and terrestrial environment from different sources. WWTPs have been recognized as one of the main discharge outlets of MPs/NPs to the ecosystem (Azizi et al., 2022). WWTPs could effectively remove 99% of influent MPs during different treatment processes (Anne Marie Mahon et al., 2017). The principal removal mechanism is retaining them in the sewage sludge (Anne Marie Mahon et al., 2017; Mohammad Mirsoleimani Azizi et al., 2021b). Reportedly, the MPs/NPs in sewage sludge ranged from 4.2×10^3 to 6.4×10^6 particles/kg of dry solids (Chand et al., 2022). Land application of sewage sludge is discarding 4.4×10^4-3×10^5 tons/year of MPs/NPs into the soil in North America (Nizzetto et al., 2016). Sewage sludge also contains other contaminants, including various persistent chemicals, pathogens, heavy metals, antibiotics, and antibiotic resistance genes (ARGs) (Dai et al., 2020a). Due to their high surface area and hydrophobicity, MPs/NPs can serve as a vector for certain pollutants (Mohammad Mirsoleimani Azizi et al., 2021b).

The presence of MPs/NPs in sludge can remarkably affect the operation stability of AD (He et al., 2021). For instance, polystyrene nanoplastics (PsNPs) can interfere with digester operation via inducing reactive oxygen species (ROS), leaching of toxic chemicals/additives, inhibiting activities of critical enzymes, and cell apoptosis via penetration of PsNPs (Azizi et al., 2022; Mohammad Mirsoleimani Azizi et al., 2021b). Also, the presence of MPs/NPs in sewage sludge can promote the proliferation of ARGs and inevitably increase the chance of ARGs transfer through land application of digestate (Azizi et al., 2022). Reportedly, THP before AD can decrease the proliferation of most ARGs throughout the AD process (C. Sun et al., 2019). However, it is still unknown whether THP could minimize ARG propagation enhanced by MPs/NPs exposure.

Although the THP process of sludge prior to AD has been adopted by AD facilities in many WWTPs worldwide (Mohammad Mirsoleimani Azizi et al., 2021a), there are still several fundamental and engineering bottlenecks associated with their practical application. Most importantly, the impact of THP on minimizing the negative environmental impacts of MPs/NPs associated with their presence in AD and anaerobic co-digestion of sewage sludge has not yet been achieved. Thus, the proposed doctoral research attention is given to the application of THP on anaerobic co-digestion of sewage sludge for enhancing energy recovery, strategies for enhancing macromolecules solubilization, and investigating how THP can influence MPs/NPs-induced stress during AD.

1.2. Scope and objectives

My doctoral thesis focuses on exploring fundamental and engineering insights into the (1) application of THP for enhancing macromolecules solubilization and energy recovery from AD of sewage sludge, and (2) impact of THP of MPs/NPs-induced stress on AD. The specific objectives of this dissertation were:

1) To explore various retrofitting schemes of low-temperature THP in AD with primary sludge fermentation.
2) To assess the impact of THP of sludge on polystyrene nanoplastics-induced stress during AD.
3) To assess the significance of solids content in THP operation on mitigating oxidative stress of polystyrene nanoplastics on sludge anaerobic digestion.
4) To examine the effect of low-temperature THP on energy recovery from semi-continuous anaerobic co-digestion of primary sludge fermentation and waste activated sludge.
5) To evaluate the potential of THP to mitigate oxidative stress from polystyrene nanoplastics during semi-continuous AD.

1.3. Thesis outline

This thesis consists of eight chapters. Chapter 1 demonstrates the background of the doctoral thesis and discusses the scope and objectives of the doctoral research. Chapter 2 provides particular attention to the low and high temperature THP as a pretreatment approach for enhancing AD of sewage sludge, the effect of MPs/NPs on AD digester performance, and insights into inhibition mechanisms of MPs/NPs. Chapter 3 investigates the efficiency of low-temperature THP on AD

process of the mixture TWAS and FPS. Chapter 4 investigates the effect of THP on minimizing the PsNPs-induced stress in AD of sewage sludge. Chapter 5 focuses on how THP affects AD of primary sludge with different TS% exposed to PsNPs. Chapter 6 provides insights into the effect of low-temperature THP on energy recovery from semi-continuous anaerobic co-digestion of FPS and TWAS. Chapter 7 evaluates the potential of THP to mitigate oxidative stress from PsNPs during semi-continuous AD. Chapter 8 summarizes the conclusion and the recommendation of future research.

Literature Review

A part of this chapter was published in Bioresource technology, 329, 124894; and the other part will be submitted in a peer-reviewed journal.

2.1. Introduction

Limiting resources of fossil fuels, growing population, progressing climate change, and industrialization confronted the world's population with a demand for searching alternative energy sources (Jankowska et al., 2017; Mosallanejad et al., 2017). Also, rapid urbanization and population growth caused excessive production of organic wastes, including food waste (FW), lignocellulosic residuals, and sewage sludge (El Gnaoui et al., 2020; X. Liu et al., 2020). It has been projected that the rising trend of the world's population will cause a 70 % increment in annual solid waste generation from ~2.0 billion tons in 2016 to 3.4 billion tons in 2050 (Dastyar et al., 2021a, 2021b). Due to a lack of sustainable organic waste management practices and policies, landfilling has been widely practiced for many decades (Dastyar et al., 2021a). Reportedly, landfilling contributes to the significant emission of greenhouse gases to the ecosystem, causing global warming, while seepage of leachate contaminates soil and groundwater (Kibler et al., 2018; Pereira de Albuquerque et al., 2021). Among them, anaerobic digestion (AD) has been widely accepted as a sustainable method for organic waste diversion from landfills and the recovery of bioenergy and biofertilizer (Dastyar et al., 2021a; Rezaee et al., 2020). Particularly, AD has recently grasped more attention due to increasing interest in renewable natural gas (RNG), triggered by changing energy policies, carbon credit, and financial incentives available for commercial-scale biogas facilities (Kassem et al., 2020; Sahoo and Mani, 2019)

AD comprises a series of biochemical steps medicated by bacteria and archaea, including hydrolysis, acidification, acetogenesis, and methanogenesis (Ai et al., 2018; Elyasi et al., 2015). Hydrolysis is mostly considered the rate-limiting step when digesters are operated with complex feedstocks containing a high level of particulate organics (Zhou et al., 2021). During hydrolysis, insoluble organic compounds and high molecular weight compounds, such as protein, carbohydrate, and lipids, break into amino acids, sugars, and fatty acids, respectively (Appels et al., 2008; S. Chen et al., 2019). At the same time, an imbalance between the kinetics of bacteria

and archaea can make methanogenesis a rate-limiting step in digesters operated with feedstocks having high levels of readily biodegradable organics (Gunaseelan, 2004; Rozzi and Remigi, 2004). Nonetheless, due to complex organics and recalcitrant organics, AD operation with most organic waste faces challenges with poor hydrolysis rates, leading to longer residence time or a larger footprint of digesters (Appels et al., 2008). Thus, pretreatment of organic waste is often critical for facilitating hydrolysis of complex organics to enhance their bioavailability during AD, thereby boosting energy recovery under shorter digestion times or higher organic loading rates (OLRs) (Song et al., 2021).

To date, various pretreatment approaches, such as physical (Nuruddin et al., 2016), chemical (T. Wang et al., 2017), biochemical (Rouches et al., 2016), and thermal (Kim et al., 2016) methods, have been studied for hydrolysis of organic waste prior to AD (El Gnaoui et al., 2020; Loow et al., 2016). Among these techniques, the thermal hydrolysis process (THP) is one of the most extensively investigated pretreatment methods, successfully applied at lab-, pilot- and industrial scales (Ariunbaatar et al., 2014a; Carrère et al., 2010). In general, THP is considered a non-oxidative process that facilitates the thermal degradation of macromolecules (Chen et al., 2012; Dasgupta and Chandel, 2019; Munir et al., 2018). In this process, the initial temperature of feedstock is increased from the ambient temperature to the desired temperature and kept for a certain exposure period (Mohammad Mirsoleimani Azizi et al., 2021a). Key benefits from THP include but are not limited to improved dewaterability of residuals (Carrère et al., 2010; Haug et al., 1978), pathogen removal for land application of digestate, and indeed improved digester process kinetics and methane recovery (Carlsson et al., 2012; Liu et al., 2012; Müller, 2001; Pilli et al., 2015; Val del Río et al., 2011). The other advantages include reduction of scum and foaming, odor generation potential of digestate, and reducing the viscosity of the digestate (Barber, 2016; Kor-Bicakci and Eskicioglu, 2019; Pilli et al., 2015). Moreover, one of the most attractive features of THP that makes it a unique pretreatment technique is the feasibility of energy recovery (Mohammad Mirsoleimani Azizi et al., 2021a). The applied heat during the THP process can be recovered using heat exchangers during the cooling process feedstock. The recovered energy can be reutilized for heating more feedstock, leading to a significant increase in energy efficiency and reducing the pretreatment expenses for industries (Pilli et al., 2015).

THP has been demonstrated to be effective for improving AD of a wide variety of organic wastes, including sewage sludge, organic fraction of municipal solid waste (OFMSW), agricultural

waste, food waste, manure, microalgae, and consequently improving their anaerobic biodegradability (H. Chen et al., 2019; Cheng et al., 2019; Pagés-Díaz et al., 2020). According to the literature, a wide spectrum of temperature (50–250 °C) and resistance time (10–120 min) have been explored for the THP (with or without steam explosion) (Ariunbaatar et al., 2014b; Carrere et al., 2016; Ferreira et al., 2014). However, depending on the operating temperatures, THP is often classified into low-temperature THP (LT-THP; ≤100°C) and high-temperature THP (HT-THP; >100°C) (Kor-Bicakci and Eskicioglu, 2019; Pilli et al., 2015) which will be further discussed in the following subsections.

2.2. LT-THP of sewage sludge

2.2.1. Significance of process parameters

Several process parameters, such as temperature, exposure time, and pH, are critical for the effectiveness of LT-THP for sewage sludge solubilization (Nazari et al., 2017). However, operating temperature and exposure times have been more studied. Nazari et al. investigated the impact of LT-THP (40–80°C, 1-5 h) on the solubilization of WAS and PS(Nazari et al., 2017). The maximum solubilizations of COD (20.3%) and VSS (38.8%) for WAS were obtained at 80°C. Analogous to WAS, 80°C contributed to the maximum solubilizations of COD (18.2%) and VSS (15.1%) for PS. Thus, for both WAS and PS, 80°C at the highest exposure time of 5 h was found as the optimum. The higher solubilization efficiencies observed for WAS are probably due to the nature of WAS comprised of numerous microorganisms, non-biodegradable debris from hydrolyzed microbial cells, a greater quantity of protein but lower levels of lipids and fibers than PS (Kor-Bicakci and Eskicioglu, 2019). Biswal et al. (Kumar Biswal et al., 2020) reported that LT-THP at 100 °C could provide the highest increase in SCOD for saline WAS, which was 9 times higher than the raw sludge. Moreover, exposure time had a considerable impact; increasing exposure time from 0.5 h to 3 h increased the SCOD concentrations by ~20%. Recently, Azizi et al. (Mohammad Mirsoleimani Azizi et al., 2021a) studied the effects of LT-THP on TWAS and fermented PS in the range of 50–90 °C and exposure time of 30-90 min. The authors found that LT-THP of TWAS alone would provide the highest solubilization efficiencies at 90˚C (60 min). In contrast, for LT-THP of TWAS and fermented PS, a slightly higher exposure time (90˚C, 90 min) would be required to achieve the highest solubilization efficiencies. However, LT-THP of TWAS alone was generally more efficient in sludge solubilization. The authors postulated that

pre-fermentation of PS possibly hydrolyzed most organics, and the remaining portion was not easily degradable under LT-THP. Overall, previous studies demonstrated that both pretreatment temperature and exposure time would be critical for LT-THP of sewage sludge

Previous studies primarily focused on optimizing temperature and exposure time, while the significance of other process parameters has often been overlooked. Nazari et al. (Nazari et al., 2017) emphasized that pH could be another pertinent variable playing a significant role in solubilization in LT-THP. According to their results from LT-THP (40–80°C, 1-5 h) of PS and WAS, the pH of 10 was the optimum for the solubilization of sewage sludge, among pH of 4, 7, and 10. The authors postulated that the observed enhancement in solubilization at alkaline pH could be attributed to (i) saponification of lipids in the cell, which solubilizes membrane leading to the release of intracellular material out of the cell (Neyens et al., 2003), (ii) dissociation of acidic groups in EPS, which creates electrostatic repulsion in the negatively charged EPS causing desorption of extracellular polymers (Nazari et al., 2017), and (iii) chemical degradation and ionization of hydroxyl groups in EPS leading to extensive swelling (Neyens et al., 2004). Conversely, LT-THP under acidic conditions could mostly hydrolyze polysaccharides to respective monosaccharides, which is considered relatively easy to hydrolyze compared to other macromolecules. Moreover, acidic conditions can cause inhibitory compounds like furfural and hydroxy-methyl-furfural (Ariunbaatar et al., 2014a; Nazari et al., 2017).

2.2.2. Solubilization of macromolecular biopolymers

Proteins represent major micromole in municipal sludge. However, proteins could be trapped by humic-like components leading to the formation of protein-humic assemblies and, consequently, making proteins less prone to microbial degradation and denaturation (Gonzalez et al., 2018). Therefore, understanding the effects of THP on the solubilization of proteins is of great interest. Protein content in the sludge is generally classified into different fractions, including total, soluble (proteins in the aqueous phase), bound (protein loosely attached to the microbial cell wall), and tightly bound or cellular (the fraction inside the microbial cell) (Dhar et al., 2012; Nazari et al., 2017). Nazari et al. studied the impact of LT-THP (at 80 °C for 5 h) on solubilization of different protein fraction in TWAS (Nazari et al., 2017). The concentration of total protein remained almost constant before and after pretreatment, while the tightly bound proteins in both WAS and PS decreased significantly followed by the increase in soluble proteins. Moreover, Biswal et al. also reported similar patterns during LT-THP (60 to 120 °C and 30 min exposure

time) of WAS (Kumar Biswal et al., 2020). The soluble protein concentration increased from 73.6 mg/L for raw WAS to 654, 1250, 2332 and 2294 mg/L at 60, 80, 100 and 120°C, respectively. These results demonstrated the solubilization of tightly bound fractions (Kumar Biswal et al., 2020). Furthermore, Azizi et al. studied the effect of LT-THP in the range of 50–90 °C and exposure time of 30-90 min under two different schemes (scheme-1: TWAS + FPS and scheme-2: TWAS only), the maximum increase in soluble protein concentrations was observed at 70°C for both schemes (Mohammad Mirsoleimani Azizi et al., 2021a). Also, their result indicated the extent of protein solubilization was higher for scheme-2 (TWAS only, 2,913 mg/L increase) than scheme-1 (TWAS + FPS, 2,313 mg/L increase) which could be attribute to the fact that after fermentation of PS, the remaining macromolecules (i.e., carbohydrates and proteins) in FPS would be more resistant to solubilization by LT-THP (Mohammad Mirsoleimani Azizi et al., 2021a). It should be noted that many WWTPs across the world implanted the fermentation of primary sludge to produce VFAs rich sludge liquor to provide readily biodegradable carbon to biological nutrient removal processes such as denitrification or enhanced biological phosphorous removal process. Thus, exploration of an optimized LT-THP process scheme would be critically important for such wastewater treatment plants.

Regarding carbohydrate solubilization, several studies have reported that low-T THP leads to significant carbohydrate solubilization. For instance, Chen et al.'s survey demonstrated that at 100 °C, the solubilization of polysaccharides increased around 13.6 fold compared to the raw sludge (Chen et al., 2017). Also, Nazari et al. found that the total carbohydrates concentration remained almost constant after the treatment (Nazari et al., 2017). At the pretreatment temperature of 80 °C and the exposure time of 5 h, soluble carbohydrate slightly increased from 109 to 220 μg/mL (Nazari et al., 2017). Additionally, Biswal et al. reported that after 3 h of pretreatment between 60 to 120 °C, soluble carbohydrate level significantly improved by 8.8–43.8 times compared to the control. This enhancement was linked to the compulsive cellulose solubilization (Kumar Biswal et al., 2020). Similarly, Azizi et al. research demonstrated a substantial increase in soluble carbohydrate concentrations for all tested conditions (50–90 °C and 30-90 min), indicating solubilization of particulate carbohydrates occurred after THP. However, no specific trends were observed for temperatures and exposure times (Mohammad Mirsoleimani Azizi et al., 2021a).

Interestingly, by comparing the quantity of released protein and carbohydrate, it can be stated that most of the mentioned studies found that the protein solubilization was higher than

carbohydrate at the same operating condition (Kumar Biswal et al., 2020; Nazari et al., 2017). The reason behind this observation could be related to the location of carbohydrate, protein, and EPS in sludge matrix. Carbohydrates are placed in exopolymers of the sludge, while proteins are mainly located inside the cells (Neyens et al., 2003). Also, protein and carbohydrates are the two main organic constituents of EPS. Therefore, carbohydrate concentration only originates from EPS decomposition, whereas releasing intracellular contents by cell rupture and also EPS decomposition contribute to the protein fraction (Kumar Biswal et al., 2020; Nazari et al., 2017).

2.2.3. Methane generation and process kinetics

Despite moderate solubilization, previous studies reported that LT-THP could still enhance the hydrolysis rate and methane yields. For instance, Nazari et al. (Nazari et al., 2017) estimated 1.1–2.5 times higher hydrolysis rate coefficient (k_{hyd}) for LT-THP of WAS and PS at 80°C (5 h), as compared to the untreated samples. Similarly, Liao et al. (Liao et al., 2016) also estimated increase in k_{hyd} values from 0.19 d^{-1} to 0.29, 0.39 and 0.39 d^{-1} for LT-THP of sewage sludge at 60, 70 and 80 °C, respectively. However, regarding methane yields, contradictory results have been reported in the literature. A study by Biswal et al. (Kumar Biswal et al., 2020) reported considerable increase in methane production from 13.7-27% for LT-THP of saline sludge at 60 and 80ºC, while methane production only slightly increased to 29% after further increasing the operating temperature to 100ºC. Besides, Azizi et al. (Mohammad Mirsoleimani Azizi et al., 2021a) reported considerable increase in methane yields with LT-THP (50–90 °C, 30-90 min) of TWAS and fermented PS and TWAS alone. For LT-THP of co-substrate, methane yield could reach as high as 56.28% (90°C, 90 min). In contrast, methane yield increased up to 43.4% (90°C, 60 min) for pretreatment of TWAS alone. Unlike these studies, Nazari et al.(Nazari et al., 2017) found 33% decrease in methane generation for WAS after THP at 80 °C for 5 h. The authors postulated that this could be attributed to the formation of melanoidins, which can commence forming even at room temperature and longer reaction time, and the inhibitory effect of ammonia which could be produced by the degradation of nitrogenous matter like proteins. Typically, ammonia present in two formations including ammonium or the ionized ammonia (NH_4^+), and free ammonia or the un-ionized ammonia (NH_3) which is poisonous for anaerobic bacteria due to its capability of penetrating the cell membrane and causing potassium deficiency and proton imbalance (Appels et al., 2008).

2.3. HT-THP of sewage sludge

2.3.1. Significance of process parameters

Temperature, residence time and sludge nature can play a significant role in determining the amount of solubilization. Jeong et al.(Jeong et al., 2019) studied the impact of HT-THP (100–220°C) on the SCOD enhancement of WAS. Their results showed a maximum increase of 55.1% in SCOD at 220°C. Moreover, Choi et al. (Choi et al., 2018) reported HT-THP at 180 °C (76 min) improved COD solubilization by 29%. Zhou et al. (Zhou et al., 2021) investigated the effect of temperature in the range of 140–180 °C and exposure time of 15–60 min on TWAS and the mixture of TWAS and FPS. They reported a maximum 49% and 40% enhancement in COD solubilization for TWAS and a mixture of TWAS and FPS, at 160°C and 30 min, respectively (Zhou et al., 2021). Additionally, they reported the highest VSS reduction (71% for TWAS and 56% for the TWAS + FPS) was observed at 180 °C and 60 min. The authors postulated that the difference in the amount of solubilization could be attributed to the difference between the initial TS content in TWAS and TWAS+FPS (Zhou et al., 2021). Also, another study suggested that the difference could be attributed to the nature of TWAS (mainly consisting of cell debris) and FPS (mainly lipid and fibers) (Nazari et al., 2017). With respect to effect of reaction (exposure) time at HT-THP, Park et al. investigated the effect of exposure time on sewage sludge at 200 °C. The results indicated that by enhancing the exposure time from 0.5 to 2 h, the SCOD increased from 57 to 215 mg/g sludge (Park et al., 2019). However, Zhou et al found that the effect of exposure time on solubilization was minimal compared to the temperature (Zhou et al., 2021). For instance, at 160 °C and different exposure times of 15, 30 and 60 min, the obtained solubilization for all three conditions was almost 34%.

2.3.2. Solubilization of macromolecular biopolymers

HT-THP can enhance protein and carbohydrate solubilization by releasing EPS components to the soluble phase (Devos et al., 2020). However, care should be taken to prevent the negative effects of excessive temperature (Gonzalez et al., 2018). At higher temperatures, the production of brownish refractory compounds is inevitable, which could be related to the conversion of proteins, carbohydrates and amino acids to melanoidins in the Maillard reaction (D. Zhang et al., 2020). Melanoidins formation is a great barrier for any further sludge biodegradability even when solubilization yield is high (Devos et al., 2020). Zhao et al.(Zhao et al., 2020) studied the effect of

temperature on solubilization of WAS at 110–230°C (Zhao et al., 2020). Reportedly, the maximum soluble protein of 1771.67 mg/L was attained at 180 °C, while at higher temperatures of 200 and 230°C, less amount of soluble protein was measured, which could be related to the occurrence of Maillard reaction. Kakar et al. (laqa Kakar et al., 2020) investigated the effect of HT-THP (150–240°C for 5–30 min) on protein and carbohydrate solubilization of TWAS. The soluble protein concentration increased from 112 mg/L for the untreated TWAS to a maximum of 2500 mg/L at 220°C and 30 min. Similarly, soluble carbohydrate increased from 703 mg/L for the raw TWAS to 2290 mg/L at 230°C and 15 min (laqa Kakar et al., 2020). However, other studies reported at a higher temperature than the melting point of sugar (170 °C), caramelization may happen leading to the formation of organic acids, aldehydes and ketones (Gonzalez et al., 2018). Also, in the temperatures range of 190 to 220 °C, denaturation and degradation of protein and, consequently, increase in the ammonia concentration is expected (Gonzalez et al., 2018).

2.3.3. Methane generation and process kinetics

Due to the enhancement in the solubilization after applying HT-THP, it is expected after increasing the bioavailability, the methane generation increase as well (Nazari et al., 2017). However, there are several contradictory results on the literature which need further investigation. Toutian et al. (Toutian et al., 2020) studied the effect of HT-THP (130-170°C) on methane production of WAS. Their results demonstrated a maximum of 27.1% enhancement in methane production at 170 °C. Despite the enhancement in ultimate methane production, the authors believed the kinetic of the process did not change, which means the required time for sludge to reach the ultimate methane production did not change considerably (Toutian et al., 2020). Moreover, Jeong et al.(Jeong et al., 2019) investigated the impact of THP (100–220°C) on methane generation of WAS with different TS% of 1, 3, 5 and 7%. The results demonstrated that 180 °C contributed to the maximum methane production with 86.1, 84.3, 76.2 and 76% enhancement for WAS with 1, 3, 5 and 7% TS%, respectively. The reduction of gas generation at higher TS contents was attributed to the mass transfer limitation and, thereby reducing the sludge solubility (Jeong et al., 2019). Notably, further increase of temperature to above 180 °C also led to the reduction of methane production. The authors ascribed the reason behind the methane reduction to an increase in NH_4^+–N concentration and decrease in the biodegradability resulted from the Maillard reaction at higher temperatures. Also, Zhou et al. (Zhou et al., 2021) investigated the effect of HT-THP

(140-180°C for 15-60 min) on the methane yield of TWAS and a mixture of TWAS and FPS. According to results, the maximum methane generation of 161% acquired from TWAS+FPS (compared to the raw sludge) under the operating conditions of 160 °C and 60 min. However, for TWAS only, maximum methane yield was obtained at 140 °C and 30 min, which was 75% higher than the raw TWAS. Reportedly, the maximum methane generation obtained from TWAS+FPS was higher than TWAS alone. The authors postulated this may have resulted from the presence of more readily biodegradable organics like VFA in the FPS. Regarding hydrolysis rate (k_{hyd}), the pretreated samples, demonstrated lower values than the raw sludges indicating longer time required for pretreated samples to reach the maximum methane production rates compared to the control (Zhou et al., 2021).

2.4. Effect of MPs/NPs on AD

2.4.1. Background

Recently, the presence of microplastics and nanoplastics in aquatic environments captured widespread attention worldwide. Notably, wastewater treatment plants have been ubiquitously identified as a major route for (nano)microplastics release to the aquatic environments, including rivers, lakes, oceans, and deep-sea sediments (Liu et al., 2019; A. M. Mahon et al., 2017; Zhang and Chen, 2020). Studies have indicated that (nano)microplastics in domestic sewage mainly originate from personal care products and laundry (Zhang et al., 2020). Therefore, significant efforts have been dedicated by research communities towards the detection of (nano)microplastics in influent, different process streams, treated effluent, sludge, and anaerobic digestates (biosolids) in wastewater treatment plants (Gies et al., 2018; A. M. Mahon et al., 2017; Mason et al., 2016; Rolsky et al., 2020; Zhang and Chen, 2020).

Microplastics are typically defined as plastic particles <5 mm in size, while plastic particles smaller than 1 μm is usually considered nanoplastics (Bhagat et al., 2020; Feng et al., 2018). About 30 types of (nano)microplastics have been detected in domestic sewage (Zhang et al., 2020). Among them, polyethylene, polyester, polyamide were identified as most abundant (Iyare et al., 2020; Liu et al., 2019). According to recent reports, up to 99% of (nano)microplastics in raw sewage can be retained in the sewage sludge (Iyare et al., 2020; A. M. Mahon et al., 2017; Zhang and Chen, 2020). In sewage sludge, concentrations of (nano)microplastics can range from 1.5×10^3 to 2.4×10^4 particles/kg dry solids (Luo et al., 2020; Zhang and Chen, 2020). Microplastics can

present in sewage sludge in different forms, including fibers, fragments, spheres, film, and microbead (A. M. Mahon et al., 2017; Rolsky et al., 2020).

Depending on their source, MPs released to the environment are universally classified as either primary or secondary MPs (Cole et al., 2011; Pellini et al., 2018). Primary MPs include particles produced intentionally to be microscopic. These plastics are typically utilized for several applications, such as facial cleansers and cosmetics, as a vector for drugs, paints, toothpaste, shampoos, and shower gels (Cole et al., 2011; Galafassi et al., 2019; Waller et al., 2017). Secondary MPs, both particles and fibers, originate from macroscopic plastic debris, as they are progressively fragmented into smaller pieces by photo-oxidation from reactive oxygen species, UV light, and other environmental conditions such as wind, waves, and temperature (Andrady, 2011; Cole et al., 2011).

The application of anaerobic digestion is a common practice for the management of sewage sludge in wastewater treatment plants, particularly in large-scale facilities (Lafratta et al., 2020; Wenjing et al., 2019; Zhou et al., 2021). Therefore, understanding the effects of (nano)microplastics on anaerobic digestion has recently attracted considerable attention. Based on the authors' knowledge, Mahon et al. (A. M. Mahon et al., 2017) first reported that the anaerobic digestion process might reduce microplastics, which was based on the characterization of biosolids samples from seven different wastewater treatment plants in Ireland. Later studies by other researchers mostly noted that certain types of (nano)microplastics, such as polyethylene, polyvinyl chloride, polystyrene, etc., could adversely affect anaerobic digestion under both short- and long-term exposures (Feng et al., 2018; Fu et al., 2018; Wei et al., 2019b, 2019a). However, different (nano)microplastics may exhibit different inhibition mechanisms depending on their physical and chemical characteristics. For instance, additives released from (nano)microplastics could directly damage microbial cells and/or inhibit the activities of key enzymes and functional genes (Wei et al., 2019c). Notably, nanoplastic particles could penetrate the microbial cell membrane (Fu et al., 2018). Some microplastics can generate reactive oxygen species (ROS) (Wei et al., 2020, 2019b). In contrast, polyamide microplastic could positively influence the anaerobic digestion of sludge (Chen et al., 2021). The additives released from microplastics could enhance the activities of some key enzymes for methanogenesis, which could improve the digester performance (Chen et al., 2021). These results suggested that the effects of different (nano)microplastics on digester

microbial communities can not be interpreted with similar mechanisms. Therefore, understanding the mechanisms underlying the impacts of (nano)microplastics on anaerobic digestion is essential.

Multiple literature reviews have recently been published on (nano)microplastics focusing on their detection/identification methods, as well as their fate and removal in the wastewater treatment process (mostly focusing on liquid treatment trains) (Iyare et al., 2020; Liu et al., 2021; Zhang et al., 2020; Zhang and Chen, 2020). However, none of them critically reviewed the underlying inhibition mechanisms behind the effects of (nano)microplastics on anaerobic digestion.

Considering the complexity of different biochemical reactions and the involvement of a diverse group of microorganisms, in anaerobic digestion, a critical review of the related academic articles will help to identify key research gaps regarding the effects of (nano)microplastics on anaerobic digestion and potential environmental risks.

Therefore, the purpose of this review article is to provide a critical overview of the current publications on the impacts of (nano)microplastics on anaerobic digestion. First, the effects of various (nano)microplastics on anaerobic digestion performance in terms of methane production, process kinetics, and solids removal are summarized. Then, underlying mechanisms affecting anaerobic digestion, such as inhibition mechanisms, effects on different biochemical pathways, key enzymes, functional genes, and microbial communities, are discussed in detail. Finally, the research gaps are identified, and an outlook for future research is prospected.

2.4.2. Impact on digester performance

Table 2.1 lists the available research findings on the impact of various (nano)microplastics on anaerobic digestion. These studies primarily amended different (nano)microplastic particles, such as polyvinyl chloride, polyethylene, polystyrene, polyamide, etc., with digester feedstocks to see the potential effects. Almost two-thirds of the studies used waste activated sludge as a feedstock, while others used synthetic wastewater (glucose). For sewage sludge, the loading of microplastic particles was primarily based on the total solids (TS) content in sludge samples. Most of the studies were carried out by batch biochemical methane potential (BMP) test, while only a few studies conducted continuous anaerobic digestion tests. Furthermore, all studies used mesophilic temperatures, possibly because mesophilic digestion is most commonly used for the stabilization of sewage sludge in wastewater treatment plants (Ruffino et al., 2020).

Table 2.1. A summary of major findings from published studies on the effects of (nano)microplastics on anaerobic digestion.

Type of MPs/NPs	Particle size	Concentration of MPs/NPs	Feedstock	Mode (temperature)	Major findings	Reference
Polyvinyl Chloride	1000 µm	10, 20, 40, 60 particles/ g-TS	Waste activated sludge	Batch (37°C)	- 10 particles/ g-TS slightly increased methane production - 20-60 particles/ g-TS led to a significant decrease in methane productivity and kinetics - Leaching of bisphenol-A (BPA) was identified as a primary reason for inhibition	(Wei et al., 2019c)
Polyethylene	40 ± 2 µm	10, 30, and 60, 100, and 200 particles/g-TS	Waste activated sludge	Batch (37°C)	- 10, 30, and 60 particles/g-TS did not affect the methane production - 100 and 200 particles/ g-TS decreased methane production by 12.4−27.5%, with a significant decrease in hydrolysis rate coefficients than the control. - Despite leaching of acetyl tri-n-butyl citrate (ATBC), synthesis of reactive oxygen species (ROS) was identified as the main reason for inhibition. - Enzymes (protease, acetate kinase, coenzyme F_{420}) associated with different stages in anaerobic digestion were negatived affected.	(Wei et al., 2019b)
Polyethylene	40 ± 2 µm	200 particles/g-TS	Waste activated sludge	Continuous (37°C)	- Daily methane production decreased by 28.8% than the control. - VS destruction decreased by 27.3 compared to the control.	(Wei et al., 2019b)

Polyester	200 μm	1, 3, 6, 10, 30, 60, 100, 200 particles/g-TS	Waste activated sludge	Batch (37ºC)	-	Methane production and hydrolysis rate coefficients decreased for all tested conditions; however, no correlation existed between different microplastics dosages	(L. Li et al., 2020)
					-	Dewaterability of digestate slightly improved by microplastics addition.	
Polyamide	500-1000 μm	5, 10, 20, and 50 particles/ g-TS	Waste activated sludge	Batch (37ºC)	-	All polyamide dosages improved methane production; the highest improvement (39.5% higher than the control) was observed for 10 particles/g-TS	(Chen et al., 2021)
					-	Leaching of caprolactam from polyamide enhanced the activities of key enzymes (protease, α-glucosidase, acetate kinase, butyrate kinase, and F_{420}) associated with methane production.	
Polystyrene	5 μm and 80 nm	0.05, 0.1, 0.2, and 0.25 g/L	Synthetic wastewater (glucose)	Batch (35ºC)	-	≤0.25 g/L did not affect methane production	(J. Zhang et al., 2020)
					-	0.25 g/L led to a significant reduction (5 μm: 17.9%; 80 nm: 19.3%) in methane production	
					-	Nanoplastic (80 nm) demonstrated a slightly higher inhibition capacity than microplastic particles (5 μm).	
Polystyrene	54.8 nm	0, 0.05, 0.1 and 0.2 g/L	Sewage sludge	Batch (37ºC)	-	Methane yields linearly decreased with increasing polystyrene concentrations.	(Fu et al., 2018)
					-	Up to 14.4% reduction in methane yield was observed for 0.2 g/L.	
					-	Pitting of microbial cells by polystyrene nanoparticles was identified as the key mechanism of inhibition.	
Polystyrene	50 ± 6 nm	0, 10, 20 and 50 μg/L	Synthetic wastewater (glucose)	Continuous (35ºC)	-	10 μg/L had no significant impacts.	(Wei et al., 2020)
					-	20 and 50 μg/L decreased methane production (by 19.0-28.6%) and COD removal (19.3-30.0%).	

					- Leaching of sodium dodecyl sulfate (SDS) and generation of ROS inhibited methane production. - Polystyrene particles accumulated into inner layer of sludge granule. - Higher dosages (20 and 50 µg/L) led to a smaller granular size.	
Polystyrene	60-80 nm	Anionic polystyrene (PS-SO_3H: 60, 80, 100 µg/mL), cationic polystyrene (PS-NH_2: 5,10, 20 µg/mL)	Synthetic wastewater (glucose)	Batch (37ºC)	- 20 µg/mL of cationic polystyrene could lead to higher inhibition of methane production than 100 µg/mL of anionic polystyrene. - Under short-term exposure, polystyrene nanoparticles could penetrate granular sludge and alter protein secondary structures of extracellular polymeric substances. - The abundance of functional genes (*mcr*A and *ACAS*) for methanogenesis decreased after exposure to polystyrene nanoparticles.	(Y. Feng et al., 2018)

Wei et al. (Wei et al., 2019c) studied the impacts of polyvinyl chloride microparticles (10-60 particles/g-TS) on the anaerobic digestion of waste activated sludge. Their results showed that the addition of 10 particles/g-TS could marginally (5.9%) increase methane production, while 20-60 particles/g-TS led to a significant decrease in methane productivity and kinetics. The methane production for 60 particles/g-TS was 75.8% of the control condition. The kinetic analysis suggested that the hydrolysis rate coefficient decreased with increased polyvinyl chloride concentration above 10 particles/g-TS. Wei et al. (Wei et al., 2019b) studied different dosages (10-200 particles/g-TS) of polyethylene microplastics in anaerobic digestion of waste activated sludge. The short-term exposure of methanogenic communities to polyethylene particles at lower concentrations (10-60 g particles/g-TS) showed a minor impact on methane production. In contrast, higher polyethylene levels (100-200 particles/g-TS) led to decreased methane production. Notably, up to 27.5% decrease in methane production was observed for polyethylene dosage of 200 particles/g-TS; hydrolysis rate coefficient also decreased by 15%. The authors further investigated the impact of inhibitory polyethylene dosage (i.e., 200 particles/g-TS) on continuous anaerobic digestion at an organic loading rate of 3 g COD/L/d for 130 days. The reduction in methane production (28.8%) during continuous operation was consistent with the batch BMP test data.

Li et al. (L. Li et al., 2020) investigated different dosages of polyester microparticles ranged from 1-200 particles/g-TS during anaerobic digestion of waste activated sludge. Compared to the control, all polyester dosages led to a decline in methane production and hydrolysis rate coefficients. Interestingly, no correlation existed between different microplastics dosages and corresponding methane potential, which was quite different from some of the previous studies done with other microplastic particles, such as polyvinyl chloride, polyethylene, etc. (discussed earlier). Moreover, digestate from polyester amended digesters showed slightly higher dewaterability. Although the mechanisms behind improved dewaterability were not revealed in their study, another study suggested that interactions between polystyrene nanoparticles and protein secondary structures in extracellular polymeric substances in activated sludge could facilitate bioflocculation of sludge (Feng et al., 2018).

Chen et al. (Chen et al., 2021) studied the impact of polyamide microplastics (5–50 particles/g-TS) on the anaerobic digestion of waste activated sludge. Interestingly, in contrast with other

studies, their results showed a positive impact of polyamide microparticles on methane production. All polyamide dosages increased methane production (5.9-39.5%) than the control. The highest increase in methane production was achieved for 10 particles/g-TS. However, hydrolysis rate coefficients for all polyamide dosages were comparable to the control. Fig. 2.1 summarizes the literature results on the effects of polyethylene, polyester, polyamide, and polyvinyl chloride microplastics (40-1000 µm) on methane production in batch anaerobic digestion of waste activated sludge. For polyvinyl chloride and polyethylene, methane production decreased with increasing microplastics levels despite significant particle size differences. Also, they showed more substantial negative impacts than polyester. Polyvinyl chloride was previously ranked as the most toxic among various microplastics found in aquatic environments (Liu et al., 2019). For polyester, no correlation was observed between the changes in methane production with different dosages. Among these four microplastics, only polyamide particles demonstrated a positive impact (Fig. 2.1).

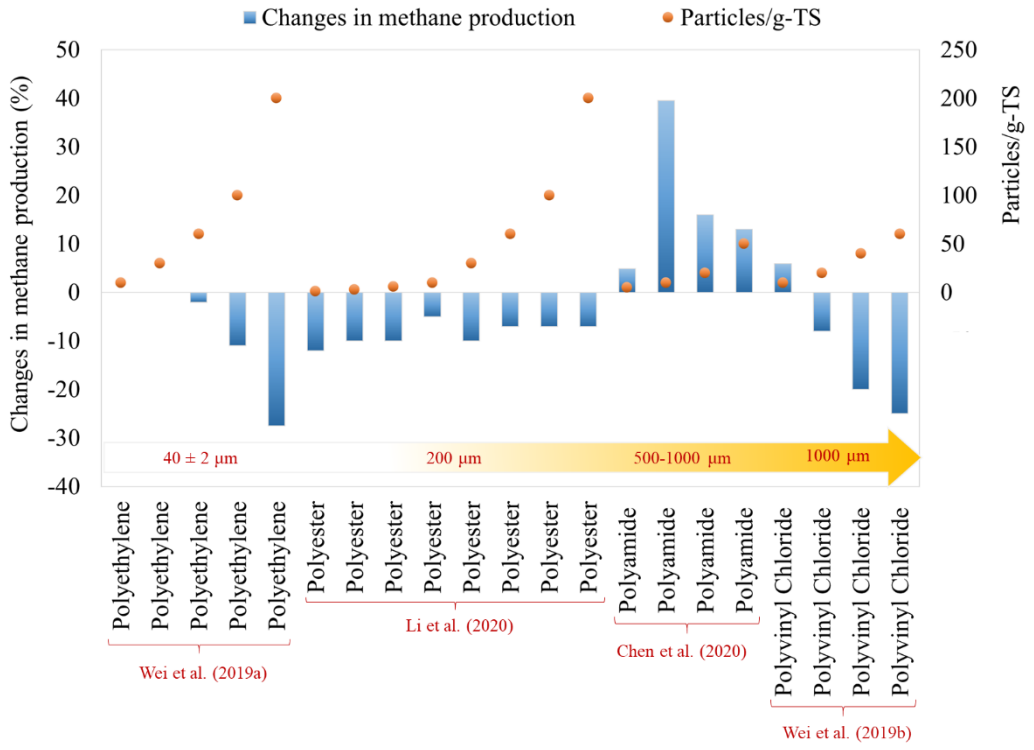

Figure 2.1. Effects of polyethylene, polyester, polyamide, and polyvinyl chloride microplastics on methane production in batch anaerobic digestion of waste activated sludge. Note. Changes in methane production (%) indicate the results compared to the control.

Among various (nano)microplastics, the effects of polystyrene on anaerobic digestion were investigated in multiple studies (Feng et al., 2020; Y. Feng et al., 2018; Fu et al., 2018; Wei et al., 2020; J. Zhang et al., 2020). Zhang et al. (2020) studied the effects of polystyrene micro and nanoparticles (80 nm and 5 μm) on anaerobic digestion. For both particles, polystyrene dosages ≤0.2 g/L did not significantly affect the anaerobic digestion. However, a concentration of 0.25 g/L led to a substantial decline (17.9-19.3%) in methane production. Moreover, nano-sized polystyrene particles caused more inhibition than micro-sized particles. Fu et al. (Fu et al., 2018) studied the impact of different concentrations (0.05–0.2 g/L) of polystyrene nanoparticles on the anaerobic digestion of sewage sludge. The polystyrene concentration of 0.2 g/L led to the highest methane potential reduction than the control (14.4% reduction). In addition to a decrease in methane production, polystyrene nanoparticles extended the lag phases compared to the control, indicating that polystyrene particles in sludge can potentially prolong the digester start-up time. Feng et al. (Y. Feng et al., 2018) studied the inhibition and recovery potential of anaerobic granular sludge under short-term exposure (210 hours) to functionalized cationic and anionic polystyrene nanoparticles. In the first cycle of the BMP test, anionic polystyrene nanoparticles (PS-SO_3H, 100 μg/mL) could reduce methane production by 17.47%. In contrast, a relatively lower concentration (20 μg/mL) of cationic polystyrene nanoparticles (PS-NH_2) could reduce methane production by 22.98%. However, methane production could be recovered in the second cycle. Wei et al. (Wei et al., 2020) studied the effects of long-term exposure of polystyrene nanoparticles (10-50 μg/L) on anaerobic granular sludge in up-flow anaerobic sludge blanket (UASB) reactors operated with synthetic wastewater at an organic loading rate of 2 kg COD/m^3/d. The digester performance was unaffected by 10 μg/L of polystyrene nanoparticles. However, the higher concentrations (20 and 50 μg/L) of polystyrene nanoparticles considerably reduced biomethane production and chemical oxygen demand (COD) efficiencies by 19.0-28.6% and 19.3-30.0%, respectively, along with higher volatile fatty acids (VFAs) accumulation. Fig. 2.2 shows the literature results on the effects of polystyrene (nano)microplastics (54.8 nm to 5 μm) on methane production in batch anaerobic digestion. For both real sludge and synthetic medium (glucose), methane production decreased with increasing polystyrene dosages. Among different studies, cationic polystyrene nanoparticles (PS-NH_2) showed the most negative impact on anaerobic digestion, suggesting that the significance of surface charge of (nano)microplastics should be an important consideration in future studies.

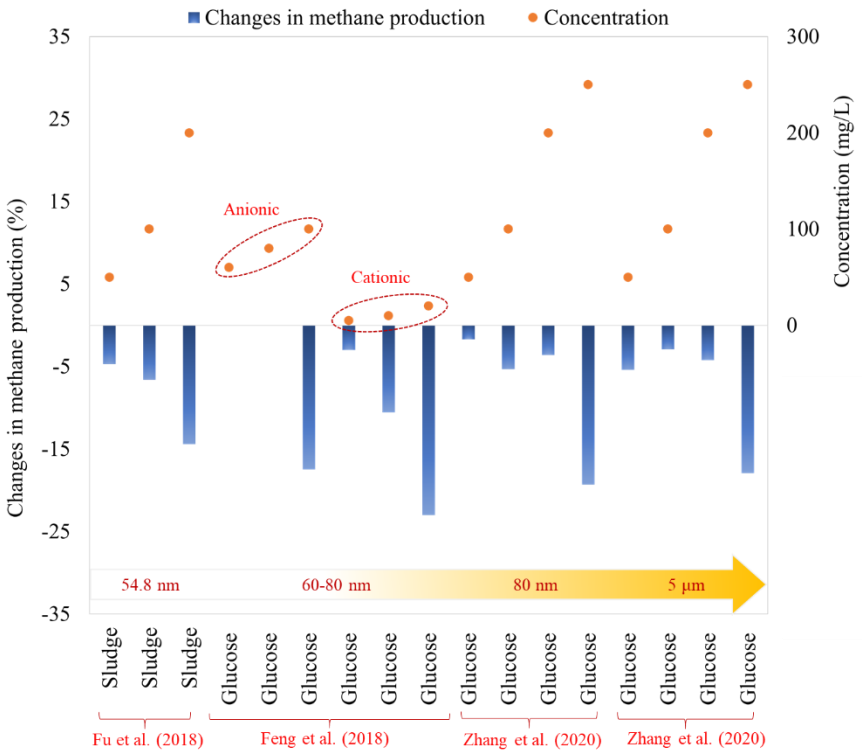

Figure 2.2. Effects of polystyrene (nano)microplastics on methane production in batch anaerobic digestion. Note. Changes in methane production (%) indicate the percentage increase/decrease compared to the control.

To date, limited information is available on the impact of (nano)microplastics on solids removal during anaerobic digestion. A few studies reported the effects on apparent volatile solids (VS) destructions in batch studies (Chen et al., 2021; Wei et al., 2019c, 2019b). Wei et al. (Wei et al., 2019c) reported a decrease in apparent VS destruction from 32.1% to 22.9% for 60 particles/g-TS of polyvinyl chloride. Analogous to methane production, Chen et al. (Chen et al., 2021) observed a ~32% increase in apparent VS destruction over the control for a polyamide concentration of 10 particles/g-TS. Notably, Wei et al. (Wei et al., 2019b) reported the impact of polyethylene microplastics on apparent VS destruction from batch BMP test as well as VS removal efficiencies for continuous anaerobic digestion. For polyethylene dosage of 200 particles/g-TS, the apparent VS destruction decreased by 24%, as compared to the control. In continuous anaerobic digestion with the same polyethylene concentration, VS destruction efficiency decreased by 27.3%, slightly higher than the decrease in the apparent VS destruction observed in the BMP test. However, the VS removal efficiencies in continuous anaerobic digestion depend on solids

residence times (SRTs) (Dhar et al., 2013). Therefore, further research is needed to understand the effects of (nano)microplastics in digesters operated under different SRTs.

Overall, most studies demonstrated decreased digester performance in terms of methane productivity, kinetics, and VS removal efficiencies. However, specific microplastics like polyamide and polyvinyl chloride (up to certain dosages) could increase methane productivity and kinetics up to certain limits (Chen et al., 2021; Wei et al., 2019c), yielding apparently contradictory results. Thus, the inhibitory effects of (nano)microplastics perhaps can be associated with physical and chemical characteristics of microplastics (e.g., type, size, shape, surface area, surface charge, etc.) and exposure time rather than the total loading.

2.4.3. Insights into inhibition mechanisms

Several mechanisms have been proposed in the literature on the inhibition of anaerobic digestion by (nano)microplastics (Fig. 2.3). First, leaching of toxic chemicals or additives from (nano)microplastics can affect microbial activities in digester by damaging microbial cells and by inhibiting activities of key enzymes associated with biochemical reactions and defense against oxidative stress (Wei et al., 2020, 2019c). For instances, Wei et al. (Wei et al., 2019c) identified the leaching of bisphenol-A (BPA) from polyvinyl chloride as the key inhibition mechanism that facilitated the rupture of microbial cell walls. The leaching of BPA (0.5-3.6 μg/L) increased with increasing the number of particles from 10 to 60 particles/g-TS. BPA concentration up to 0.5 μg/L could increase methane production slightly over the control, while higher concentrations (1.8-3.6 μg/L) hindered methane production. The role of BPA in methanogenesis inhibition was also confirmed through additional experiments by spiking corresponding BPA concentrations in digesters. Wei et al. (2020) also found that sodium dodecyl sulfate leached from polystyrene nanoparticles could contribute to methanogenesis inhibition. Regarding the underlying mechanisms, Wei et al. (Wei et al., 2019c) postulated that BPA leached from polyvinyl chloride could facilitate the rupture of microbial cells and solubilization of extracellular polymeric substances. This explanation was justified by the higher release of unknown soluble chemical oxygen demand (SCOD) fractions in polyvinyl chloride particles amended digesters. The unknown SCOD could be attributed to lipids and nucleic acids released from damaged microbial cells and solubilized extracellular polymeric substances. Nonetheless, further studies would be needed to get more insights into the fundamental role of BPA in methanogenesis inhibition. As an emerging

contaminant in sewage sludge, previous studies investigated the fate of BPA in anaerobic digestion (Phan et al., 2018; Samaras et al., 2014; Yang et al., 2017). These studies reported no removal to 80% removal of BPA in anaerobic digesters. Also, there has been no report on any adverse impact of BPA on anaerobic digestion. Thus, it is possible that digester operating conditions may also influence the threshold BPA concentration for inhibition or BPA removal efficiency (Samaras et al., 2014). Wei et al. (Wei et al., 2019b) also investigated the leaching of potential additives from polyethylene, such as acetyl tri-n-butyl citrate (ATBC), diethylhexyl phthalate (DEHP), and Irgafos 168 phosphate (plastic antioxidant). Only the leaching of ATBC was observed, while the leaching of other additives was insignificant. Further tests with direct spiking of ATBC in digesters revealed no adverse impact of ATBC on methanogenic communities. Moreover, Chen et al. (Chen et al., 2021) found that caprolactam released from polyamide microparticles could increase the activities of key enzymes involved in anaerobic digestion (discussed later).

Second, (nano)microplastics can catalyze the generation of reactive oxygen species (ROS), such as H_2O_2, •OH, etc. (Wei et al., 2020, 2019b) (Fig. 2.3b). Wei et al., 2019a found that the exposure of (nano)microplastics (e.g., polyethylene, polystyrene) could considerably increase the intracellular ROS levels, which also aligned with the viability of microbial biomass. Previous studies also suggested that (nano)microplastics exposure can induce the generation of ROS under aerobic conditions (Hwang et al., 2019; Prata et al., 2019). The high surface area of (nano)microplastic particles can promote ROS generation via the catalytic reaction between free radicals and molecular dioxygen (Wei et al., 2019b). However, the mechanisms of ROS generation under anaerobic condition are still ambiguous. A few recent reports suggested ROS generation in anaerobic bioreactors at sub-micromolar concentrations of oxygen when exposed to the unfavorable metabolic environment (e.g., presence of inhibitors, pH changes) (Tian et al., 2019; Zheng et al., 2019). Thus, further research is needed to understand the ROS generation mechanism by (nano)microplastics under anaerobic conditions.

Third, (nano)microplastics may directly damage the microbial cells and inhibit metabolic functions (Fu et al., 2018) (Fig. 2.3c). However, the inhibition mechanisms depend on the characteristics (e.g., type, concentrations, size, etc.) of (nano)microplastics (Chen et al., 2021; Wei et al., 2019b, 2019c; J. Zhang et al., 2020). Notably, nanoplastic particles can penetrate microbial cell membranes through the gaps between biopolymers chain and cause damage to proteins and

phospholipids (Zhang and Chen, 2020). For instance, Fu et al. (Fu et al., 2018) investigated the impact of polystyrene nanoplastics on a model fermentative bacterium *Acetobacteroides hydrogenigenes* that can utilize carbohydrates to produce hydrogen (a precursor for hydrogenotrophic methanogenesis). The addition of polystyrene nanoplastic at a concentration of 0.2 g/L led to decreased glucose fermentation to hydrogen. The microscopic imaging suggested that polystyrene nanoparticles were attached to the surface of microbial cells and caused the pitting of cell walls. Thus, polystyrene nanoparticles could inhibit fermentative bacteria and thereby disrupt their syntrophic partnership with methanogens. However, further research would be needed to evaluate the possible damage of archaeal cells (i.e., methanogens) by nanoplastic particles. Anaerobic granular sludge has been reported to be more resistant to unfavorable metabolic conditions than suspended biomass (Elbeshbishy et al., 2017; Sheng et al., 2010). However, Feng et al. (Y. Feng et al., 2018) found that functionalized anionic and cationic polystyrene nanoparticles could penetrate anaerobic granular sludge and alter the protein secondary structures of extracellular polymeric substances even under short-term exposure (210 hours). Moreover, cationic polystyrene nanoparticles showed higher inhibition capacity. Extracellular polymeric substances are typically negatively charged (Zhang and Chen, 2020); thus, catatonic polystyrene nanoparticles could be readily combined with them. Moreover, Wei et al. (Wei et al., 2020) recently found that long-term exposure (86 days) of polystyrene nanoparticles (20-50 μg/L) decreased the generation of extracellular polymeric substances and led to smaller sludge granule in up-flow anaerobic sludge blanket (UASB) reactor operated with synthetic wastewater (glucose). Fluorescence imaging of granular sludge showed that polystyrene nanoparticles were agglomerated/accumulated on the outer layer of sludge granule as well as transferred into inner layers of sludge granule over long-term exposure (Fig. 2.3d).

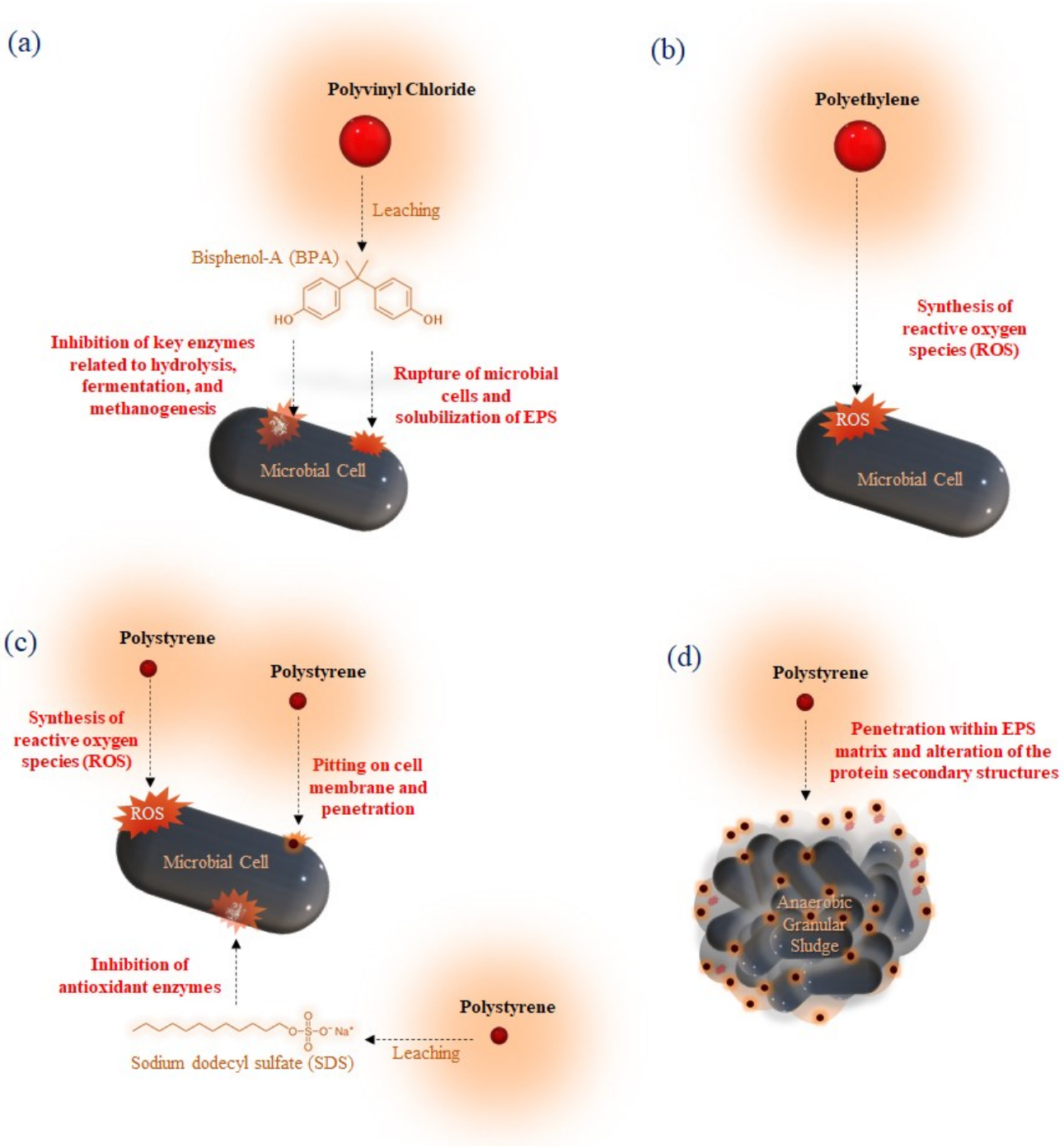

Figure 2.3. Mechanisms of (a) polyvinyl chloride, (b) polyethylene, (c, d) polystyrene (nano)microplastics induced inhibition of anaerobic digestion. Figures were drawn based on the mechanisms proposed in the literature (Y. Feng et al., 2018; Fu et al., 2018; Wei et al., 2020, 2019b, 2019c).

2.4.4. Impact of different biochemical pathways associated with anaerobic digestion

The process of anaerobic digestion presents a complex biochemical process combining acidogenic (hydrolysis and fermentation) and methanogenesis steps. In general, the methanogenesis step is considered to be more sensitive or susceptible to unfavorable environmental conditions (Karakashev et al., 2005; Luo et al., 2020). Moreover, the inhibition of the acidogenic step can ultimately lead to the deterioration of methanogenesis, as these steps are syntrophycally linked. Although most of the studies focused on the impact of (nano)microplastics on the digester performance, a few studies also looked into their effects on acidogenic (hydrolysis and fermentation) and methanogenesis stages (Wei et al., 2019a; Zhang et al., 2020). The investigations were based on monitoring profiles of COD, proteins, carbohydrates, VFAs, activities of key enzymes, and microbial communities in digesters in response to (nano)microplastics exposure.

Wei et al. (Wei et al., 2019c) found that polyvinyl chloride exposure could increase soluble COD concentrations while the generation of VFAs considerably decreased. Interestingly, the unknown fraction of SCOD increased with increasing polyvinyl chloride concentrations. The authors postulated that the increase in unknown SCOD fractions could be attributed to lipids and nucleic acids released from the rupture of microbial cells and solubilization of extracellular polymeric substances by bisphenol-A leached from polyvinyl chloride. Although the hydrolysis process seemed to be unaffected or improved (based on the increase in SCOD), the abundance of various known hydrolytic bacteria decreased along with fermentative bacteria. Thus, polyvinyl chloride negatively impacted the acidogenic step, indicated by low VFAs generation. Wei et al. (Wei et al., 2020) found that polystyrene nanoparticle exposure decreased the overall VFAs generation while increased propionate concentration. Thus, their results suggested that both fermentation efficiency and pathways would be affected by polystyrene nanoparticles. In contrast to these studies, Chen et al. (Chen et al., 2021) found that COD, proteins, and carbohydrates solubilization were comparable for both polyamide amended and control digesters, indicating hydrolysis was not affected by polyamide addition. However, VFAs production in polyamide amended reactor with 10 particles /g-TS increased by 23.5%, suggesting a positive impact on the fermentation step. As mentioned earlier, except for polyamide, higher concentrations of other (nano)microplastics exhibited adverse effects on anaerobic digestion.

A few studies conducted supplementary experiments with model organic compounds to understand the impacts of (nano)microplastics on acidogenic and methanogenic steps more explicitly (Wei et al., 2019a; Zhang et al., 2020). For instance, Wei et al. (Wei et al., 2019b) investigated the effects of polyethylene microplastics on the acidogenic step; the experiments were conducted with model monosaccharide and amino acid compounds. There was no significant difference in glucose (model monosaccharide compound) degradation under control and different polyethylene dosages. In contrast, the degradation of glutamate (model amino acid) was considerably reduced at higher polyethylene concentrations (100-200 particles /g-TS), suggesting microbial communities capable of fermenting proteins would be more vulnerable to polyethylene microplastics. The authors also observed a 24.1% decrease in the relative abundance of *Proteiniclasticum* species, known to ferment proteins to acetate.

Zhang et al. (J. Zhang et al., 2020) found no significant differences in profiles of pH, VFAs, and ammonia nitrogen after exposure of digesters to polystyrene nanoparticles. The authors further conducted experiments to understand the impact of polystyrene particles on acidogenic (with glucose as a substrate) and methanogenesis (using acetate as a substrate). The results suggested an adverse impact on both steps, while methanogenic activity was more disturbed than the acidogenic activity due to polystyrene exposure.

2.4.5. Effects on enzymes and functional genes associated with anaerobic digestion

When exposed to (nano)microplastics, methane productivity and kineties are positively or negatively affected depending on their physical and chemical features as well as (perhaps) digester operating conditions. It was also evident that (nano)microplastics can potentially influence different biochemical stages in anaerobic digestion (discussed in the previous section). The activities of key enzymes involved in different stages in anaerobic digestion are expected to be affected by environmental conditions, such as pH, temperature, etc. (Dai et al., 2016; Lu et al., 2020; Zhang et al., 2014). The changes in digester performance after (nano)microplastics exposure have been reported to be a result of changes in activities of key enzymes, such as protease, cellulase, α-glucosidase, acetate kinase, butyrate kinase, coenzyme F_{420}, etc., involved in different biochemical reactions (Chen et al., 2021; Wei et al., 2019c). Protease, cellulase, and α-glucosidase are extracellular hydrolases that play key roles in the hydrolysis of complex organics (e.g., proteins and carbohydrates) (Chen et al., 2021; Tian et al., 2017; Wang et al., 2015; X. Wang et al., 2017;

Wei et al., 2019c; Yang et al., 2019). Acetate kinase catalyzes the conversion of acetyl-CoA to acetic acids, while butyrate kinase facilitates the formation of short-chain VFAs from amino acids (Chen et al., 2021; Wang et al., 2015; X. Wang et al., 2017; Wei et al., 2019c). The cofactor F_{420} is an essential coenzyme for methanogenesis (Chen et al., 2021; Wang et al., 2015; Wei et al., 2019c).

Wei et al. (Wei et al., 2019c) studied the changes in activities of four selected key enzymes (protease, cellulase, acetate kinase, coenzyme F_{420}) during anaerobic digestion of sewage sludge amended with polyvinyl chloride microplastics (10-60 particles/g-TS). In general, their study showed a negative impact of polyvinyl chloride particles on methanogenesis. Except for cellulase, the relative activities of the other three enzymes decreased considerably than the control with increasing polyvinyl chloride dosages. The highest reductions in activities of protease, acetate kinase, F_{420} were observed at 60 particles/g-TS, which also corroborated with the highest reduction in methane production for this specific polyvinyl chloride dosage. Chen et al. (Chen et al., 2021) studied the impact of polyamide particles (5–50 particles/g-TS) on five different key enzymes (protease, α-glucosidase, acetate kinase, butyrate kinase, and F_{420}) during anaerobic digestion of waste activated sludge. The results suggested that polyamide particles enhanced enzymatic activities. Notably, the activity of coenzyme F_{420} increased by up to 200% of the control for 10 particles/g-TS, which was also supported by the highest methane production. The authors postulated that the leaching of caprolactam (CPL) from polyamide microparticles could play a key role in boosting enzymatic activities. The direct spiking of CPL to the digesters also supported this notion. Interestingly, a comparison of SCOD, soluble proteins and soluble carbohydrates suggested a trivial effect of polyamide on hydrolysis, while the activities of enzymes related to hydrolysis also improved. This could attribute to the fact that solubilization could also be a non-microbial process (Wei et al., 2019b). Moreover, in addition to enzymatic activity, the distribution of enzymes on surface-active sites of the sludge would be equally important for hydrolysis (Ruan et al., 2019). Previous studies also suggested that enzymatic activities may not correspond to methane production in anaerobic digestion (Tian et al., 2017). Also, to date, only coenzyme F_{420} has been used as a biomarker to evaluate the impact of microplastics on methanogenic activity (Chen et al., 2021; Wei et al., 2019c). The activity of coenzyme F_{420} may not provide an accurate estimation of acetoclastic methanogenic activity in anaerobic digesters (Dolfing and Mulder, 1985;

Heyer et al., 2015), while acetoclastic methanogenesis has been identified as the dominant methanogenesis pathways in sewage sludge anaerobic digester (Guo et al., 2015). Therefore, future studies related to microplastics should consider other biomarkers (e.g., cofactor F_{430}) as suggested in the recent literature (Passaris et al., 2018).

In addition to enzymes associated with different biochemical reactions, (nano)microplastics can impact the defense antioxidant enzymes of methanogens (Wei et al., 2020). Although methanogens are strictly anaerobic, some taxonomically diverse methanogens have various antioxidant enzymes (e.g., superoxide dismutase, superoxide reductase, catalase, peroxidase, etc.) to scavenge ROS (Horne and Lessner, 2013; Wu et al., 2021). Wei et al. (Wei et al., 2020) found that sodium dodecyl sulfate (SDS) leached from polystyrene nanoparticles could restrain the activities of two antioxidant enzymes (superoxide dismutase and catalase), thereby diminished the resistance of methanogenic communities to oxidative stress induced by nanoplastics.

Moreover, Feng et al. (Y. Feng et al., 2018) found that polystyrene nanoparticles could negatively affect two functional genes for methanogenesis: methyl-coenzyme M reductase (*mcr*A) and acetyl-CoA synthetase (*ACAS*). *mcr*A can be used as a biomarker for hydrogenotrophic methanogen (Morris et al., 2014; Zakaria and Dhar, 2019). *ACAS* encodes key enzymes for converting acetate to acetyl-CoA and indicates the acetoclastic methanogenic activity (Guo et al., 2019).

2.4.6. Impact on digester microbial communities

The impact of (nano)microplastics on the digester microbiome is critical, as there has been evidence that microplastics can alter the structure and metabolic pathways of microbial communities in different wastewater systems (Zhang and Chen, 2020). Wei et al. (Wei et al., 2019c) studied the changes in digester microbial communities after exposure to 60 particles/g-TS of polyvinyl chloride. Notably, compared to the control, the abundances of various hydrolytic/fermentative bacteria, such as *Rhodobacter* sp., *Proteiniborus* sp., etc., decreased in the digester exposed to polyvinyl chloride particles. These changes also corroborated with a decrease in the generation of various VFAs. Moreover, the abundance of methanogenic *Methanosaeta* sp. decreased by 16.5% than the control. Wei et al. (Wei et al., 2019b) also showed similar effects for 200 particles/g-TS of polyethylene on digester microbial communities. Their results showed a

decrease in relative abundances of various hydrolytic/fermentative bacteria (*Rhodobacter* sp., *Bacteroides* sp., *Proteiniclasticum* sp., etc.). Moreover, relative abundances of known hydrogenotrophic (*Methanobacterium* sp., *Methanoculleus* sp., and *Methanospirillum* sp.) and acetoclastic methanogens (*Methanosaeta* sp.) decreased in the test digester. Acetoclastic methanogens were still dominant in both reactors, indicating polyethylene exposure did not alter the methanogenesis pathway. Although it was evident that polyethylene exposure adversely affected all biochemical steps involved in anaerobic digestion, a comparison of SCOD and substrate degradation profiles suggested that the methanogenesis step was the most seriously affected by polyethylene exposure. Analogous to microplastics, polystyrene nanoparticles showed a similar impact on digester microbial communities; abundances of various fermentative bacteria (e.g., *Longilinea* sp., *Paludibacter* sp., etc.) and methanogens (e.g., *Methanosaeta* sp.) decreased due to long-term exposure to nanoplastic particles (Wei et al., 2020). Thus, these studies demonstrated the adverse impact of microplastic particles on bacterial and archaeal communities in digesters (Wei et al., 2020, 2019c, 2019b).

However, Fu et al. (Fu et al., 2018) found that different microorganisms might have different tolerance to polystyrene nanoparticles. For instance, the relative abundances of some families (e.g., *Cloacamonaceae*, *Porphyromonadaceae*, *Anaerolinaceae*, and *Gracilibacteraceae*) decreased by the addition of polystyrene nanoparticles in digesters. In contrast, the relative abundances of some other families (*Anaerolinaceae*, *Clostridiaceae*, *Geobacteraceae*, *Dethiosulfovibrionaceae*, and *Desulfobulbaceae*) increased. Previous studies also reported that the increase in abundances of some of those families (e.g., *Clostridiaceae, Desulfobulbaceae,* etc.) in aerobic bioreactors exposed to various microplastics, such as polyether sulfone, polyvinyl chloride (Qin et al., 2020; Seeley et al., 2020). However, a previous study suggested partial inhibitory effects of polyvinyl chloride and polybutylene terephthalate-hexane acid on *Geobacter metallireducens* GS15 belong to *Geobacteraceae* family (Li et al., 2020). Thus, shifts in microbial communities may depend on the type and characteristics of (nano)microplastics. Apparently, most of the (nano)microplastics studied to date could affect the digester microbial communities, thereby impacting the performances of digesters. Except for a few cases (Wei et al., 2020, 2019b), these results were from short-term exposure to (nano)microplastics. There is no information available in the literature on whether anaerobic microbial communities can adapt to (nano)microplastics over long-term

exposure. Therefore, understanding the effects of exposure time of (nano)microplastics on digester microbial communities should be further investigated.

Previous studies substantiated the impact of (nano)microplastics on the diversity of microbial communities in aerobic bioreactors as well as in natural environments (Miao et al., 2019; Seeley et al., 2020; Zhang and Chen, 2020). As the anaerobic digestion process is a multi-step biochemical process involving complex syntrophy between diverse bacterial and archaeal populations (Barua and Dhar, 2017), understanding the impact of (nano)microplastics on microbial diversity merit investigation. The effect of (nano)microplastics on microbial diversity and richness has not been well reported. Nonetheless, according to few reports, the diversity of the microbial communities seems not to be affected considerably by exposure to polyvinyl chloride, polyethylene, polystyrene, and polyester particles (Fu et al., 2018; Wei et al., 2020, 2019c, 2019b).

2.4.7. Outlook and research needs

Most of the (nano)microplastics researched to date have been found to deteriorate anaerobic digestion performance (Table 1). Notably, various inhibition mechanisms have been revealed, including (1) releasing of toxic additives/chemicals, (2) affecting activities of key enzymes and functional genes, (3) producing ROS, (4) damaging/penetrating microbial cells, (5) altering protein structures in granular sludge (Fig. 3). Nonetheless, investigations on the effects of (nano)microplastics on anaerobic digestion are still in an early stage. Several knowledge gaps related to underlying mechanisms, the role of digester process parameters, and environmental consequences should be addressed in future research.

Previous studies primarily focused on understanding the effects of individual (nano)microplastic compounds on anaerobic digestion, while sewage would have more than one type of (nano)microplastics. Thus, further research is still needed to understand possible synergistic and antagonistic interactions among different types of microplastics. Previous studies used waste activated sludge as a substrate to study the effects of (nano)microplastics on anaerobic digestion (see Table 1). However, co-digestion of primary and waste activated sludges is commonly practiced in wastewater treatment plants (Lafratta et al., 2020; Zhou et al., 2021). Based on previous reports, ~70% of microplastics could be removed during preliminary and primary treatment processes in wastewater treatment plants (Bui et al., 2020; Iyare et al., 2020). Thus, it is

expected that the microplastics concentrations would be higher in primary sludge than waste activated sludge. Therefore, future research should focus on understanding the effects of co-digestion of primary and waste activated sludge.

Except for a few studies (Wei et al., 2020, 2019b), most of the studies have been performed in batch (i.e., BMP test), while a thorough investigation of the effects of (nano)microplastics on continuous anaerobic digestion is needed. Notably, the impact of SRTs on the fate of (nano)microplastics remains unknown. Moreover, there was evidence that most microplastics would be retained in sludge in the form of fibers rather than fragments or spheres (A. M. Mahon et al., 2017; Rolsky et al., 2020). Therefore, systematic evaluation of the effects of various physical characteristics of (nano)microplastics on anaerobic digestion should be considered in future studies. Future studies should also consider reporting the mass of nano(microplastics) (e.g., g/kg of dry sludge) rather than particle counts to allow meaningful comparison of results among different studies. Despite similar particle counts, the total weight of (nano)microplastics can be significantly different due to the differences in particle sizes (Rolsky et al., 2020).

In most of the current literature, researchers amended digesters with (nano)microplastics to evaluate their effects and barely reported their removal efficiencies, possibly because of a lack of standard analytical methods or equipment. Thus, the quality of digestate in terms of residual (nano)microplastics has been overlooked. Nonetheless, Mahon (A. M. Mahon et al., 2017) found that regardless of the removal of microplastics during anaerobic digestion, accumulation of microplastics in biosolids would be inevitable. The land application of biosolids is common in many countries (A. M. Mahon et al., 2017; Riau et al., 2010; Rolsky et al., 2020). Therefore, assessing the presence of (nano)microplastics in biosolids and their potential environmental consequences need more attention. There is a possibility that the land application of biosolids would facilitate the transport of (nano)microplastics into soil environments (He et al., 2018; Ngo et al., 2019). The transmission of (nano)microplastics via land application of biosolids could have significant environmental consequences. For instance, (nano)microplastics can adsorb various environmental pollutants, including antibiotics and heavy metals (Li et al., 2018; Mao et al., 2020; Rolsky et al., 2020). Notably, (nano)microplastics can also serve as carriers for antimicrobial resistance genes (ARGs) (Dong et al., 2021; Shi et al., 2020). The land application of digestate (i.e., biosolids) has been widely considered one of the major routes for transmitting ARGs to the

environment (García et al., 2020; Wu et al., 2016; J. Zhang et al., 2019). Although current guidelines for land application of biosolids are primarily based on levels of pathogen and vector attraction reductions (Iranpour et al., 2004), future studies on the effects of (nano)microplastics should consider evaluating the digestate quality concerning these aspects. However, a quick, simple, and standardized method for (nano)microplastics detection in sludge and biosolids are critically needed. Various analytical methods already developed for (nano)microplastics detection in soils (He et al., 2018) should be considered/adopted by the anaerobic digestion research community to accelerate research on these aspects.

2.4.8. Conclusions

Previous studies provided essential evidence that the presence of (nano)microplastics in sewage sludge can influence the anaerobic digestion process through different mechanisms. However, future research should focus on more systematic studies to understand the significance of various physical and chemical characteristics of (nano)microplastics on different inhibition mechanisms. Moreover, the presence and impact of (nano)microplastics on biosolids quality have not been researched adequately. Notably, potential environmental risks, such as the possible transmission of antibiotic resistance genes and heavy metals via the land application (nano)microplastic-contaminated biosolids, needs in-depth research.

Chapter 3

Low-temperature thermal hydrolysis for anaerobic digestion facility in wastewater treatment plant with primary sludge fermentation

A version of this chapter was published in Chemical Engineering Journal, vol. 426, 130485.

3.1. Introduction

With increasing population growth, urbanization, and stricter environmental regulations, wastewater treatment, and subsequent sludge generation increases worldwide (Kor-Bicakci and Eskicioglu, 2019; Pilli et al., 2015). In Canada, the annual sewage sludge production was estimated at around 0.7 million tons of dry sludge, equal to 10-75 g of dry sludge per capita per day (Kor-Bicakci and Eskicioglu, 2019). The sludge management and disposal costs in a typical wastewater treatment plant (WWTP) have been estimated at 50-70% of the total operating costs (Appels et al., 2008; Cano et al., 2015). Thus, efficient and economic sludge management techniques are critical for the wastewater industry to achieve energy-neutral or even energy-positive wastewater treatment. Among various sludge handling/disposal approaches, anaerobic digestion (AD) is most widely used in large-scale WWTPs (Hosseini Koupaie et al., 2018; Mohammad Mirsoleimani Azizi et al., 2021b). AD is considered as a cost-effective and eco-friendly approach for sludge volume reduction, stabilization, and energy recovery through methane-rich biogas generation (Jianwei Liu et al., 2020; Y. Zhang et al., 2019).

AD is a complex biochemical process that includes four major steps: hydrolysis, acidogenesis, acetogenesis, and methanogenesis (Appels et al., 2008; Kim et al., 2015). The hydrolysis step is recognized as a rate-limiting step in sludge anaerobic digestion (Nazari et al., 2017). During hydrolysis, insoluble and high-molecular weight macromolecular compounds (e.g., lipids, polysaccharides, and proteins) are degraded into low-molecular weight soluble organics, such as amino acids, sugars, and fatty acids (Appels et al., 2008). Various pre-treatment methods can accelerate sluggish hydrolysis kinetics (Appels et al., 2008). To date, several pre-treatment approaches, such as chemical (alkali, acid, and oxidants) (Li et al., 2012; Rajesh Banu et al., 2017), thermal (conventional and microwave heating) (Appels et al., 2010; Eftaxias et al., 2018), mechanical (ultrasonic, high-pressure homogenization, etc.) (Le et al., 2016; Nguyen et al., 2017),

biological (enzyme and ensilage) (Ding et al., 2017; Liu et al., 2017), and hybrid processes (Nazari et al., 2017; Peng et al., 2018) have been investigated for enhancing AD process. Among them, the thermal hydrolysis process (THP) has been mostly implemented in full-scale AD facilities in WWTPs (Jianwei Liu et al., 2020). The key benefits of THP include enhanced energy and heat recovery and increasing biosolids acceptability and sludge volume reduction by high solids removal (Jeong et al., 2019; Wilson and Novak, 2009).

Typically, THP can be divided into two different categories: high-temperature (>100ºC) and low-temperature (<100ºC) (Kor-Bicakci and Eskicioglu, 2019). Both low and high-temperature approaches were reported to enhance the solubilization of particulate organics in sewage sludge (Liu et al., 2012; Xue et al., 2015; Zhang et al., 2016). Although a wide range of temperatures (50-270ºC) and exposure times (15-90 min) have been explored in previous studies, most of them focused on high-temperature regimes (>100ºC). Compared to low-temperature THP (<100ºC), the operation of THP at high temperatures consumes more energy, requiring high operating costs that considerably reduce the profitability of the process (Appels et al., 2010; Xue et al., 2015). Moreover, high-temperature THP operated ≥180ºC can often lead to the formation of refractory and inhibitory compounds that can adversely affect the process kinetics and biomethane recovery (Jeong et al., 2019; Zhou et al., 2021).

Although low-temperature THP (<100ºC) has relatively been under-investigated, a handful of studies evidently demonstrated its effectiveness for sludge solubilization and subsequent enhancement of AD (Dhar et al., 2012; Kumar Biswal et al., 2020; Nazari et al., 2017). For instance, Dhar et al. reported that THP (50-90 °C and 30 min) of waste activated sludge (WAS) could increase methane production up to 19% (Dhar et al., 2012). However, previous studies suggested that the effectiveness of low-temperature THP would be contingent on several pertinent variables, including THP conditions (mainly temperature and exposure times) and sludge characteristics. For instance, Nazari et al. reported 80ºC (pH=10, 5 h) as optimum among different low-temperature THP conditions (40-80ºC, pH=4-10, exposures times 1-5 h) for solubilization of chemical oxygen demand (COD) and volatile suspended solids (VSS) in WAS (Nazari et al., 2017). The similar THP condition (80ºC, pH=10, 5 h) also led to significant solubilization of COD and VSS for primary sludge (PS). However, the methane potential decreased by 33% for a THP-treated PS sample with higher soluble carbohydrates. Thus, intrinsic differences in

macromolecular (e.g., proteins, carbohydrates) composition of different types of sludges may lead to varying results. Therefore, characterizing macromolecular compounds during THP would be essential to get more scientific insights into the effectiveness of THP.

With growing concerns about reducing nutrients (nitrogen and phosphorous) discharge, many WWTPs adopted PS fermentation to produce sludge fermentation liquor rich in volatile fatty acids (VFA) that can be utilized as an exogenous readily biodegradable carbon source for biological nutrient removal (e.g., biological phosphorus removal and denitrification) process (Barua et al., 2019; Liu et al., 2018; Zhou et al., 2021). The remaining solid residue, usually called fermented primary sludge (FPS), is then used as a co-substrate with thickened waste activated sludge (TWAS) for the AD facility (Zhou et al., 2021). However, to date, limited information is available on the effects of different THP conditions for anaerobic co-digestion of FPS and TWAS. Recently, we investigated the impact of various retrofitting schemes of high-temperature THP (140-180^{o}C, 15-60 min) for an AD facility in a WWTP with primary sludge fermentation (Zhou et al., 2021). Our results also suggested that a higher degree of solubilization during high-temperature THP would not necessarily lead to higher methane yields, possibly due to the differences in macromolecular composition in FPS and TWAS. However, as per the authors' knowledge, no studies investigated the low-temperature THP (<100ºC) on macromolecular compounds solubilization and subsequent methane yields from co-digestion of TWAS and FPS.

Given these research gaps, this present study comprehensively investigated low-temperature THP (<100ºC) of FPS and TWAS under two different process schemes. The objectives of the present study were to evaluate: a) effectiveness of various THP conditions (50-90ºC, 30-90 min) on solubilization of COD, VSS, proteins, carbohydrates, volatile fatty acids (VFA), ammonia nitrogen; b) changes in functional groups associated with macromolecular compounds; c) the methane potential and kinetics, and d) a preliminary economic assessment to compare potential net savings in AD cost per metric tonne dry biosolids produces in both schemes. To the best of our knowledge, this study presents the first experimental assessment of low-temperature THP (<100^{o}C) for enhancing anaerobic co-digestion of TWAS and FPS along with comprehensive profiling of macromolecular compounds solubilization.

3.2. Materials and methods

3.2.1. Sludge and inoculum

The TWAS, FPS, and digested sludge used in this study were collected from the Gold Bar WWTP (Edmonton, Alberta, Canada) in July 2020. The fermentation of primary sludge is used at the Gold Bar WWTP to produce volatile fatty acids (VFAs) and reduce the sludge volumes to the anaerobic digesters. Four fermenter/thickeners are used to achieve fermentation. The solids residence time (SRT) is 5-8 days, and the hydraulic residence time is 35 – 73 hrs. The VFAs-rich supernatant (known as sludge liquor) is used as an exogenous carbon source in the anaerobic zone in the biological nutrient removal (BNR) process. The thickened FPS is then mixed with TWAS before mesophilic AD at 37 °C. The volume ratio of 1:1 was selected to mimic the operating condition in WWTP. A simplified process flow diagram is provided in the Supplementary Information (Fig. A1). After collection, samples were stored at 4ºC in a cold room. Prior to the biochemical methane potential (BMP) test, the digested sludge was pre-incubated for three days at 37ºC for acclimation of microbial communities, as well as depletion of residual organics. The characteristics of inoculum, FPS, TWAS, and FPS+TWAS are summarized in Table 3.1.

Table 3.1. Characteristics of substrate and inoculum.

Parameters	**Inoculum**	**Substrate**		
	Digested sludge	**FPS**	**TWAS**	**FPS+TWAS**
TSS (mg/L)	23,000 ± 1,750	48,666 ± 2,897	51,500 ± 250	50,083 ± 1,573
VSS (mg/L)	15,583 ± 1,181	32,083 ± 2,529	40,083 ± 577	36,083 ± 1,553
TCOD (mg/L)	24,447 ± 621	56,147 ± 13,155	60,548 ± 1,943	58,347 ± 1,342
SCOD (mg/L)	1,283 ± 2,29	6,104 ± 59	1,002 ± 61	3,553 ± 50
Total protein (g/L)	–	10.60	16.41	13.5
Soluble protein (g/L)	–	0.44	1.33	0.88
Total carbohydrate (g/L)	–	9.27	8.03	9.13
Soluble carbohydrate (g/L)	–	0.05	0.45	0.25
TVFA (mg COD/L)	40 ± 3	4,502 ± 23	615 ± 42	2,558 ± 30
TAN (mg/L)	1,303 ± 24	33.76 ± 2.7	37.6 ± 4.52	35.68 ± 1.7

pH	7.10 ± 0.01	4.59 ± 0.01	6.28 ± 0.01	5.44 ± 0.04

3.2.2. Low-temperature thermal pre-treatment

The low-temperature THP of TWAS and FPS was conducted with a 2 L batch hydrothermal reactor (Parr 4848, Max. temperature: 350ºC, Max. pressure: 1900 psi, Parr Instrument Company, Moline, IL, USA) (Zhou et al., 2021). For each experiment, 400 mL of sample was added. The reactor was tightly sealed and heated by a heating jacket covering the entire reactor. The sludge was stirred at a constant speed of 150 rpm throughout the process (Zhou et al., 2021). The sludge temperature was monitored with a thermocouple equipped with the reactor. After the temperature reached the desired values (50, 70, and 90ºC), the target exposure times (30, 60, and 90 min) were maintained. After this exposure periods, the heating was turned off. Then, cold water was recirculated through the designated recirculation tubes to decrease the sludge temperature down to room temperature.

The THP experiments were conducted in two schemes (Zhou et al., 2021). The schematic illustration of two schemes is provided Fig. 3.1. In scheme 1, THP was applied to the mixture (volume ratio 1:1) of FPS and TWAS. However, in scheme-2 (Fig. 3.1b), THP was performed only on the TWAS, and then it was mixed with the raw FPS (volume ratio 1:1) before the BMP test. For each scheme, nine pre-treatment tests were performed at three temperatures (50, 70, and 90^{o}C) and three exposure times (30, 60, and 90 min). The experimental ranges of temperature and exposure time were selected based on the literature. Most low-temperature THP studies have been performed between 50^{o}C to 90^{o}C (Dhar et al., 2012; Nazari et al., 2017; Xue et al., 2015). Moreover, the typical exposure times used in commercial THP technologies (e.g., Cambi^{TM}, Exelys^{TM}, etc.) are <90 min (Abu-Orf and Goss, 2012; Barber, 2016).

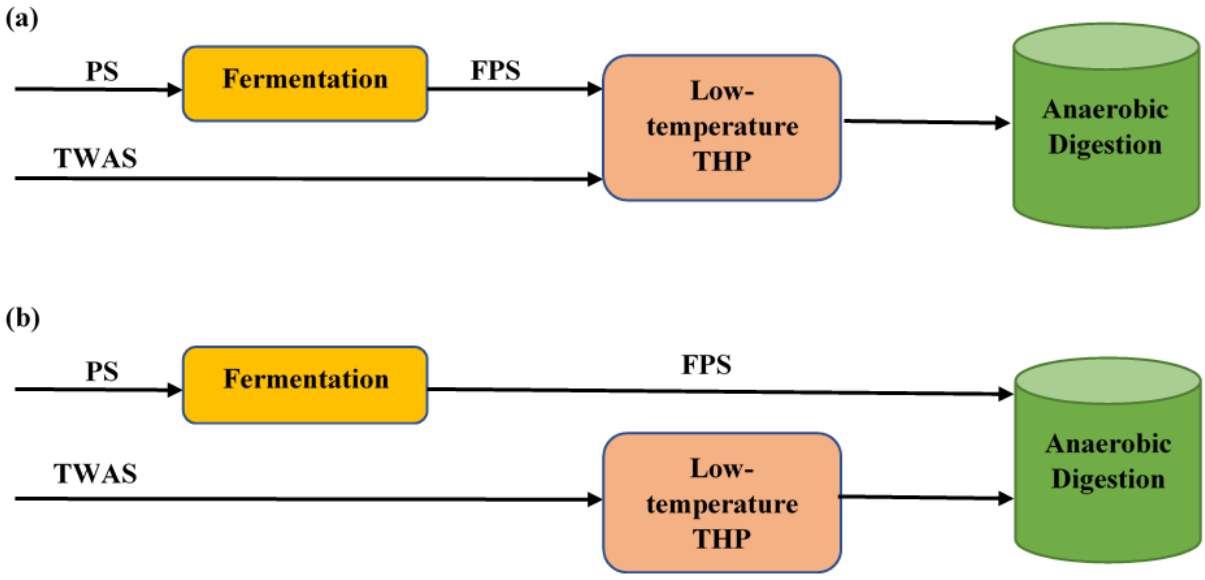

Figure 3.1. Conceptual schematic of THP schemes: (a) scheme-1 and (b) scheme-2. In scheme-1, THP was conducted for a mixture of FPS and TWAS (volume ratio of 1:1). In scheme-2, THP was conducted only for TWAS, and then mixed with FPS before biochemical methane potential test (BMP).

3.2.3. BMP tests

Fifty-four anaerobic glass bioreactors (ISES-Canada, Vaughan, ON, Canada) with a working volume of 350 mL and a 150 mL headspace were used to evaluate biochemical methane potential (BMP) of pretreated samples. The BMP tests were conducted using a food-to-microorganism (F/M) ratio of 2 (g total chemical oxygen demand (TCOD)/g volatile solids (VS)). Previous THP studies also used F/M of ≤2 to avoid any potential process disturbances (e.g., acidification via accumulation of organic acids) due to organics overloading (Dhar et al., 2012; Toutian et al., 2020; Zhou et al., 2021). After loading the estimated volumes of sludge and inoculum, N_2 gas was purged for almost 3 min to create an anaerobic environment. Additionally, reactors were equipped with a mechanical agitator plus an electric motor for continuous mixing at 300 rpm during the experiment. The operating temperature of bioreactors was maintained at mesophilic conditions (37 ± 2°C) using water baths (General Purpose Water Bath, Digital, 20 L, PolyScience, Illinois, USA). The produced methane from each bioreactor was directly collected using gas bags connected with a CO_2 sequestration unit. In each CO_2 absorption unit, 3M NaOH solution with thymolphthalein indicator was used to absorb CO_2 and other acidic gases (e.g., H_2S) from the biogas (Barua et al.,

2018). The generated methane volume was manually measured using a frictionless glass syringe daily (Barua et al., 2018). Moreover, untreated samples were used with inoculum as the control, and inoculum with deionized water was used as the blank to determine the methane produced from the seed. All BMP tests were performed in triplicate for 45 days.

3.2.4. Analytical methods

The total suspended solids (TSS) and VSS concentrations were measured using standard methods (2540 Solids) (Association et al., 1915). Total ammonium nitrogen (TAN), TCOD, and soluble chemical oxygen demand (SCOD) concentrations were analyzed utilizing HACH reagent kits (HACH, Loveland, CO, USA). For TAN and SCOD, samples were prepared by using 0.45 μm membrane filters. The concentration of major VFAs (acetate, propionate, and butyrate) were measured using an ion chromatograph machine (Dionex™ ICS-2100, Sunnyvale, USA) equipped with an electrochemical detector (ECD) and microbore AS19, 2mm column. The operating temperature of 30 and 35 ºC were selected for the column and the conductive detector, respectively. The eluent was 7.00 mM KOH, and its flow rate was 0.25 mL/min using an eluent generator (EGC II KOH, Thermo Scientific). The samples for VFAs analysis were filtered with 0.2 µm membrane filters. The IC was calibrated with five different concentrations of VFA mix (Volatile Free Acid Mix CRM46975, Sigma Aldrich, Canada).

For measuring the total and soluble proteins, total Kjeldahl nitrogen (TKN) kit (HACH, Loveland, CO, USA) was used. The Kjeldahl method indirectly quantifies the protein content by nitrogen measurement (Mariotti et al., 2008; Sáez-Plaza et al., 2013). For quantifying the soluble protein, samples were filtered using 0.45 μm membrane filters. Additionally, the total and soluble carbohydrates were determined using the modified phenol-sulfuric acid method using glucose as a standard (Dubois et al., 1956). Glucose was used as the standard solution. Briefly, 2.5 mL of sample was mixed with 6.25 ml of concentrated sulfuric acid. Then 1.5 mL of 8% phenol was mixed in and the mixture stayed for 10 min at room temperature. Subsequently, the mixture was incubated at 95ºC for 5 min. Afterward, the samples were cooled down at room temperature. Then, the absorbance was read at 490 nm with a spectrophotometer within 10 minutes for both standard and test samples (Jiao et al., 2010).

Fourier-transform infrared spectroscopy (FTIR) analysis was conducted for the control and pretreated samples. Samples were dried at 105 °C for 24 h. Afterward, 2 mg of samples were mixed with 200 mg of KBr (FTIR Grade) in an agate mortar to homogenize the sample. Infrared spectra for the samples were measured over the range of 4,000–400 cm^{-1} with an FTIR Perkin-Elmer 2,000 spectrophotometer.

3.2.5. Calculation, kinetic modeling, and statistical analyses

COD solubilization and VSS reduction after THP were calculated as follows (Nazari et al., 2017):

$$COD\ solubilization = \frac{SCOD_t - SCOD_0}{TCOD_0} \quad (1)$$

$$VSS\ reduction = \frac{VSS_0 - VSS_t}{VSS_0} \quad (2)$$

Where, subscripts (t) and (0) refer to the treated and untreated samples, respectively.

The first-order kinetic and modified Gompertz were used, as illustrated in Eqs. (3) and (4) respectively (Jibao Liu et al., 2020a; Vu et al., 2020; Zhang et al., 2016), to evaluate methanogenesis kinetics from the BMP test experimental data:

$$V\ (t) = V_m\ (\ 1 - e^{-kt}) \quad (3)$$

$$V\ (t) = V_m\ .\exp\left\{-\exp\left[\ 1 + (\lambda\ -\ t)\ \frac{Re}{V_m}\right]\right\} \quad (4)$$

Where, V(t) is the cumulative methane production at time t (mL), V_m is the experimental ultimate methane production potential (mL), k is the kinetic methanogenesis rate constant (d^{-1}), t is the cumulative time for the production of methane (days), e is a mathematical constant (2.718282), λ is the lag phase for methane production (days), and R is the maximum production rate of methane (mL/d). Non-linear regression analyses were performed to estimate the values of the kinetic constants (k, λ, and R). Based on the measured methane production from the BMP tests, the initial estimated values were used to attain the best fit model of the data. The comparison of experimental and simulated methane production data using first-order and modified Gompertz kinetic models are provided in the Supplementary Materials (Figs. A2-A4).

Statistical analyses such as one-way analysis of variance (ANOVA) , Kruskal-Wallis Test, and Tukey Pairwise Comparisons in Minitab™ 19 were performed to determine the similarity and significant differences between the characteristics of pretreated samples in the different conditions. 95% confidence level (i.e., to be considered significant, p-values <0.05) was aimed to compare the significant differences in the values of the mean of the data sets. Additionally, using Minitab 19; the principal component analysis (PCA) and cluster analysis were implemented to emphasize and assess the potential relationships and variations between the pre-treatment conditions in the two schemes (Jolliffe, 2002; Siddiqui, 2013).

3.2.6. Techno-economic evaluation

A preliminary techno-economic evaluation was performed based on the experimental results. The heat and electricity requirement for THP was calculated from the amount of energy required to increase the sludge temperature from the initial temperature to the desired values. The energy requirement for sludge heating was calculated using Eq. (5) (Kavitha et al., 2016; Raso et al., 1999):

$$E_{heat} = \rho_{sl} V_{sl} C_p \left(T_{final} - T_{initial}\right) \quad (5)$$

where E_{heat} is the energy needed to heat the sludge (kJ), ρ_{sl} is the density of sludge (kg/m^3), V_{sl} is the volume of sludge (m^3), C_p is the specific heat of sludge (4.2 kJ/kg ℃), $T_{initial}$ is the initial temperature of sludge (℃), and T_{final} is the final temperature of sludge (℃).

The THP operating costs were calculated based on the following information: (I) initial sludge temperature of 15ºC (Dhar et al., 2012); (II) 20% heat loss with 80% heat recovery from the pretreated sludge with a heat exchanger (Dhar et al., 2012); (III) after reaching the desired temperature (e.g., 70ºC), the temperature will decrease 2ºC in every 20 min which will lead to additional energy required to raise the sludge temperature to the desired value. The electricity cost was estimated at $0.07/kWh (Barua et al., 2019). Similarly, there will be a saving in biosolids handling (dewatering, transportation, and landfill) costs since THP can reduce the suspended solids, which was appraised as $280/ton dry solids (Kumar Biswal et al., 2020). Besides, considering price of natural gas, per m^3 increase in the methane generation leads to an additional

monetary income of $0.28 (Dhar et al., 2012). The net revenue can be calculated according to Eq. 6:

Net saving compared to the control ($) = Increase in methane generation ($) + Reduction in the cost of dewatering, transportation, and landfill ($) - Pre-treatment cost ($) (6)

It should be noted that the capital investment for THP was not considered in this preliminary assessment. In general, long-term continuous and pilot-scale studies are required to acquire complete insight into the scale-up of THP schemes prior to a comprehensive techno-economic analysis. Furthermore, capital costs may vary depending on the selection of specific commercial THP technologies (e.g., Cambi^{TM}, Exelys^{TM}, etc.) (Abu-Orf and Goss, 2012). These aspects were not considered within the scope of this study.

3.3. Results and discussion

3.1. Solubilization of COD and suspended solids

Fig. 3.2 illustrates the impact of different THP conditions on COD solubilization. TCOD concentrations in the pretreated sludge remained almost constant for both schemes (Fig. 3.2a and b), indicating volatilization of organics did not occur for the tested THP conditions. As compared to the control, SCOD concentrations increased in all pretreated samples. However, COD solubilization increased marginally after further increases in pre-treatment temperature and exposure time from 50ºC, 30 min, respectively. The highest increase in SCOD solubilization (15.57 and 20.4% for scheme-1 and 2, respectively) was achieved at 90ºC, 90 min. Comparing two schemes, it can be noticed that scheme-2 provided slightly higher COD solubilization efficiencies than scheme-1, which could be due to differences in characteristics between TWAS+FPS and TWAS. The COD solubilization is attributed to the disintegration and hydrolysis of macromolecular biopolymers (proteins, lipids, and carbohydrates) to soluble monomers due to the THP (Appels et al., 2010; Xue et al., 2015). The concentrations of proteins and carbohydrates were different in TWAS+FPS and TWAS samples (Table 1), while different macromolecular compounds in sludge may respond differently under THP (Bougrier et al., 2007).

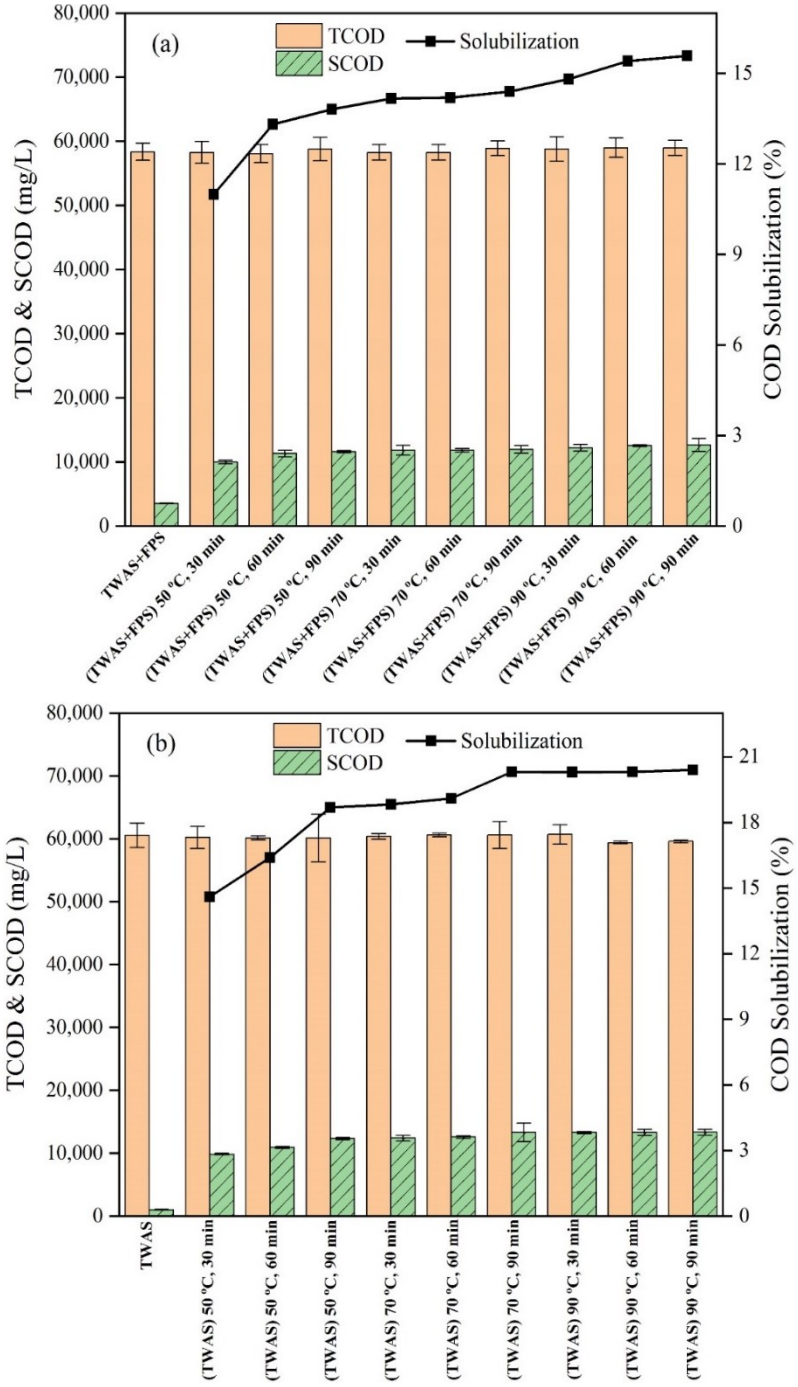

Figure 3.2. TCOD and SCOD concentrations of raw and pretreated sludge samples: (a) scheme-1 (FPS+TWAS) and (b) scheme-2 (TWAS only). Bars that do not share a letter are significantly different ($p < 0.05$).

The changes in suspended solids also showed similar trends (Fig. 3.3). The highest VSS solubilization (26.12%) for scheme-1 was achieved at 90°C, 90 min (Fig. 3.3a). The same operating condition (90ºC, 90 min) in scheme-2 provided 25.11% VSS solubilization (Fig. 3.3b). The minor inconsistencies between the COD and VSS solubilization efficiencies could probably be due to the solubilization of organics between particle sizes above 0.45 µm and lower than 1.2 µm (usually referred to as colloidal matters) (Nazari et al., 2017). The SCOD indicates organics with particle sizes less than 0.45 µm, while VSS represents organic solids with particle sizes larger than 1.2 µm [15]. To the best of authors' knowledge, this study first reports low-temperature THP for TWAS+FPS. Nonetheless, the VSS solubilization efficiencies observed in both schemes were within the range (10-38%) previously reported for low-temperature THP (50-100ºC) of TWAS (Dhar et al., 2012; Kumar Biswal et al., 2020; Nazari et al., 2017).

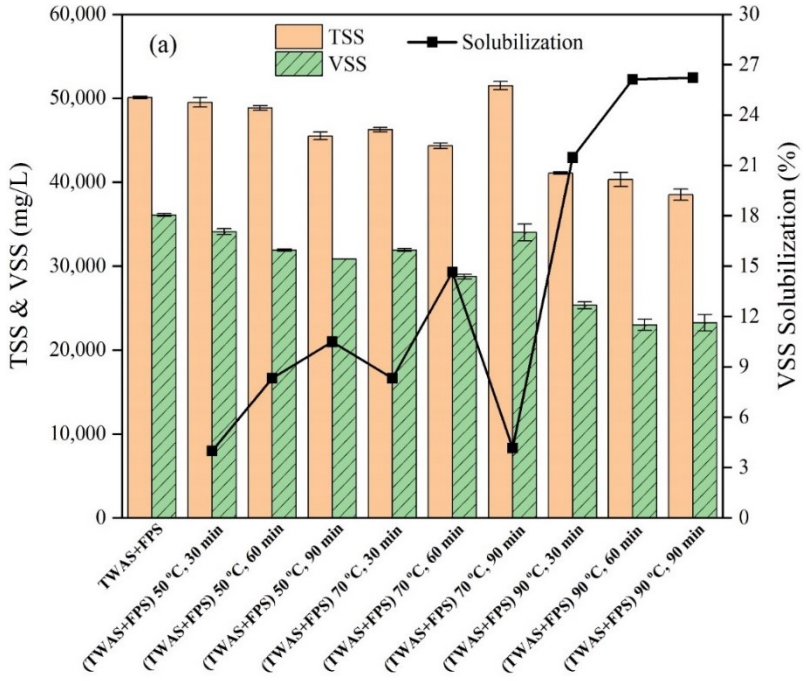

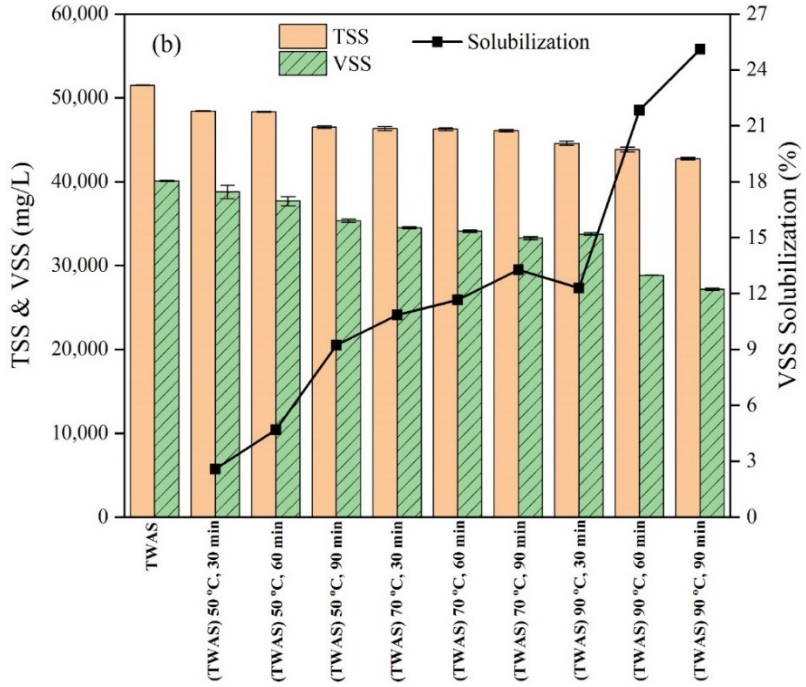

Figure 3.3. TSS and VSS concentrations of raw and pretreated sludge samples: (a) scheme-1 (FPS+TWAS) and (b) scheme-2 (TWAS only).

3.3.2. Changes in VFAs

Fig. 3.4 depicted the concentration of VFAs before and after pre-treatment. The initial VFAs concentrations in FPS (4,502 mg COD/L) was much higher than TWAS (615 mg COD/L). This could be attributed to the fermentation process that caused higher VFAs in FPS (Moretto et al., 2019). For both schemes, VFAs increased in all pretreated samples. However, for scheme-1 (TWAS+FPS), there were no considerable differences among the pretreated samples. At 50ºC, 30 min, VFAs concentration increased from 2,558 mg COD/L (TWAS+FPS) to 3,189 mg COD/L. For further increase in temperature and exposure time, increases in VFAs concentration was insignificant (p-value=0.38). For scheme-2 (TWAS only), 90ºC (60-90 min) led to a relatively higher VFAs increase (i.e., statistically not significant (p-value=0.33)) compared to other test conditions. Notably, an increase of 2.7 times (615 mg COD/L to 1,652 mg COD/L) in VFAs concentration was observed at 90ºC, 90 min. However, the maximum increase in VFAs was higher in scheme-2 (TWAS only, 615 to 1,652 mg COD/L) than scheme-1 (TWAS+FPS, 2,500 mg COD/L to 3,189 mg COD/L). The increase in VFAs is usually attributed to the breakdown of unsaturated lipids (Liao et al., 2018; Wilson and Novak, 2009). It is possible that the fermentation

of primary sludge already degraded a major portion of unsaturated lipids into VFAs, and the remaining portion in FPS was not easily degradable under low-temperature THP. As discussed later, FTIR results also corroborated with this hypothesis.

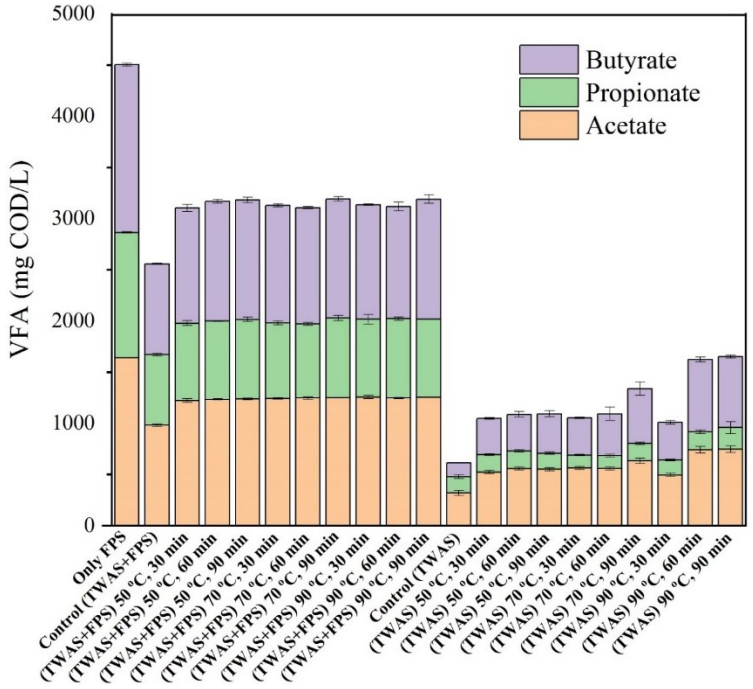

Figure 3.4. Impact of various pretreatment conditions on VFAs concentrations.

3.3.3. Solubilization of macromolecular compounds

The solubilization of macromolecular compounds was assessed with the measurement of carbohydrates and proteins (Fig. 3.5 and 3.6). Furthermore, FTIR analysis of solids was performed to evaluate the changes in functional groups of various macromolecules (Fig. 3.7). Fig. 3.5 illustrates the total and soluble carbohydrate concentrations in raw and pretreated samples from both schemes. The total carbohydrate concentration in TWAS+FPS was marginally higher than TWAS, while the soluble carbohydrate concentration was slightly higher in TWAS (Table 3.1). Comparing the raw and pretreated samples, the total carbohydrate concentrations remained almost constant for both schemes, indicating no volatilization of carbohydrates during low-temperature THP. In contrast, soluble carbohydrate concentrations considerably increased for all tested conditions, indicating solubilization of particulate carbohydrates occurred after THP (Fig. 3.5b). However, no specific trends were observed for temperatures and exposure times. For both

schemes, only a marginal but statistically insignificant (p-value=0.73 and 0.92 for scheme 1 and 2, respectively) increase in soluble carbohydrates was observed after increasing temperature from 50ºC. Also, different exposure times had minimal impact at all temperatures. Nonetheless, as compared to the control, higher increases in soluble carbohydrates were observed in scheme-2 (775.9 mg/L increase) than scheme-1 (459.8 mg/L increase).

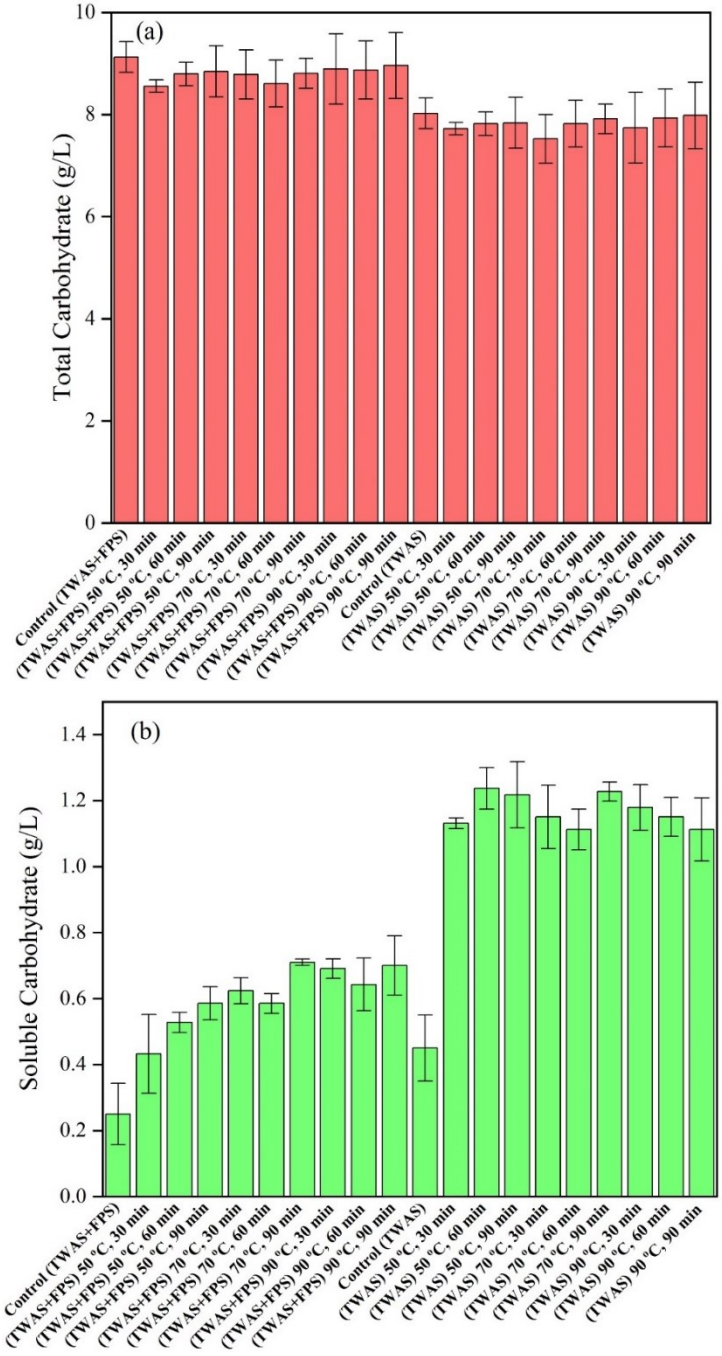

Figure 3.5. (a) Total carbohydrate, and (b) soluble carbohydrate concentrations for raw and pretreated sludge samples.

Both total and soluble protein concentrations in TWAS was higher than TWAS+FPS (see Table 3.1); the high levels of total protein was attributed to activated biomass in TWAS (Abudi et al., 2016). Analogous to carbohydrates, the total protein concentrations also remained nearly constant in raw and pretreated samples, while soluble protein concentrations increased for both schemes (Fig. 3.6b). The maximum increase in soluble protein concentrations was observed at 70ºC for both schemes. However, like soluble carbohydrates, increasing temperature from 50ºC, the further increase in soluble protein concentration was marginal. Moreover, the extent of protein solubilization was higher for scheme-2 (TWAS only, 2,913 mg/L increase) than scheme-1 (TWAS+FPS, 2,313 mg/L increase); this trend was also comparable to soluble carbohydrates. Thus, these results indicated that after fermentation of primary sludge, the remaining macromolecules (i.e., carbohydrates and proteins) in FPS would be more resistant to solubilization by low-temperature THP.

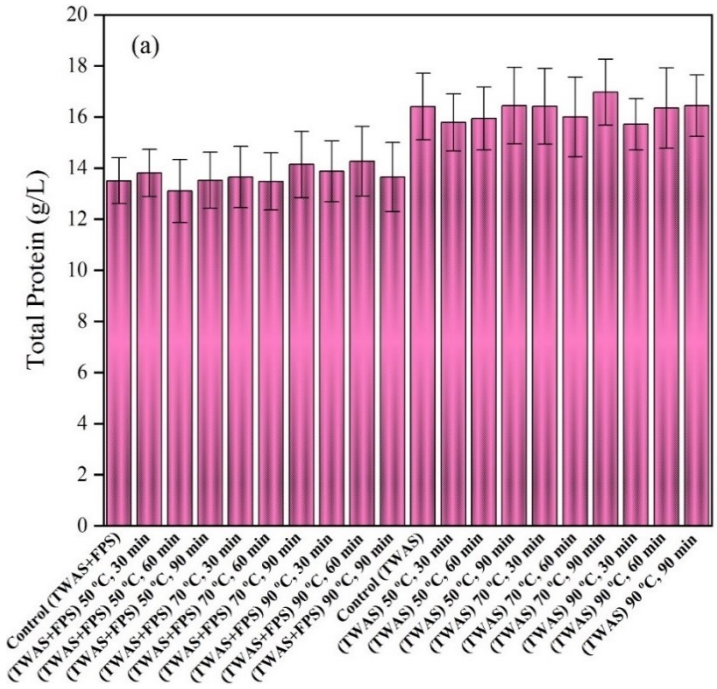

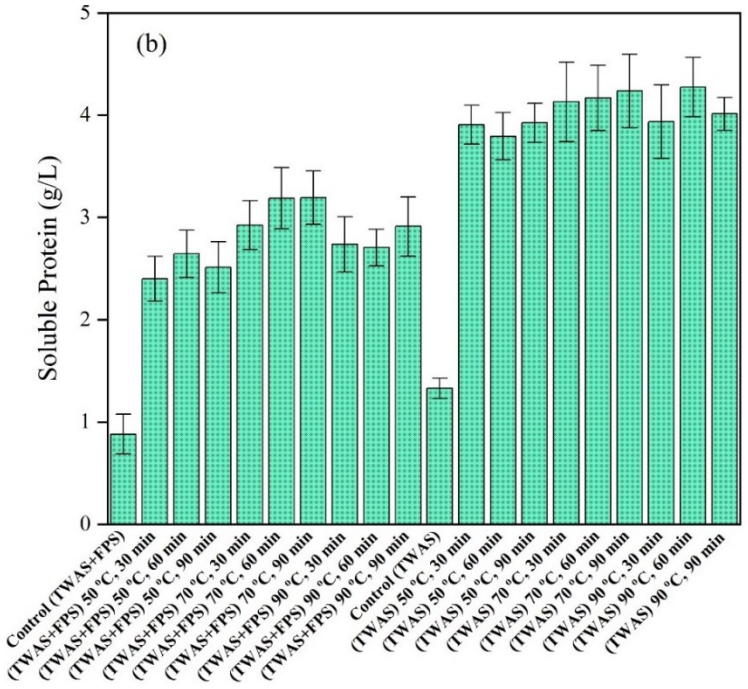

Figure 3.6. (a) Total protein, and (b) soluble protein concentrations for raw and pretreated sludge samples.

Fig. 3.7 illustrates the FTIR spectrum of solids content in raw and untreated samples. For both schemes, the most intense absorbance peaks were observed for the control samples (i.e., TWAS +FPS and TWAS for scheme-1 and scheme-2, respectively). Peaks at different wavelengths could be related to different macromolecules present in the sludge (Böcker et al., 2017; Jones et al., 1952). Thus, the changes in the intensities of the peaks could indicate changes in functional groups and solubilization of particulate macromolecules. The absorption peak around 865-1,200 cm^{-1} is assigned to C-O stretching of polysaccharides and the Si-O of silicate (Senesi et al., 2003; Zhao et al., 2013). The peak between 1,000-1,100 cm^{-1} demonstrates the vibration in carbohydrates, polysaccharides, and aromatic ethers (Chowdhury et al., 2019). The absorption peaks in the 1,650-1,700 cm^{-1} region correspond to the proteins, esters carbonyl, etc. (Réveillé et al., 2003). Moreover, the intense peak between the 2,800-3,000 cm^{-1} region and the shoulder around 1,455 cm^{-1} are ascribed to the aliphatic C-H stretching and bending. Thus, these peaks are related to fats and lipids degradation (Grube et al., 2006). The intense peak between 3,300-3,500 cm^{-1} is associated with O-H vibration of carboxylic and alcoholic groups (Chowdhury et al., 2019). As compared to the control, the intensity of these absorption peaks decreased for solids samples from both THP schemes, indicating solubilization of particulate macromolecular compounds

(proteins, carbohydrates, and lipids) occurred due to low-temperature THP. However, the FTIR spectrum mostly overlapped for all pretreated samples in both schemes, indicating the same level of solubilization of these macromolecular compounds. Still, there is a difference in absorption peaks between the control and all pretreated samples. Although these results suggest that 50ºC, 30 min was optimum for macromolecular compounds solubilization, the biodegradability of the solubilized organics may vary widely depending on the THP operating conditions that can ultimately influence the digester performance (Lu et al., 2018). Nonetheless, FTIR analysis results are in good agreement with the quantitative measurements of protein and carbohydrate concentrations, as indicated by marginal changes in their concentrations after increasing THP temperature from 50ºC, 30 min. Moreover, the reduction in lipids and fats indicated in FTIR was also corroborated with the increase in VFAs. As illustrated in Fig. 3.4, increases in VFAs were also marginal for further increase in temperature from 50ºC, which was also in agreement with overlapped FTIR spectrum for pretreated samples.

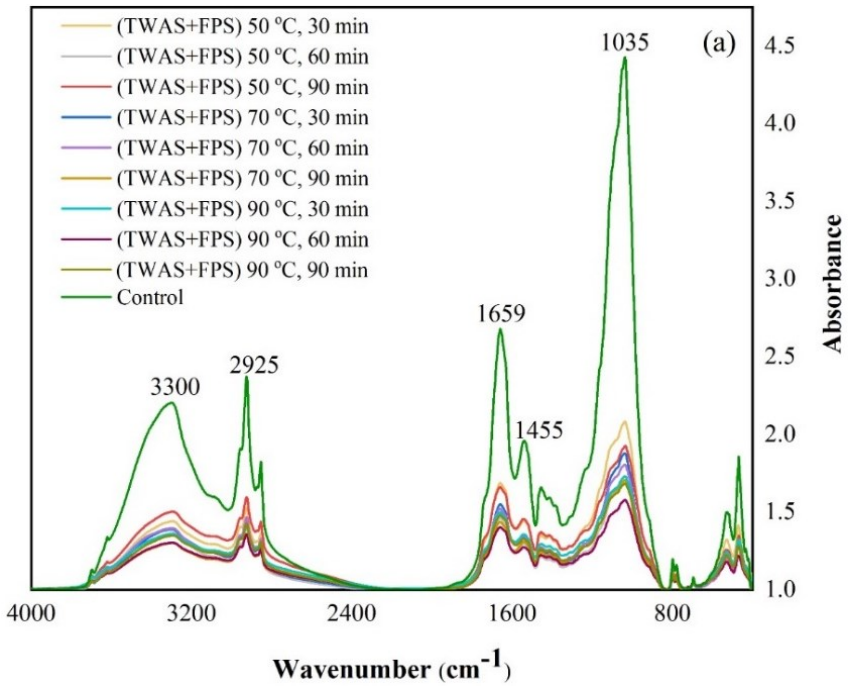

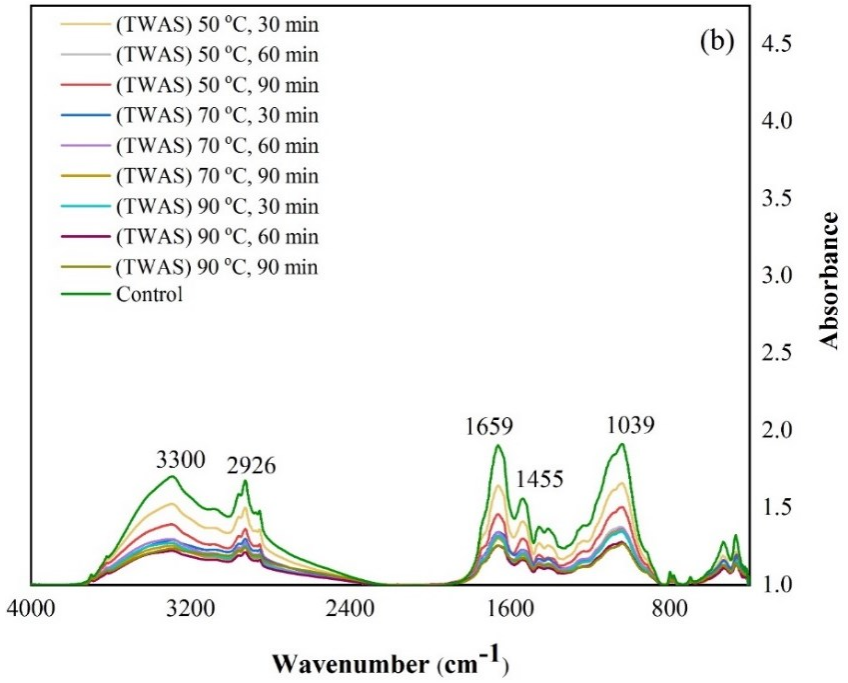

Figure 3.7. FTIR spectrum of raw and pretreated sludge samples for (a) scheme-1 (FPS+TWAS), and (b) scheme-2 (TWAS only).

The PCA was performed to further elucidate the relative influence of two THP schemes on macromolecular compounds solubilization (Fig. 3.8). Scheme-1 (TWAS+FPS) samples were clustered together in the top quadrants. In contrast, scheme-2 (TWAS) samples were mostly grouped in the left-bottom quadrant. Compared to control (untreated), carbohydrates, lipids, and proteins in THP samples were considerably varied. The variations in the PC1 direction contributed to 96.2% of the total variations, and this attribute to the broad separation of THP samples from the control in this direction. For scheme-2, the characteristic peaks associated with proteins, lipids, and carbohydrates were greatly reduced and directed to the opposite direction as compared to untreated TWAS (Fig. 3.8). Nonetheless, scheme-1 samples exhibited a better association with carbohydrates loading vector where the carbohydrates peaks were positively shifted towards the top quadrant. As stated earlier, the PCA also emphasized a minor increase in solubilization of macromolecular compounds after increasing temperatures and exposure times from 50°C, 30 min in both schemes. This matches the positive scores of those conditions on PC1 and their relative positions in the same part with control.

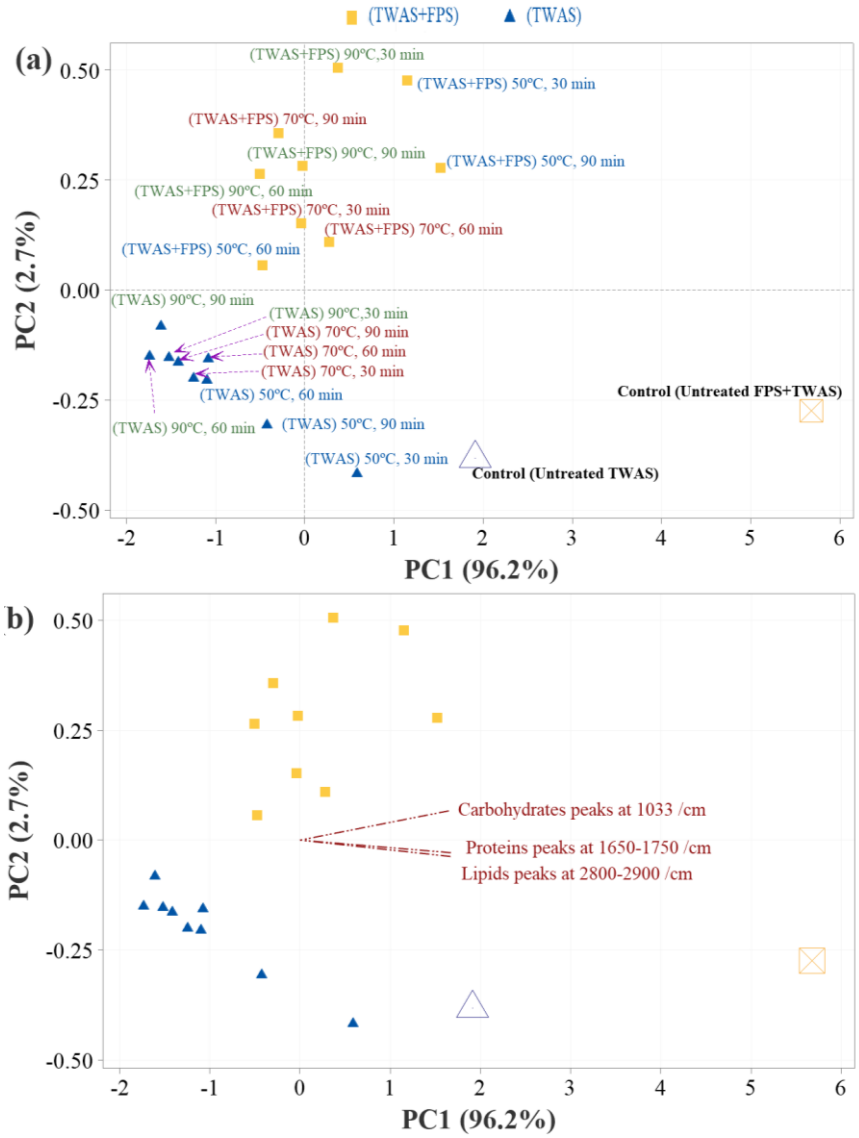

Figure 3.8. (a) Score plot for PCA analysis of all pretreated samples, PC 1 (96.2%) and PC 2 (2.7%), (b) Biplot and loading plot of PC1 and PC2 with project lines of all pretreated samples where sample loadings are represented as vectors radiating from the origin. Sample scores are indicated by symbols (according to each scheme), samples that are chemically similar will plot near to each other (clustered together), samples are color-coded by substrate source.

To grasp a better understanding, the PCA analysis was re-examined to evaluate the relative influence of two THP schemes on macromolecular compounds, COD, and VSS solubilization (results not shown). The respective contribution to the total variance in PCA analysis of all pretreated samples was manifested by variation percentages of 63.8 (PC 1 axis) and 26.9 (PC 2

axis). Although the VSS solubilization was positively correlated and associated with TWAS+FPS, TWAS samples attained another key solubilization difference. For the analysis of COD and carbohydrates solubilization, the PCA results revealed high efficiency of scheme-2 compared to scheme-1 (i.e., as noticed from low peaks in FTIR analysis; see Fig. A2b). Notably, TWAS samples were intensified in the direction vectors of COD, carbohydrates, and protein solubilization, demonstrating the outperformance of scheme-2 in solubilization of COD and macromolecular compounds. In the same sense and with respect to COD solubilization, the PCA verified a positive association among proteins, carbohydrates, and COD solubilization. The cluster analysis similarly emphasized two main clusters of data at a similarity level of 86.29 in which cluster 1 encompassed proteins, carbohydrates, and COD solubilization and cluster 2 included the VSS solubilization only. The results indicated that solubilization metrics based on carbohydrates, proteins, VSS, and COD are favorable for PCA assessment to categorize THP conditions based on their relative solubilization performances. Also, the relative differences demonstrated by PCA are evidence for future investigations of the efficiency of low-temperature THP conditions concerning the types of sludge and solubilization of macromolecular compounds.

3.3.4. Ammonia nitrogen solubilization

Ammonia nitrogen in sludge can play a significant role in maintaining AD process stability by providing buffering capacity (Chowdhury et al., 2019). However, high ammonia levels can hinder methanogenic activity and lead to process inhibition (Rajagopal et al., 2013). Depending on the feedstocks and digester operating conditions, free ammonia nitrogen (FAN) concentration 215-1,450 mg/L can inhibit methanogenic communities under mesophilic conditions (Yenigün and Demirel, 2013). Several studies raised concerns about high ammonia nitrogen in thermally pretreated sludge (Nazari et al., 2017; Rajagopal et al., 2013; Wilson and Novak, 2009; Zhou et al., 2021). The hydrolysis of nitrogenous compounds (e.g., proteins, amino acids, urea, etc.) during THP can increase ammonia levels (Bougrier et al., 2008). Given these facts, TAN concentrations in raw and predated sludge samples were analyzed (see Fig. 3.9). TAN concentrations in the pretreated samples (163.1-272.3 mg/L) for scheme-1 (TWAS+FPS) was nearly 4.5-7.6 times higher than control (35.68 mg/L). Also, for scheme-2 (TWAS only), THP caused a significant enhancement (7.43-9.92 times, p-value=0.001) in TAN concentrations compared to the control (i.e., raw TWAS). However, for scheme-1, it appeared that the increases in TAN levels at 90ºC

were considerably lower than 50ºC and 70ºC, which could be attributed to the ammonia volatilization at higher temperatures (Eskicioglu et al., 2008; Kumar Biswal et al., 2020). For scheme-2, TAN concentrations increased with increased exposure times at 70ºC and 90ºC. The maximum TAN concentration was attained at 90ºC and 90 min. However, ammonia volatilization might also occur in scheme-2. For instance, TAN concentration at 70ºC (30 min) was considerably lower than that observed at 50ºC (30 min). In all pretreated samples, TAN concentrations remained <400 mg/L, indicating FAN concentrations would be much lower than the inhibitory level reported in the literature. Comparing the two schemes, the increase in TAN levels in scheme-2 was higher than scheme-1, which showed a good agreement with protein solubilization. However, non-linearity between TAN and soluble proteins can be credited to ammonia volatilization.

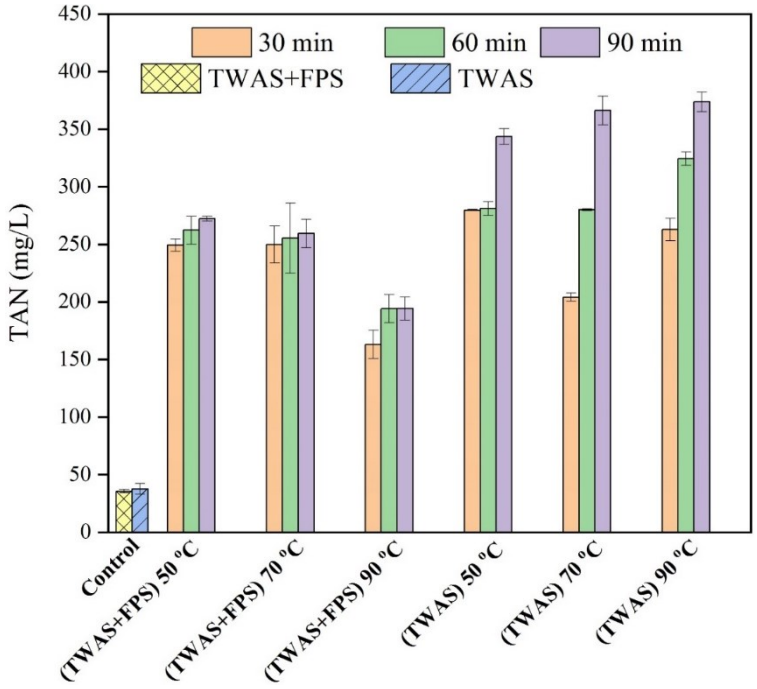

Figure 3.9. Effect of various pretreatment conditions on TAN concentrations.

3.3.5. Biomethane yield and process kinetics

Fig. 3.10 shows the cumulative methane production profiles. Noteworthy, methane generation initiated instantly on the first day of the BMP test without any noticeable lag phases. Overall, the application of THP considerably enhanced the biomethane generation compared to control. For instance, the control generated a considerably lower methane yield (93 mL CH_4/g COD) than the pretreated samples from scheme-1 (Fig. 3.10a). For this scheme, the maximum methane yield

(145.33 mL CH_4/g COD; 56.28% increase over the control), was achieved at 90ºC, 90 min. The total cumulative methane yields increased with increasing temperature. However, at each temperature, increasing exposure time had a minor effect in enhancing methane yields. In scheme-2, the enhancements in biomethane yields compared to the control varied between 6.06-43.4%. The maximum biomethane yield (133.4 mL CH_4/g COD) for this scheme was achieved at 90ºC, 60 min. In most cases, the effects of temperatures and exposure times showed similar patterns like scheme-1. To the best of the authors' knowledge, this study first reports the low-temperature THP (<100ºC) on co-digestion of FPS and TWAS, while most of the previous studies focused on low-temperature THP on TWAS (Dhar et al., 2012; Kumar Biswal et al., 2020; Nazari et al., 2017). These studies reported up to a 30% increase in methane yield for low-temperature THP of TWAS. In this study, increases in methane yields reached up to 56.28%, which could be attributed to the synergistic effects of co-digestion (Villamil et al., 2020, 2019). Particularly, FPS contained considerably higher levels of VFAs. Also, despite higher solubilization efficiencies in scheme-2, scheme-1 was more efficient for enhancing methane yields which could be correlated with VSS reduction rather than COD and macromolecular compounds solubilization. A previous study on high-temperature THP (140-180ºC) by Zhou et al. also reported that THP of TWAS + FPS could provide higher methane yields than THP of TWAS alone (Zhou et al., 2021).

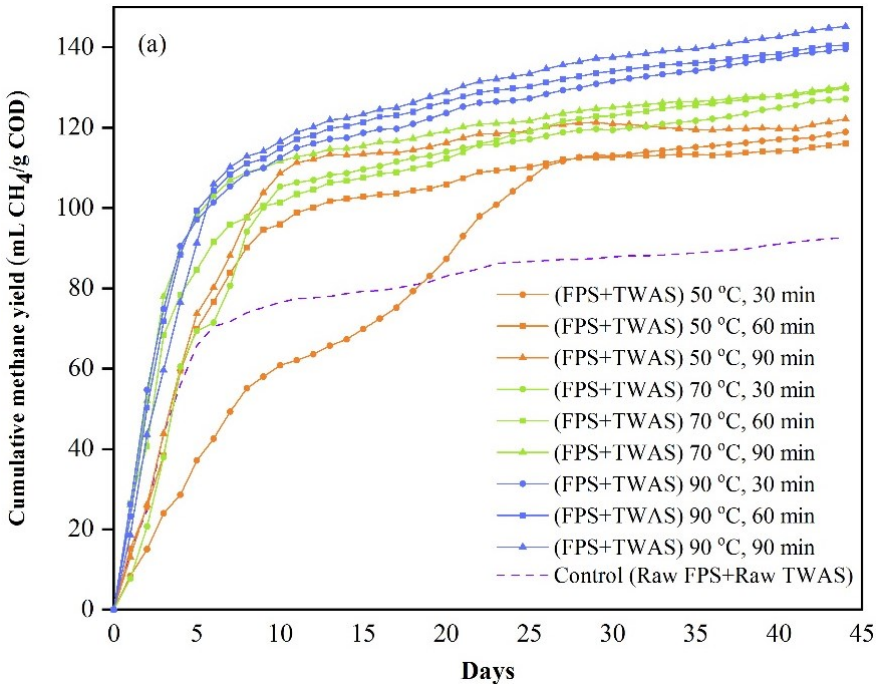

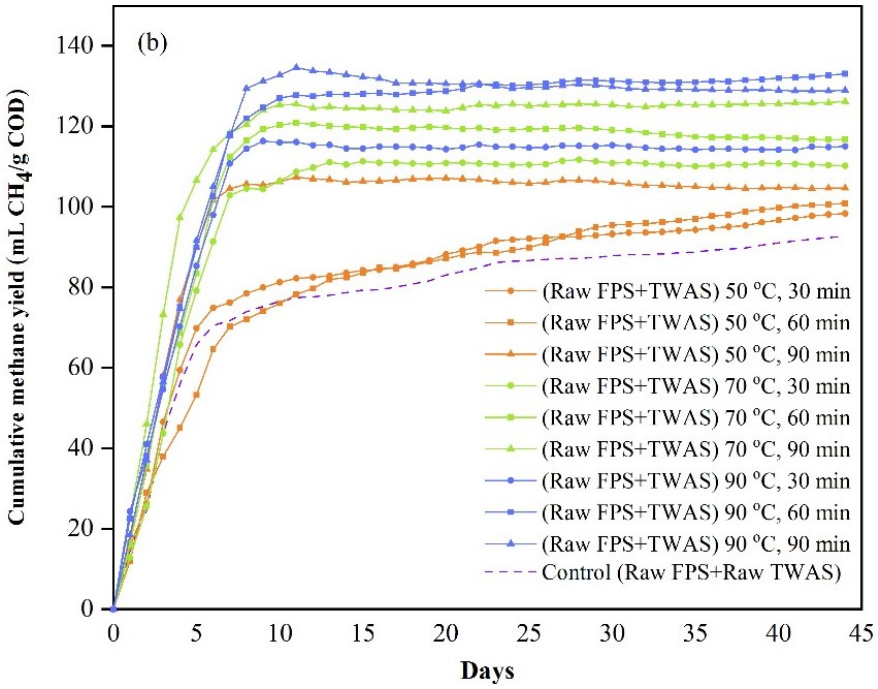

Figure 3.10. The time-course profile of cumulative methane yields for (a) scheme-1 (pretreated FPS + TWAS), and (b) scheme-2 (untreated FPS + pretreated TWAS).

To assess methanogenesis kinetics, the first-order kinetic model was used to estimate the methanogenesis rate constant (k) and maximum methane production (V_m) (Table 3.2). For both schemes, the highest V_m values were estimated at 90ºC for 60-90 min exposure times (1,689-1,782 mL). Moreover, the differences between estimated V_m and experimentally measured total cumulative methane production were ≤10%. Nonetheless, most of the pre-treatment conditions in scheme-1 showed quite comparable or slightly lower k values than the control. Moreover, no specific trends were observed withing increasing temperatures and exposure times. For instance, the maximum k value was achieved at 70ºC, 90 min (0.28 d^{-1}), which was higher than the control (0.22 d^{-1}). In contrast, some THP conditions showed k values lower than the control (50ºC, 30-90 min: 0.06-0.18 d^{-1}; 70ºC, 30-60 min: 0.16-0.21 d^{-1} and 90ºC, 90 min: 0.19 d^{-1}). Unlike scheme-1, k values estimated for scheme-2 were higher than the control in most cases. Thus, it was apparent that higher methane yields observed for pre-treatment conditions than the control could be attributed to superior maximum methanogenesis rates (R) and/or reduced lag phases (λ). Therefore, the BMP test results were further analyzed with a modified Gompertz kinetic model.

Similar to the first-order model, the differences between the estimated V_m with the modified Gompertz model and experimental total cumulative methane production were very marginal (see Table 3.2). In scheme-1, most pretreated TWAS+FPS samples showed negative λ, suggesting methane production commenced without any substantial lag phases. However, R values (151-217 mL/d) were considerably higher than the control (135 mL/d) for this scheme. Thus, reduced lag phases and higher maximum methane production rates contributed to the higher methane yields in scheme-1. With respect to the scheme-2 (TWAS), except for 50ºC, 60 min, R values were higher than the control (144-356 mL/d vs. 135 mL/d). Interestingly, λ values for this scheme were slightly higher than the values estimated for the control and scheme-1. Notably, samples from scheme-2 at 50 and 90ºC (90 min) and 70ºC (30-60 min) showed more extended lag phases, indicating that these conditions require a longer time than the control to achieve the maximum methane production rates. This finding indicates that methanogens might slowly adopt some of the solubilized organics (inhibitory compounds) released during the THP of TWAS alone, which led to differences in kinetic features observed under two schemes. As suggested in the literature, the acclimatization of microbial communities to potential inhibitory compounds over the long-term continuous operation of digesters can reduce lag phases (Jiang et al., 2019; Silva et al., 2014) and may not pose significant operational concerns, except for more extended digester start-up times.

PCA was investigated again to assess variations and differences in THP samples based on various process parameters (e.g., time, temperature, COD solubilization, VSS solubilization, methane yield, VFA increase, solubilization of carbohydrates and proteins). The score, biplot, and loading plots established for all pretreated samples in scheme-1 (TWAS+ FPS) and scheme-2 (TWAS) are provided in the Supplementary Materials (Fig. A5). All pretreated samples were noticeably separated in PC1 (55.6%) and PC2 (31%). The loading vectors of the six parameters emphasize distinctive differences in the samples.

Table 3.2. Kinetic parameters estimated with the first-order and modified Gompertz model.

Experimental conditions	First Order Model				Modified Gompertz Model						Experimental	Differences	
	Methanogenesis rate constant k (d^{-1})	Standard error of k	Estimated Maximum methane production V_m (mL)	Standard error of V_m	Maximum methane production V_m (mL)	Standard error of V_m	Maximum Methane Production Rate, R (mL/d)	Standard error for R	Lag phase, λ (d)	Standard error for λ	Measured maximum methane production Vm (mL)	First Order Model	Modified Gompertz Model
(TWAS+FPS) 50ºC, 30 min	0.06	0.0026	1680	30.60	1580	24.64	57	2.49	-2.5	0.6	1527	-10%	-4%
(TWAS+FPS) 50ºC, 60 min	0.18	0.0048	1446	7.63	1424	8.45	151	7.71	-0.53	0.27	1490	3%	4%
(TWAS+FPS) 50ºC, 90 min	0.18	0.0052	1548	8.28	1525	4.94	184	5.31	0.04	0.13	1572	1%	3%
(TWAS+FPS) 70ºC, 30 min	0.16	0.0055	1569	11.70	1534	11.12	159	9.30	-0.08	0.31	1630	4%	6%
(TWAS+FPS) 70ºC, 60 min	0.21	0.0109	1559	14.83	1579	17.54	105	9.81	-4.42	0.89	1668	7%	5%
(TWAS+FPS) 70ºC, 90 min	0.28	0.0118	1581	9.80	1574	11.44	217	18.75	-1.13	0.38	1674	6%	6%
(TWAS+FPS) 90ºC, 30 min	0.24	0.0121	1670	13.96	1679	16.34	143	13.76	-3.12	0.71	1791	7%	6%
(TWAS+FPS) 90ºC, 60 min	0.23	0.0098	1702	12.18	1698	14.74	172	14.96	-1.94	0.52	1800	5%	6%
(TWAS+FPS) 90ºC, 90 min	0.19	0.0074	1782	12.65	1765	15.29	177	13.86	-1.33	0.46	1880	5%	6%
TWAS (50ºC, 30 min) + FPS	0.22	0.0099	1190	9.10	1177	10.33	144	12.80	-0.87	0.42	1262	6%	7%
TWAS (50ºC, 60 min) + FPS	0.14	0.0050	1137	9.11	1126	11.44	76	5.24	-2.34	0.58	1193	5%	6%
TWAS (50ºC, 90 min) + FPS	0.32	0.0163	1366	9.76	1356	2.92	319	8.82	0.56	0.06	1339	-2%	-1%
TWAS (70ºC, 30 min) + FPS	0.24	0.0118	1433	11.46	1417	2.31	263	4.71	0.76	0.05	1409	-2%	-1%
TWAS (70ºC, 60 min) + FPS	0.26	0.0137	1535	12.29	1524	5.18	282	10.76	0.51	0.11	1493	-3%	-2%
TWAS (70ºC, 90 min) + FPS	0.32	0.0118	1613	8.13	1601	1.95	356	5.62	0.28	0.04	1620	0%	1%
TWAS (90ºC, 30 min) + FPS	0.28	0.0124	1484	9.93	1475	4.89	261	9.90	0.17	0.12	1473	-1%	0%
TWAS (90ºC, 60 min) + FPS	0.24	0.0080	1689	9.13	1674	3.94	257	6.37	0.05	0.09	1707	1%	2%
TWAS (90ºC, 90 min) + FPS	0.26	0.0137	1685	14.23	1672	6.03	299	11.82	0.54	0.12	1651	-2%	-1%
Control (TWAS+FPS)	0.22	0.0099	1120	8.56	1108	9.72	135	12.05	-0.87	0.42	1188	6%	7%

The differences in THP schemes and test conditions were assessed using cluster observation analysis (Fig. A6). The analysis divided the data into 6 main clusters at a similarity level of 71.93. For example, clusters 3 and 6 encompassed TWAS+FPS samples at 90ºC (30-90 min) and TWAS samples at 70ºC (90 min) and 90ºC (60-90 min), respectively. Notably, the PCA showed such positive correlations and clustering (Fig. A5). The highest contribution of methane production with scheme-1 at 70 and 90ºC can be clearly distinguished with the clustering of the samples closely in the bottom-left of the graph. Furthermore, solubilization of COD and carbohydrates, VFAs increase have a positive relationship with TWAS samples, particularly at (70 and 90ºC) since their position was in the same quadrant (positive score of PC1). Overall, more effectiveness of THP in terms of high levels of solubilization efficacy (COD, VFAs, carbohydrates, and proteins solubilization) for TWAS compared to TWAS+FPS can be confirmed. On examining the relationships between pre-treatment time and temperature, it can be remarked that the minimal impact at low temperature (50ºC) on enhancing most of these parameters. However, the enhancement in most of the factors (e.g., solubilization of COD, carbohydrates and proteins, VFAs, and methane yields) were positively correlated with increasing temperature and time, particularly at 70 and 90ºC and pre-treatment time 60-90 min. The results suggested that temperature had more impact on sludge solubilization than exposure times, and notably, 90ºC was the most effective. The increase in the variations of PC2 can be attributed to the orientation of the methane production (i.e., loading vector of methane production was positioned towards 90 °C; high methane producing conditions in scheme 1) in the direction of PC2 axis. Such high association of methane yields in both axis confirms earlier observations in which the three maximum methane yield values for conditions of TWAS samples were observed at 90ºC (60 and 90 min) and 70ºC (60 min). Thus, higher temperatures (70 and 90ºC) and longer exposure times (60-90 min) enhanced solubilization of organics and methane production in both schemes. In contrast, low temperature in scheme-1 could still favor methane yield. With respect to sludge nature, mixing fermented primary sludge, changes of the temperature and exposure time and favoring solubilization enhancement, the distinctions between THP alternatives were supported and demonstrated by PCA observations. Such performance patterns can be further deployed in the assessment and foreseeing the effectiveness of THPs in full scale WWTPs.

Overall, the results demonstrated that low-temperature THP under scheme-1 (TWAS+FPS) was more effective in enhancing methane yield despite scheme-2 (TWAS only) seem to be quite effective in the solubilization of COD and macromolecular compounds. So far, a previous study by Zhou et al. has investigated similar process schemes for high-temperature THP (140-180ºC) for a WWTP with primary sludge fermentation (Zhou et al., 2021). Their results also suggested similar trends of more effectiveness of co-treatment of TWAS and FPS in enhancing methane yield. Based on the extensive literature search, no studies could be found on low-temperature THP for co-digestion of TWAS and FPS. Interestingly, compared to scheme-1, scheme-2 in this study was more effective in proteins and carbohydrates solubilization. The surface hydrophobicity of sludge is usually associated with proteins (Liao et al., 2001). Various refractory hydrophobic dissolved organics and humic substances can be released during protein solubilization by THP (Lu et al., 2018). Thus, it can be hypothesized that higher solubilization of proteins during scheme-2 (TWAS only) might release more hydrophobic recalcitrant compounds, which warrants further investigation. Nonetheless, it was evident that solubilization efficiencies of macromolecular compounds are inadequate to distinguish their biodegradability. Therefore, detailed profiling of dissolved organic matters released by THP and their degradability during AD should be further investigated.

3.3.6. Energy and economic evaluation

Although THP has been implemented in the full-scale (mostly at high-temperature regimes), there is limited information available on the economic feasibility of low-temperature THP for WWTPs with primary sludge fermentation. Therefore, the preliminary cost estimate of low-temperature THP operation was performed based on a ton of solids (TSS basis). Compared to conventional AD without THP, the economic viability was assessed based on energy demand in THP operation, the increment in methane production, and the decrease in solids handling cost (Dhar et al., 2012; Kumar Biswal et al., 2020). As summarized in Table 3.3, most of the THP conditions in both schemes (except for 70ºC, 90 min in scheme-1) led to a net saving of $6.94-79.55/ dry metric ton solids. Among all conditions, THP at 90ºC, 90 min in scheme-1, was the most economically feasible. The same THP condition (90ºC, 90 min) also led to the highest net saving ($44.93) in scheme-2. A previous study by Dhar et al. reported that increasing temperature in low-temperature THP of TWAS (50, 70, 90ºC at 30 min exposure time) linearly decreased net

saving from $78 to $45 per ton of dry solids (Dhar et al., 2012). The results of this study suggest that THP at 90ºC will be economically more viable for AD facilities in WWTPs integrated with primary sludge fermentation. Moreover, increasing exposure times at 90ºC can further increase the economic effectiveness. We note that these economic assessments were based on batch BMP tests. Comprehensive techno-economic and environmental assessment (including capital costs, carbon credits, etc.) based on long-term continuous anaerobic digestion studies, particularly at different solid residence times, is required to acquire complete insight into the feasibility of different schemes.

Table 3.3. Economic assessment for different pretreatment processes compared to the control.

Set of pre-treatments		Pre-treatment cost ($/tonne dry solids)	Increase in methane production ($/tonne dry solids)	Dewatering, transportation, and landfill cost ($/tonne dry solids)	Net saving ($/tonne dry solids)
Scheme-1	(TWAS+FPS) 50°C, 30 min	11.93	15.56	3.31	6.94
	(TWAS+FPS) 50°C, 60 min	12.92	14.04	7.10	8.22
	(TWAS+FPS) 50°C, 90 min	13.92	19.17	26.03	31.29
	(TWAS+FPS) 70°C, 30 min	18.55	21.72	21.77	24.93
	(TWAS+FPS) 70°C, 60 min	19.55	24.61	32.66	37.71
	(TWAS+FPS) 70°C, 90 min	20.54	21.47	-8.05	-7.12
	(TWAS+FPS) 90°C, 30 min	25.18	33.40	51.12	59.33
	(TWAS+FPS) 90°C, 60 min	26.18	34.51	55.38	63.72
	(TWAS+FPS) 90°C, 90 min	27.17	40.93	65.79	79.55
Scheme-2	TWAS (50°C, 30 min)	11.60	3.45	17.03	8.88
	TWAS (50°C, 60 min)	12.57	4.90	17.49	9.82
	TWAS (50°C, 90 min)	13.53	7.19	27.62	21.28
	TWAS (70°C, 30 min)	18.04	10.56	28.54	21.05
	TWAS (70°C, 60 min)	19.01	14.59	29.00	24.58
	TWAS (70°C, 90 min)	19.98	20.72	29.92	30.66
	TWAS (90°C, 30 min)	24.49	13.88	38.21	27.60
	TWAS (90°C, 60 min)	25.46	25.51	40.35	42.40
	TWAS (90°C, 90 min)	26.42	23.02	48.33	44.93

3.4. Conclusions

In this study, two different low-temperature THP schemes were investigated for enhancing methane yields from co-digestion of TWAS and FPS. Although scheme-2 (THP of TWAS alone) was more effective in the solubilization of macromolecular compounds, VSS reduction was substantially more profound in scheme-1 (THP of TWAS+FPS). THP at 90ºC showed a more significant enhancement in methane production for both schemes, as evidenced by 56.28% (scheme-1) and 43.4% (scheme-2) higher methane yields over control. Nonetheless, methane yields were correlated with VSS reduction rather than COD and macromolecular compounds solubilization. Thus, despite higher macromolecular compounds solubilization in scheme-2, scheme-1 was more efficient for enhancing methane yields. A preliminary economic assessment showed that low-temperature THP would be economically feasible except for one condition (scheme-1 at 70ºC, 90 min). The highest net saving ($79.55/ton dry solids) in operating cost was estimated for scheme-1 at 90ºC, 90 min. As implementing THP is considered a promising option for the AD facility's process intensification, these findings will guide WWTPs with primary sludge fermentation.

Chapter 4

Thermal hydrolysis of sludge counteracts polystyrene nanoplastics-induced stress during anaerobic digestion

A version of this chapter was published in ACS ES &T Engineering, vol. 7, 1306-1315.

4.1. Introduction

Plastics play an indispensable role in our daily life, while their extensive production, utilization, and uncontrolled disposal have led to significant environmental concerns (Cole et al., 2011). In 2018, around 320 million tons of plastic were produced globally (Wei et al., 2019b), and it has been estimated that the world plastic waste generation may reach about 12 billion metric tons by 2050 (Cox et al., 2019). Discarded plastics contribute to the formation of microplastics (MPs), with particle sizes from 1 μm to 5 mm, via multiple natural fragmentation processes, such as mechanical wear, weathering, ultraviolet radiation, and microbial degradation (C. Wang et al., 2021; Wei et al., 2020). MPs can further break down into smaller fragments (1 to 1000 nm), called nanoplastics (NPs) (Al-Sid-Cheikh et al., 2018). Moreover, intentionally manufactured NPs for specific applications, such as facial cleansers and cosmetics, electronics, paints, etc., intensify the discharge of NPs to the environment (Lehner et al., 2019; M. Hernandez et al., 2017). Due to high stability, mobility, and surface area, NPs demonstrated a greater potential to adsorb and desorb dissolved metals, persistent chemical and biological pollutants (Fu et al., 2018). Also, because of their small size, NPs are bioavailable even for small aquatic invertebrates and other biotas (fish, shrimps, etc.), which can have a detrimental effect on biotas and facilitate the transfer of toxins to humans through food webs (Tourinho et al., 2010). Monitoring efforts indicated that MPs/NPs are already present in freshwaters (J. Sun et al., 2019), oceans (Cole et al., 2011), air (Chen et al., 2020), and soils (Guo et al., 2020). The negative effect of MPs/NPs pollution has been reported for humans and more than 600 aquatic organisms (O'Connor et al., 2016).

The wastewater treatment plants (WWTPs) have been considered as major routes for MPs/NPs discharge to the aquatic and terrestrial environment (Mohammad Mirsoleimani Azizi et al., 2021b). MPs/NPs in wastewater mainly include microbeads from personal care products, fibers

from synthetic clothing and fabrics during laundry washing, and so on (Galafassi et al., 2019). Reportedly, ~30 types of MPs/NPs have been detected in domestic sewage, with a concentration in the range of 2.6×10^5 to 3.2×10^5 particles/m^3 (Mohammad Mirsoleimani Azizi et al., 2021b). WWTPs can remove up to 99% of MPs/NPs from liquid treatment trains, mainly retaining them in the sewage sludge (Anne Marie Mahon et al., 2017; Mohammad Mirsoleimani Azizi et al., 2021b). MPs/NPs concentrations in the sewage sludge range from 1.5×10^3 to 2.4×10^4 MPs/kg dry solids (Mohammad Mirsoleimani Azizi et al., 2021b), while they present in different forms such as spheres, microbeads, films, fragments, and fibers (Anne Marie Mahon et al., 2017). Polystyrene (PS), polyvinyl chloride (PVC), polypropylene (PP), polyethylene terephthalate (PET), and polyethylene (PE) are the most common MPs/NPs found in sewage sludge (Wei et al., 2019b).

Anaerobic digestion (AD) is a widely applied sludge stabilization method that produces methane-rich biogas (Dastyar et al., 2021a, 2021b). Based on the abovementioned context, understanding the impact of MPs/NPs on the AD process has recently attracted substantial attention (Mohammad Mirsoleimani Azizi et al., 2021b). Previous studies evidently demonstrated that most MPs/NPs could inhibit methane production via several mechanisms, including leaching of toxic additives, inducing reactive oxygen species (ROS), restraining activities of key enzymes (Fu et al., 2018). Moreover, NPs, like polystyrene nanoplastics (PsNPs), could directly damage cells via penetration (Mohammad Mirsoleimani Azizi et al., 2021b). Despite many WWTPs adopting sludge pretreatment processes prior to AD (Mohammad Mirsoleimani Azizi et al., 2021a), existing literature provides almost no information on the effects of MPs/NPs in AD with sludge pretreatment. For instance, the thermal hydrolysis process (THP) is a widely implemented method for sludge pretreatment in full-scale AD facilities (Mohammad Mirsoleimani Azizi et al., 2021a). Enhanced biogas recovery by improving hydrolysis, high solids removal, pathogen removal, and enhanced dewaterability of biosolids are the key benefits of THP (Jeong et al., 2019). Furthermore, heat recovery from thermally hydrolyzed sludge provides an excellent opportunity for minimizing the operating cost (Mohammad Mirsoleimani Azizi et al., 2021a). However, based on an extensive literature search, no reports could be found on how THP can influence MPs/NPs-induced stress during AD.

Moreover, previous studies provide limited information on secondary risks of MPs/NPs in AD. For instance, MPs/NPs can act as carriers for other contaminants, including heavy metals, persistent chemicals, antibiotics, and, most importantly, antibiotic resistance genes (ARGs) (Dai et al., 2020a). Antibiotic resistance is one of the most alarming global health challenges. It has been reported that MPs/NPs can stimulate the propagation of ARGs in different environmental media (Pereira de Albuquerque et al., 2021). Although published reports related to ARG in AD exposed to MPs/NPs have still been limited (Zhang et al., 2021), it can be postulated that MPs/NPs can potentially increase risks of ARGs transmission via land application of digestate. THP prior to AD can decrease ARG propagation during AD (C. Sun et al., 2019). However, it is still unknown whether THP could minimize ARGs propagation enhanced by MPs/NPs exposure.

Given these research gaps, for the first time, this study systematically investigated how THP impacts AD of sewage sludge exposed to PsNPs. Specifically, we compared sludge exposed to PsNPs alone (50, 100, and 150 µg/L), and with thermal hydrolysis (80 and 160ºC) of sludge exposed to PsNPs in terms of methane production, ARGs propagation, extracellular polymeric substances (EPS), ROS levels, and microbial communities.

4.2. Methodology

4.2.1. Sludge and inoculum

The primary sludge (PS), thickened waste activated sludge (TWAS), and anaerobically digested sludge was collected from the Gold Bar WWTP (Edmonton, Alberta, Canada) and stored in a cold room (4ºC) before the experiment. A mixture of PS and TWAS (volume ratio of 1:1) was used as a feedstock for AD. The characteristics of digested sludge, PS, TWAS, and PS+TWAS are provided in Table B1.

4.2.2. Experiments

PsNPs (50 nm, 2.5% solids (w/v) aqueous suspension, Density=1.06 g/cm^3) used in this study was purchased from Polysciences (Niles, IL, USA). For PsNPs exposure experiments, three concentrations of 50, 100, and 150 µg/L of PsNPs were prepared and added to the mixture of TWAS and PS. Then, the sludge samples were placed in an ultrasonic water bath for 15 min for homogeneous dispersion (Zakaria et al., 2018). Afterward, the THP of mixed sludge containing

PsNPs was performed with a batch hydrothermal reactor covered with a heating jacket (2L, Parr 4848, maximum pressure: 1900 psi, maximum. temperature: 350ºC, Parr Instrument Company, Moline, IL, USA). After loading 400 mL of sludge sample, the reactor was tightly sealed and then heated. The sludge was stirred at a constant speed of 150 rpm during the process, and the temperature was monitored with a thermocouple. The heating rate was 2–3ºC/min. After reaching the desired temperatures (80 and 160ºC) and the exposure period of 60 minutes, the heating was switched off. Then, the system was cooled down to room temperature using cold water recirculation through a designated recirculation tube. The THP experiments at 80 and 160ºC with 60 min exposure time were performed for both samples containing PsNPs and samples without PsNPs (control).

The effects of PsNPs and THP on anaerobic biodegradability were assessed with the biochemical methane potential (BMP) tests using a feed-to-inoculum (F/I) ratio of 2 (g total chemical oxygen demand (TCOD)/g volatile solids (VS)). Prior to the test, the digested sludge was pre-acclimatized for 3 days at 37ºC. A detailed description of the batch reactors (working volume of 300 mL) used for BMP tests could be found in the literature (Mohammad Mirsoleimani Azizi et al., 2021a). Different test conditions included were: (I) untreated sludge as the control, (II) sludge pretreated at 80 and 160ºC, (III) sludge amended with PsNPs (50,100, and 150 µg/L), and (IV) PsNPs-amended sludge (50,100, and 150 µg/L) pretreated at 80 and 160ºC. Furthermore, the BMP of inoculum and deionized water served as the blank to determine the methane production from the inoculum. The reactors were placed in water baths to maintain 37ºC. The liquid medium was continuously mixed at 300 rpm. All tests were performed in triplicate.

4.2.3. ROS measurement

ROS measurement was performed according to the literature (Limbach et al., 2007; Wei et al., 2019b) with slight modification. Briefly, 2’7’-dichlorodihydrofluorescein diacetate (H_2DCFDA; Molecular Probes, Eugene, USA) can be oxidized to fluorescent dichlorofluorescein (DCF) by intracellular ROS. H_2DCFDA was diluted in Dimethyl sulfoxide (DMSO) to reach 50µmol/L. The samples were centrifuged at 10,000 rpm for 10 min, and then the pellets were washed using Phosphate-buffered saline (PBS, pH 7.4) for three times. Afterward, 50 µmol/L H_2DCFDA was added to the samples and incubated in the dark at 35±1ºC for 60 min. Then, the pellets were centrifuged for 10 min and plated into a 96-well plate. Fluorescence measurements of

DCF were conducted by fluorescence spectroscopy (SpectraMax M3, Molecular Devices LLC, California, USA) with an excitation wavelength of 485 nm and an emission wavelength of 520 nm.

4.2.4. Characterization of microbial communities and ARGs

The microbial communities in digestate samples were characterized using 16S rRNA sequencing. A detailed description of the sample preparation protocol, sequencing, and data analysis are provided in the Supporting Information. Quantitative polymerase chain reaction (qPCR) used for targeting thirteen frequently detected antibiotics resistance genes **(**ARGs) including tetracycline resistance genes (*tet*A, *tet*B, *tet*C, *tet*W, *tet*M, *tet*Q, *tet*X), sulfonamides resistance genes (*sul*1, *sul*2), macrolide resistance genes (*erm*B, *erm*C), ß-lactam resistance genes (bla_{OXA}, bla_{TEM}), and integrons (*intl1*, *intl2*), and 16s rRNA were also quantified. The primers of the selected genes are provided in Table B2. The detailed quantification procedure can be found elsewhere (Zakaria and Dhar, 2020, 2021).

4.2.5. Analytical methods

The total suspended solids (TSS) and volatile suspended solids (VSS) concentrations were quantified using standard methods (Association et al., 1915). Total ammonium nitrogen (TAN), TCOD, and soluble chemical oxygen demand (SCOD) concentrations were measured with HACH reagent kits (HACH, Loveland, CO, USA). For TAN and SCOD, samples were prepared using 0.45 μm membrane filters. The concentrations of major volatile fatty acids (VFAs) were measured using an ion chromatograph (Dionex™ ICS-2100, Sunnyvale, USA); the samples were filtered with 0.2 µm membrane filters before the analysis. EPS extraction was performed with the heating method (Xu et al., 2013; Zakaria and Dhar, 2020). The carbohydrate content was determined using the modified phenol-sulfuric acid method (Dubois et al., 1956), using glucose as the standard. Pierce™ Modified Lowry Protein Assay Kit (Thermo Fisher, USA) was utilized to determine the protein contents of the EPS according to the manufacturer's instructions. The detailed sample preparation and analytical protocol are provided in the Supporting Information. Fourier-transform infrared spectroscopy (FTIR) analysis was conducted for all samples, according to a method described in our previous study (Mohammad Mirsoleimani Azizi et al., 2021a).

4.2.6. Microscopic imaging

To understand the interaction between microbial cells and PsNPs, a transmission electron microscope (TEM) and a scanning electron microscope (SEM) imaging of sludge samples was carried out after the completion of PsNPs exposure. A detailed description of the sample preparation protocol and methods are provided in the Supporting Information.

4.2.7. Kinetic and statistical analyses

The first-order kinetic and modified Gompertz models were used to assess process kinetics from the BMP test data; details are provided in the Supporting Information. A one-way analysis of variance (ANOVA) using Microsoft Excel was performed to determine the statistical significance of the results at a 95% confidence level (i.e., to be considered significant, p-values <0.05).

4.3. Results and discussion

4.3.1. Methane generation

Fig. 4.1a shows the cumulative methane production profiles under different experimental conditions. For all samples, methane production started immediately on the first day without any noticeable lag phases. The cumulative methane yield from the control was 170±3 mL CH_4/g COD. Interestingly, 50 µg/L of PsNPs slightly increased methane yield to 192±2 mL CH_4/g COD. However, with increased PsNPs concentrations to 100 and 150 µg/L, cumulative methane yields reached 139±2 and 120±1 mL CH_4/g COD, 17.98% and 29.34% lower than control. Thus, PsNPs stimulated methane production at a lower level while suppressing the methanogenesis process at elevated concentrations.

However, THP could completely compensate for the negative impact of higher PsNPs levels (100-150 µg/L) on methanogenesis. For instance, 80ºC-100 µg/L and 160ºC-100 µg/L resulted in a 5.52% and 19.67% enhancement in cumulative methane yields. Similarly, 11.93% decrease and 1.0% increase were achieved for 80ºC-150 µg/L and 160ºC-150 µg/L. In contrast, 150 µg/L of PsNPs resulted in a 29.3% reduction in cumulative methane yield. Thus, THP at 80ºC was adequate to completely counteract the negative impact on methane yields by 150 µg/L of PsNPs, however, without any further increase. In contrast, THP at 160ºC was effective in further improving methane

yield for 150 µg/L of PsNPs. Thus, it was evident that THP could offset the adverse impact of a high level of PsNPs (100-150 µg/L) and improve methane production. The application of THP alone could also increase methane production due to the solubilization of organics (see Table B3), which is consistent with numerous previous studies (Dhar et al., 2012; Kumar Biswal et al., 2020; Mohammad Mirsoleimani Azizi et al., 2021a; Zhou et al., 2021). Despite providing higher methane yields, THP at 160ºC led to extended lag phases for all PsNPs concentrations (see Fig. 4.1a and Table B4), demonstrating a more prolonged time required for microbial adoption to solubilized organics (often refractory and/or inhibitory compounds). Such observations have also been reported in the literature for high-temperature THP (Zhou et al., 2021). Overall, our results showed that PsNPs levels (100-150 µg/L) induced inhibitory effects on methanogenesis, whereas THP could relieve PsNPs-induced inhibition.

4.3.2. ROS generation

As reported in the literature (Wei et al., 2020), ROS induced by PsNPs is a recognized fundamental mechanism that can arrest methanogenic activity (Wei et al., 2020). Briefly, ROS may include superoxide ($O_2^{\bullet-}$), hydrogen peroxide (H_2O_2), and hydroxyl radical ($OH^{\bullet}$) (Wei et al., 2019b). These species are known to cause oxidative stress in cells (Mu and Chen, 2011). The high surface area of MPs/NPs particles can promote ROS generation via the catalytic reaction between free radicals and molecular dioxygen (Wei et al., 2019b). However, the mechanisms of ROS generation under anaerobic condition are still ambiguous. A few recent reports suggested ROS generation in anaerobic bioreactors at sub-micromolar concentrations of oxygen when exposed to the unfavorable metabolic environment (e.g., presence of inhibitors, pH changes) (Tian et al., 2019; Zheng et al., 2019). As shown in Fig. 4.1b, the exposure to PsNPs remarkably affected the ROS levels. Compared to the control, there was a marginal decrease in ROS level (-4.9%) for 50 µg/L of PsNPs, whereas higher PsNPs levels increased ROS levels by 17.1% (100 µg/L PsNPs) and 34.84% (150 µg/L PsNPs). A few recent studies also reported that high MPs/NPs levels would increase the ROS generation in AD (Z. Wang et al., 2021; Wei et al., 2019d). Interestingly, THP could reduce ROS levels for sludge exposed to high PsNPs levels (100-150 µg/L). For instance, ROS levels in 80ºC-100 µg/L and 160ºC-100 µg/L decreased by 7.8% and 3.5% compared to 100 µg/L of PsNPs alone. These findings indicated that THP could reduce ROS levels induced by exposure to higher PsNPs levels in digesters.

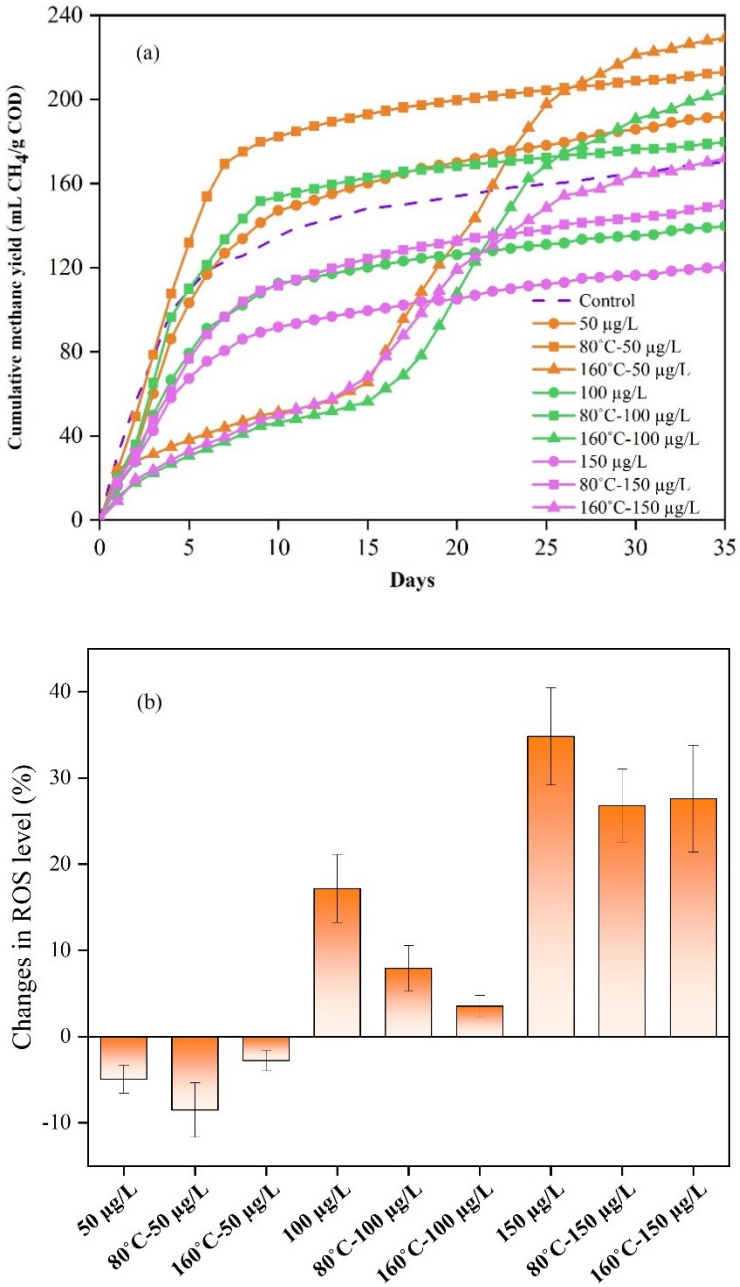

Figure 4.1. (a) Cumulative methane yields, and (b) relative changes in ROS levels for different experimental conditions compared to the control.

4.3.3. Microscopic imaging

The morphological changes in the sludge biomass after PsNPs exposure was visualized using SEM and TEM imaging (See Fig. B1). SEM images suggested that PsNPs were mostly attached

to cells and agglomerated together. Moreover, there was a layer covering the cells, which could be related to the excretion of EPS (Zakaria and Dhar, 2020). TEM images revealed that some cells could protect themselves by forming a protective EPS layer against PsNPs. Nonetheless, PsNPs could still penetrate some cells, leading to rupturing the cell membrane. This is consistent with previous reports on EPS solubilization and pitting of cell walls by PsNPs (Fu et al., 2018; Mohammad Mirsoleimani Azizi et al., 2021b). These findings indicated that the tolerance against PsNPs might vary for different microorganisms since PsNPs could penetrate some of the cells, whereas some remained intact.

4.3.4. Changes in EPS composition

Previous studies suggested that MPs/NPs can interfere or alter EPS structures (Z. Wang et al., 2021). In this study, EPS polysaccharides and proteins were characterized as the major constituents of sludge EPS (Zakaria and Dhar, 2020). Compared to the control, 50 µg/L of PsNPs exposed sludge showed increased EPS polysaccharides and proteins concentrations by 2.41% and 13.2%, respectively (Fig. 4.2a). However, at higher PsNPs levels (100-150 µg/L), EPS protein content decreased from 322 (control) to 232.5 and 241.5 mg/g sludge, respectively. Whereas EPS polysaccharide content substantially increased (p-value <0.001) from 207.5 (control) to 333 and 364 mg/g sludge for 100 and 150 µg/L PsNPs, respectively. Thus, EPS protein showed an opposite trend to polysaccharides at higher PsNPs levels.

For sludge containing 50 µg/L of PsNPs, THP consistently maintained higher proteins than polysaccharides (Fig. 4.2a). However, EPS levels for THP (80ºC-50 µg/L and 160ºC-50 µg/L) were substantially lower than the control and 50 µg/L of PsNPs. Compared to 100 µg/L of PsNPs without pretreatment, THP (80ºC-100 µg/L and 160ºC-100 µg/L) decreased EPS protein content by 18.5 and 9.6%, respectively. Likewise, polysaccharides were also reduced by 13.5% and 53.9%, respectively. THP of sludge containing 150 µg/L of PsNPs (80ºC-150 µg/L and 160ºC-150 µg/L) demonstrated almost similar decreasing trends for proteins and polysaccharides (Fig. 2a). Thus, THP could decrease EPS protein and polysaccharides content in sludge containing PsNPs. In general, compared to the control and 50 µg/L PsNPs, EPS proteins were considerably lower for all test conditions. In contrast, EPS polysaccharides were higher for higher PsNPs levels (100 and 150 µg/L) and corresponding THP samples at 80ºC.

4.3.5. FTIR spectrum

Fig. 4.2b illustrates the FTIR spectrum of the functional groups associated with EPS. Peaks at different wavelengths could be related to different functional groups (Böcker et al., 2017; Mohammad Mirsoleimani Azizi et al., 2021a). Thus, the changes in the intensities of the peaks are associated with changes in functional groups (Mohammad Mirsoleimani Azizi et al., 2021a). The bands in the range of 500-1,000 cm^{-1} are ascribed to the fingerprint region (Wei et al., 2020). The peak between 1,000–1,100 cm^{-1} demonstrates the vibration in polysaccharides and aromatic ethers (Chakravarty et al., 2010). The peaks at 1,550 and 1,650 cm^{-1} belonged to the amido-II and amido-I of proteins, respectively (Mu et al., 2012). Besides, the peak at 2,920 cm^{-1} and the shoulder around 1,450 cm^{-1} are belonged to the aliphatic C–H stretching and bending (Mohammad Mirsoleimani Azizi et al., 2021a). The intense peak between 3,300–3,500 cm^{-1} is associated with the O–H vibration of carboxylic and alcoholic groups (Mohammad Mirsoleimani Azizi et al., 2021a). As compared to the control, the intensity of the mentioned peaks changed for the samples containing PsNPs. For instance, the most intense peak at 1,060 cm^{-1} is for 150 µg/L, demonstrating the highest amount of polysaccharide. Interestingly, at 1,650 cm^{-1} the highest achieved peak is for 50 µg/L, indicating an increase in EPS protein content. The absorption peak decreased for all THP samples, suggesting a decrement in the protein and polysaccharide content. However, there are some overlaps for different peaks, which could be related to very close concentrations of different components in each sample.

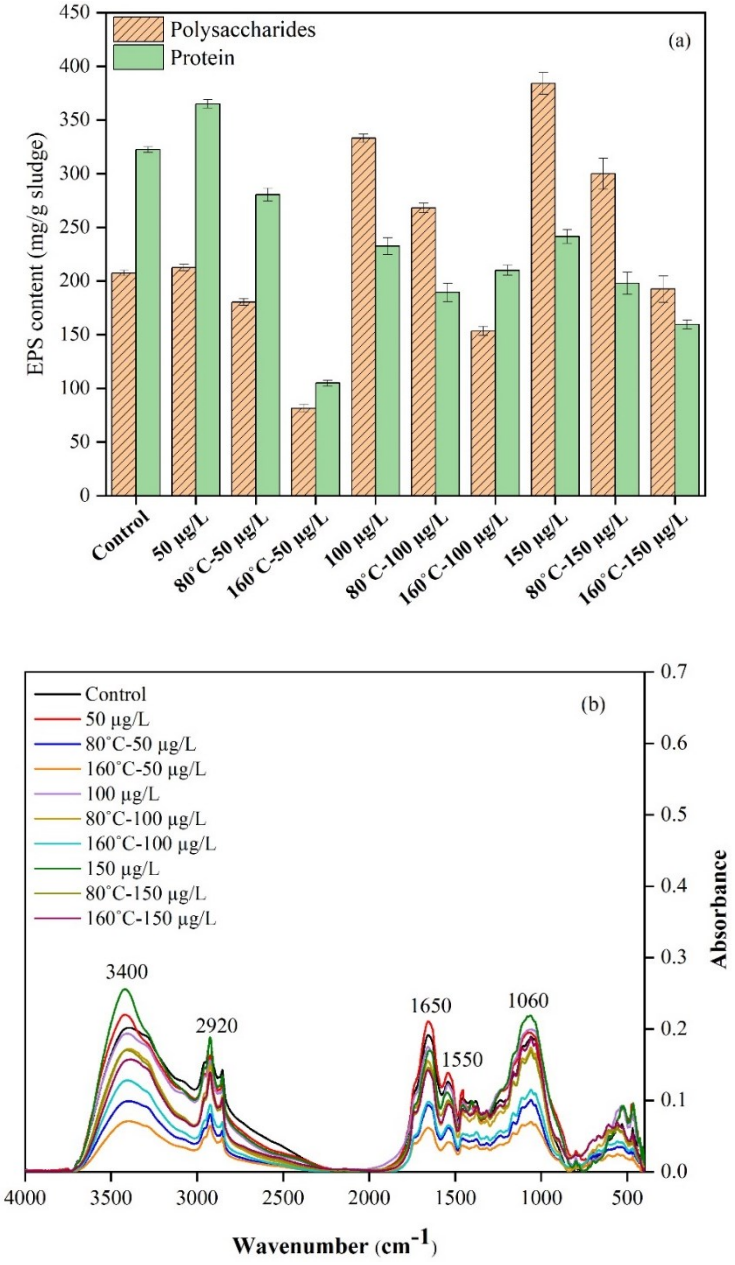

Figure 4.2. (a) EPS content, (b) FTIR spectra of the digestate samples.

4.3.6. ARG propagation

As shown in Fig. 4.3, increased PsNPs concentration from 50 µg/L to 100 and 150 µg/L enhanced propagation of most ARGs. For instance, the abundance of *sul1* increased from 4.59×10^4 copies/g sludge (control) to 1.08×10^5, 1.17×10^5, and 1.4×10^5 copies/g sludge for PsNPs concentrations of 50, 100, and 150 µg/L, respectively. Likewise, *sul2* abundance for 100, and 150

µg/L also increased by 1.36 and 1.5-fold than the control, respectively (Fig. 4.3a). Dung et al. (Pham et al., 2021) also previously reported that exposure to polystyrene increased the abundance of *sul1* and *sul2* in the aerobic activated sludge process. The relative (compared to the control) fold of *intl1*, increased from 1.59 to 2.28 with increasing PsNPs from 50 to 150 µg/L (Fig. 4.3b). Compared to the control, the abundance of *intl2* also increased after PsNPs exposure. *Intl1* is considered a horizontal gene transfer (HGT) indicator, one of the most prevalent mobile genetic elements (MGEs) found in the environment (Wright et al., 2008). Previous researches also reported that MPs/NPs could increase integrons (*Intl1* and *intl2)* abundance in different wastewater systems (Dai et al., 2020b; Eckert et al., 2018).

Fig. 4.3c shows the changes in abundances of various *tet* genes. After exposure to PsNPs, the abundance of most *tet* genes (except for *tet*M and *tet*X) increased than the control. Notably, *tet*W, which encodes a ribosomal protection protein (Zhang et al., 2021), exhibited the highest abundances in both control and PsNPs samples. However, PsNPs had the highest impact on the abundance of *tet*B. The *tet*B abundance in control was 1.19×10^2 copies/g sludge, while it increased up to 4.73×10^3 copies/g sludge for 50 µg/L (39-fold increase). Zhang et al. (Zhang et al., 2021) also reported the increased abundance of several *tet* genes in dairy waste digestate after exposure to polyethylene MPs (1 g/L). Furthermore, ß-lactam resistance genes (bla_{OXA}, bla_{TEM}) abundance increased up to 2-fold after PsNPs exposure (Fig. 4.3d). However, there were no significant changes in macrolide resistance genes (*erm*B, *erm*C); their abundances remained almost constant after PsNPs exposure (Fig. 4.3e). Nonetheless, PsNPs increased the abundance of most ARGs, which could be attributed to the fact that MPs/NPs can serve as a reservoir of ARGs (Shi et al., 2020).

Although PsNPs elevated ARG abundances than the control, THP decreased their abundances. For instance, 80ºC-50 µg/L and 160ºC-50 µg/L conditions decreased the abundance of *Sul1* by 28% and 92% compared to the sample without pretreatment (i.e., 50 µg/L PsNPs). Also, *Sul2* abundance in 80ºC-50 µg/L and 160ºC-50 µg/L reduced by 63.2% and 80.30%, respectively. Similar trends were also observed for samples exposed to high PsNPs levels (100-150 µg/L). Fig. 4.3b shows a considerable decrease in integrons abundance for THP samples, indicating a substantial reduction in HGT potential. The changes in tetracycline and ß-lactam resistance genes also showed similar decreasing patterns with THP (Fig. 4.3c and d). The decrease of ARGs after

THP was consistent with previous reports (Ma et al., 2011; Tong et al., 2019), which could be attributed to the reduction of potential hosts carrying various ARGs (Tong et al., 2017, 2016; Wang et al., 2019). The number of 16S rRNA gene copies for the pretreated samples was significantly lower (p-value <0.001) than the control and untreated PsNPs samples (see Fig. B2). Thus, potential ARG hosts in the incoming sludge might be destroyed by THP, thereby minimizing the ARG propagation that PsNPs could enhance.

However, the abundance of *erm*B and *erm*C increased for the THP samples exposed to 100 and 150 µg/L of PsNPs (Fig. 4.3e). For instance, the abundance of *erm*B in the sample 150 µg/L was around 5.4×10^3 copies/g sludge, which increased to 5.55×10^3 and 6.2×10^3 copies/g sludge in the 80ºC-150 µg/L and 160ºC-150 µg/L, respectively. Previous studies also demonstrated that some ARGs and MGEs might rebound during AD despite decreased abundances due to THP before the AD (Ma et al., 2011; Pei et al., 2016). Nonetheless, THP could reduce the abundance of most ARGs and MGEs prompted by PsNPs exposure and minimize the risks of ARG transmission through digestate biosolids.

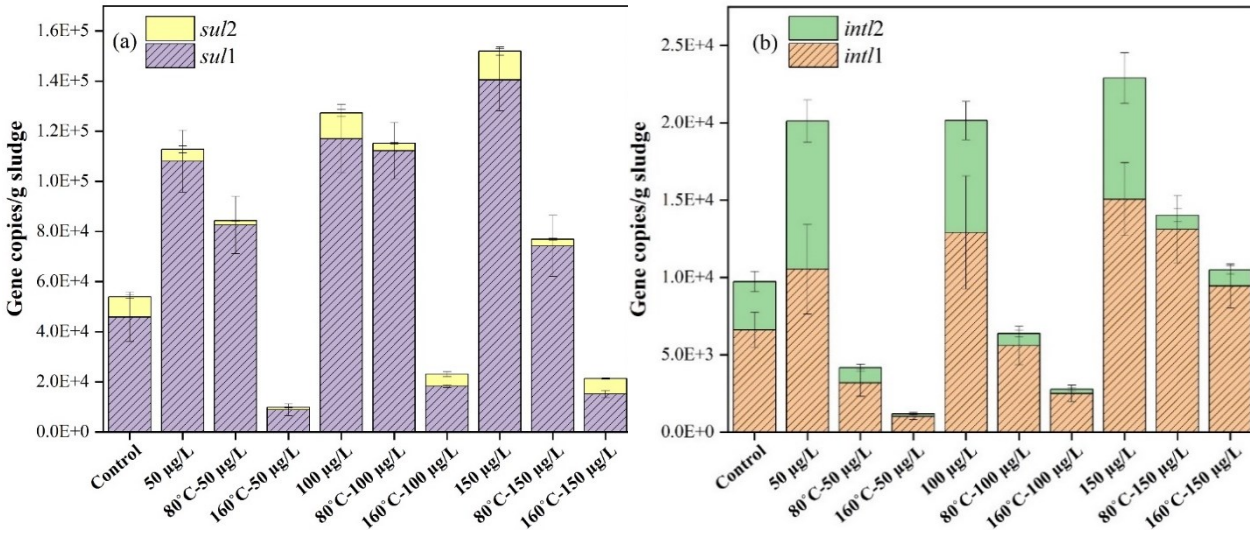

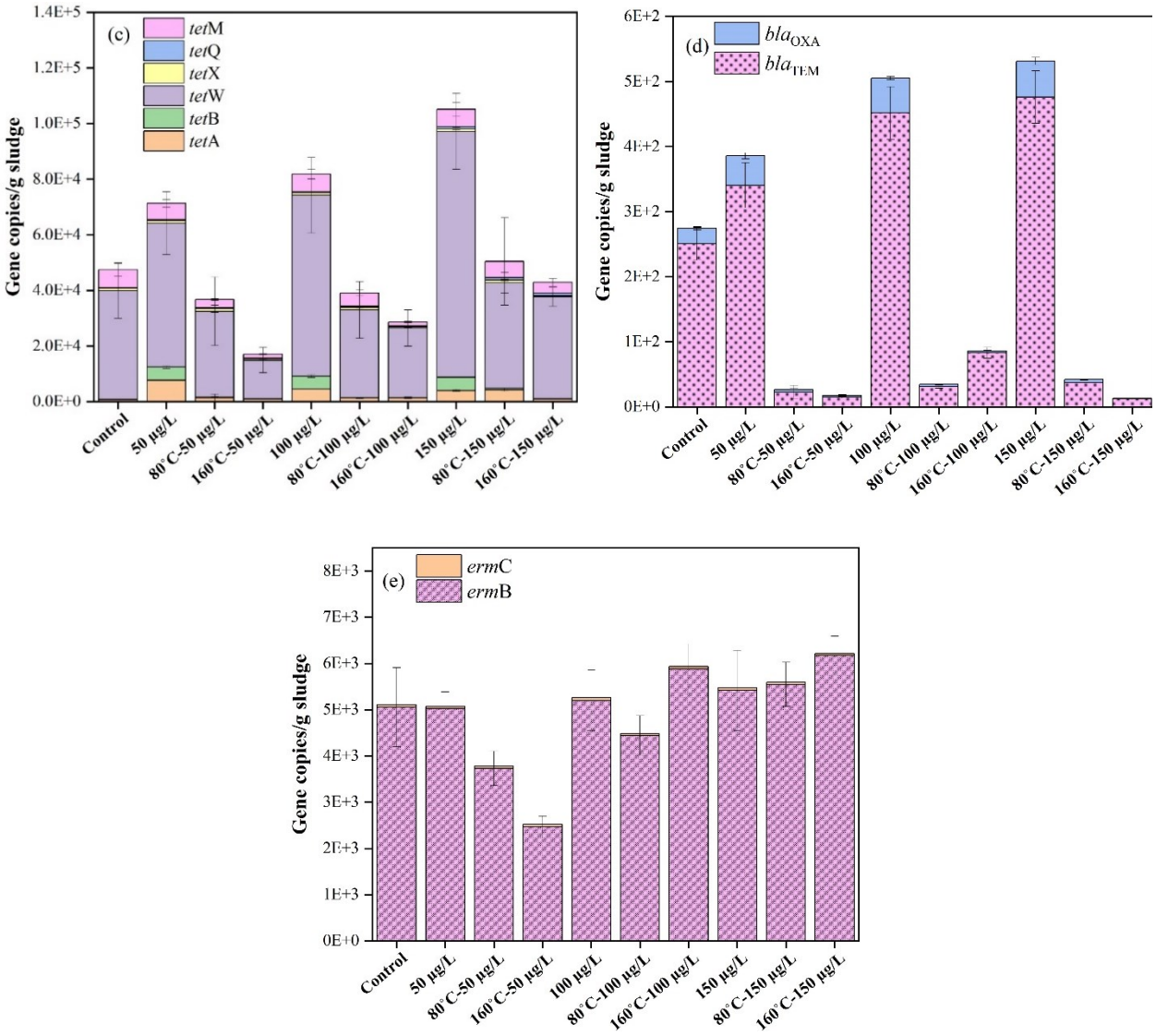

Figure 4.3. Concentrations of (a) sulfonamide (*sul*), (b) integron (*intI*), (c) tetracycline (*tet*), (d) macrolide (*erm*), and (e) ß-lactam (*bla*) resistance genes under different experimental conditions.

4.3.7. Microbial community

As shown in Fig. B2, 16S rRNA gene copies significantly decreased from 1.16×10^{10} copies/g (control) to 1.23×10^{9}, 1.34×10^{9}, and 1.28×10^{9} copies/g sludge for the samples exposed to 50, 100, and 150 µg/L of PsNPs. Also, THP further decreased the 16S rRNA gene copies. For instance, gene copies in 80ºC-50 µg/L and 160ºC-50 µg/L, reached 2.3×10^{7} and 2.23×10^{6} copies/g sludge, respectively. Thus, the quantity of microbial population was affected by both THP and the toxicity

of PsNPs. Alpha diversity indices were calculated to assess microbial diversity under different conditions (see Table B5). Compared to the control, both PsNPs and THP + PsNPs demonstrated more diverse microbial communities, indicated by higher Chao1, OTUs, and Shannon index scores. It was previously reported that MPs/NPs exposure or THP could result in a more diverse digester microbiome (Zakaria and Dhar, 2020).

The exposure to PsNPs and THP reduced the abundances of most of the bacterial genera (Fig. 4. 4a). *Cloacamonaceae*_W22 was the most dominant genus (37%) in control. Their abundance decreased to 22.4% for 150 µg/L of PsNPs. THP at 160ºC (160ºC-150 µg/L) further decreased their abundance to 17.2%. The abundance of the second most dominant genus *Anaerolinaceae*_T78 (22%) had similar relative abundances in control and PsNPs samples, while their relative abundances decreased after THP. *Treponema* (8%), *Bacteroides* (8.4%), and *Cloacamonaceae*_W5 (4%) were other dominant genus in the control. *Treponema* and *Cloacamonaceae*_W5 demonstrated a marginal decrease in response to PsNPs and THP, whereas *Bacteroides* abundance remained almost constant. This indicates that different bacterial genera have different tolerance levels to PsNPs and THP operating temperatures. Some other genera, such as *Clostridia* and *Acinetobacter*, represented a tiny portion of the microbial community (~2%).

The relative abundance of archaea at the genus level is illustrated in Fig. 4.4b. *Methanosaeta* (41%), *Methanosarcina* (29%), *Methanoculleus* (16%), and *Methanobacterium* (14%) were the most dominant in control. They also constituted the majority (48-90%) of archaeal communities in test reactors. However, the abundance of known acetoclastic *Methanosaeta* decreased due to PsNPs exposure (e.g., decreased to 25% for 150 µg/L of PsNPs). Previous studies also indicated that MPs/NPs could reduce the abundance of *Methanosaeta* sp. (Wei et al., 2019d, 2019a). However, THP at 80ºC could increase *Methanosaeta* abundance compared to the control and PsNPs without THP. In contrast, THP at 160ºC considerably decreased their abundance and reached as low as 8% for 160ºC-150 µg/L. Given that acetoclastic methanogens are more sensitive to environmental conditions, such observation could be attributed to the formation refractory or inhibitory compounds under high-temperature THP (Zhou et al., 2021). The abundance of *Methanosarcina*, which is recognized as metabolically versatile archaea (Lambie et al., 2015), significantly decreased for both PsNPs and PsNPs/THP conditions (Fig. 4.4b). However, strictly hydrogenotrophic *Methanoculleus* enriched after exposure to PsNPs. For instance, exposure of 50,

100, and 150 µg/L of PsNPs, increased their abundance to 22, 31, and 31%, respectively. In contrast, the abundance of hydrogenotrophic *Methanobacterium* species remained almost constant or slightly increased after exposure to PsNPs as well as their combination with THP. Thus, the results are consistent with the fact that hydrogenotrophic methanogens are more resilient to harsh environmental conditions (Jiang et al., 2019).

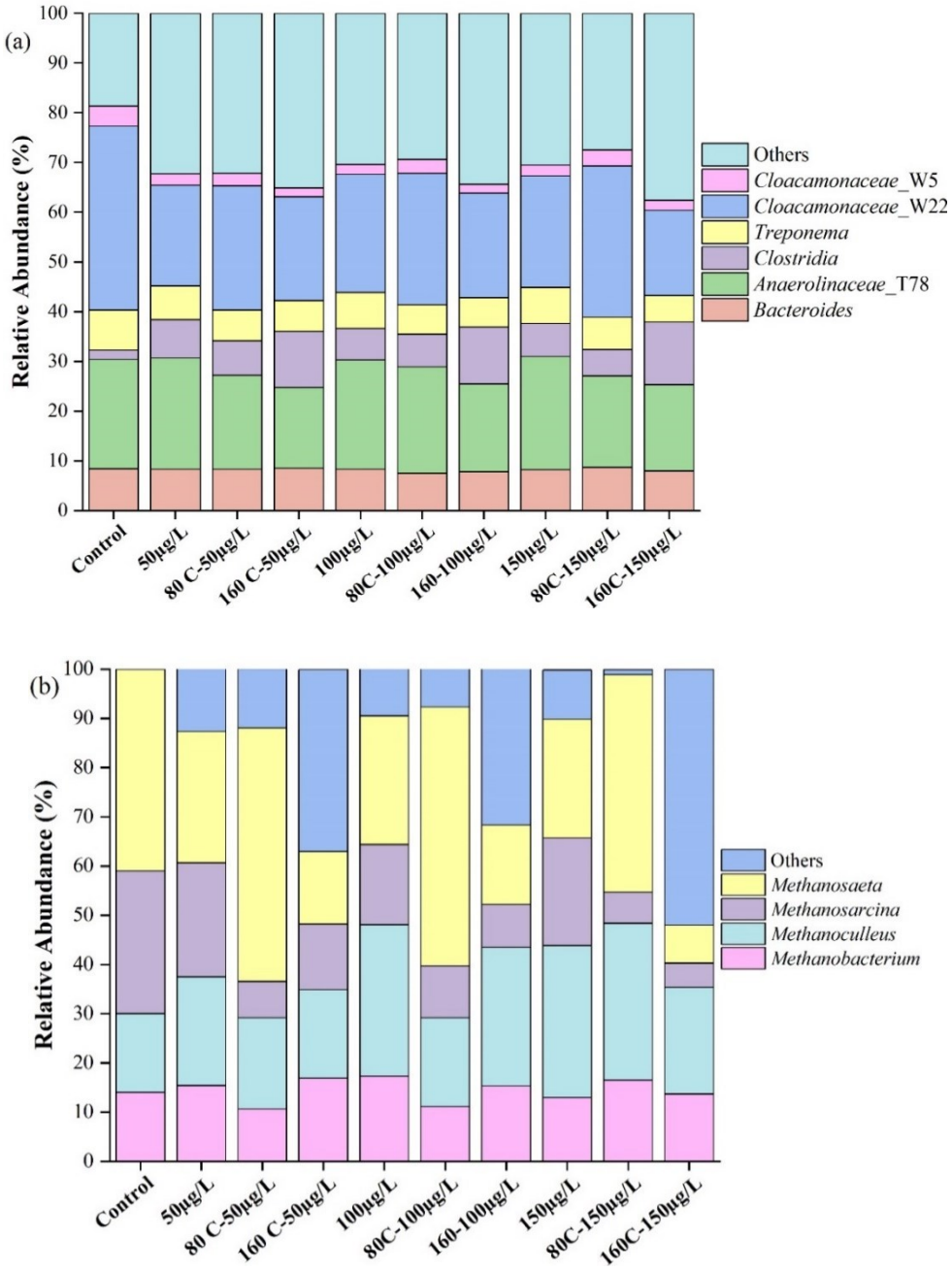

Figure 4.4. Relative abundance of (a) bacterial, and (b) archaeal communities at the genus level.

4.4. Discussion

For the first time, the present study reports that THP can relieve oxidative stress on methanogenesis and ARG propagation induced by the high levels of PsNPs. However, it appeared that high-temperature THP (e.g., 160^{o}C) might be required depending on the levels of PsNPs in sludge. The higher PsNPs levels could decrease methane yields, which agrees with several recent reports (Fu et al., 2018; Wei et al., 2019b).

PsNPs can penetrate or adhere to the cell surface, damaging cells or inhibiting cellular metabolism and growth (Fu et al., 2018). Thus, the higher concentrations are expected to have a more pronounced impact leading to a significant decrease in methanogenic activity. Microscopic imaging also confirmed that PsNPs could cause the pitting of cell walls leading to membrane permeation and cell rupture. The qPCR results also showed a decrease in 16S rRNA gene copies with increasing PsNPs levels. In addition to direct damage of cells, ROS induced by PsNPs can play a key role in methanogenic inhibition. High ROS levels can cause redox imbalance and peroxidation of cells, leading to metabolic disturbance and inhibition (Wei et al., 2020). Antioxidant enzymes, such as superoxide dismutase (SOD) and catalase (CAT) (Wei et al., 2020), can serve as ROS scavengers (Das and Roychoudhury, 2014). However, leaching additives from MPs/NPs (e.g., sodium dodecyl sulfate) can restrain the activities of such key enzymes, thereby alleviating microbial resistance to oxidative stress induced by MPs/NPs(Mohammad Mirsoleimani Azizi et al., 2021b). Thus, it can be inferred that an increase in ROS levels at 100-150 µg/L of PsNPs compared to the control negatively affected methanogenesis. In contrast, relatively lower ROS levels observed after introducing THP could be attributed to the thermal degradation of PsNPs that might reduce ROS generation potential.

Despite a decrease in 16S rRNA gene copies compared to the control, 50 µg/L of PsNPs marginally improved methane yield with decreased ROS levels. Wei et al. (Wei et al., 2020) previously reported that exposure to <10 µg/L of PsNPs had no noticeable impact on AD, while higher levels (~50 µg/L) dropped the methane production by 28.6%. The mechanisms behind the enhanced methanogenesis by low levels of (nano)microplastics are still ambiguous. However, a recent report suggested that leached additives from (nano)microplastics might enhance solubilization and activity of key enzymes (Chen et al., 2021). Interestingly, 50 µg/L of PsNPs

showed higher VFAs accumulation than the control (see Fig. B4). This could be attributed to enhanced hydrolysis/acidification by PsNPs exposure or inhibition of VFAs consumers (e.g., methanogens). Despite higher VFAs accumulation, 50 µg/L of PsNPs enhanced methane productivity. In contrast, higher PsNPs concentrations (100 and 150 µg/L) decreased methane production, while VFAs accumulation was almost similar or slightly lower than the control. Thus, enhanced hydrolysis/acidification by 50 µg/L is more probable.

A recent study suggested that PsNPs particles can alter protein secondary structures of sludge EPS (L. J. Feng et al., 2018). Our results also indicated significant changes in EPS composition due to PsNPs exposure. Notably, at higher PsNPs levels, protein content decreased, while polysaccharide content increased. Polysaccharides are recognized as fine strands that attach to the cell surface and constitute a complex network (Flemming and Wingender, 2010). Its secretion around the cell could be a response of microorganisms to protect themselves from the direct contact of the reactive sites PsNPs (Li et al., 2019). In contrast, higher EPS protein content might enhance the number of exoenzymes that can facilitate methane production (Li et al., 2019). The exoenzymes are the prevailing ingredient of EPS proteins that can assist electron shuttling between syntrophic partners (bacteria and archaea) in digesters (Li et al., 2019). However, THP could decrease both proteins and polysaccharides compared to PsNPs samples without THP. Such observations could be attributed to THP breaking the sludge EPS network and releasing the organics into the soluble phase (Sun et al., 2016). Besides, previous studies demonstrated a substantially negative linear correlation between protein/polysaccharide ratio and the surface charge and adsorption capacity of EPS. Thus, decreasing the protein/polysaccharide ratio might promote the PsNPs adsorption to EPS (Dai et al., 2020b), leading to pitting and rupturing microbial cells and EPS solubilization (Mohammad Mirsoleimani Azizi et al., 2021b). In this study, increasing PsNPs concentration from 50 to 100 and 150 µg/L decreased protein/polysaccharide ratios from 1.71 to 0.63, indicating a higher likelihood of PsNPs adsorption. However, after applying THP, protein/polysaccharide ratios dramatically increased for the samples containing higher PsNPs concentrations. For instance, for 80ºC-100 µg/L and 160ºC-100 µg/L, this ratio increased to 0.71 and 1.37 from 0.69 (100 µg/L of PsNPs alone). Based on these findings, it can be implied that THP (especially high-temperature THP) was more effective in the thermal decomposition of PsNPs, thereby preventing their role in EPS alteration.

4.5. Environmental implications

Our findings provide new information demonstrating that THP prior to AD could counteract adverse impacts imposed by PsNPs, such as arresting of methanogenesis and ARG propagation. To date, 75+ AD facilities worldwide adopted or currently considering THP as a pretreatment for AD (Barber, 2016). The drivers behind THP installation primarily include increased biogas production and high-quality biosolids generation (Mohammad Mirsoleimani Azizi et al., 2021a). The evidence for such added benefits of minimizing negative impacts of PsNPs is encouraging. Organic polymers are usually sensitive to high temperatures that can induce changes in their polymeric structures (Oliveira et al., 2020). However, their thermal stability depends on the physicochemical characteristics and composition of polymer blends (Pud et al., 2003). Thus, the results do not prove the effectiveness of THP for a wide variety of MPs/NPs found in sewage sludge. Further research is warranted to understand the fate of other MPs/NPs in THP followed by AD. The present work can serve as a pilot for further investigation and optimization of THP as a potential remediation method for minimizing (nano)microplastics-induced stress on AD and ARG transmission risks of biosolids.

Chapter 5

Sludge thermal hydrolysis for mitigating oxidative stress of polystyrene nanoplastics in anaerobic digestion: significance of solids content

A version of this chapter was published in ACS Sustainable Chemistry & Engineering, vol. 18, 7253-7262

5.1. Introduction

Due to the extensive production, use, and uncontrolled disposal of plastics to the environment, microplastics (MPs, a particle size of <5 mm) and nanoplastics (NPs, 1 to 1000 nm) are released into the environment (Azizi et al., 2022). Considering their ubiquitous detection in oceans, freshwater, air, soils, and polar region and a potential menace to the environment (J. Sun et al., 2019). Also, recent studies indicated the existence of MPs/NPs in human placentas, lung tissues, and blood (Jenner et al., 2022), which can cause detrimental and severe health issues.

MPs/NPs can enter the aquatic and terrestrial environment from different sources. However, wastewater treatment plants (WWTPs) have been recognized as one of the main discharge outlets of MPs/NPs to the ecosystem (Azizi et al., 2022). WWTPs could effectively remove 99% of influent MPs during different treatment processes (Anne Marie Mahon et al., 2017). The principal removal mechanism is retaining them in the sewage sludge (Mohammad Mirsoleimani Azizi et al., 2021b). Reportedly, the MPs/NPs in sewage sludge ranged from 4.2×10^3 to 6.4×10^6 particles/kg of dry solids (Chand et al., 2022). Land application of sewage sludge is discarding 4.4×10^4–3×10^5 tons/year of MPs/NPs into the soil in North America (Nizzetto et al., 2016). Sewage sludge also contains residual antibiotics and antibiotic resistance genes (ARGs) (Azizi et al., 2023; Dai et al., 2020a). Due to their high surface area and hydrophobicity, MPs/NPs can be vectors for various pollutants, including antibiotics and ARGs (Mohammad Mirsoleimani Azizi et al., 2021b).

Anaerobic digestion (AD) has been widely implemented for sludge stabilization, resource recovery, pathogens removal, as well as production of methane-rich biogas (Dastyar et al., 2021b; Pereira de Albuquerque et al., 2021). MPs/NPs in sludge can remarkably affect the operational

stability of digesters (He et al., 2021). For instance, polystyrene nanoplastics (PsNPs) can interfere with digester operation by inducing reactive oxygen species (ROS), leaching of toxic chemicals/additives, inhibiting activities of critical enzymes, and cell apoptosis via penetration (Azizi et al., 2022; Mohammad Mirsoleimani Azizi et al., 2021b). Also, MPs/NPs in sewage sludge can promote ARG proliferation and inevitably increase the chance of spreading ARGs through land application of digestate (Azizi et al., 2022).

The thermal hydrolysis process (THP) is a commonly used pretreatment approach for enhancing sludge solubilization, hydrolysis rate, methane recovery, and solids removal in AD. THP can disintegrate sludge, particularly the matrix of extracellular polymeric substances (EPS), solubilizing particulate organics and enhancing methanogenesis (Haffiez et al., 2022a). THP before AD can decrease the proliferation of most ARGs throughout the digestion process (Haffiez et al., 2022a). Most recently, Azizi et al. (Azizi et al., 2022) found that THP can provide dual benefits of mitigating the adverse impact of PsNPs in AD and reducing ARG proliferation encouraged by PsNPs. However, knowledge of the effect of different operational features of THP, particularly the total solids (TS) content of sludge, on MPs/NPs-induced stress during AD is still limited. The TS content of sewage sludge plays an indispensable role in the AD performance and process economics of THP. Operating THP at higher TS% can reduce energy consumption; however, higher TS% can increase sludge viscosity leading to reduced heat transfer efficiencies (Toutian et al., 2021). Numerous studies previously emphasized the significance of TS% on the efficiency of the THP process in terms of solubilization and its subsequent impact on AD (Li and Chen, 2022). For instance, Jong et al. found that THP of sludge with 8% TS was the most advantageous among different TS% (5%, 8%, 10%, 12%, and 15%), resulting in the highest levels of sludge disintegration and methane production (Gong et al., 2019). Similarly, Li et al. found that 6% TS was the most effective within a wide range of TS% (2% to 12%) in enhancing THP efficiency regarding sludge solubilization and methane production (Li and Chen, 2022). Moreover, TS content beyond certain levels may induce challenges in mixing, ammonia and organic acids stress, ultimately resulting in process disturbance (Li and Chen, 2022). Thus, it is crucial to comprehend how the solids content influences THP efficiency and subsequent AD performance and other inhibitory factors. To the best of our knowledge, no reports have been published to date

on how different solids content in sludge influences the effectiveness of THP in mitigating MPs/NPs-induced oxidative stress and ARG proliferation.

Given these research gaps, the research questions in this study were to investigate how the THP affects the AD of sewage sludge with different TS% (4, 8, and 12%) when exposed to PsNPs. Specifically, the effectiveness of THP was evaluated in terms of mitigating oxidative stress induced by PsNPs and the propagation of ARGs. Furthermore, the study aimed to explore fundamental linkages between process variables (PsNPs, TS%, and THP) and ROS levels, EPS, and ARG abundance.

5.2. Material and methods

5.2.1. Sludge and Inoculum

The primary sludge (PS) and anaerobically digested sludge (DS) used in this research were collected from the Gold Bar WWTP (Edmonton, Alberta, Canada). After collecting PS and DS, samples were stored at 4 ºC in a cold room. To achieve the desired TS% of 4, 8, and 12%, a series of centrifugation steps (10 min for each step) was performed at 3500 rpm. The characteristics of DS and PS are summarized in Table C1.

5.2.2. Experiments

For PsNPs exposure experiments, 150 µg/L of PsNPs were prepared (Azizi et al., 2022) and added to the PS with different TS% (4, 8, and 12%). According to the literature, recent studies examining the impact of TS% on THP efficiency selected 2%-15% as their appropriate operating TS content (Gong et al., 2019; Li and Chen, 2022). Thereby, TS content in this range was selected. As reported in a previous study, 150 µg/L of PsNPs could have a more detrimental effect on AD than 50 and 100 µg/L (Azizi et al., 2022). The thermal hydrolysis of sludge was conducted using a bench-scale hydrothermal reactor; the detailed operating procedure was described elsewhere (Azizi et al., 2022). The THP was conducted at 160 ˚C (60 min), which was more effective in alleviating the PsNPs-induced stress in AD than 80 ˚C (Azizi et al., 2022). An exposure time of 60 min was selected for THP based on our previous studies (Azizi et al., 2022; Zhou et al., 2021).

The anaerobic biodegradability of different samples was evaluated with the biochemical methane potential (BMP) test. The detailed experimental protocol can be found in literature (Azizi et al., 2022). The BMP test conditions included: (I) untreated sludge with three different TS% (4, 8, and 12%) as controls, (II) pretreated PS (4, 8, and 12%) at 160 ºC (60 min exposure time), (III) sludge (4, 8, and 12%) amended with 150 µg/L of PsNPs, and (IV) PsNPs-amended sludge (4, 8, and 12%) pretreated at 160 ºC and 60 min exposure time. All tests were performed in triplicate. Methane yields were expressed based on the initial total COD of the feed sludge added to the reactors.

5.2.3. Quantification of antibiotics resistance genes

Quantitative polymerase chain reaction (qPCR) was utilized for targeting the most frequently detected ARGs and mobile genetic elements (MGEs) in sewage sludge (Haffiez et al., 2022b). Tetracycline resistance genes (*tet*A, *tet*B, *tet*W, and *tet*M), sulfonamides resistance genes (*sul*1, *sul*2), ß-lactam resistance gene (bla_{TEM}), macrolide resistance gene (*erm*B), MGEs (*intl*1, *intl*2) and 16S rRNA were quantified. The primers of these genes are provided in the supplementary information (Table C2). The quantification procedure was described in detail in our previous studies (Zakaria and Dhar, 2021)

5.2.4. Analytical methods

Detailed analytical methods for the reactive oxygen species (ROS), extracellular polymeric substances (EPS), total suspended solids (TSS), volatile suspended solids (VSS), total chemical oxygen demand (TCOD), soluble chemical oxygen demand (SCOD), volatile fatty acids (VFAs), and total ammonium nitrogen (TAN) concentrations can be found elsewhere (Azizi et al., 2022).

5.2.5. Data analysis

The first-order kinetic and modified Gompertz models were implemented to evaluate process kinetics and lag phases from the BMP test results (Mohammad Mirsoleimani Azizi et al., 2021a). Student's t-test using Microsoft Excel was carried out to determine the statistical significance (95% confidence level) of the results. Additionally, using Origin 2021, the principal component analysis (PCA) and correlative analysis were performed to examine the potential relationships and variations between different test conditions and parameters (Meshref et al., 2021). The Spearman's

rank correlation was used, and the correlation coefficient values ranged from -1 to +1 (Haffiez et al., 2022a). The alpha value of 0.05 was selected for the correlation confidence intervals.

5.3. Results and discussion

5.3.1. Methane Production

The cumulative methane yields for controls (Control-4%TS, Control-8%TS, and Control-12%TS) were 208.31±1, 193.92±2.3, and 157.81±2 mL CH_4/g COD (Fig. 5.1). Thus, with increasing solids content, methane yields decreased (p-value=0.006), which could be related to increased sludge viscosity and mass transfer limitation at higher solids content (Ahn and Chang, 2021). THP at 160 ºC increased methane yield (Table C3) for the sample with 12% TS (THP-12%TS), indicating THP at higher solids content could alleviate such mass transfer limitation by disintegrating sludge flocks (Mohammad Mirsoleimani Azizi et al., 2021a) and thereby increasing the methane yield up to 62% compared to the corresponding control (Control-12%TS) (Fig. C1). Also, THP enhanced the methane production by ~10% for samples with 4% and 8% TS (THP-4%TS and THP-8%TS) compared to their respective controls (Control-4%TS and Control-8%TS).

With the addition of PsNPs, methane yields from samples with 4% and 8% TS (PsNPs-4%TS and PsNPs-8%TS) reached 176.80±2.9 and 179.82±2.9 mL CH_4/g COD, which were 15.07 (p-value=0.005) and 7.25% (p-value=0.025) lower than their respective controls. However, with an increased TS% to 12% (PsNPs-12%TS), the cumulative methane yield reached 168.21±3.6 mL CH_4/g COD, which was 6.65% higher (p-value= 0.012) than its respective control (Control-12%TS). Thus, PsNPs enhanced methane generation at a higher TS (12%) while suppressing methane production at lower TS (4% and 8%). This could be attributed to a lower EPS content, higher ROS generation (discussed later), and leaching of potentially toxic additives. As suggested in the literature, additives (e.g., sodium dodecyl sulfate (SDS)) leached from PsNPs can inhibit the activity of key enzymes related to the microbial defense against oxidative stress and suppress the methanogenesis process (Mohammad Mirsoleimani Azizi et al., 2021b). A higher methane production at higher TS% (PsNPs-12%TS) could be due to higher secretion of EPS (discussed later), providing a defense line against external toxic substances like PsNPs (Xu et al., 2021). Also, EPS can act as a wetting agent and coat the surface of MPs/NPs leading to the alteration of hydrophobic surface properties of PsNPs (Xu et al., 2021). Notably, this can facilitate the

agglomeration of MPs/NPs and associated microbial communities, owing to the entanglement of PsNPs in the EPS matrix (Summers et al., 2018). This can decrease PsNPs abundance in the media and decrease the chance of their adherence and penetration into the cells (Mohammad Mirsoleimani Azizi et al., 2023). As a result, the MPs/NPs are less likely to induce stress, ultimately decreasing cell apoptosis. Also, the decreased VS removal in the PsNPs-12%TS (compared to PsNPs-4%TS and PsNPs-8%TS) can support this postulation (see Fig. C2). A higher TS content can enhance EPS production, which in turn can facilitate the agglomeration of PsNPs and decrease their abundance in the media resulting in reduced cell apoptosis and decreased VS removal efficiency.

Interestingly, PsNPs-4%TS and PsNPs-8%TS showed a higher VFA accumulation than their respective controls (see Fig. C3). This might be related to damage to cells and the release of intracellular content after PsNPs exposure (Chen et al., 2021). Owing to the strong adsorption affinity, MPs/NPs can directly attach to the cell under low EPS levels leading to cell membrane permeation and cell rupture (Wei et al., 2020). Nevertheless, at higher TS% (PsNPs-12%TS), a lower VFA accumulation was observed than its corresponding control. Thus, inhibition of VFA consumers (e.g., methanogens) could be the more probable reason behind high VFA accumulation in PsNPs-4%TS and PsNPs-8%TS than in corresponding controls.

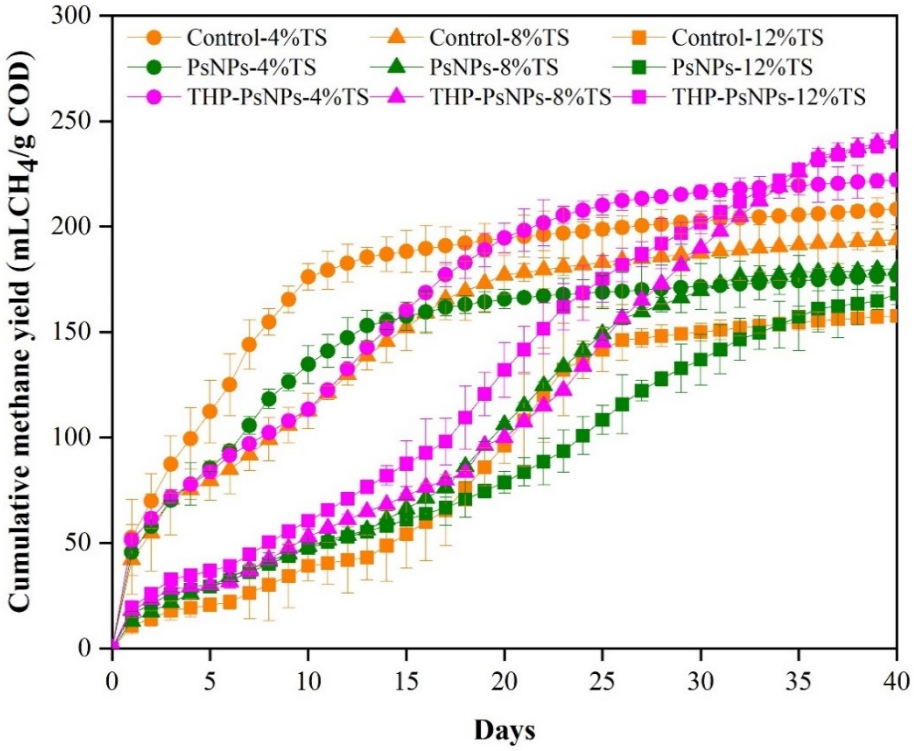

Figure 5.1. Cumulative methane yields for different experimental conditions (4,8, and 12%TS, PsNPs (150 µg/L), THP (160 ºC and 60 min)).

Notably, applying THP could entirely offset the negative impact of PsNPs at lower TS%. For instance, THP-PsNPs-4%TS and THP-PsNPs-8%TS resulted in 6.70 and 24.60% increases in methane production (compared to their controls), respectively. Similarly, 52.40% enhancement (compared to Control-12%TS) was achieved for THP-PsNPs-12%TS. Thus, THP could completely offset the negative impact of PsNPs on methane production at lower TS% while improving the methane generation for 12% TS content. This could be due to the solubilization of organics by THP, as suggested in previous studies (Jeong et al., 2019; laqa Kakar et al., 2019). Despite increasing methane generation, THP led to a prolonged lag phase (Text C1 and Table C4). For instance, PsNPs-12%TS exhibited 4.56 d lag phase, whereas the lag phase increased to 5.54 d for THP-PsNPs-12%TS. This observation suggests that methanogens might need longer to adopt some refractory and/or inhibitory compounds released due to the THP of sewage sludge or additives released from PsNPs (Mohammad Mirsoleimani Azizi et al., 2021a). Also, the first-order kinetic model for THP samples demonstrated a lower methanogenesis rate constant (k), indicating that THP samples took longer to achieve maximum methane production than the controls. For

instance, k values of 0.17, 0.11, and 0.06 d^{-1} were obtained in Control-4%TS, Control-8%TS, and Control-12%TS, respectively, whereas k values decreased to 0.09, 0.06, and 0.07 d^{-1} in THP-PsNPs-4%TS, THP-PsNPs-8%TS, and THP-PsNPs-12%TS. Overall, our results illustrated that PsNPs could cause an inhibitory effect on methanogenesis at lower solids content (4% and 8% TS), whereas THP can counteract the PsNPs-induced inhibition. Thus, digesters operated under lower solids content would be more vulnerable to PsNPs-induced inhibition.

5.3.2. ROS generation

ROS induced by PsNPs is a principal mechanism that can affect methanogenesis and induce oxidative stress on cells (Wei et al., 2020). ROS typically includes superoxide ($O_2^{\bullet-}$), hydrogen peroxide (H_2O_2), and hydroxyl radical ($OH^{\bullet}$) (Wei et al., 2019b). The interaction of electron donors' active sites on the surface of NPs with the submicromolar oxygen concentration in anaerobic conditions can produce nanomolar quantities of $O_2^{\bullet-}$ and H_2O_2, leading to ROS generation via dismutation and Fenton chemistry (Nel et al., 2006). As illustrated in Fig. 5.2, the addition of PsNPs substantially affected ROS generation. Compared to the controls, 16.21, 16.70, and 8.79% increase in ROS level was attained in PsNPs-4%TS, PsNPs-8%TS, and PsNPs-12%TS, respectively. Thus, increasing TS content to 12% decreased ROS levels under similar PsNPs concentrations. The decreased ROS level at 12%TS could be attributed to the fact that higher TS content in sludge can impede the transport of submicromolar oxygen through the sludge, decreasing the amount of ROS generated by microbial metabolism (Gao et al., 2023). This could be due to the limited availability of oxygen, which is a key component in producing ROS by microbial metabolism (Gao et al., 2023). Additionally, as the TS content increases, higher secretion of EPS (discussed later) might happen, and the sludge floc structure becomes denser, which can improve the ability of external parthenogenetic bacteria to scavenge ROS, thus preventing damage to the anaerobic bacteria within the floc from ROS attack (Gao et al., 2023). Moreover, some previous studies also reported that exposure to MPs/NPs can induce ROS generation in AD (Azizi et al., 2022; Wei et al., 2019d). This ROS level increment may lead to cell peroxidation and redox imbalance, causing inhibition and metabolic disturbance (Wei et al., 2020). Most of the cells can mediate oxidative stress via antioxidant enzymes such as catalase and superoxide dismutase (Wei et al., 2020), which can act as the ROS scavengers and defense line against ROS-induced damage. However, leaching some additives like SDS from PsNPs can restrict

the activities of ROS scavengers, reducing microbial resistance to oxidative stress (Azizi et al., 2022). Nevertheless, THP could decrease ROS levels for all samples. For instance, ROS levels in THP-PsNPs-4%TS decreased by 7% compared to PsNPs-4%TS. Despite being resistant to biodegradation, MPs/NPs may undergo physical changes and some level of degradation upon exposure to high temperatures (Dilara Hatinoglu and Dilek Sanin, 2022). As the temperature increases and reaches the glass transition temperature of MPs/NPs (e.g., 106 ˚C for PsNPs) (Paik and Kar, 2006), it becomes more susceptible to degradation by cleavage of ester linkage (Dilara Hatinoglu and Dilek Sanin, 2022). The reduction in ROS production potential could be ascribed to altering the physicochemical characteristics of PsNPs during THP (Azizi et al., 2022). Although ROS generation could cause cell toxicity, it is not solely responsible for AD inhibition (Wei et al., 2019b). Direct damage to the microbial cells, inhibiting key enzymes and metabolic functions, and leaching of toxic chemicals/additives are other potential inhibition mechanisms proposed in the literature (Mohammad Mirsoleimani Azizi et al., 2021b). Nonetheless, the dominant inhibition mechanism among them remains unknown.

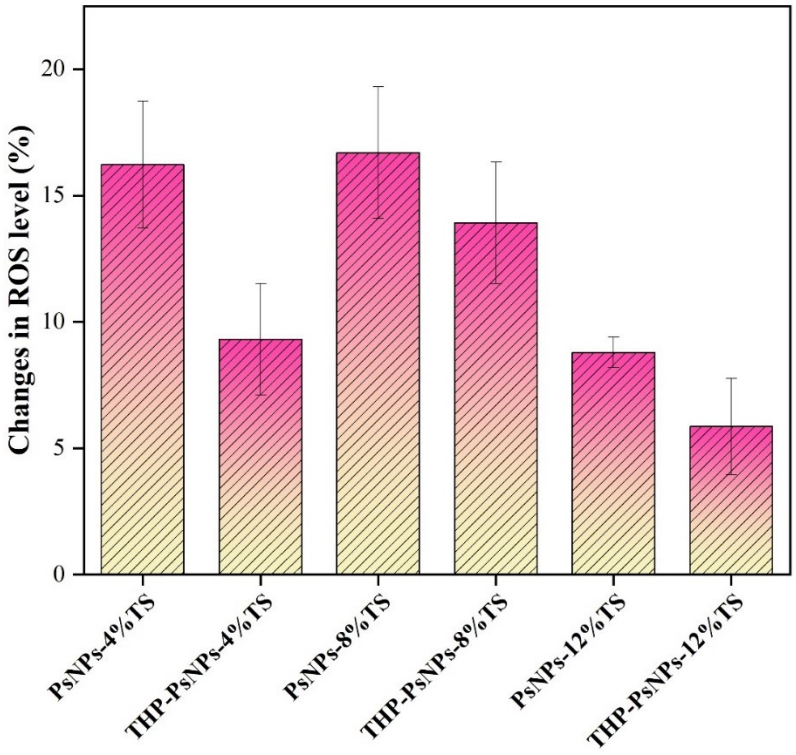

Figure 5.2. Relative changes in ROS levels for different experimental conditions (PsNPs (150 µg/L), THP (160 ºC and 60 min)) compared to the respective controls (4,8, and 12%TS).

5.3.3. Changes in total EPS composition

The EPS can provide a defensive shield against the harsh environment (e.g., high salinity, extreme pH and temperature) and the presence of PsNPs (Azizi et al., 2022). As shown in Fig. 5.3a, EPS polysaccharide and protein contents in control samples increased with increasing TS%. For instance, protein contents in Control-4%TS, Control-8%TS, and Control-12%TS samples were 210, 240, and 292 mg/g sludge (p-value=0.009), respectively. According to previous studies, PsNPs can alter EPS structures (Azizi et al., 2022). Compared to the controls, exposure to PsNPs decreased protein content in PsNPs-4%TS and PsNPs-8%TS by 14.28 and 10.10%, whereas a 6.16% increase was achieved in PsNPs-12%TS. Increasing EPS protein content can facilitate methane production since protein can serve as an electron shuttle and enhance the number of exoenzymes participating in extracellular electron transfer (EET) (Haffiez et al., 2022a; Li et al., 2019). The improvement of EET can outweigh the negative effect of mass transfer limitation at higher TS%, thereby stimulating methane production (Li et al., 2019). Notably, EPS polysaccharides demonstrated an opposite trend to protein, and a dramatic shift was observed after exposure to PsNPs. For instance, a 10.70, 9.33, and 4.53% enhancement (compared to respective controls) in EPS polysaccharide concentration was attained in PsNPs-4%TS, PsNPs-8%TS, and PsNPs-12%TS, respectively. This increased (p-value=0.005) polysaccharide content could be attributed to microorganisms' protection mechanism, which forms a protective layer by using polysaccharides secretion to shield from the reactive sites of PsNPs (Li et al., 2019).

Moreover, the EPS contents for THP samples were remarkably lower than controls. Compared to the controls, THP decreased the protein content by 23.80, 8.33, and 10.62% in THP-PsNPs-4%TS, THP-PsNPs-8%TS, and THP-PsNPs-12%TS, respectively. Similarly, polysaccharides were also reduced by 13.90, 16.33, and 33.61%. So, the effect of THP is more prominent at higher TS%. This finding could be ascribed to the disintegration of the sludge EPS network by THP and the release of the intracellular and extracellular material into the soluble phase (Azizi et al., 2022).

5.3.4. FTIR spectrum

FTIR analysis of digestate samples was performed to examine the changes in different functional groups related to EPS (Fig. 5.3b). Peaks at different wavelengths could be associated

with different EPS components, and the intensity of each peak could demonstrate the changes in the functional groups and EPS solubilization (Mohammad Mirsoleimani Azizi et al., 2021a). The peaks in the range of 500-1,000 cm^{-1} are typically considered fingerprint regions (Wei et al., 2020). The band in the 1,000–1,100 cm^{-1} indicates the vibration in polysaccharides and aromatic ethers. As illustrated in Fig. 5.3b, the most intense peak in this range belongs to the PsNPs-12%TS, demonstrating the highest polysaccharide content consistent with EPS results. Besides, the peaks at 1,550 and 1,650 cm^{-1} can associate with the amido-II and amido-I of proteins, respectively (Mu et al., 2012). Analogous to polysaccharides, the most intense peak in this range is for PsNPs-12%TS, demonstrating an enhancement in EPS protein content.

Moreover, the shoulder around 1,450 cm^{-1} and the band at 2,920 cm^{-1} are associated with the aliphatic C–H bending and stretching (Azizi et al., 2022; Mohammad Mirsoleimani Azizi et al., 2021a). The sharp peak in the range of 3,300–3,500 cm^{-1} belongs to the O–H vibration of alcoholic and carboxylic functional groups (Azizi et al., 2022; Mohammad Mirsoleimani Azizi et al., 2021a). Notably, increasing the TS% increased the intensity of all mentioned peaks in most samples. Remarkably, the absorption peak reduced for all THP samples, demonstrating a decreasing trend in the EPS proteins and polysaccharides. Nonetheless, there are some overlaps for different functional groups, indicating similar concentrations of different components in each sample (Azizi et al., 2022).

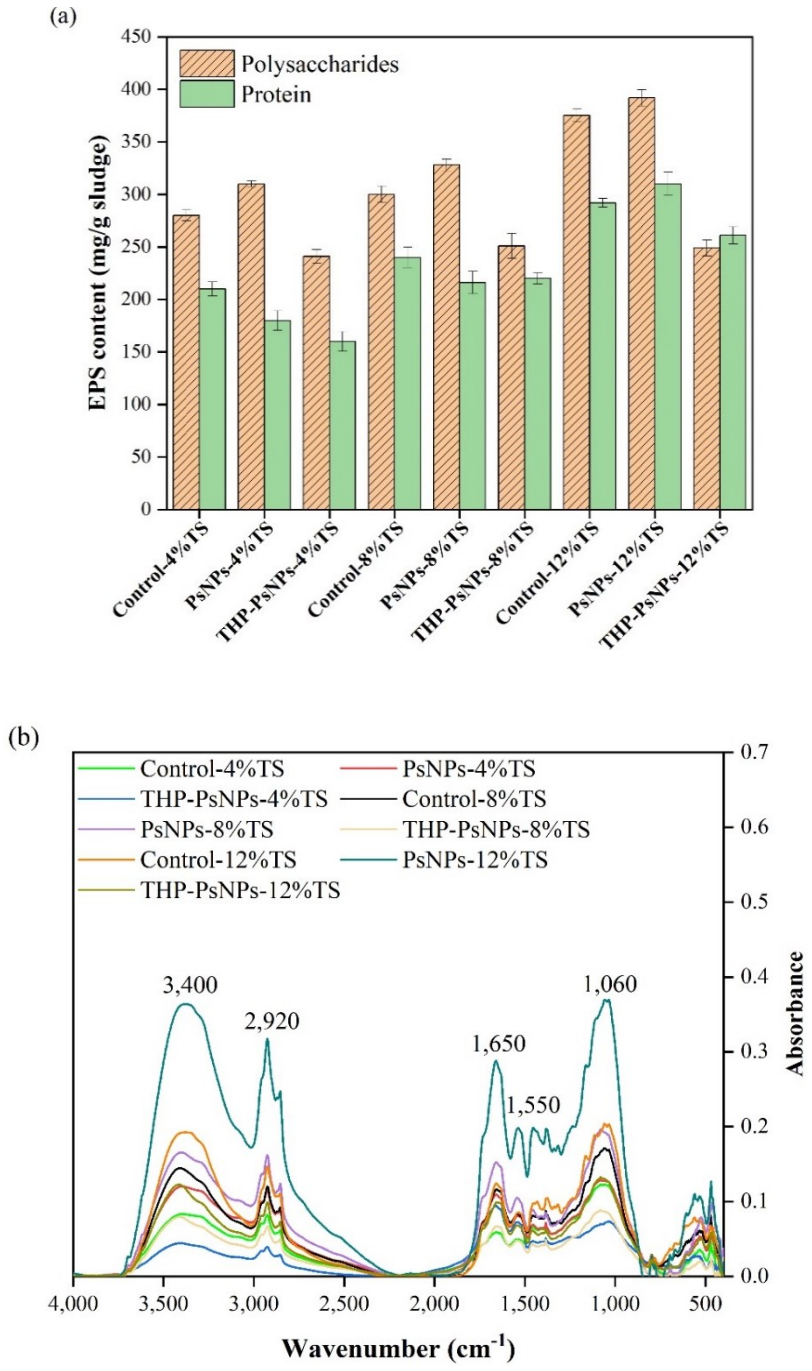

Figure 5.3. (a) EPS content and (b) FTIR spectra of digestate samples under different experimental conditions (4,8, and 12%TS, PsNPs (150 µg/L), THP (160 ºC and 60 min)).

5.3.5. Propagation of antibiotics resistance genes

Despite the ability of AD to remove certain ARGs, the proliferation of various ARGs may still occur during the process, as indicated by previous studies (Yun et al., 2021; Zang et al., 2020).

Moreover, the abundance of ARGs in digestate is influenced by various operating conditions, such as temperature (mesophilic, thermophilic), residence time, solid content, number of stages, and feedstock pretreatment (e.g., THP, Ozonation, ultrasonic). Other factors that may contribute to ARG propagation include the presence of heavy metals, exposure to MPs/NPs, and the use of conductive additives (Haffiez et al., 2022b). In this study, the targeted ARGs including *tet*W, *tet*A, *tet*B, *tet*M, *sul*1, *sul*2, bla_{TEM}, *erm*B, and MGEs (*intl*1 and *intl*2) were detected in the digestate (Fig 5.4a-d). Among all ARGs, *sul*1 (14-48%) and *intl*1 (17-43%), followed by *tet*W (14-26%), were the most abundant in all samples. As demonstrated in Fig. 5.4a, the abundance of *sul*1 increased (p-value=0.028) from 1.07×10^4 copies/g sludge (Control-4%TS) to 1.86×10^4 and 1.95×10^4 copies/g sludge for Control-8%TS and Control-12%TS, respectively. However, Control-4%TS demonstrated the highest abundance of *sul*2 (1.45×10^3 copies/g sludge), gradually decreasing with increasing TS%. Nonetheless, exposure to PsNPs enhanced the propagation of both *sul*1 and *sul*2. For instance, the abundance of *sul*1 in the PsNPs-4%TS, PsNPs-8%TS, and PsNPs-12%TS, increased by 8, 1.1, and 1.2-fold than the controls, respectively (Fig. 5.4a). A previous study indicated that exposure to polystyrene could proliferate *sul*1 and *sul*2 (Pham et al., 2021). Analogous to *sul*1, the abundance of *intl*1 in the controls increased (p-value=0.005) with increasing TS% from 4 to 12% (Fig. 5.4b). *Intl*1 is one of the most frequently detected mobile genetic elements (MGEs) and an indicator of horizontal gene transfer (HGT) (Wright et al., 2008). Notably, a 1.14, 1.10, and 1.2-fold (compared to the controls) increase in the abundance of *intl*1 was obtained in the PsNPs-4%TS, PsNPs-8%TS, and PsNPs-12%TS, respectively. Likewise, *intl*2 abundance for PsNPs-4%TS, PsNPs-8%TS, and PsNPs-12%TS also enhanced by 3, 3.40, and 5.50-fold than the controls, respectively. Previous studies also demonstrated that exposure to PsNPs could enhance the propagation of integrons (*intl*1 and *intl*2) (Azizi et al., 2022).

As demonstrated in Fig. 5.4c, the abundance of different *tet* genes changed with increased TS% and exposure to PsNPs. Notably, the abundances of *tet*A and *tet*B were elevated with increasing TS%, whereas no specific trend was found in *tet*W and *tet*M. As an example, for *tet*W, which encodes a ribosomal protection protein (Zhang et al., 2021), 1.07×10^4, 1.80×10^4, and 1.09×10^4 copies/g sludge (p-value=0.031) was attained for Control-4%TS, Control-8%TS, and Control-12%TS, respectively. Besides, PsNPs samples indicated the proliferation of *tet*A, *tet*W, and *tet*M, which is consistent with previous studies (Azizi et al., 2022; Zhang et al., 2021).

Interestingly, no substantial change was observed in the abundance of *tet*B, and it remained almost unaffected after PsNPs exposure. Besides, the macrolide resistance gene (*erm*B) increased with increasing TS%. After exposure to PsNPs, the abundance increased (compared to control) by 1.14, 1.33, and 1.06-fold in PsNPs-4%TS, PsNPs-8%TS, and PsNPs-12%TS, respectively (Fig. 5.4d). However, as depicted in Fig. 5.4d, ß-lactam resistance gene (bla_{TEM}) exhibited minor changes in both controls and PsNPs samples. Overall, PsNPs enhanced the propagation of most ARGs. This observation might be related to the fact that MPs/NPs can act as a reservoir of ARGs. PsNPs can alter microbial community composition by harming certain microorganisms, while promoting the growth of others (Azizi et al., 2022). Thereby, exposure to NPs can intensify the selective pressure for ARG proliferation (Haffiez et al., 2022b). For instance, Shi et al. found that exposure to NPs increased the prevalence of those bacteria which were potential ARG hosts (Shi et al., 2020). Further, the increased ROS production after exposure to NPs could damage the bacterial cell and increase their membrane permeability, potentially causing more bacteria to become ARG receptors via the intra-bacterial community transfer of MGEs (Shi et al., 2020). Besides, the hydrophobic surface of MPs/NPs is a hub for the microorganisms and stimulates the constitution of biofilms called 'plastisphere' (Dong et al., 2021). This biofilm formation for a longer time enables a forceful interaction between microbes and a high-nutrient-rich environment. It increases the syntrophic interactions among microorganisms, promoting antibiotic resistance (Zettler et al., 2013). Also, the risk of gene mutation and HGT can be enhanced by the accumulation of antibiotics on MPs/NPs.

The absolute abundances of ARGs were 7.91×10^4, 9.07×10^4, and 9.56×10^4 copies/g sludge (p-value=0.003) in Control-4%TS, Control-8%TS, and Control-12%TS, respectively, indicating the increase of total ARGs with increasing TS%. Additionally, the absolute abundance of total ARGs in the PsNPs amended samples was much higher than the controls. Specifically, the ARGs abundance in PsNPs-4%TS, PsNPs-8%TS, and PsNPs-12%TS samples were 2.03×10^5, 1.15×10^5, and 1.45×10^5 copies/g sludge (p-value=0.028), respectively. Although PsNPs enhanced the proliferation of ARGs, THP decreased their abundance. As shown in Fig. 5.4e, ARG abundance of 2.34×10^5, 7.52×10^4, and 7.33×10^4 copies/g sludge (p-value=0.13) were obtained in the digestate samples from THP-PsNPs-4%TS, THP-PsNPs-8%TS, and THP-PsNPs-12%TS, respectively. Thus, THP-PsNPs-4%TS might encourage rebounding and increase ARG concentrations during

the subsequent AD, which is consistent with previous studies (Haffiez et al., 2023; Ma et al., 2011). The ARG rebounding effect in the AD process implies that THP might induce a selection pressure for certain microbial hosts carrying ARGs (Sun et al., 2022). Also, ARGs may respond differently to the digester operating conditions, such as TS content (Ma et al., 2011). For instance, Sun et al. found that operating AD with higher TS content is more effective in ARG removal than its low TS content counterpart (W. Sun et al., 2019). Although the authors did not reveal the mechanisms behind decreased abundance at higher TS content, another study suggested microbial mobility as a critical factor in HGT for ARG propagation (Zhang et al., 2018). As a result, higher TS content and increasing sludge viscosity can impact the abundance of ARGs in the digesters.

However, THP-PsNPs-8%TS and THP-PsNPs-12%TS could avail the ARG reduction by 34.58% and 49.43% compared to PsNPs-8%TS, and PsNPs-12%TS samples, respectively. For instance, THP-PsNPs-8%TS and THP-PsNPs-12%TS reduced the abundance of *tet*W by 52% and 31% (compared to the samples without THP), whereas THP-PsNPs-4%TS demonstrated 107% increases in the abundance. Also, similar trends were observed for *tet*B and bla_{TEM} (Fig. 5.4c and d). THP samples indicated a substantial reduction in integrons abundance (Fig. 5.4b) and showed a considerable reduction in HGT potential (Azizi et al., 2022). As reported in previous studies (Haffiez et al., 2022a), this decrement in ARGs after applying THP could be due to decreasing potential hosts carrying several ARGs (Haffiez et al., 2022a). To further elucidate the ability of the microbiome to carry ARGs in the digestate, the 16S rRNA gene copies were quantified (Haffiez et al., 2022a). As demonstrated in Fig. C4, the number of 16S rRNA gene copies for the THP samples was remarkably less (p-value=<0.001) than in the controls and PsNPs samples. This may indicate the destruction of potential ARG hosts after THP, leading to minimizing the ARG proliferation, which PsNPs could increase (Azizi et al., 2022). Although THP proliferated ARGs at 4%TS, it efficiently decreased most ARGs increased by PsNPs exposure and minimized the risk of ARGs spread through digestate at higher TS%.

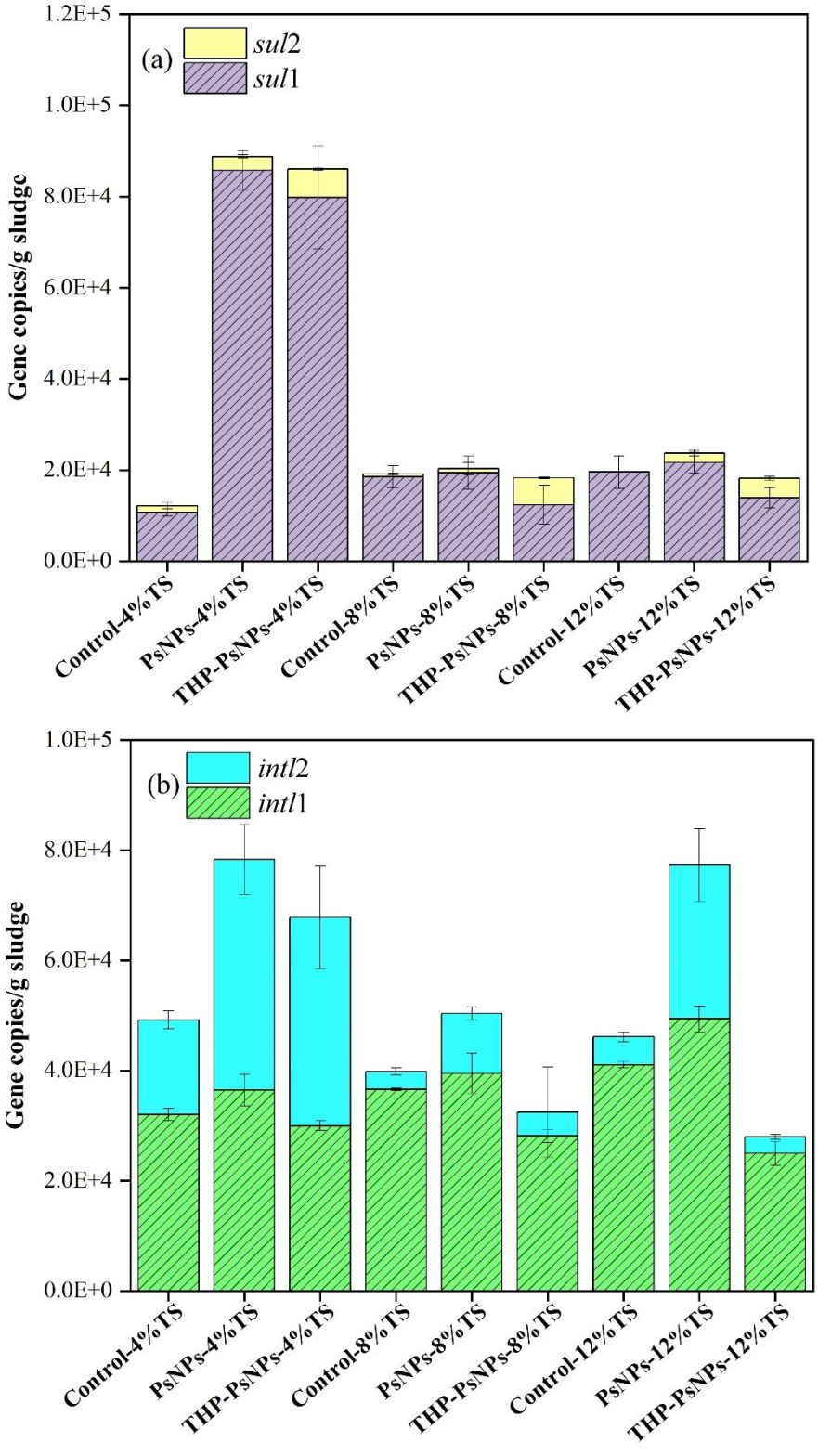
(a)
sul2
sul1
Gene copies/g sludge
1.2E+5
1.0E+5
8.0E+4
6.0E+4
4.0E+4
2.0E+4
0.0E+0
Control-4%TS
PsNPs-4%TS
THP-PsNPs-4%TS
Control-8%TS
PsNPs-8%TS
THP-PsNPs-8%TS
Control-12%TS
PsNPs-12%TS
THP-PsNPs-12%TS
(b)
intl2
intl1
Gene copies/g sludge
1.0E+5
8.0E+4
6.0E+4
4.0E+4
2.0E+4
0.0E+0
Control-4%TS
PsNPs-4%TS
THP-PsNPs-4%TS
Control-8%TS
PsNPs-8%TS
THP-PsNPs-8%TS
Control-12%TS
PsNPs-12%TS
THP-PsNPs-12%TS

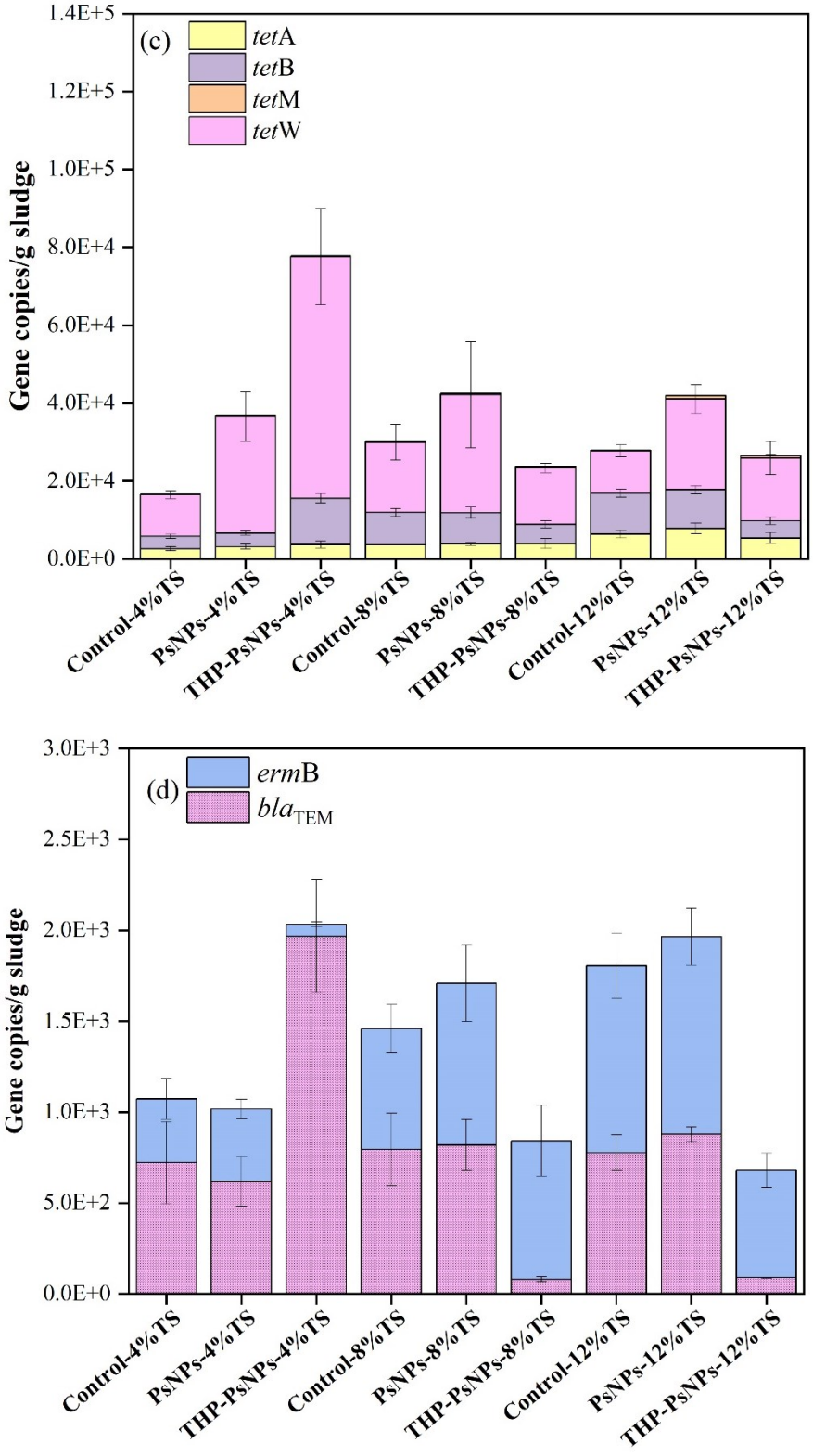
(c)
tetA
tetB
tetM
tetW
Gene copies/g sludge
1.4E+5
1.2E+5
1.0E+5
8.0E+4
6.0E+4
4.0E+4
2.0E+4
0.0E+0
Control-4%TS
PsNPs-4%TS
THP-PsNPs-4%TS
Control-8%TS
PsNPs-8%TS
THP-PsNPs-8%TS
Control-12%TS
PsNPs-12%TS
THP-PsNPs-12%TS
(d)
ermB
bla TEM
Gene copies/g sludge
3.0E+3
2.5E+3
2.0E+3
1.5E+3
1.0E+3
5.0E+2
0.0E+0
Control-4%TS
PsNPs-4%TS
THP-PsNPs-4%TS
Control-8%TS
PsNPs-8%TS
THP-PsNPs-8%TS
Control-12%TS
PsNPs-12%TS
THP-PsNPs-12%TS

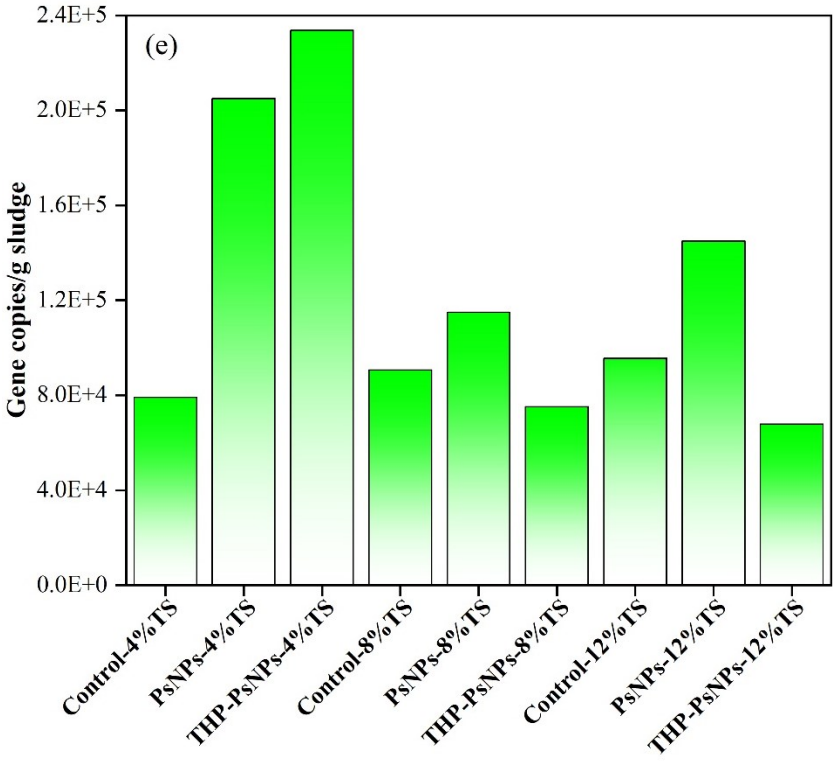

Figure 5.4. (a) Sulfonamide resistance genes, (b) integrons, (c) tetracycline resistance genes, (d) macrolide and β-lactam resistance genes, and (e) total ARGs in digested sludge.

5.3.6. Multivariate Analysis

A multivariate analysis was performed to get more insights into the correlations among TS%, PsNPs, and THP-PsNPs, with ROS, ARGs, and EPS contents. As demonstrated in Fig. 5.5a, TS% has a strong positive correlation with ARGs, EPS-polysaccharides, EPS protein, and ROS, indicating that with increasing TS% from 4 to 12%, the values for all of these parameters substantially increased. Moreover, exposure to PsNPs was positively correlated with EPS-polysaccharides and EPS-protein (Fig. 5.5b), demonstrating that with increasing TS%, polysaccharide and protein secretion increased. However, ARGs and ROS were negatively correlated (r=-0.65 and -0.14) with PsNPs exposure and increasing TS%. As shown in Fig. 2, when TS% increased from 4% to 12%, the ROS level decreased from 16.20% to 8.79%. Thus, results suggest that even though exposure to PsNPs resulted in induced ROS generation, there is an inverse correlation between ROS production and increased TS%. Regarding ARGs, the highest abundance after adding PsNPs was achieved at 4%TS (PsNPs-4%TS) (see Fig. 5.4e), decreasing in PsNPs-

8%TS. However, with further increasing TS% to 12%, a higher total ARGs (compared to PsNPs-8%TS) was attained. Thus, although PsNPs proliferated ARGs abundance (compared to the control), ARGs abundance is negatively correlated with increasing TS%. Moreover, Fig. 5.5c illustrated that total ARGs were negatively (r=-0.87) correlated with THP-PsNPs. This indicates that the application of THP on the samples containing PsNPs mainly decreased ARGs abundance. In contrast, EPS contents and ROS exhibited a positive correlation. For instance, for EPS-polysaccharides and EPS-proteins, a robust positive correlation coefficient (r=1 and 0.99) was attained, indicating that although THP is disintegrating the sludge EPS network, EPS secretion substantially increased with increasing TS%.

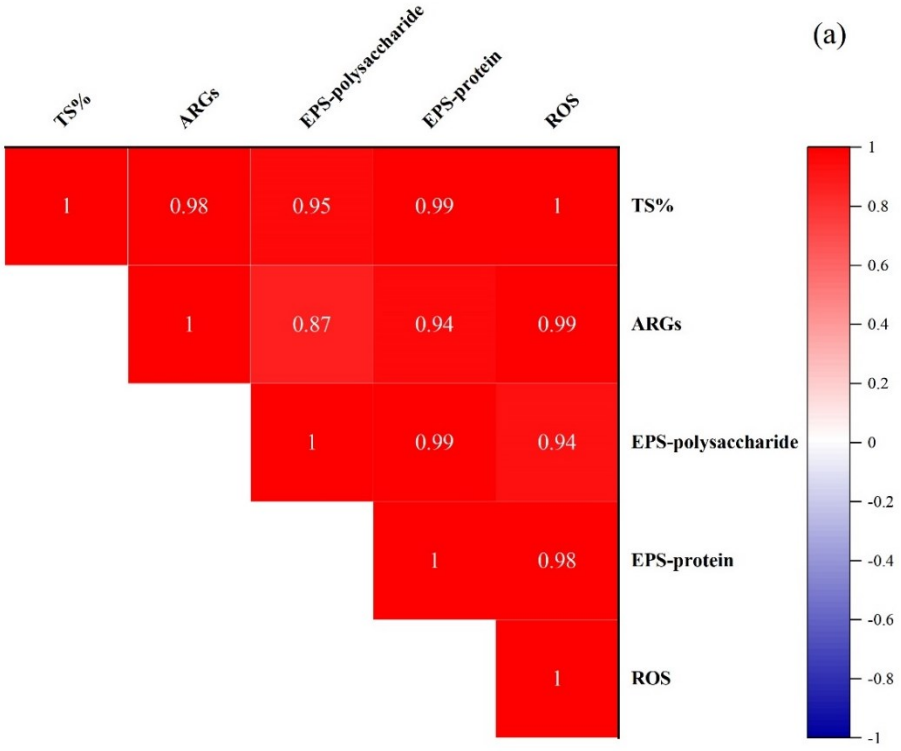

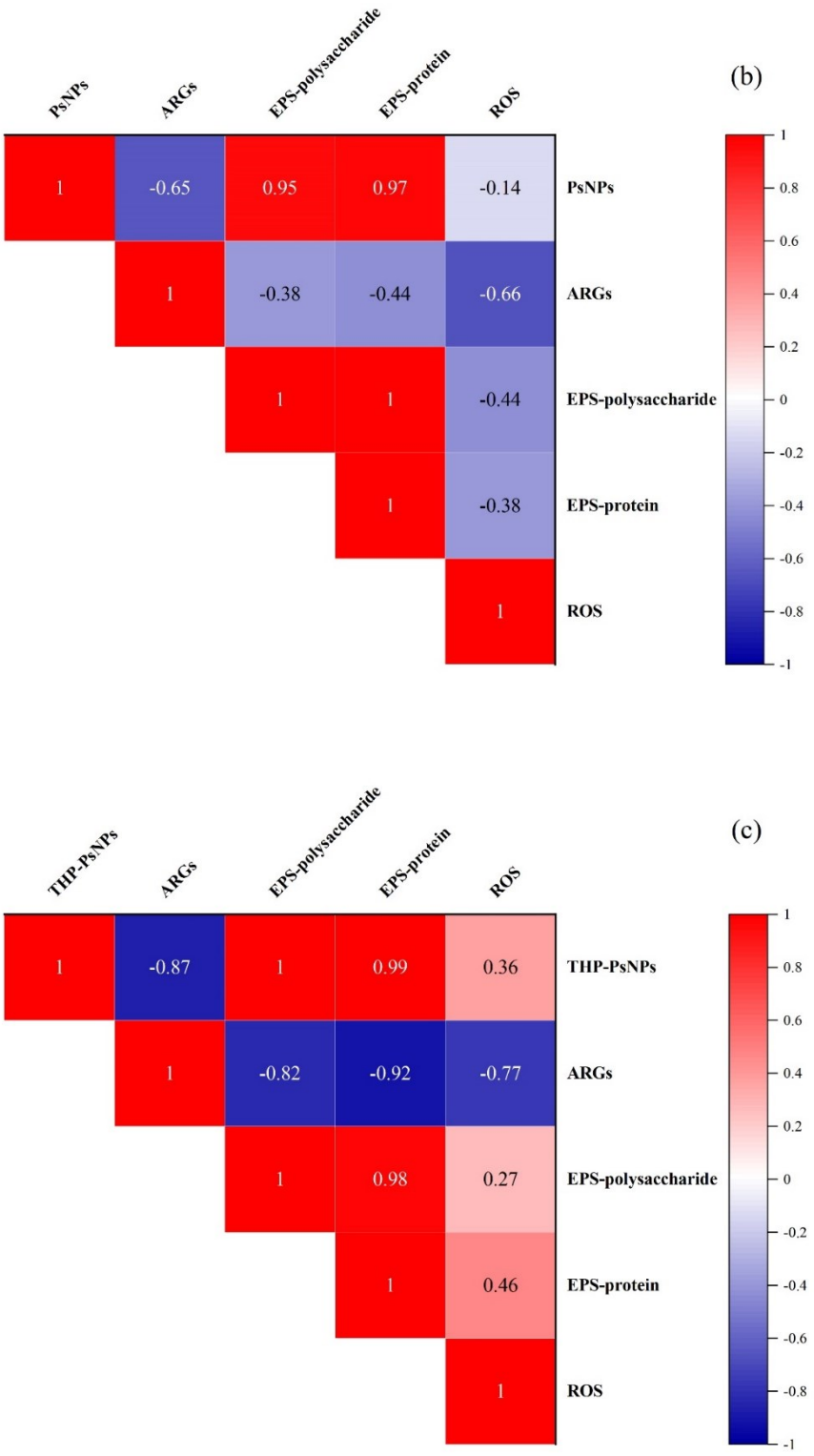

Figure 5.5. Correlation analysis of EPS content, ARGs, and ROS levels based on (a) TS% (4, 8, and 12%), (b) PsNPs (150 µg/L), and (c) THP-PsNPs (160 ºC, 60 min, PsNPs (150 µg/L)).

5.3.7. Principal Component Analysis (PCA)

The PCA was conducted to examine the relative effectiveness, variations, and similarities of TS%, THP, and PsNPs on AD performance. As shown in Fig. 5.6a, PsNPs-12%TS and Control-12%TS were clustered together in the top-left quadrant. EPS-polysaccharides and EPS-proteins vector were shifted towards these two samples indicating a higher EPS secretion at 12%TS. This increased secretion may be due to the microbial self-defense mechanism, as suggested in the literature (Haffiez et al., 2022a; Li et al., 2019). In contrast, samples with 4 and 8%TS (i.e., PsNPs-8%TS, THP-PsNPs-8%TS, PsNPs-4%TS, and THP-PsNPs-4%TS) were grouped together in the top and bottom-right quadrants. The ROS, VFA, and VS removal loading vectors were shifted towards the top-right quadrant, suggesting increased hydrolysis, VS destruction, and ROS generation in PsNPs-8%TS and THP-PsNPs-8%TS. This might be linked to damage to cells and the release of intracellular content after PsNPs exposure (Chen et al., 2021), ultimately leading to decreased methane production, compared to 12% TS samples. Notably, the ARGs loading vector radiated towards the bottom-right quadrant where PsNPs-4%TS and THP-PsNPs-4%TS were positioned, indicating a positive association between these samples and ARGs propagation. The increased ARG abundance in these samples could be associated with the operating conditions of the digester, such as TS content (Ma et al., 2011). Furthermore, Control-4%TS and Control-8%TS were clustered in the bottom-left quadrant. Compared to the controls, applying THP and adding PsNPs, considerably affected the samples with 4 and 8% of TS.

Fig. 5.6b illustrates the PCA of ARGs under different experimental conditions. It can be found that *sul*1, *tet*W, *intl*2, and bla_{TEM} vectors radiated towards the THP-PsNPs-4%TS, indicating that THP might amplify ARG rebounding during subsequent AD. Also, *tet*M, *tet*B, *tet*A, *erm*B, and *intl*1 loading vectors were shifted towards the top-left quadrant, indicating a very high abundance of these genes in PsNPs-8%TS, PsNPs-12%TS, and Control-12%TS. Notably, PsNPs-4%TS and Control-4%TS were grouped in the bottom-right quadrant, and *sul*2 vectors radiated towards them, indicating that lower TS% enhanced the abundance of *sul*2. Overall, most ARGs were radiated toward the four samples located in the top quadrant, suggesting that these samples can play a significant role in ARG propagation.

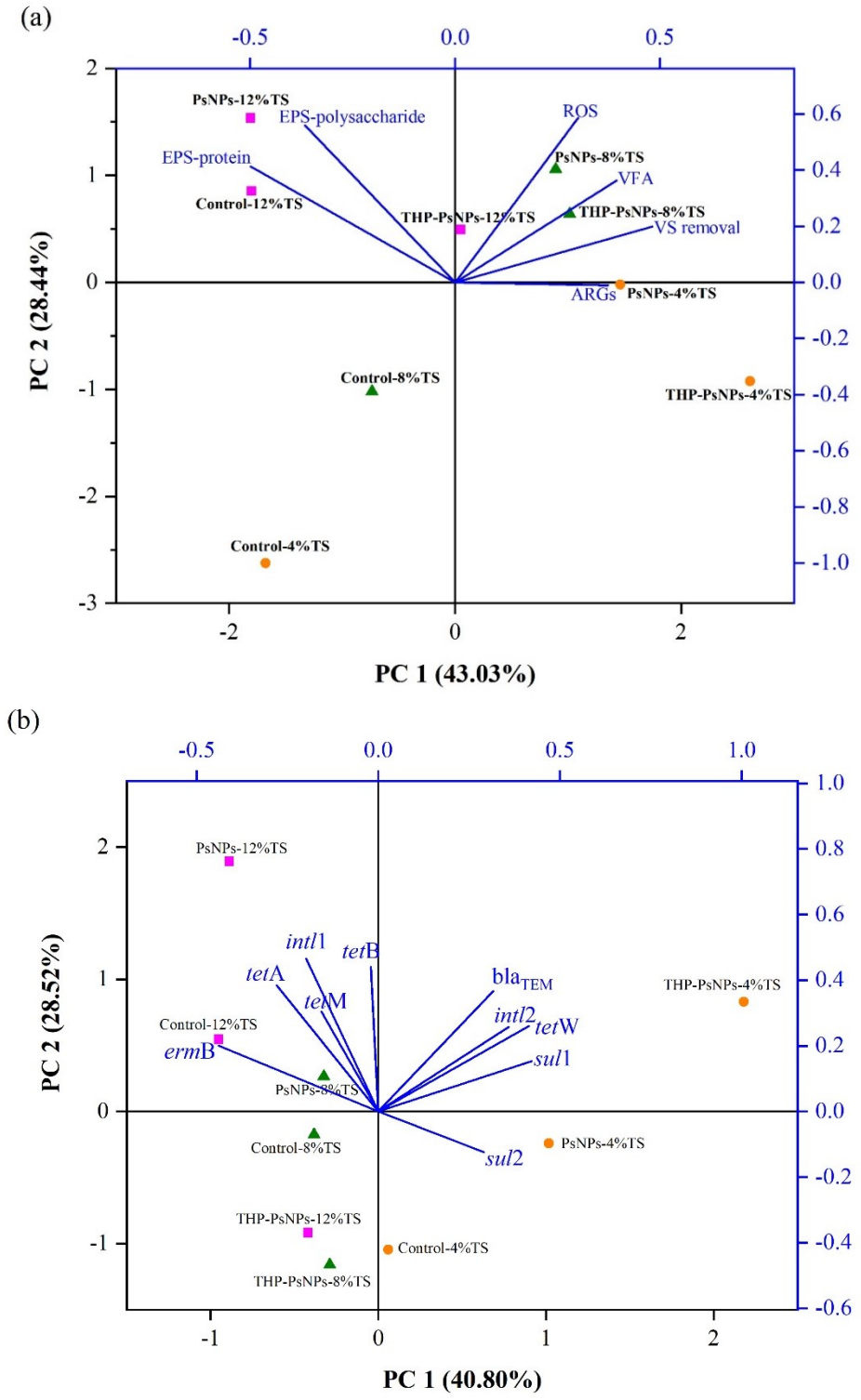

Figure 5.6. (a) PCA of EPS, content, ROS, ARGs, VFA, and VS removal (b) PCA of different ARGs under different experimental conditions (4,8, and 12%TS, PsNPs (150 µg/L), THP (160 ºC and 60 min)).

5.4. Conclusion

The results demonstrated that the oxidative stress of PsNPs would be more intense in anaerobic digesters operated under lower solids content (4% and 8% TS). In contrast, the digester with higher TS content of 12% showed relatively lower ROS levels with sustained methane production, indicating that possibly higher EPS content provided protective barriers. For all TS contents, PsNPs increased ARGs in digestate, with 4% TS showing the highest increase in ARG abundance among PsNPs samples. THP was effective in alleviating oxidative stress of PsNPs at 4-8% TS. However, THP was ineffective in mitigating the ARG abundance of the PsNPs-4%TS sample; instead, it increased ARGs. Nevertheless, THP effectively mitigated the ARG abundance of PsNPs samples under 8% and 12% TS. It was evident that operating AD with THP would be more beneficial for sludge with higher TS% for both energy recovery and remediation of PsNPs and ARGs. This study was focused explicitly on PsNPs, whereas various other types of MPs/NPs are also found in sludge. Thus, the results of this study do not necessarily imply that THP would be effective in reducing stress induced by a wide variety of MPs/NPs. Further research is warranted to understand the efficacy of THP in mitigating oxidative stress caused by exposure to different types of MPs/NPs at varying levels of solids content.

Chapter 6

Low-Temperature Thermal Hydrolysis for Boosting the Performance of Semi-Continuous Anaerobic Digestion of Fermented Primary Sludge and Antibiotic Resistance Genes Management

A version of this chapter will be submitted in a journal for peer-review and publication

6.1. Introduction

Anaerobic digestion (AD) is a widely employed technology in large-scale wastewater treatment plants (WWTPs) for handling and disposal of sludge (Hosseini Koupaie et al., 2018; Mohammad Mirsoleimani Azizi et al., 2021b). AD is considered as an eco-friendly and promising approach that not only helps in decreasing sludge volume but also harnesses the potential of sewage sludge to produce methane-rich biogas (Jianwei Liu et al., 2020; Zhang et al., 2019). The limited availability of readily biodegradable substances in sludge leads to reduced methane generation and prolonged solid retention time (SRT) ranging from 15 to 30 days. In order to overcome these challenges, several pretreatment technologies have been devised to disrupt the structures of sludge, increase the solubility of organic compounds, and improve their biodegradability. These pretreatments primarily focus on enhancing the hydrolysis step, which is considered the rate-limiting in sludge AD, and enhance the overall performance of the AD process (Nazari et al., 2017).

The thermal hydrolysis process (THP) has emerged as a extensively adopted pretreatment method in full-scale AD facilities within WWTPs (Jianwei Liu et al., 2020). This pretreatment approach can be categorized into two main types: high-temperature (>100ºC) and low-temperature (<100ºC) (Kor-Bicakci and Eskicioglu, 2019). Both high-temperature and low-temperature THP methods have been shown to effectively increase the solubilization of particulate organic matter in sewage sludge. However, low-temperature THP, in particular, has received less attention in research despite its lower operating costs, which can significantly enhance the economic feasibility of the process (Appels et al., 2010; Xue et al., 2015). THP offers several advantages, including improved energy and heat recovery, increased acceptance of biosolids, sludge volume reduction

through efficient solids removal, and enhanced dewaterability (Kor-Bicakci and Eskicioglu, 2019; Pilli et al., 2015). Moreover, THP has been shown to be effective in the removal of pathogens from AD digestate (Haffiez et al., 2022a). Recent studies have also demonstrated that THP has the potential to decrease the proliferation of antibiotic resistance genes (ARGs), which is recognized as a global health issue with alarming implications (Haffiez et al., 2023, 2022a). A recent study by Haffiez et al. demonstrated that application of THP on AD of sewage sludge can substantially decrease most of ARGs detected in the sewage sludge under both low and high temperature THP (80 ºC -170 ºC) (Haffiez et al., 2023, 2022a). Notably, prior investigations of THP have predominantly focused on batch mode experiments, while the investigation of its effects on semi-continuous AD of sludge remains limited. Understanding the specific impacts of low-temperature THP on the performance and efficiency of AD systems can provide valuable insights for optimizing the process and maximizing its benefits in sludge management.

Amid growing concerns over reducing nutrient discharge in WWTPs, many full scale facilities have adopted primary sludge (PS) fermentation to generate sludge fermentation liquor rich in volatile fatty acids (VFA). These VFAs serve as an external carbon source that is easily biodegradable, playing a vital role in supporting crucial biological nutrient removal processes, such as biological phosphorus removal and denitrification. (Barua et al., 2019; Liu et al., 2018; Zhou et al., 2021). The solid residue remaining after PS fermentation, known as fermented primary sludge (FPS), is combined with thickened waste activated sludge (TWAS) and subjected to the AD (Mohammad Mirsoleimani Azizi et al., 2021a). Nevertheless, there is currently limited available data concerning the effects of various THP conditions for the anaerobic co-digestion of FPS and TWAS. Recently, we conducted a study to investigate the the influence of different retrofitting schemes involving low-temperature THP (operating at 50-90°C for 30-90 minutes) on an AD facility in a WWTP with primary sludge fermentation under batch mode (Mohammad Mirsoleimani Azizi et al., 2021a). Our findings indicated that the application of low-temperature THP can significantly enhance COD solubilization and subsequently increase methane production by 56% compared to the control (Mohammad Mirsoleimani Azizi et al., 2021a). Nevertheless, based on the literature review, no studies have explored the effects of low-temperature THP on COD solubilization and resulting methane yields during the co-digestion of TWAS and FPS under semi-continuous mode.

Meanwhile, SRT is a crucial operational parameter in AD that plays a significant role in determining the organic loading rate and biomass retention in the digester (Feng et al., 2019; Jianwei Liu et al., 2020). It is essential to monitor SRT periodically in continuous and semi-continuous AD to guarantee the process's performance and stability (Jianwei Liu et al., 2020; Neumann et al., 2018). Proper control and management of the SRT can help optimize the efficiency of methane production and ensure the reliable operation of anaerobic digesters over extended periods. Furthermore, SRT has a pronounced impact on the metabolic rate of anaerobic microorganisms (Montañés Alonso et al., 2016). It is crucial to maintain an adequate SRT to foster the gradual and steady growth of methanogens, as a reduced SRT can impede methane production and disrupt the methanogenesis process (Jianwei Liu et al., 2020). Additionally, a short SRT can carry the risk of microbial washout, leading to the failure of the AD process (Feng et al., 2019; Gil et al., 2018). Thus, maintaining a sufficient SRT is crucial to ensure the stability and performance of AD digesters. However, it is essential to consider that the SRT also affects the size of continuous anaerobic digesters, and in certain scenarios, a shorter SRT may be preferred to reduce digester volume and investment costs, especially in large-scale biogas plants (Gil et al., 2018; Jianwei Liu et al., 2020). Therefore, conducting a thorough investigation into the impact of SRT on anaerobic digestion processes becomes crucial to strike the optimal balance between efficient methane recovery and cost-effectiveness in AD operations.

With these research gaps, the current study conducted a comprehensive investigation into the impact of low-temperature THP on the AD of FPS and TWAS under various SRTs. The effects of THP were evaluated using different retrofitting schemes. Additionally, the study assessed the combined impact of THP and SRTs on AD performance, focusing on methane production, organics solubilization, and the propagation of ARGs.

6.2. Material and method

6.2.1. Experimental set-up.

The study involved the use of three identical glass anaerobic bioreactors (ISES-Canada, Vaughan, ON, Canada) with a capacity of 1.5 liters for working volume and 2 liters for total volume. These bioreactors were equipped with mechanical agitators powered by electric motors

and were stirred at a speed of 200 rpm. To ensure a consistent mesophilic operating condition at a temperature of 37 ± 1 °C, the bioreactors were operated in a water bath (VWR Water bath 28L, 120V, VWR Canada, Mississauga, ON, Canada).

6.2.2. Sludge characteristics

The digested sludge (inoculum), and the AD feed sludge (thickened waste activated sludge (TWAS) and FPS) used in the experiments were obtained from Goldbar WWTP in Edmonton, Alberta, Canada. The digested sludge was collected once during the initial phase of the reactor startup, while the TWAS and FPS were collected monthly. All samples were stored at a temperature of 4 °C in a cold room for a period of 2 to 6 weeks, depending on the sampling frequency. Prior to starting the reactors, the inoculum was pre-incubated for 5 days at 37 °C to allow for the acclimation of microbial communities and degradation of residual organics. The average characteristics of the different types of sludge are provided in Table 6.1.

Table 6.2. Characteristics of substrate and inoculum.

Parameters	**Inoculum**	**Substrate**		
	Digested sludge	**FPS**	**TWAS**	**FPS+TWAS**
TSS (mg/L)	20,000 ± 1,200	62,600 ± 1,400	38,700 ± 1,900	41,600 ± 1,400
VSS (mg/L)	16,400 ± 800	56,400 ± 1,000	34,300 ± 1,700	37,200 ± 1,600
TCOD (mg/L)	29,682 ± 824	89,281 ± 6,868	53,685 ± 3,243	71,483 ± 6,739
SCOD (mg/L)	4,717 ± 44	12,356 ± 687	3,242 ± 26	8,922 ± 2,777
TVFA (mg COD/L)	89 ± 11	8,602 ± 239	925 ± 84	4,763± 295
TAN (mg/L)	1,323 ± 3	181 ± 5	36 ± 3	134 ± 1
pH	6.95 ± 0.01	4.87 ± 0.01	6.1 ± 0.01	5.84 ± 0.04

6.2.3. Low-temperature thermal pre-treatment

The low-temperature-THP of TWAS and FPS was carried out using a 2 L batch hydrothermal reactor (Parr 4848, Max. temperature: 350°C, Max. pressure: 1900 psi, Parr Instrument Company, Moline, IL, USA) (Mohammad Mirsoleimani Azizi et al., 2021a). Each experiment involved adding 900 mL of sample into the reactor, which was tightly sealed. The reactor was heated using a heating jacket that covered the entire reactor. Throughout the process, the sludge was stirred

continuously at a fixed speed of 150 rpm (Mohammad Mirsoleimani Azizi et al., 2021a). The temperature of the sludge was monitored using a thermocouple attached to the reactor. Once the desired temperature (90°C) was reached, the sludge was exposed for the specified target duration (90 min). After the exposure period, the heating was turned off, and cold water was circulated through designated recirculation tubes to rapidly cool the sludge down to room temperature.

6.2.4. Start-up, operation, and experimental phases

During start-up, the inoculum and substrate (mixture of FPS and TWAS with 1:1 volume ratio) were mixed together based on a food-to-microorganisms (F/M) ratio of 2 (g TCOD/g VS). Different test conditions included were (I) control, (II) pretreated TWAS+FPS (scheme1), and (III) pretreated TWAS, and untreated FPS (scheme 2). To ensure anaerobic conditions, the bioreactors were purged with nitrogen gas for 5 min. The reactors were initially operated in batch mode for the first 5 days, where the entire contents were treated as a single batch. After this initial period, the operation mode was switched to a semi-continuous mode. In the semi-continuous mode, the bioreactors were continuously fed with the new substrate while a portion of the digested material was removed. Three different solid residence times (SRTs) were chosen for the experiment: 20, 15, and 10 d. These SRTs represent the amount of time the sludge spends in the bioreactors, simulating different AD conditions. To achieve this, the sludge was introduced into the bioreactors using peristaltic pumps (Longer Pump BT100−2 J, Langer Instruments Corp, Tucson, AZ) at rates of 75, 100, and 150 mL/day. These rates corresponded to specific organic loading rates (OLRs) of 3.57, 4.77, and 7.15 kg COD/m³/day for the 20, 15, and 10-day SRTs, respectively.

To establish a baseline for later comparison, all three reactors underwent an initial operational phase referred to as the "pre-experimental phase." During this phase, all reactors were operated under similar conditions, without the introduction of pretreated sludge. The pre-experimental phase lasted for 30 days and aimed to ensure consistency in biogas yield and quality across all reactors. By confirming this consistency, it provided a reliable baseline for commencing the experimental phase and evaluating the effects of the introduced treatments. Following the completion of the pre-experimental phase, the experimental phase commenced. During this phase, specific reactors received the pretreated sludge according to the desired SRTs of 20, 15, and 10 d. Notably, each SRT lasted for two cycles, and the reactors were operated for a total duration of 120

days. This approach facilitates a reliable comparison of the impact of SRT and THP of retrofitting scheme on AD performance. By systematically evaluating these different factors, their individual contributions to AD performance can be assessed and compared.

6.2.5. Analytical methods

The TSS and VSS were determined using established standard methods. TCOD, SCOD, TAN, and alkalinity levels were measured using HACH reagent kits (HACH Co., Loveland, CO, USA). The pH of the samples was measured using a bench-top pH meter (Accumet AR15, Fisher Scientific, Pittsburgh, PA, USA).

6.2.6. Quantification of antibiotic resistance genes

Quantitative polymerase chain reaction (qPCR) was employed to evaluate the presence of eight commonly observed antibiotic resistance genes (ARGs) in the samples. These genes encompassed tetracycline resistance genes (*tet*A, *tet*B, *tet*W, *tet*X, *tet*Q, and *tet*M), sulfonamide resistance genes (*sul*1, *sul*2), ß-lactam resistance gene (bla_{TEM}, bla_{OXA}), macrolide resistance gene (*erm*C, *erm*B), as well as mobile genetic elements like integrons (*intl*1, *intl*2) and 16S rRNA. The specific primers used for amplifying these genes can be found in the Supporting Information of the study. The protocols for sample preparation, sequencing procedures, and data analysis are available in our previous publications, providing detailed information on these aspects (Haffiez et al., 2022a, 2023; Mirsoleimani Azizi et al., n.d.).

6.3. Results and discussions

6.3.1. Anaerobic digestion performance

Figure 6.1 illustrates the daily methane generation from digesters during a 120-day operation period under different operating conditions. Initially, from days 1 to 30, all reactors ran under the same conditions as a pre-experimental phase, without the addition of PsNPs and THP, to establish a benchmark for future comparisons. During the initial 22 days of operation, methane generation in all digesters exhibited significant fluctuations. Subsequently, in the following week, the daily methane production rate experienced a slight increase and eventually stabilized. This stable production level was maintained for just over a week, between days 22 and 30. The average daily

methane generation in the control, scheme 1, and scheme 2 digesters during this period was comparable, with values of 0.30 ± 0.04, 0.31 ± 0.03, and 0.31 ± 0.03 L $CH_4/L_{reactor}/d$, respectively. Additionally, the methane content in the biogas generated from these reactors was around 52-55% (vol.%). Despite minor fluctuations, all reactors demonstrated comparable methane productivity during this phase, establishing it as the baseline for introducing the pretreated samples.

Starting on day 31, the experimental phase commenced for all reactors with a SRT of 20 d (days 31 to 70). Subsequently, the SRT was reduced to 15 d for the period between days 71 and 100, and further decreased to 10 d for days 101 to 120. The impact of SRT and THP on average methane production is summarized in Table 6.2. The results indicated that as the SRT decreased from 20 days to 10 days, the production of biomethane increased across all reactors. This increase can be attributed to the higher influent of sludge, which provides more organic material to the reactors (Jianwei Liu et al., 2020). Also, it can demonstrates that the available microbial community could metabolize the provided organics and prevents from organic overload (Nges and Liu, 2010). However, despite this increase in biomethane production, the yield of biomethane decreased as the SRT decreased. For instance, in the control reactor, the methane yield decreased from 100.1 to 81.90 and further to 61.34 mL/g COD as the SRT decreased from 20 d to 15 d and 10 d, respectively. The reduction in methane production can be explained by the fact that, although both methane generation and sludge intake increased, the rate of improvement in methane production was not as high as the inflow of incoming organic matter. This finding aligns with several previous studies that have reported similar trends (Jibao Liu et al., 2020b; Jianwei Liu et al., 2020; Nges and Liu, 2010). For instance, Liu et al. studies indicated that while by decreasing SRT from 25 to 15 d, led to an increase in methane production from 70 mL/L·d to 75 mL/L·d, the biomethane yield dropped from 98.9 mL/g VS to 65.6 mL/g VS (Jianwei Liu et al., 2020).

Table 6.2. The impact of SRT and THP on average daily methane production (L $CH_4/L_{reactor}/d$)

	Average daily methane production (L $CH_4/L_{reactor}/d$)		
SRT (d)	**Control**	**Scheme-1**	**Scheme-2**
20	0.36	0.48	0.46
15	0.39	0.54	0.51

10	0.44	0.59	0.55

Regarding the effect of THP on methane production, the results indicated (Fig. 6.1 and Table 6.2) that application of THP can enhance methane production under both scheme 1 and 2, compared to the control. For instance, scheme 1 led to a 34.4% increase in biomethane production compared to the control at an SRT of 20 d. This improvement can be attributed to the increased solubilization of organic content (discussed later) and improved microbial availability facilitated by THP (Mohammad Mirsoleimani Azizi et al., 2021a). Furthermore, when comparing scheme 1 and scheme 2 under the same SRT conditions, it was observed that scheme 1 (0.48-0.59 L $CH_4/L_{reactor}/d$) generated higher methane production than scheme 2 (0.46-0.55 L $CH_4/L_{reactor}/d$). This difference can be related to the synergistic effects of co-digestion and THP application on both TWAS and FPS (Villamil et al., 2020, 2019). This finding is consistent with our previous study which was performed under the batch mode (Mohammad Mirsoleimani Azizi et al., 2021a). Additionally, it was noted that the increase in methane production after applying THP was more pronounced when the SRT was decreased from 20 d to 15 d (37.9% vs. 34.4 %). Overall, the results indicate that scheme 1 with an SRT of 15 d yielded more methane than the control with an SRT of 20 d. Therefore, in terms of methane yield, the application of THP has the potential to decresae the SRT of sludge AD by more than 25%. Notably, the superior performance of the digester at an SRT of 15 d can be attributed to the establishment of a favorable equilibrium. At this SRT, the AD system may have provided the microbial community with sufficient time to adapt and effectively utilize the available organic matter. This optimal balance likely resulted in enhanced methane production compared to the longer SRT of 20 d which had a lower OLR. Also, the better performance compared to 10 d SRT could be related to this fact that under this SRT, microbial community did not have adequate time for optimal growth and substrate utilization. These findings underscore the importance of optimizing operating conditions and considering the interactions between SRT, and THP to maximize methane yield and enhance the performance of AD processes.

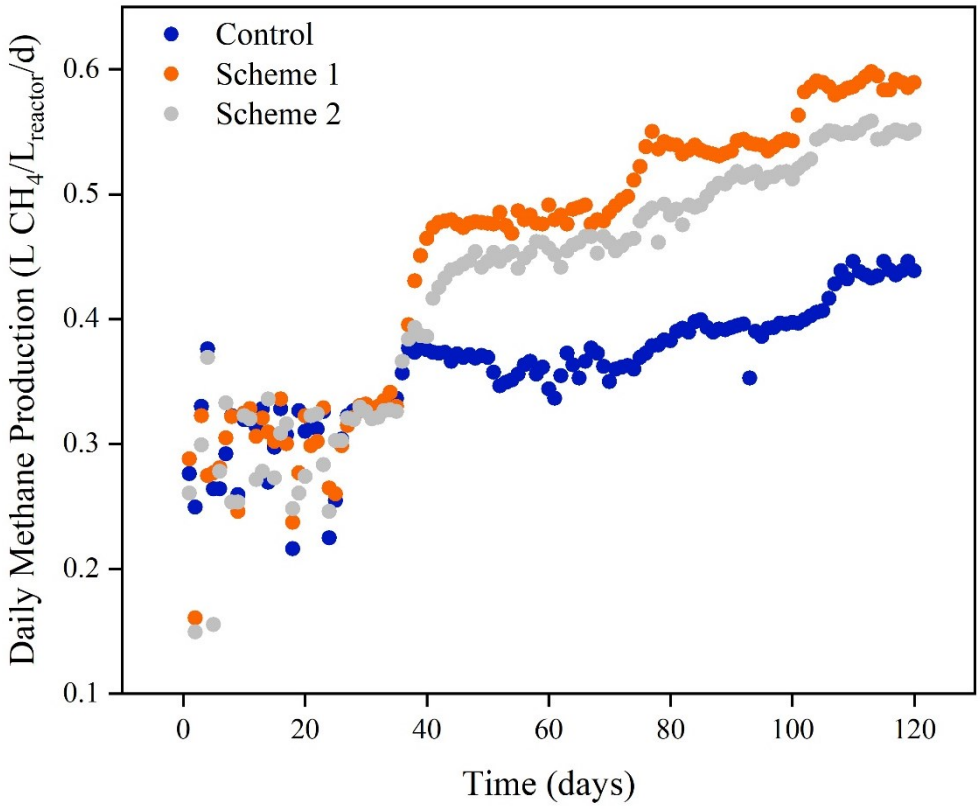

Figure 6.1. Daily biomethane production under different operating conditions.

6.3.2. Organic matters solubilization and removal

Fig. 6.2 illustrates the impact of low-temperature THP on the solubilization of organic content. After THP at 90°C, SCOD concentrations increased to 19,586 and 15,265 mg/L under scheme 1 and 2, respectively, representing a solubilization efficiency of 16.45% and 22.31% (Fig. 6.2a). This rise in SCOD indicates the decomposition of particulate biopolymers (proteins, lipids, and carbohydrates) into soluble monomers as well as the release of water-soluble components following THP (Appels et al., 2010; Xue et al., 2015). However, TCOD concentrations remained constant, suggesting that there was no volatilization of organics during the process. (Mohammad Mirsoleimani Azizi et al., 2021a). Comparing the two schemes, scheme-2 exhibited marginally greater COD solubilization performance than scheme-1, possibly due to the distinct characteristics between TWAS + FPS and TWAS (Mohammad Mirsoleimani Azizi et al., 2021a). Additionally, THP led to decreased TSS and VSS concentrations in the pretreated samples, with VSS solubilization reaching 24.43% and 23.56% for scheme-1 and 2, respectively (Fig. 6.2b).

In Fig. 6.2c, the TVFA concentration in scheme 1 raised from 2,934 mg COD/L (raw TWAS+FPS) to 3,681 mg COD/L after THP. Similarly, scheme 2 (TWAS only) exhibited an increase in TVFA to 1,072 mg COD/L, which was 1.94 times higher than the raw TWAS. The elevated VFAs are ascribed to the breakdown of unsaturated lipids during the process (Liao et al., 2018; Wilson and Novak, 2009). However, THP application on scheme-1 was less efficient compared to scheme-2, likely due to the fermentation process in FPS, which had already degraded a significant portion of unsaturated lipids into VFAs, making the remaining portion less susceptible to degradation under low-temperature THP (Mohammad Mirsoleimani Azizi et al., 2021a).

In comparison to the raw sludge, all pretreated samples exhibited an increase in TAN concentrations (Fig. 6.2d). In scheme-1 (TWAS + FPS), the pretreated sample showed TAN concentrations of 234 mg/L, which were 2.1 times higher than the control (108 mg/L). Similarly, in scheme-2 (TWAS only), THP led to a significant enhancement (8.85 times) in TAN concentrations compared to the raw TWAS (36 mg/L). This rise in TAN concentrations can be attributed to the hydrolysis of nitrogenous compounds (such as proteins, amino acids, urea, etc.) during THP, which increases ammonia levels. (Bougrier et al., 2008). Despite the significant increase in TAN after THP treatment, TAN levels in both pretreated samples remained below inhibitory TAN concentrations (4.2 g/L) that have been previously reported for AD (Haffiez et al., 2022a).

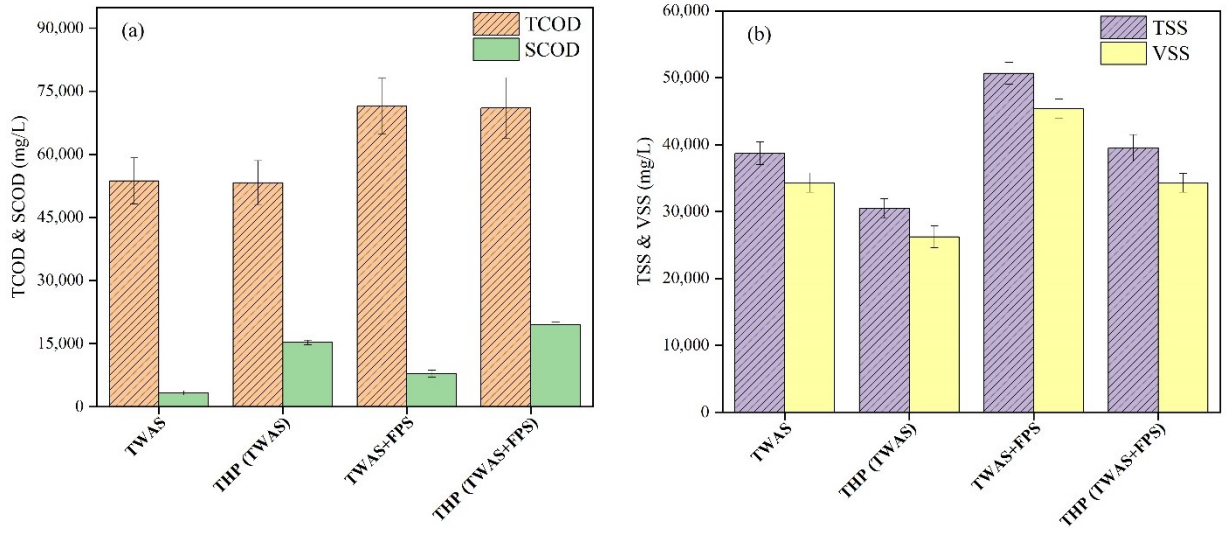

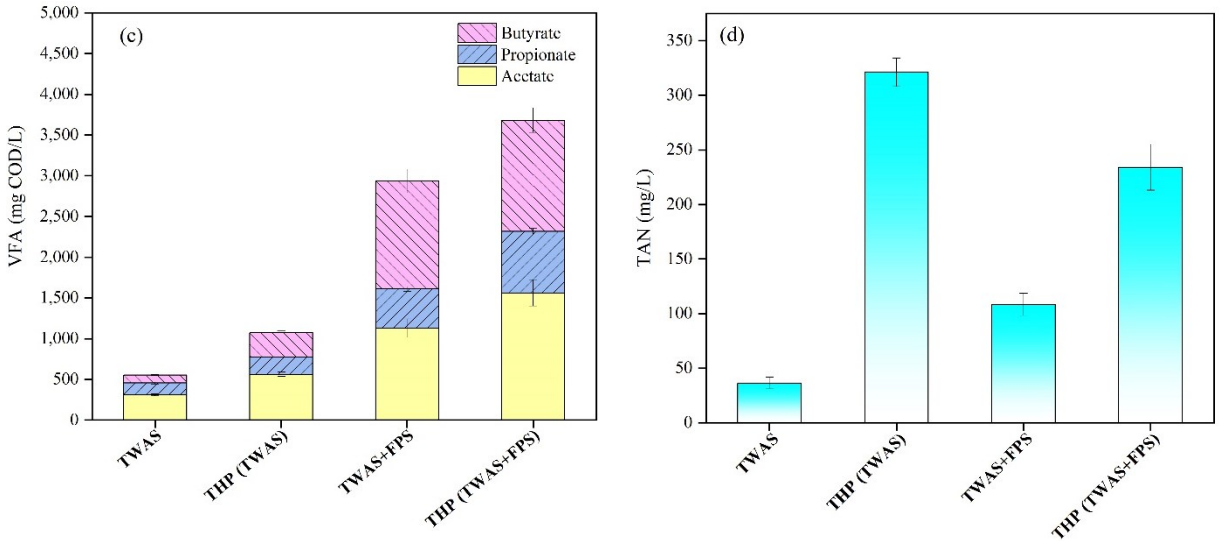

Figure 6.2. The effect of low-temperature THP on organic matters concentration under different operating condition (a) TCOD and SCOD, (b) TSS and VSS, (c) VFA, (d) TAN.

Figure D1 demonstrates effluent TSS, VSS, TCOD, and SCOD under different operating conditions. The results indicated that the removal efficiency of VSS and TCOD decreased with the reduction of SRT in all reactors. For instance, VSS reduction in control was 45.76, 43.52, and 41.75% under 20, 15, and 10 d SRT, respectively (Fig. D1a). Notably, it is generally considered acceptable for sludge digestion processes operating under mesophilic conditions to achieve a 40-60% reduction in VS (Nges and Liu, 2010). Following the application of THP, there was an improvement in COD removal compared to the control reactor (Fig. D1b). This enhancement can be ascribed to the decomposition and hydrolysis of macromolecular compounds, such as proteins, lipids, and carbohydrates, into soluble monomers facilitated by THP (Appels et al., 2010; Xue et al., 2015). The observed increase in VSS and COD removal aligns with the methane production profiles. When evaluating the theoretical methane yield of 395 mL CH_4/g $COD_{removed}$ at 37 ˚C, the COD mass balances, calculated using the experimental methane production and TCOD removal data, showed a closure of 90% to 105% for the control, scheme 1, and scheme 2 reactors, emphasizing data reliability (Table S1). Moreover, in all three reactors, the effluent's concentration of TVFA showed a decline, likely attributed to the conversion of VFA to methane during the AD process (Fig. D1c). Interestingly, the pretreated samples exhibited higher VFA concentrations in the effluent compared to the control, with decreasing SRT leading to increased VFA concentration. This finding is consistent with previous studies in the literature (Jianwei Liu et al., 2020; Nges and

Liu, 2009). Additionally, during AD, further hydrolysis resulted in TAN concentrations of 1,346-1,853 mg/L in the digestate samples (Fig. D1d). The reduction of SRT correlated with an increase in TAN concentrations in all three reactors, with this effect being more pronounced in the pretreated samples. Notably, no evidence of system acidification was observed, as the concentration of VFAs remained relatively low, and the presence of TAN provided effective buffering capacity.

6.3.3. Antibiotic resistance genes

In this study, the presence of targeted ARGs including *tet*A, *tet*B, *tet*W, *tet*X, *tet*Q, *tet*M, *sul*1, *sul*2, bla_{TEM}, bla_{OXA}, *erm*B, *erm*C, and MGEs (*intl*1 and *intl*2) was investigated in the digestate (Fig 6.3a-d). Among these ARGs, *sul*1 (31.4%-41.1%), *tet*W (22.1%-43.8%), and *intl*1 (5.6%-11.8%) were found to be the most abundant across all reactors. Interestingly, decreasing SRT from 20 to 15 and 10 d resulted in a higher abundance of most ARGs in the digesters. For example, in the control reactor with an SRT of 20 d, the abundance of *tet*W was 3.91×10^4 copies/g sludge, whereas it increased to 4.11×10^4 and 4.32×10^4 copies/g sludge under 15 and 10 d SRT, respectively (Fig. 3a). A similar pattern was noticed for most ARGs, with the exception of bla_{TEM} and *erm*C (Fig .3d and e). Overall, 1.16×10^{10}, 9.71×10^9, and 8.84×10^9 copies/g sludge of total ARGs was detected in the control under 20, 15, and 10 d SRT (Fig. 3f). These findings are consistent with previous studies reported in the literature (Haffiez et al., 2022b; Ma et al., 2011; Sun et al., 2019). The lower abundance of ARGs observed at longer SRTs can be attributed to factors such as reduced microbial diversity and the development of oligotrophic conditions over extended residence times (Haffiez et al., 2022b; Sun et al., 2019). Under these conditions, some Antibiotic-Resistant Bacteria (ARB) may be reduced, and the likelihood of new cell reproduction could be limited (Qian et al., 2021). Additionally, higher rates of antibiotic biodegradation may occur during longer residence times, contributing to the lower abundance of ARGs (Haffiez et al., 2022b; Nnadozie et al., 2017).

Notably, the application of THP led to decrease in the abundance of most targeted ARGs in scheme-1 and scheme-2, compared to the control across three different SRTs. The frequently detected Mobile Genetic Elements (MGEs) *intl*1 and *intl*2, known for their involvement in horizontal gene transfer (HGT), exhibited substantial reductions in pretreated samples. For

instance, under 20 d SRT, the abundance of *intl*1 decreased from 6.61×10^3 copies/g sludge (control) to 4.59×10^3 and 6.01×10^3 copies/g sludge in scheme-1 and scheme-2, respectively (Fig. 3c). Likewise, *tet*W abundance decreased from 6.61×10^3 copies/g sludge to 2.36×10^4 and 3.38×10^4 copies/g sludge in scheme-1 and scheme-2, respectively (Fig. 6.3a). The similar trend was also observed for *sul*1 and *sul*2 (Fig. 6.3b). Nonetheless, bla_{TEM} abundance increased by 1.07 and 1.55-fold in scheme-1 and scheme-2, respectively (Fig. 6.3d). This increase in ARG abundance suggests a rebounding effect after THP, as reported in previous studies (Haffiez et al., 2023, 2022a). Some specific ARG host microbes can resist harsh environmental conditions during THP by forming endospores to endure stressful conditions (Haffiez et al., 2022a; O'sullivan et al., 2015). Indeed, after the return of favorable conditions, these endospores can germinate, releasing active bacteria and promoting their proliferation (Rampelotto, 2010). Overall, a substantial reduction of up to 43% (compared to control) in total ARGs was observed in scheme 1 and 2 under different SRTs. This reduction in ARGs after the application of THP can be attributed to a decrease in potential hosts carrying multiple ARGs, as previously observed (Haffiez et al., 2022a).

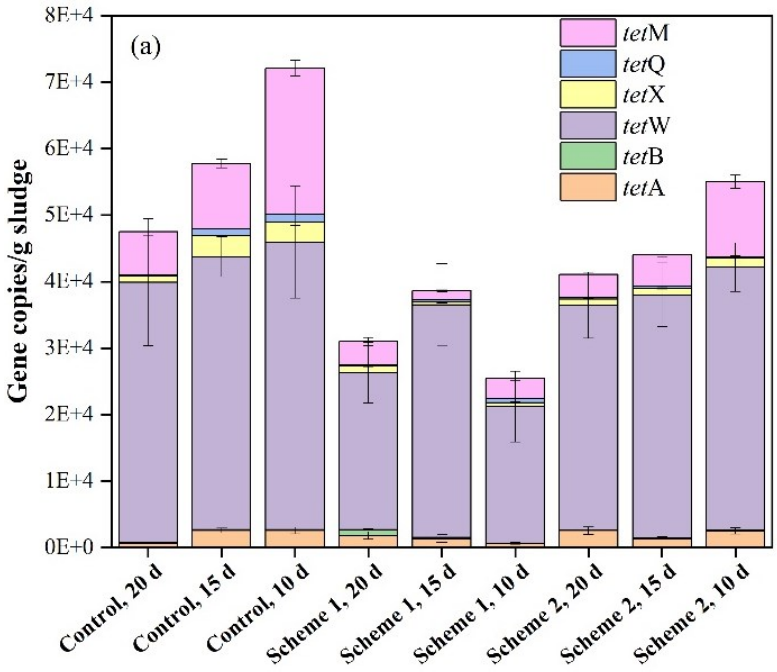

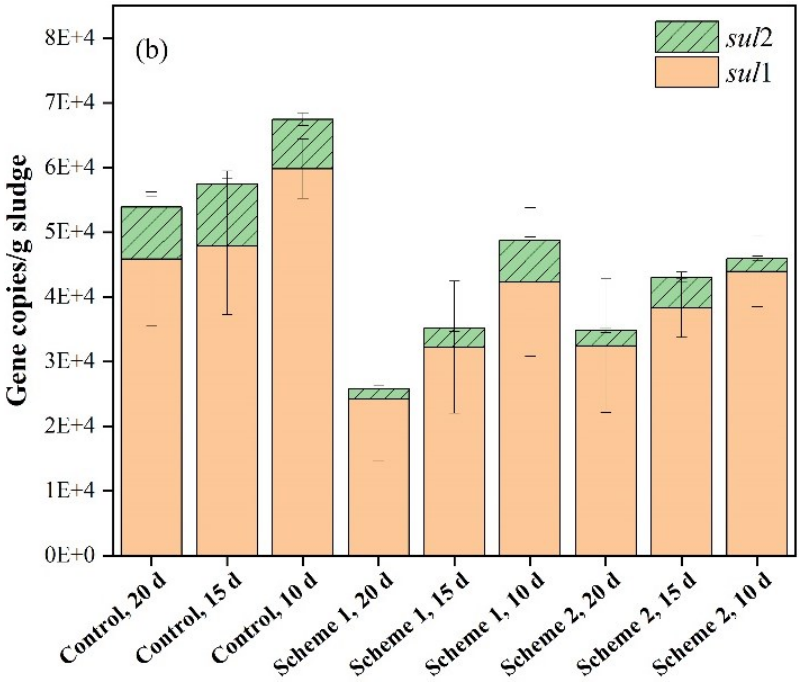
(b)
sul2
sul1
Gene copies/g sludge
8E+4
7E+4
6E+4
5E+4
4E+4
3E+4
2E+4
1E+4
0E+0
Control, 20 d
Control, 15 d
Control, 10 d
Scheme 1, 20 d
Scheme 1, 15 d
Scheme 1, 10 d
Scheme 2, 20 d
Scheme 2, 15 d
Scheme 2, 10 d

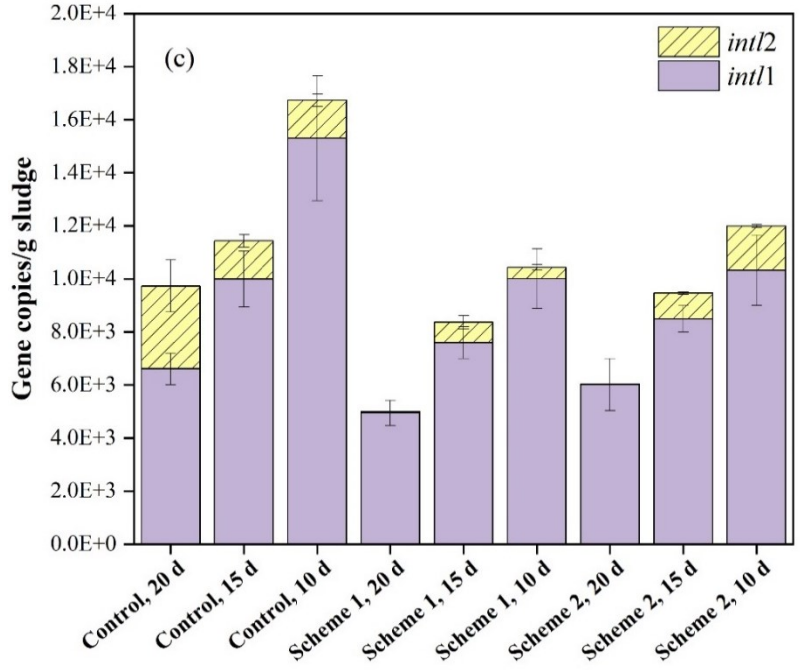
(c)
intl2
intl1
Gene copies/g sludge
2.0E+4
1.8E+4
1.6E+4
1.4E+4
1.2E+4
1.0E+4
8.0E+3
6.0E+3
4.0E+3
2.0E+3
0.0E+0
Control, 20 d
Control, 15 d
Control, 10 d
Scheme 1, 20 d
Scheme 1, 15 d
Scheme 1, 10 d
Scheme 2, 20 d
Scheme 2, 15 d
Scheme 2, 10 d

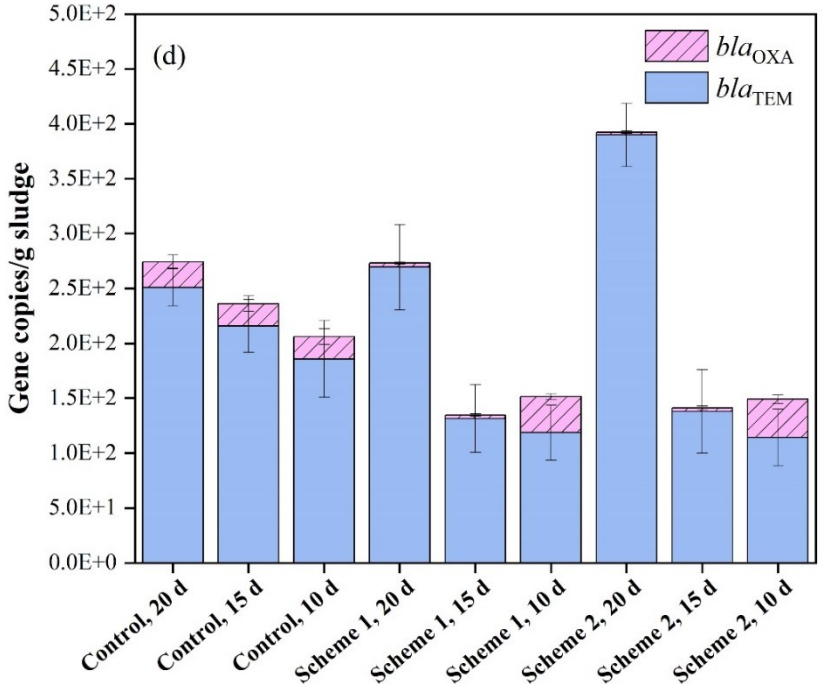
(d)
bla_{OXA}
bla_{TEM}
Gene copies/g sludge
5.0E+2
4.5E+2
4.0E+2
3.5E+2
3.0E+2
2.5E+2
2.0E+2
1.5E+2
1.0E+2
5.0E+1
0.0E+0
Control, 20 d
Control, 15 d
Control, 10 d
Scheme 1, 20 d
Scheme 1, 15 d
Scheme 1, 10 d
Scheme 2, 20 d
Scheme 2, 15 d
Scheme 2, 10 d

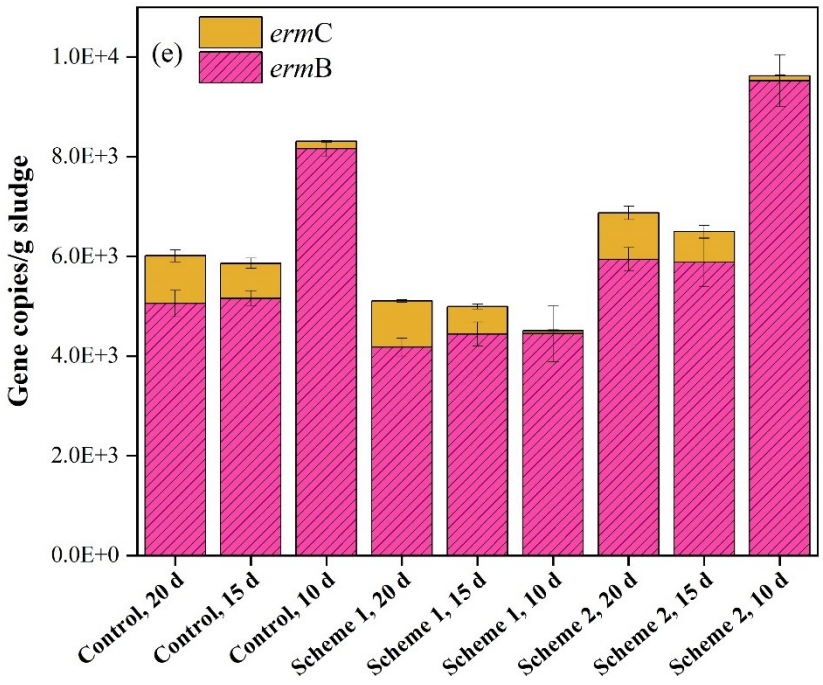
(e)
ermC
ermB
Gene copies/g sludge
1.0E+4
8.0E+3
6.0E+3
4.0E+3
2.0E+3
0.0E+0
Control, 20 d
Control, 15 d
Control, 10 d
Scheme 1, 20 d
Scheme 1, 15 d
Scheme 1, 10 d
Scheme 2, 20 d
Scheme 2, 15 d
Scheme 2, 10 d

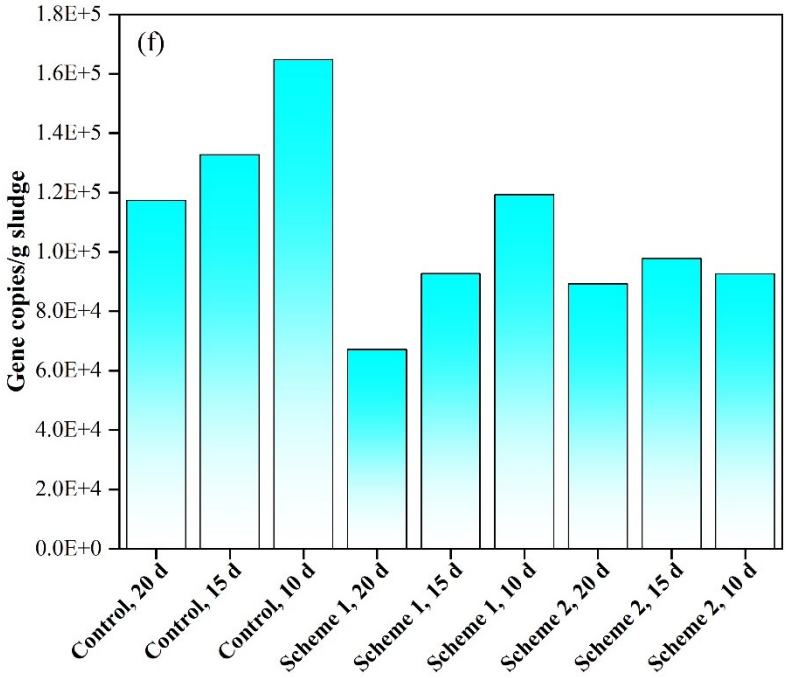

Figure 6.3. Concentrations of (a) tetracycline (*tet*) resistance genes, (b) sulfonamide (*sul*) resistance genes, (c) integron (*intl*), (d) ß-lactam (bla) resistance genes, (e) macrolide (erm) resistance genes, and (f) total ARGs under different experimental conditions.

To gain further insight into the microbiome's capacity to harbor ARGs in the digestate, the abundance of 16S rRNA gene copies was measured (Haffiez et al., 2022a). As depicted in Fig. D2, the THP samples exhibited a notable decrease in the number of 16S rRNA gene copies compared to the control. This suggests the potential disruption or elimination of potential hosts for ARGs after THP treatment, which may contribute to the reduction in ARGs proliferation (Azizi et al., 2022). In conclusion, the application of THP showed promising results in decreasing the abundance of targeted ARGs. These findings highlight the potential of THP as a strategy to mitigate ARGs dissemination in AD systems.

6.4. Conclusion

This study explored the impact of two low-temperature THP schemes on methane generation during co-digestion of TWAS and FPS under different SRTs. Results showed that decreasing SRT led to reduced methane yield, but THP significantly enhanced methane production by up to 37.9% in scheme-1 (TWAS+FPS) and 31.2% in scheme-2 (TWAS only) under 15 d SRT. Comparing the

methane yield in the control and pretreated samples, the implementation of THP has the capability to shorten the SRT of sludge AD by more than 25%, thus accelerating the digestion process. Furthermore, decreasing SRTs lead to the ARGs proliferation whereas THP effectively decreased the abundance of most ARGs, showing promise in mitigating antibiotic resistance in AD process. These findings highlight THP's potential for sustainable sludge management. Further research is needed to optimize THP implementation and understand underlying mechanisms.

Chapter 7

Exploring the Potential of Thermal Hydrolysis to Mitigate Oxidative Stress from Polystyrene Nanoplastics during Semi-continuous Anaerobic Digestion

A version of this chapter will be submitted in a journal for peer-review and publication

7.1. Introduction

The widespread production, usage, and improper disposal of plastics have resulted in a concerning environmental issue: the widespread presence of microplastics (MPs) and nanoplastics (NPs) in various ecosystems (Cole et al., 2011). MPs are particles with sizes less than 5 mm, while NPs range from 1 to 1000 nm (Al-Sid-Cheikh et al., 2018; Wei et al., 2020). These particles have been detected in oceans, freshwater, soils, polar regions, etc., posing significant threats to the environment (Guo et al., 2020; J. Sun et al., 2019). Even more concerning is the recent discovery of MPs/NPs in human placentas, lung tissues, and blood, raising potential health risks (Jenner et al., 2022). With millions of tons of plastic produced annually, the problem continues to escalate, leading to further fragmentation and generation of MPs. Additionally, NPs are intentionally manufactured for various applications, contributing to their discharge into the environment (Lehner et al., 2019; M. Hernandez et al., 2017). Due to their small size, NPs have a higher potential to adsorb and desorb harmful substances, affecting aquatic organisms and potentially transferring toxins through the food chain (Tourinho et al., 2010). The existence of MPs/NPs in different ecosystems emphasizes the urgency of addressing plastic pollution's pervasive impacts on both the environment and public well-being.

Wastewater treatment plants (WWTPs) have been identified as the main sources of MPs/NPs discharge into the ecosystem (Azizi et al., 2022). Notably, during different treatment processes, WWTPs can effectively eliminate up to 99% of influent MPs/NPs (Anne Marie Mahon et al., 2017). The primary removal mechanism involves capturing MPs/NPs in sewage sludge, where reports have indicated MPs/NPs concentrations ranging between 4.2×10^3 to 6.4×10^6 particles/kg of dry solids (Chand et al., 2022). Alongside MPs/NPs, sewage sludge encompasses leftover antibiotics and antibiotic resistance genes (ARGs) with potential environmental implications

(Azizi et al., 2023; Dai et al., 2020a). Given the substantial surface area and hydrophobic characteristics of MPs/NPs, they have the potential to serve as harbors for diverse contaminants like antibiotics and ARGs, further complicating the environmental impact of their presence in WWTPs' effluent and sewage sludge (Mohammad Mirsoleimani Azizi et al., 2021b).

Anaerobic digestion (AD) serves as a broadly adopted method for sludge stabilization, resource recovery, producing valuable methane-rich biogas (Dastyar et al., 2021b; Pereira de Albuquerque et al., 2021). Moreover, the success of AD relies on crucial operational parameters like the Solids Retention Time (SRT). The SRT, which determines organic loading rates and biomass retention in the digester, holds notable importance in maintaining the process's performance and stability (Feng et al., 2019; Jianwei Liu et al., 2020). Optimizing SRTs is essential in continuous and semi-continuous AD systems to ensure reliable digester operation over extended periods (Jianwei Liu et al., 2020; Neumann et al., 2018). Nevertheless, recent attention has focused on the potential influence of MPs/NPs on the AD process (He et al., 2021). Studies have shown that these particles can significantly hinder methane production through various mechanisms, such as releasing of harmful additives, induction of reactive oxygen species (ROS), and inhibition of crucial enzyme activities (Azizi et al., 2022; Mohammad Mirsoleimani Azizi et al., 2021b). Moreover, certain NPs, like polystyrene nanoplastics (PsNPs), have been found to directly damage cells through penetration (Mohammad Mirsoleimani Azizi et al., 2021b). It is crucial to comprehend the implications of MPs/NPs on AD under different SRTs, as they can disrupt the operational stability of digesters and impact the dissemination of antibiotic resistance genes (ARGs) by land application of digestate (Azizi et al., 2022).

The thermal hydrolysis process (THP) stands as an extensively adopted technique for pre-treating sludge in large-scale AD facilities (Mohammad Mirsoleimani Azizi et al., 2021a). It offers several key benefits, including increased biogas recovery through enhanced hydrolysis, high solids removal, pathogen elimination, and improved biosolids dewatering capabilities (Jeong et al., 2019). Moreover, harnessing heat recovery from thermally hydrolyzed sludge presents a remarkable opportunity to reduce operational expenses (Mohammad Mirsoleimani Azizi et al., 2021a). Notably, THP before AD has decreased the induced stress caused by MPs/NPs throughout the digestion process (Haffiez et al., 2022a). Recent research by Azizi et al. demonstrated that THP could offer a dual advantage of alleviating the negative effects of PsNPs in AD and reducing ARG

propagation that PsNPs might promote (Azizi et al., 2022). By effectively managing the induced-stress caused by MPs/NPs, THP offers a promising approach to ensure the continued efficacy of the AD process. However, despite its advantages, previous investigations of THP have primarily focused on batch mode experiments, with limited exploration of its effects on the semi-continuous AD of sludge containing PsNPs. Further investigation is warranted to fully comprehend the capability of THP in managing PsNPs and induced-stress while maximizing its benefits in AD facilities.

Given these research gaps, this study represents the first systematic investigation into the effect of THP on AD of sewage sludge when subjected to PsNPs under semi-continuous mode at different SRTs. The main focus was to compare the effects of adding sludge exposed to PsNPs with thermally pretreated (90°C) sludge containing PsNPs on AD performance under different SRTs (20, 15, and 10 d). The effectiveness of THP was evaluated by examining its potential to mitigate oxidative stress and hinder the proliferation of ARGs in the AD process.

7.2. Material and methods

7.2.1. Experimental set-up

The study involved the use of three identical glass anaerobic bioreactors (ISES-Canada, Vaughan, ON, Canada) with a capacity of 1.5 liters for working volume and 2 liters for total volume. These bioreactors were equipped with mechanical agitators powered by electric motors and were stirred at a speed of 200 rpm. To maintain a consistent mesophilic operating condition at a temperature of 37 ± 1 °C, the bioreactors were operated in a water bath (VWR Water bath 28L, 120V, VWR Canada, Mississauga, ON, Canada).

7.2.2. Sludge characteristics

The digested sludge (inoculum), and the AD feed sludge (thickened waste activated sludge (TWAS) and FPS) used in the experiments were obtained from Goldbar WWTP in Edmonton, Alberta, Canada. The digested sludge was collected once during the initial phase of the reactor startup, while the TWAS and FPS were collected monthly. All samples were stored at a temperature of 4 °C in a cold room for a period of 2 to 6 weeks, depending on the sampling

frequency. Prior to starting the reactors, the inoculum was pre-incubated for 5 days at 37 °C to allow for the acclimation of microbial communities and degradation of residual organics. The average characteristics of the different types of sludge are provided in Table 7.1.

Table 7.3. Characteristics of substrate and inoculum.

Parameters	**Inoculum**	**Substrate**		
	Digested sludge	**FPS**	**TWAS**	**FPS+TWAS**
TSS (mg/L)	20,000 ± 1,200	62,600 ± 1,400	38,700 ± 1,900	41,600 ± 1,400
VSS (mg/L)	16,400 ± 800	56,400 ± 1,000	34,300 ± 1,700	37,200 ± 1,600
TCOD (mg/L)	29,682 ± 824	89,281 ± 6,868	53,685 ± 3,243	71,483 ± 6,739
SCOD (mg/L)	4,717 ± 44	12,356 ± 687	3,242 ± 26	8,922 ± 2,777
TVFA (mg COD/L)	89 ± 11	8,602 ± 239	925 ± 84	4,763± 295
TAN (mg/L)	1,323 ± 3	181 ± 5	36 ± 3	134 ± 1
pH	6.95 ± 0.01	4.87 ± 0.01	6.1 ± 0.01	5.84 ± 0.04

7.2.3. Low-temperature thermal pre-treatment

The low-temperature-THP of TWAS and FPS was carried out using a 2 L batch hydrothermal reactor (Parr 4848, Max. temperature: 350°C, Max. pressure: 1900 psi, Parr Instrument Company, Moline, IL, USA) (Mohammad Mirsoleimani Azizi et al., 2021a). Each experiment involved adding 900 mL of sample into the reactor, which was tightly sealed. The reactor was heated using a heating jacket that covered the entire reactor. Throughout the process, the sludge was stirred continuously at a fixed speed of 150 rpm (Mohammad Mirsoleimani Azizi et al., 2021a). The temperature of the sludge was monitored using a thermocouple attached to the reactor. Once the desired temperature (90°C) was reached, the sludge was exposed for the specified target duration (90 min). After the exposure period, the heating was turned off, and cold water was circulated through designated recirculation tubes to rapidly cool the sludge down to room temperature.

7.2.4. Start-Up, operation, and experimental phases

During start-up, the inoculum and substrate (mixture of FPS and TWAS with 1:1 volume ratio) were mixed together based on a food-to-microorganisms (F/M) ratio of 2 (g TCOD/g VS). Different test conditions included were (I) control, (II) PsNPs amended sludge (mixture of FPS and TWAS with 1:1 volume ratio), and (III) pretreated PsNPs-amended sludge (THP-PsNPs). For PsNPs (50 nm, 2.5% solids (w/v) aqueous suspension, density = 1.06 g/cm3) exposure experiments, 150 µg/L of PsNPs were prepared and added to the reactor. To ensure anaerobic conditions, the bioreactors were purged with nitrogen gas for 5 min. The reactors were initially operated in batch mode for the first 5 days, where the entire contents were treated as a single batch. After this initial period, the operation mode was switched to a semi-continuous mode. In the semi-continuous mode, the bioreactors were continuously fed with the new substrate while a portion of the digested material was removed. Three different solid residence times (SRTs) were chosen for the experiment: 20, 15, and 10 d. These SRTs represent the amount of time the sludge spends in the bioreactors, simulating different AD conditions. To achieve this, the sludge was introduced into the bioreactors using peristaltic pumps (Longer Pump BT100−2 J, Langer Instruments Corp, Tucson, AZ) at rates of 75, 100, and 150 mL/day. These rates corresponded to specific organic loading rates (OLRs) of 3.57, 4.77, and 7.15 kg COD/m^3/day for the 20, 15, and 10-day SRTs, respectively.

To establish a baseline for later comparison, all three reactors underwent an initial operational phase referred to as the "pre-experimental phase." During this phase, all reactors were operated under similar conditions, without the introduction of pretreated or PsNPs amended sludge. The pre-experimental phase lasted for 30 days and aimed to ensure consistency in biogas yield and quality across all reactors. By confirming this consistency, it provided a reliable baseline for commencing the experimental phase and evaluating the effects of the introduced treatments. Following the completion of the pre-experimental phase, the experimental phase commenced. During this phase, specific reactors received the addition of pretreated sludge and PsNPs amended sludge according to the desired SRTs of 20, 15, and 10 d. Notably, each SRT lasted for two cycles, and the reactors were operated for a total duration of 120 days. This approach facilitates a reliable comparison of various parameters, including SRT, the impact of THP, and the effects of PsNPs on

AD performance. By systematically evaluating these different factors, their individual contributions to AD performance can be assessed and compared.

7.2.5. Analytical methods

The TSS and VSS were determined using established standard methods. TCOD, SCOD, TAN, and alkalinity levels were measured using HACH reagent kits (HACH Co., Loveland, CO, USA). The pH of the samples was measured using a bench-top pH meter (Accumet AR15, Fisher Scientific, Pittsburgh, PA, USA). Detailed analytical methods for reactive oxygen species (ROS) analysis can be found elsewhere (Azizi et al., 2022).

7.2.6. Quantification of antibiotic resistance genes

Quantitative polymerase chain reaction (qPCR) was employed to evaluate the presence of eight commonly observed antibiotic resistance genes (ARGs) in the samples. These genes encompassed tetracycline resistance genes (*tet*A, *tet*B, *tet*W, *tet*X, *tet*Q, and *tet*M), sulfonamide resistance genes (*sul*1, *sul*2), ß-lactam resistance genes (bla_{TEM}, bla_{OXA}), macrolide resistance genes (*erm*C, *erm*B), as well as mobile genetic elements like integrons (*intl*1, *intl*2) and 16S rRNA. The specific primers used for amplifying these genes can be found in the Supporting Information of the study. The protocols for sample preparation, sequencing procedures, and data analysis are available in our previous publications, providing detailed information on these aspects (Azizi et al., 2022; Haffiez et al., 2023, 2022a).

7.3. Results and Discussion

7.3.1. Anaerobic digestion performance

Fig. 7.1 illustrates the daily methane generation from digesters during a 120-day operation period under different operating conditions. Initially, from days 1 to 30, all reactors ran under the same conditions as a pre-experimental phase, without the addition of PsNPs and THP, to establish a benchmark for future comparisons. Throughout the initial 22-day operational period, methane generation in all digesters exhibited significant fluctuations. Following this, in the subsequent week, the daily methane generation rate experienced a slight increase and eventually stabilized. This stable production level was maintained for just over a week, between days 22 and 30. The

average daily methane generation in control, PsNPs, and THP-PsNPs reactors during this period was comparable, with values of 0.30 ± 0.04, 0.30 ± 0.02, and 0.32 ± 0.01 L $CH_4/L_{reactor}/d$, respectively. Additionally, the biogas generated from these reactors exhibited a methane content of around 52-55% (vol.%). Despite minor fluctuations, all reactors demonstrated comparable methane productivity during this phase, establishing it as the baseline for introducing the pretreated samples.

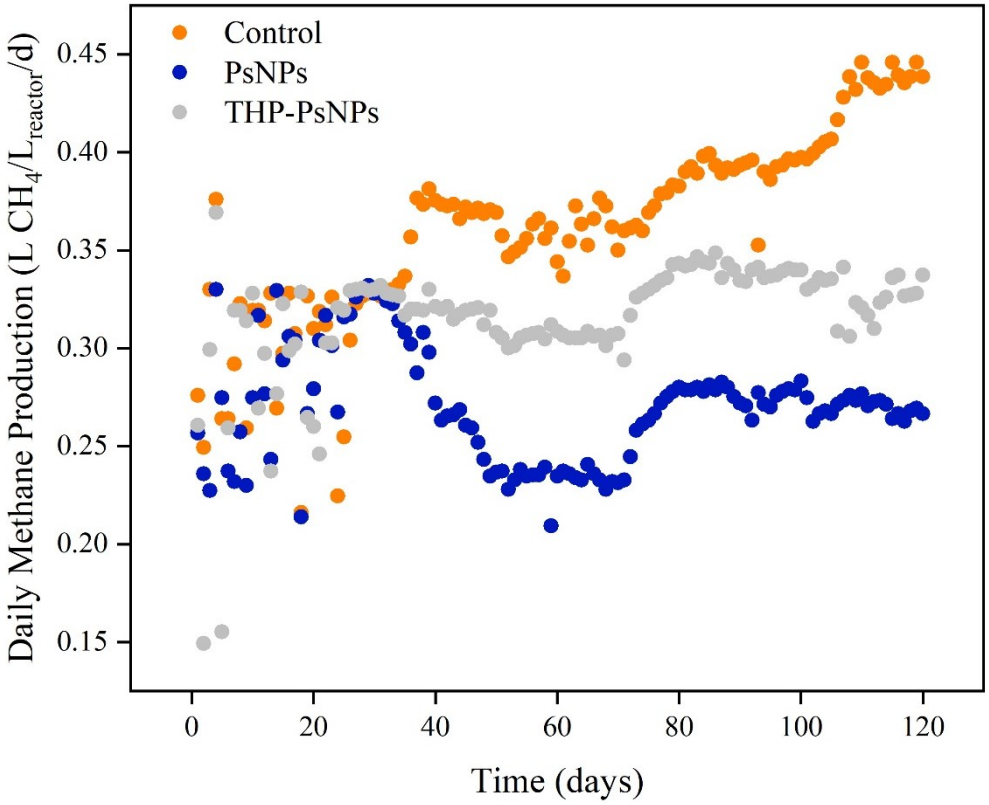

Figure 7.1. Daily biomethane production under different operating conditions.

Starting on day 31, the experimental phase commenced for all reactors with an SRT of 20 d (days 31 to 70). Subsequently, the SRT was reduced to 15 d for the period between days 71 and 100, and further decreased to 10 d for days 101 to 120. The impact of varying SRTs, pretreatment, and PsNPs exposure on methane production is summarized in Table 2. The results indicated that as the SRT decreased from 20 days to 10 days, the production of biomethane increased in control. This increase can be attributed to the higher influent of sludge, which provides more organic material to the reactors (Jianwei Liu et al., 2020). Also, it can demonstrate that the available

microbial community could metabolize the provided organics and prevents organic overload (Nges and Liu, 2010). However, despite this increase in biomethane production, the yield of biomethane decreased (data not shown) as the SRT decreased. For instance, in the control reactor, the methane yield decreased from 100.1 to 81.90 and further to 61.34 mL/g COD as the SRT decreased from 20 d to 15 d and 10 d, respectively. The reduction in methane production can be explained by the fact that, although both methane generation and sludge intake increased, the rate of improvement in methane production was not as high as the inflow of incoming organic matter. This finding aligns with several previous studies that have reported similar trends (Jibao Liu et al., 2020b; Jianwei Liu et al., 2020; Nges and Liu, 2010).For instance, Liu et al. studies indicated that while by decreasing SRT from 25 to 15 d, led to an increase in methane production from 70 mL/L·d to 75 mL/L·d, the biomethane yield dropped from 98.9 mL/g VS to 65.6 mL/g VS (Jianwei Liu et al., 2020).

Table 7.2. The impact of THP and PsNPs on average daily methane production (L $CH_4/L_{reactor}$/d) under different SRTs.

	Average daily methane production (L $CH_4/L_{reactor}$/d)		
SRT (d)	**Control**	**PsNPs**	**THP-PsNPs**
20	0.36±0.01	0.26±0.01	0.31±0.01
15	0.39±0.01	0.28±0.02	0.36±0.02
10	0.44±0.02	0.27±0.01	0.33±0.02

Notably, PsNPs amendment decreased (compared to the control) methane production by 28.2, 29.3, and 38.8% under 20, 15, and 10 d SRT, respectively (Fig. 1 and Table 2). The presence of PsNPs in the anaerobic digester can impede methane production through various pathways, including the generation of high levels of ROS, direct cellular damage, and the leaching of potentially toxic additives (Mohammad Mirsoleimani Azizi et al., 2021b). According to the literature, PsNPs can release additives like sodium dodecyl sulfate (SDS), which can hinder the functioning of crucial enzymes engaged in microbial defense mechanisms, consequently suppressing the methanogenesis process (Mirsoleimani Azizi et al., n.d.). Interestingly, the inhibitory effect of PsNPs (compared to the control) became more pronounced when the SRT was

decreased. This can be ascribed to the direct inhibition of methanogens responsible for methane generation and the alteration of microbial metabolic pathways, which affects their capacity to degrade organic matter and generate methane (Wei et al., 2020). With a shortened SRT, there is limited time available for the recovery and regrowth of these microorganisms, resulting in a reduced capacity for methane production.

Despite the inhibitory impacts of PsNPs on methane generation, the application of THP demonstrated a mitigating effect (Fig. 1 and Table 2). Notably, the average methane production in the THP-PsNPs digester under SRT conditions of 20, 15, and 10 d reached 0.31, 0.36, and 0.33 L $CH_4/L_{reactor}/d$, respectively, which were 19.2, 28.6, and 22.2% higher compared to the PsNPs digester. Therefore, the application of THP under PsNPs exposure at different SRTs, was able to counteract the negative impact of PsNPs and improve methane production. This improvement can be ascribed to the enhanced breakdown of organic matter and the degradation of PsNPs facilitated by the application of THP, as suggested by previous studies (Jeong et al., 2019; laqa Kakar et al., 2020; Mirsoleimani Azizi et al., n.d.). Notably, the superior performance of the digester at an SRT of 15 d can be attributed to the establishment of a favorable balance. At this SRT, the AD system may have provided the microbial community with sufficient time to adapt and effectively utilize the available organic matter. The improved methane production is likely due to finding the right balance in operating conditions. This balance seems to have a better impact compared to using a longer SRT of 20 days, which may have had a lower OLR. On the other hand, it also outperformed a shorter SRT of 10 days, which might not have provided enough time for the microbial community to grow optimally and efficiently use the available substrates. These findings underscore the importance of optimizing operating conditions and considering the interactions between MPs/NPs, SRT, and THP to maximize methane yield in the AD processes.

Fig. 7.2 demonstrates effluent TSS, VSS, TCOD, and SCOD under different operating conditions. It was found that the removal efficiency of VSS and TCOD decreased with the reduction of SRT in all reactors. For instance, VSS reduction in control was 45.33, 43.32, and 41.72% under 20, 15, and 10 d SRT, respectively. Likewise, 44.18, 37.91, and 30.41% TCOD removal were obtained in control under 20, 15, and 10 d SRT, respectively. Following PsNPs amendment and applying THP on the sample containing PsNPs, there was an improvement in VSS and COD removal compared to the control reactor. This enhancement can be ascribed to the

breakdown and hydrolysis of large biopolymers, such as proteins, lipids, and carbohydrates, into soluble individual units by THP (Appels et al., 2010; Xue et al., 2015). Also, the increased VSS removal observed in the PsNPs sample could be attributed to cell damage and the subsequent release of intracellular contents following exposure to PsNPs (Mirsoleimani Azizi et al., n.d.; Wei et al., 2020). This is due to a notable adsorption affinity of MPs/NPs, which allows them to directly attach to the cell membrane, thereby inducing membrane permeation and cell damage (Azizi et al., 2022; Mohammad Mirsoleimani Azizi et al., 2021b).

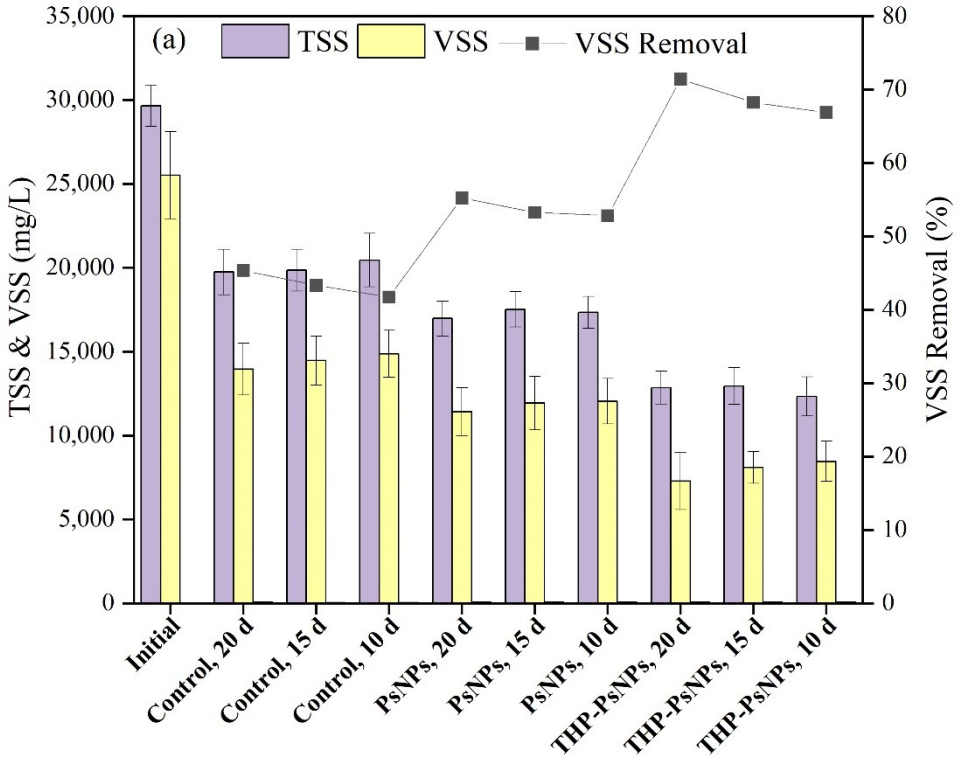

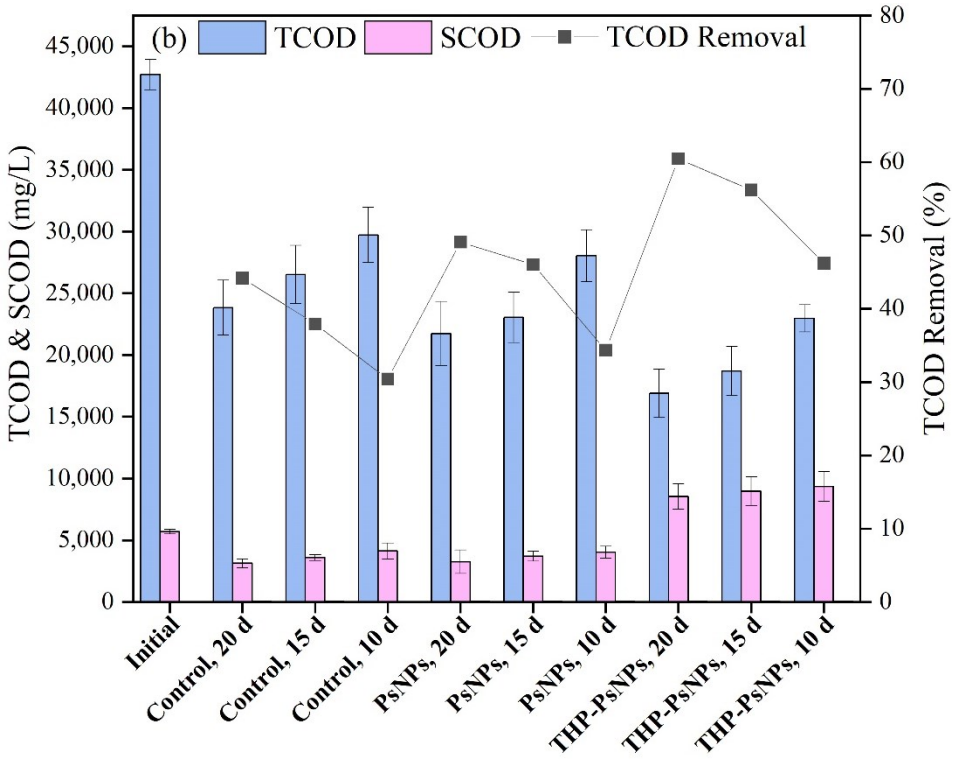

Figure 7.2. (a) Effluent TSS, VSS, and VSS removal, (b) Effluent TCOD, SCOD, and TCOD removal.

7.3.2. ROS Generation

ROS production induced by PsNPs is a critical element that affects the methanogenesis process and induces detrimental oxidative stress within cells. (Wei et al., 2020). ROS encompasses several radicals, including superoxide ($O_2^{\bullet-}$), hydrogen peroxide (H_2O_2), and hydroxyl radical ($OH^{\bullet}$) (Wei et al., 2019b). The interplay involving PsNPs surface and the limited oxygen levels present in anaerobic conditions leads to the generation of $O_2^{\bullet-}$ and H_2O_2. This, in turn, gives rise to the ROS production through mechanisms such as dismutation and Fenton chemistry (Nel et al., 2006). As demonstrated in Fig. 7.3, PsNPs amendment significantly increased ROS production under different operating conditions. Compared to the control, 32, 34.9, and 41.3% increase in ROS levels were attained for PsNPs sample under 20, 15, and 10 d SRT. The lower ROS level under longer SRT could be related to this fact that longer SRTs provide more time for the microbial community to adapt and recover from any stressors, potentially resulting in a reduced production of ROS. This extended time frame allows the microorganisms to enhance their antioxidant defense mechanisms, including the synthesis and activation of ROS scavenger enzymes (Mirsoleimani

Azizi et al., n.d.). As a result, longer SRTs may promote the upregulation and effectiveness of enzymes like catalase (CAT) and superoxide dismutase (SOD), which help neutralize ROS and maintain cellular homeostasis (Ray et al., 2012; Wei et al., 2020). Consequently, a reduced production of ROS is anticipated under longer SRT conditions. Conversely, the accelerated turnover of biomass in shorter SRTs may disrupt the balance between ROS production and scavenging, leading to an imbalance favoring increased ROS levels. Additionally, the prolonged presence of PsNPs in AD reactors can lead to increased leaching of SDS from the PsNPs. This leaching of SDS has the potential to inhibit the activity of ROS scavenger enzymes, further contributing to elevated ROS levels (Das and Roychoudhury, 2014; Mohammad Mirsoleimani Azizi et al., 2021b). Nevertheless, THP resulted in a decrease in ROS levels in the THP-PsNPs reactor. The ROS levels in the THP-PsNPs reactor were 24.8%, 26.34%, and 32.65% under SRTs of 20, 15, and 10 d, respectively. This decrement (compared to PsNPs) in potential ROS generation can be attributed to the modification of the physicochemical properties of the PsNPs that occur as a result of the THP (Azizi et al., 2022; Mirsoleimani Azizi et al., n.d.). The THP process may induce changes in the structure and characteristics of the PsNPs, potentially altering their reactivity and reducing their potential to generate ROS (Mirsoleimani Azizi et al., n.d.). Overall, further research is warranted to investigate the interplay between SRTs, ROS production, and THP operating conditions to gain a comprehensive understanding of the oxidative stress dynamics in AD systems.

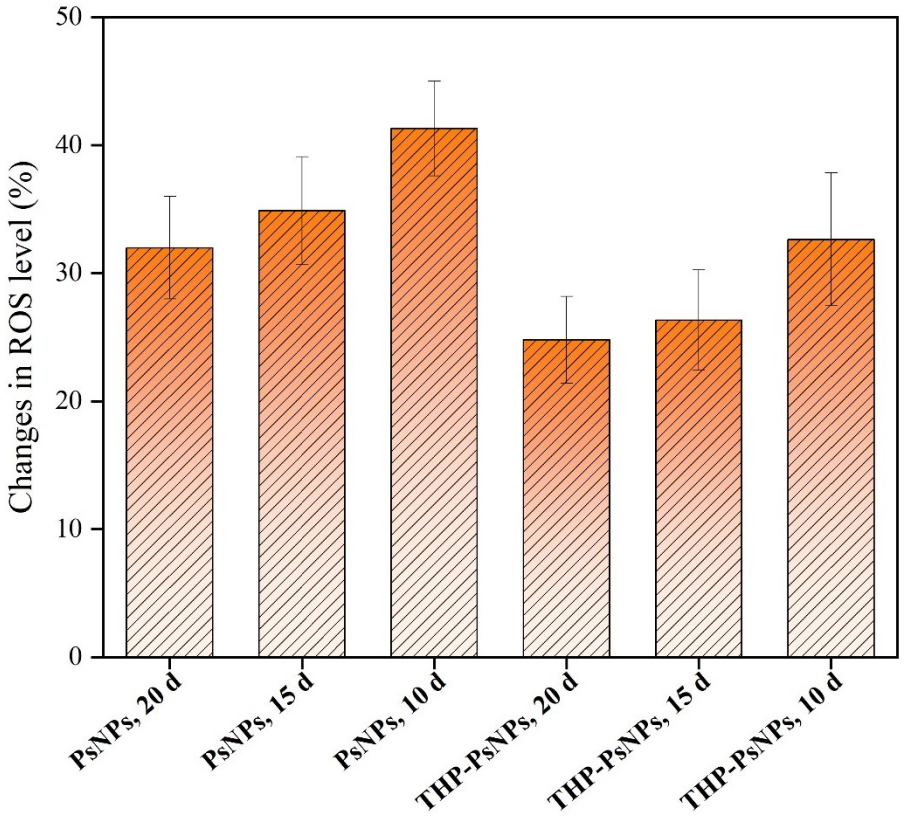

Figure 7.3. Relative changes in the ROS level under different experimental conditions.

7.3.3. Antibiotic resistance genes

In this study, the presence of targeted ARGs including *tet*A, *tet*B, *tet*W, *tet*X, *tet*Q, *tet*M, *sul*1, *sul*2, bla_{TEM}, bla_{OXA}, *erm*B, *erm*C, and MGEs (*intl*1 and *intl*2) was investigated in the digestate (Fig 7.4a-e). Among these ARGs, *sul*1 (33.5%-42.1%), *tet*W (26.2%-33.3%), and *intl*1 (5.6%-11.8%) were found to be the most abundant across all reactors. Interestingly, decreasing SRT from 20 to 15 and 10 d resulted in an enhancement in the abundance of most ARGs in the digesters. For example, in the control reactor with an SRT of 20 d, the abundance of *tet*W was 3.91×10^4 copies/g sludge, whereas it increased to 4.11×10^4 and 4.32×10^4 copies/g sludge under 15 and 10 d SRT, respectively (Fig. 7.4a). likewise, for *sul*1, the abundance was 4.59×10^4, 4.78×10^4, and 5.98×10^4 copies/g sludge in the control under 20, 15, and 10 d SRT, respectively (Fig. 7.4b). This trend was also observed for integrons (Fig. 7.4c), bla_{OXA}, and *erm*B. However, the abundance of bla_{TEM} and *erm*C decreased as the SRT was reduced from 20 to 10 d (Fig. 7.4d and e). Overall, 1.16×10^{10}, 9.71×10^9, and 8.84×10^9 copies/g sludge of total ARGs were detected in control under 20, 15, and

10 d SRT (Fig. 7.4f). These findings are consistent with previous studies reported in the literature (Haffiez et al., 2022b; Ma et al., 2011; W. Sun et al., 2019). The lower abundance of ARGs observed at longer SRTs can be attributed to factors such as reduced microbial diversity and the development of oligotrophic conditions over extended residence times (Haffiez et al., 2022b; W. Sun et al., 2019). Under these conditions, some Antibiotic-Resistant Bacteria (ARB) may be eliminated, and the likelihood of new cell proliferation could be limited (Qian et al., 2021). Additionally, higher rates of antibiotic biodegradation may occur during longer residence times, contributing to the lower abundance of ARGs (Haffiez et al., 2022b; Nnadozie et al., 2017).

Moreover, the exposure to PsNPs led to a notable enhancement in the proliferation of most ARGs across all operational conditions. For instance, the abundance of *sul*1 increased by 1.20, 1.4, and 1.36-fold compared to the control under 20, 15, and 10 d SRT, respectively. The frequently detected Mobile Genetic Elements (MGEs), *intl*1 and *intl*2, known for their involvement in horizontal gene transfer (HGT), also exhibited substantial increases. For instance, the abundance of *intl*1 rose from 6.61×10^3 copies/g sludge in the control to 1.05×10^4 copies/g sludge in the PsNPs reactor under an SRT of 20 d. Similarly, *intl*2 abundance increased by 3.07-fold, 7.15-fold, and 5.48-fold compared to the control under SRTs of 20, 15, and 10 d, respectively. These findings are consistent with prior studies highlighting the role of PsNPs in promoting MGE proliferation (Dai et al., 2020a; Mirsoleimani Azizi et al., n.d.). Additionally, exposure to PsNPs resulted in an increased abundance of specific ARGs. Fig. 4a demonstrates that the abundance of *tet*A, *tet*B, and *tet*W increased by 3.02-11.82-fold, 31.37-39.76-fold, and 1.32-1.58-fold, respectively, following PsNPs exposure across all three SRTs. However, a notable reduction in the abundance of *tet*X (4.77%-70.92%), *tet*Q (7.54%-65.09%), and *tet*M (8.67%-71.84%) was observed. This decrease can be attributed to the impact of PsNPs on microbial community composition, favoring the growth of certain microorganisms while suppressing others (Azizi et al., 2022). Consequently, the presence of nanoparticles intensifies the selective pressure for ARGs propagation (Haffiez et al., 2022b). Overall, in the PsNPs reactors, the total abundance of ARGs was consistently higher compared to the control reactor under SRTs of 20, 15, and 10 d, with increases of 40.01%, 38.93%, and 27.84% respectively. This rise in abundance can be attributed to the heightened production of ROS triggered by exposure to nanoparticles. The generated ROS have the potential to cause damage to bacterial cells, increase membrane permeability, and aid in the transmission of ARGs

within the bacterial community through MGEs like integrons (*intl*1, *intl*2) (Shi et al., 2020). Moreover, the hydrophobic properties and the extensive surface area of MPs/NPs enable them to adsorb diverse environmental pollutants, including antibiotics and heavy metals (He et al., 2021). This adsorption process intensifies interactions between microorganisms and creates an environment rich in nutrients, thereby promoting syntrophic interactions among microorganisms and facilitating the development of antibiotic resistance (Zettler et al., 2013).

Although PsNPs contributed to the increased propagation of ARGs, application of THP demonstrated a contrasting pattern, leading to a reduction in the abundance of nearly all specified ARGs. For example, the abundance of *intl*1in THP-PsNPs decreased by 14.08, 15.75, and 21.48% compared to PsNPs under 20, 15, and 10 d SRT, respectively. This trend was also observed in total ARGs. For instance, under an SRT of 15 days, the PsNPs reactor had a total ARGs abundance of 1.84×10^5 copies/g sludge, whereas the THP-PsNPs reactor showed a decrease to 1.15×10^5 copies/g sludge, representing a 37.52% reduction in total ARGs (Fig. 7.4e). This reduction in ARGs after the application of THP can be attributed to a decrease in potential hosts carrying multiple ARGs, as observed in previous studies (Haffiez et al., 2022a).

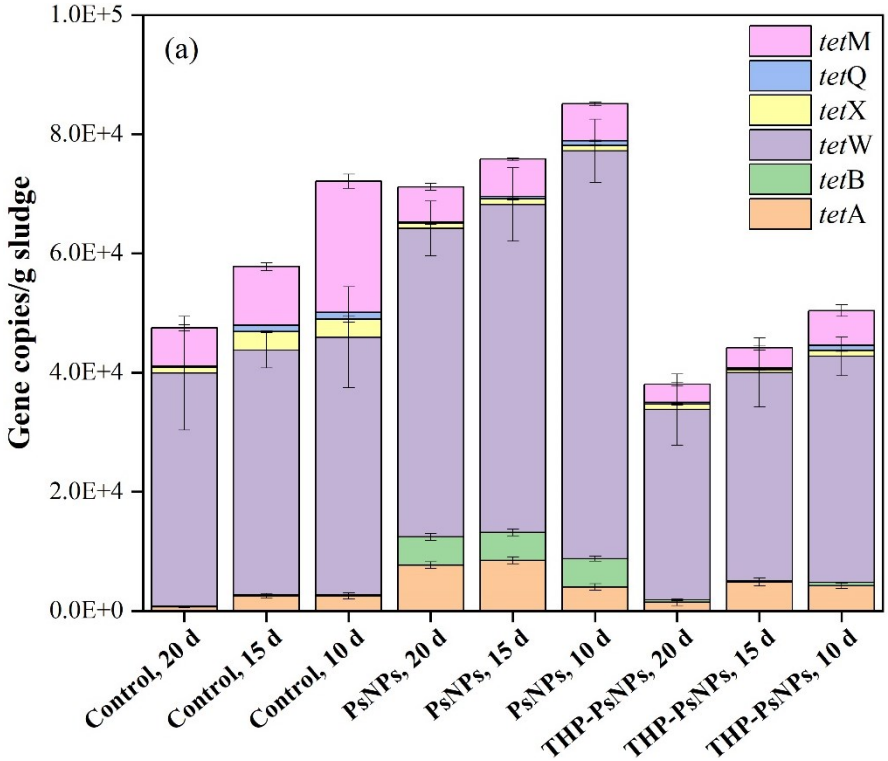

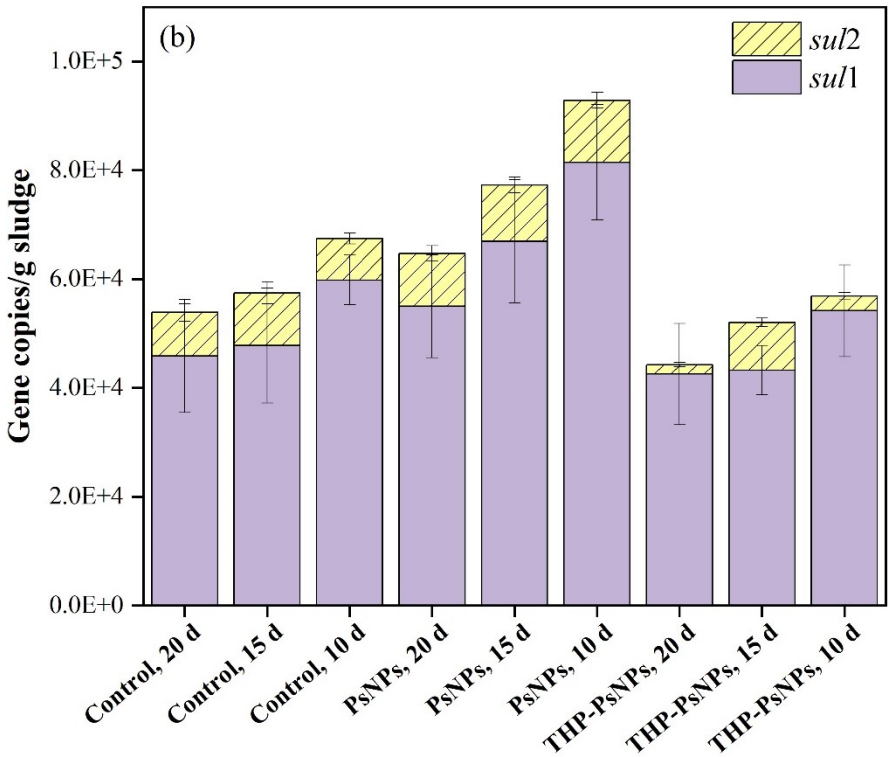
(b)
sul2
sul1
Gene copies/g sludge
1.0E+5
8.0E+4
6.0E+4
4.0E+4
2.0E+4
0.0E+0
Control, 20 d
Control, 15 d
Control, 10 d
PsNPs, 20 d
PsNPs, 15 d
PsNPs, 10 d
THP-PsNPs, 20 d
THP-PsNPs, 15 d
THP-PsNPs, 10 d

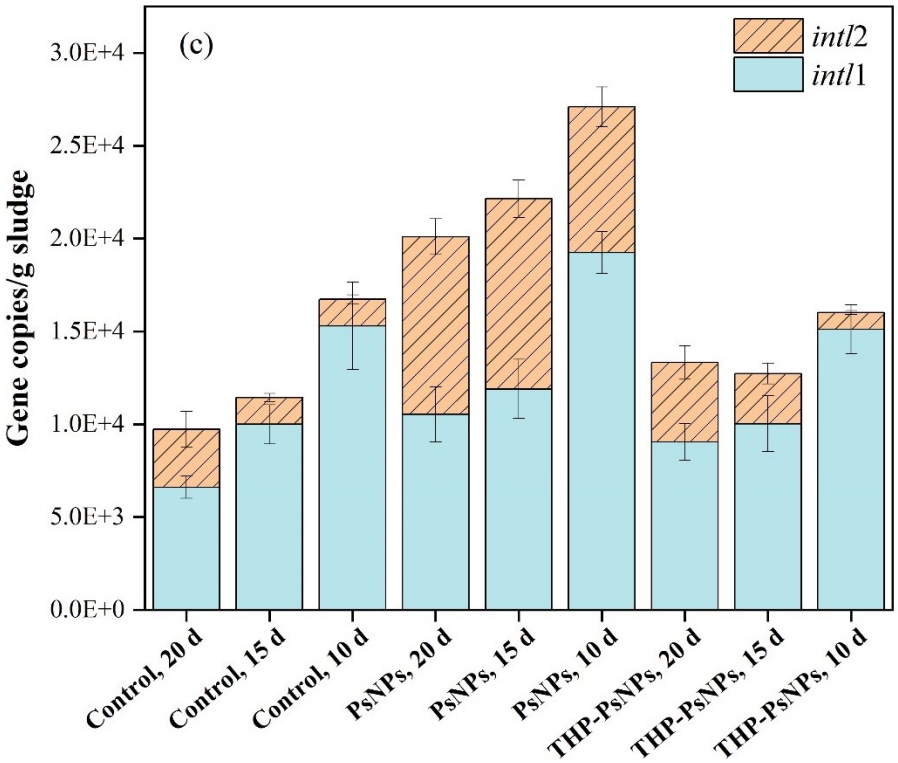
(c)
intl2
intl1
Gene copies/g sludge
3.0E+4
2.5E+4
2.0E+4
1.5E+4
1.0E+4
5.0E+3
0.0E+0
Control, 20 d
Control, 15 d
Control, 10 d
PsNPs, 20 d
PsNPs, 15 d
PsNPs, 10 d
THP-PsNPs, 20 d
THP-PsNPs, 15 d
THP-PsNPs, 10 d

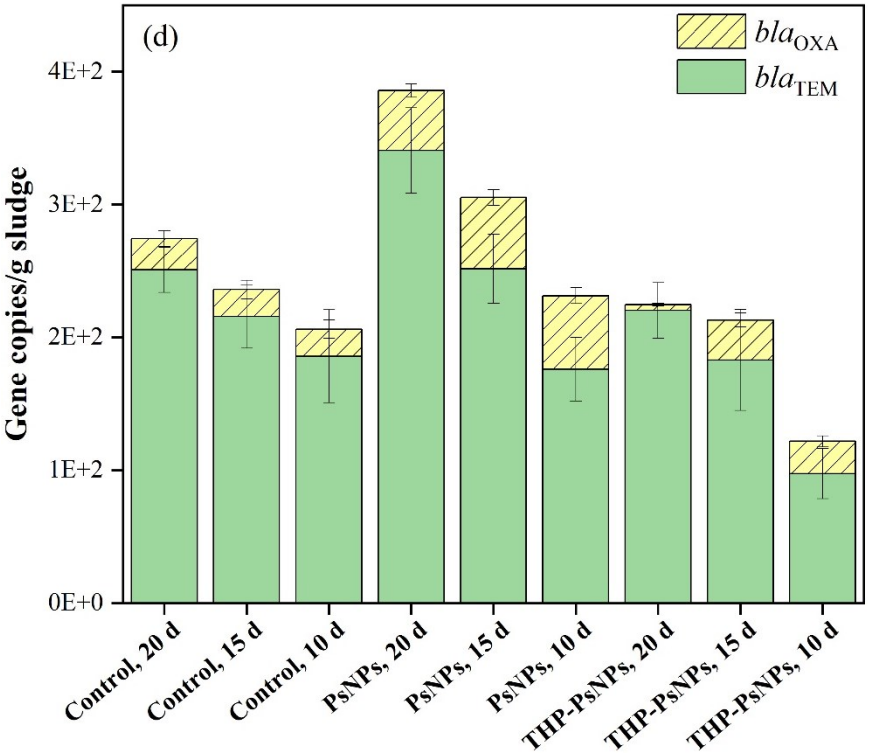
(d)
bla_{OXA}
bla_{TEM}
Gene copies/g sludge
4E+2
3E+2
2E+2
1E+2
0E+0
Control, 20 d
Control, 15 d
Control, 10 d
PsNPs, 20 d
PsNPs, 15 d
PsNPs, 10 d
THP-PsNPs, 20 d
THP-PsNPs, 15 d
THP-PsNPs, 10 d

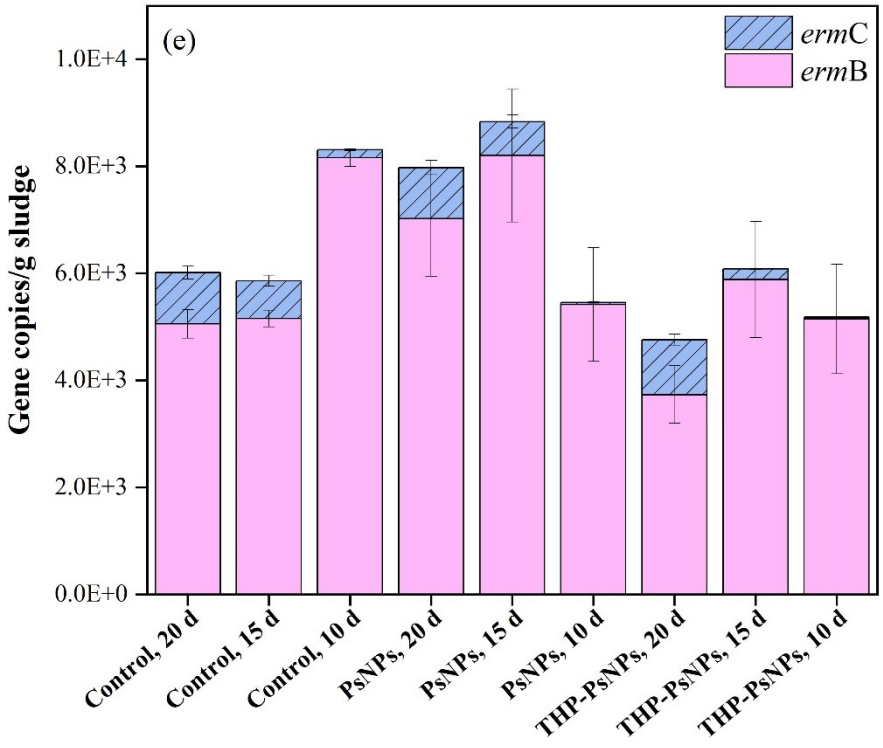
(e)
ermC
ermB
Gene copies/g sludge
1.0E+4
8.0E+3
6.0E+3
4.0E+3
2.0E+3
0.0E+0
Control, 20 d
Control, 15 d
Control, 10 d
PsNPs, 20 d
PsNPs, 15 d
PsNPs, 10 d
THP-PsNPs, 20 d
THP-PsNPs, 15 d
THP-PsNPs, 10 d

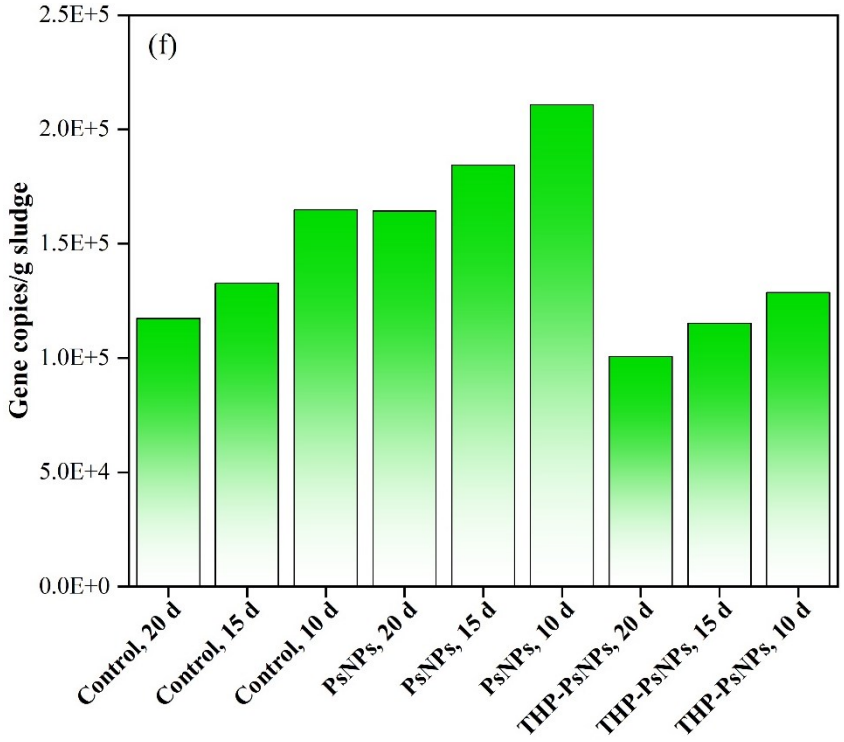

Figure 7.4. Concentrations of (a) tetracycline (*tet*) resistance genes, (b) sulfonamide (*sul*) resistance genes, (c) integron (*intl*), (d) ß-lactam (bla) resistance genes, (e) macrolide (erm) resistance genes, and (f) total ARGs under different experimental conditions.

To gain further insight into the microbiome's potential to harbor ARGs in the digestate, quantification of 16S rRNA gene copies was performed (Haffiez et al., 2022a). As depicted in Fig. E1, the THP samples exhibited a notably reduced count of 16S rRNA gene copies in comparison to the control and PsNPs samples. This suggests the potential disruption or elimination of potential hosts for ARGs after THP treatment, which may contribute to the reduction in ARG proliferation that could otherwise be increased by PsNPs (Azizi et al., 2022). In conclusion, the application of THP showed promising results in decreasing the abundance of targeted ARGs, countering the increased propagation observed with PsNPs. These findings highlight the potential of THP as a strategy to mitigate ARG dissemination in AD systems. Further research is warranted to explore the underlying mechanisms and optimize the implementation of THP, taking into consideration factors such as SRT, PsNPs, and their interactions to effectively manage ARGs within wastewater treatment processes.

7.4. Conclusion

This research aimed to assess the impact of low-temperature THP and PsNPs on AD performance at varying SRTs. The results revealed that the presence of PsNPs led to a notable inhibition of methane production, with this effect becoming more pronounced at lower SRTs. Furthermore, it was observed that PsNPs induced higher oxidative stress levels at lower SRTs. In contrast, the application of THP not only reduced the ROS levels but also demonstrated a mitigating effect, resulting in increased methane production compared to PsNPs. In addition, the presence of PsNPs caused a substantial rise in the prevalence of ARGs in the digestate, with the 10d SRT displaying the most notable surge in ARGs abundance. However, the implementation of THP demonstrated its effectiveness in decreasing the abundance of ARGs under various operating conditions. These findings underscore the potential of THP as a sustainable approach for managing sludge containing PsNPs. Nonetheless, further research is necessary to optimize the AD performance of sewage sludge containing PsNPs under different SRTs. Exploring potential improvements in this area will be crucial for ensuring efficient and environmentally friendly sludge management practices.

Chapter 8

Conclusions and Recommendations

8.1. Conclusions

This doctoral thesis focused on exploring various retrofitting schemes of low-temperature THP in AD under batch and semi-continuous conditions and assessing the impact of THP of sludge on MPs/NPs stress during AD.

This thesis examined low-temperature THP (50–90°C, 30–90 min) for enhancing co-digestion of FPS and TWAS. The experiments were conducted under two schemes: scheme-1 (THP of TWAS + FPS) and scheme-2 (THP of TWAS only). Scheme-1 resulted in a greater enhancement in methane production over the control (scheme-1: 56.28% at 90°C, 90 min vs. scheme-2: 43.4% at 90°C, 60 min). Thus, these results suggested that low-temperature THP of TWAS alone (scheme-2) would result in the solubilization of refractory macromolecular compounds, leading to a relatively lower positive impact on methane yields than scheme-1. The preliminary economic assessment considering THP operating cost, enhancement in energy recovery, and saving in biosolids handling costs indicated that THP at 90°C (90 min) under scheme-1 could provide the highest net saving of $79.55/dry tonne solids compared to the control (AD without THP). These results will provide technical guidance in adopting THP in WWTPs with PS fermentation.

To determine the impact of THP on alleviating oxidative stress of MPs/NPs in AD, different PsNPs concentrations of 50, 100, and 150 μg/L were tested. Our results showed that higher PsNPs levels were found to decrease methane yields compared to the control. However, THP counteracted the suppression of methane production imposed by PsNPs concentrations and reduced the levels of reactive oxygen species (ROS) and the propagation of antibiotic resistance genes (ARGs). This suggests that THP holds significant potential as a remediation method for MPs/NPs in WWTPs.

The thesis further examined the efficiency of THP in counteracting MPs/NPs oxidative stress under different TS content. The presence of PsNPs substantially enhanced ROS levels at lower TS content compared to higher TS, resulting in reduced methane production. Nevertheless, applying

THP effectively mitigated ROS-induced stress and the propagation of most ARGs. These results provide insights into the significance of sludge solids content in THP for co-remediation of PsNPs-induced oxidative stress and ARGs propagation during AD.

For a more realistic representation of industrial AD conditions, the study investigated the impact of THP on the mixture of FPS+TWAS and TWAS alone, under semi-continuous mode, with different SRTs. The application of THP led to substantial methane production enhancements in both cases. However, the presence of PsNPs caused significant inhibition of methane production, which was effectively mitigated by THP.

In conclusion, this thesis provides valuable insights into various retrofitting schemes for low-temperature THP in AD and its potential to mitigate the impact of MPs/NPs on the AD process. The findings offer crucial guidance for optimizing THP applications in WWTPs and contribute to the understanding of AD processes under different operating conditions.

8.2. Recommendations

- A preliminary economic assessment showed that low-temperature THP would be economically feasible. However, performing a comprehensive techno-economic analysis considering the life cycle assessments of THP implementation in WWTPs. This analysis should include capital and operational costs, energy consumption, and environmental benefits, to provide a holistic view of the technology's feasibility.
- Given that the thermal stability of MPs/NPs depends on the physicochemical characteristics and composition of polymer blends, the results of this study do not necessarily imply that THP would be effective in reducing stress induced by a wide variety of MPs/NPs. Further research is warranted to understand the efficacy of THP in mitigating oxidative stress caused by exposure to different types of MPs/NPs.
- Conducting microbial community analysis to understand the changes in the anaerobic microbiome during AD with THP is of great importance. Identifying key microbial groups involved in the degradation of MPs/NPs and organic matter will enhance our understanding of the underlying mechanisms.
- Investigating the fate and behavior of MPs/NPs throughout the AD process is needed to understand their transformation and potential accumulation in digestate biosolids. This

comprehensive understanding will lead to a more holistic approach in addressing MPs/NPs pollution.

- Significant research gaps persist in the safe disposal of AD digestate. Further investigations are needed to quantify the remaining MPs/NPs in the digestate and to understand the environmental impact of the disposal of these products. Additionally, a thorough analysis of the metal content is essential. This will contribute to a more comprehensive understanding and responsible management of the digestate.

References

Abu-Orf, M., Goss, T., 2012. Comparing thermal hydrolysis processes (CAMBI^{TM} and EXELYS^{TM}) for solids pretreatmet prior to anaerobic digestion. Digestion 16, 8–12.

Abudi, Z.N., Hu, Z., Sun, N., Xiao, B., Rajaa, N., Liu, C., Guo, D., 2016. Batch anaerobic co-digestion of OFMSW (organic fraction of municipal solid waste), TWAS (thickened waste activated sludge) and RS (rice straw): Influence of TWAS and RS pretreatment and mixing ratio. Energy 107, 131–140. https://doi.org/10.1016/j.energy.2016.03.141

Ahn, J.-Y.Y., Chang, S.-W.W., 2021. Effects of Sludge Concentration and Disintegration/Solubilization Pretreatment Methods on Increasing Anaerobic Biodegradation Efficiency and Biogas Production. Sustainability 13, 12887. https://doi.org/10.3390/SU132212887

Ai, S., Liu, H., Wu, M., Zeng, G., Yang, C., 2018. Roles of acid-producing bacteria in anaerobic digestion of waste activated sludge. Front. Environ. Sci. Eng. 12, 1–11.

Al-Sid-Cheikh, M., J. Rowland, S., Stevenson, K., Rouleau, C., B. Henry, T., C. Thompson, R., 2018. Uptake, Whole-Body Distribution, and Depuration of Nanoplastics by the Scallop Pecten maximus at Environmentally Realistic Concentrations. Environ. Sci. & Technol. 52, 14480–14486. https://doi.org/10.1021/acs.est.8b05266

Appels, L., Baeyens, J., Degrève, J., Dewil, R., 2008. Principles and potential of the anaerobic digestion of waste-activated sludge. Prog. Energy Combust. Sci. https://doi.org/10.1016/j.pecs.2008.06.002

Appels, L., Degrève, J., Van der Bruggen, B., Van Impe, J., Dewil, R., 2010. Influence of low temperature thermal pre-treatment on sludge solubilisation, heavy metal release and anaerobic digestion. Bioresour. Technol. 101, 5743–5748. https://doi.org/10.1016/j.biortech.2010.02.068

Ariunbaatar, J., Panico, A., Esposito, G., Pirozzi, F., Lens, P.N.L., 2014a. Pretreatment methods to enhance anaerobic digestion of organic solid waste. Appl. Energy. https://doi.org/10.1016/j.apenergy.2014.02.035

Ariunbaatar, J., Panico, A., Frunzo, L., Esposito, G., Lens, P.N.L., Pirozzi, F., 2014b. Enhanced anaerobic digestion of food waste by thermal and ozonation pretreatment methods. J. Environ. Manage. 146, 142–149. https://doi.org/10.1016/J.JENVMAN.2014.07.042

Association, A.P.H., Association, A.W.W., Federation, W.P.C., Federation, W.E., 1915. Standard methods for the examination of water and wastewater. American Public Health Association.

Azizi, S.M.M., Haffiez, N., Zakaria, B.S., Dhar, B.R., 2022. Thermal Hydrolysis of Sludge Counteracts Polystyrene Nanoplastics-Induced Stress during Anaerobic Digestion. ACS ES&T Eng. 7, 1306–1315. https://doi.org/10.1021/acsestengg.1c00460

Azizi, S.M.M., Haffiez, N., Zakaria, B.S., Elbeshbishy, E., Dhar, B.R., 2023. Chapter 15 - Nano- and microplastics as carriers for antibiotics and antibiotic resistance genes. Elsevier, pp. 361–385. https://doi.org/10.1016/B978-0-323-99908-3.00005-1

Barber, W.P.F., 2016. Thermal hydrolysis for sewage treatment: A critical review. Water Res. https://doi.org/10.1016/j.watres.2016.07.069

Barua, S., Dhar, B.R.B.R., 2017. Advances towards understanding and engineering direct interspecies electron transfer in anaerobic digestion, Bioresource Technology. https://doi.org/10.1016/j.biortech.2017.08.023

Barua, S., Zakaria, B.S., Chung, T., Hai, F.I., Haile, T., Al-Mamun, A., Dhar, B.R., 2019. Microbial electrolysis followed by chemical precipitation for effective nutrients recovery from digested sludge centrate in WWTPs. Chem. Eng. J. 361, 256–265. https://doi.org/10.1016/j.cej.2018.12.067

Barua, S., Zakaria, B.S., Dhar, B.R., 2018. Enhanced methanogenic co-degradation of propionate and butyrate by anaerobic microbiome enriched on conductive carbon fibers. Bioresour. Technol. 266, 259–266. https://doi.org/10.1016/j.biortech.2018.06.053

Bhagat, J., Zang, L., Nishimura, N., Shimada, Y., 2020. Zebrafish: An emerging model to study microplastic and nanoplastic toxicity. Sci. Total Environ. https://doi.org/10.1016/j.scitotenv.2020.138707

Böcker, U., Wubshet, S.G., Lindberg, D., Afseth, N.K., 2017. Fourier-transform infrared

spectroscopy for characterization of protein chain reductions in enzymatic reactions. Analyst 142, 2812–2818.

Bougrier, C., Delgenès, J.P., Carrère, H., 2008. Effects of thermal treatments on five different waste activated sludge samples solubilisation, physical properties and anaerobic digestion. Chem. Eng. J. 139, 236–244. https://doi.org/10.1016/j.cej.2007.07.099

Bougrier, C., Delgenès, J.P., Carrère, H., 2007. Impacts of thermal pre-treatments on the semi-continuous anaerobic digestion of waste activated sludge. Biochem. Eng. J. 34, 20–27. https://doi.org/10.1016/j.bej.2006.11.013

Braet, F., De Zanger, R., Wisse, E., 1997. Drying cells for SEM, AFM and TEM by hexamethyldisilazane: a study on hepatic endothelial cells. J. Microsc. 186, 84–87.

Bui, X.T., Vo, T.D.H., Nguyen, P.T., Nguyen, V.T., Dao, T.S., Nguyen, P.D., 2020. Microplastics pollution in wastewater: Characteristics, occurrence and removal technologies. Environ. Technol. Innov. https://doi.org/10.1016/j.eti.2020.101013

Cano, R., Pérez-Elvira, S.I., Fdz-Polanco, F., 2015. Energy feasibility study of sludge pretreatments: A review. Appl. Energy. https://doi.org/10.1016/j.apenergy.2015.03.132

Carlsson, M., Lagerkvist, A., Morgan-Sagastume, F., 2012. The effects of substrate pre-treatment on anaerobic digestion systems: A review. Waste Manag. 32, 1634–1650. https://doi.org/10.1016/j.wasman.2012.04.016

Carrere, H., Antonopoulou, G., Affes, R., Passos, F., Battimelli, A., Lyberatos, G., Ferrer, I., 2016. Review of feedstock pretreatment strategies for improved anaerobic digestion: From lab-scale research to full-scale application. Bioresour. Technol. 199, 386–397. https://doi.org/10.1016/J.BIORTECH.2015.09.007

Carrère, H., Dumas, C., Battimelli, A., Batstone, D.J., Delgenès, J.P., Steyer, J.P., Ferrer, I., 2010. Pretreatment methods to improve sludge anaerobic degradability: A review. J. Hazard. Mater. https://doi.org/10.1016/j.jhazmat.2010.06.129

Chakravarty, S., Mohanty, A., Sudha, T.N., Upadhyay, A.K., Konar, J., Sircar, J.K., Madhukar, A., Gupta, K.K., 2010. Removal of Pb (II) ions from aqueous solution by adsorption using

bael leaves (Aegle marmelos). J. Hazard. Mater. 173, 502–509. https://doi.org/10.1016/J.JHAZMAT.2009.08.113

Chand, R., Kohansal, K., Toor, S., Pedersen, T.H., Vollertsen, J., 2022. Microplastics degradation through hydrothermal liquefaction of wastewater treatment sludge. J. Clean. Prod. 335, 130383. https://doi.org/10.1016/J.JCLEPRO.2022.130383

Chen, G., Feng, Q., Wang, J., 2020. Mini-review of microplastics in the atmosphere and their risks to humans. Sci. Total Environ. 703, 135504. https://doi.org/10.1016/J.SCITOTENV.2019.135504

Chen, H., Rao, Y., Cao, L., Shi, Y., Hao, S., Luo, G., Zhang, S., 2019. Hydrothermal conversion of sewage sludge: Focusing on the characterization of liquid products and their methane yields. Chem. Eng. J. 357, 367–375. https://doi.org/10.1016/J.CEJ.2018.09.180

Chen, H., Tang, M., Yang, X., Tsang, Y.F., Wu, Y., Wang, D., Zhou, Y., 2021. Polyamide 6 microplastics facilitate methane production during anaerobic digestion of waste activated sludge. Chem. Eng. J. 408, 127251. https://doi.org/https://doi.org/10.1016/j.cej.2020.127251

Chen, S., Dong, B., Dai, X., Wang, H., Li, N., Yang, D., 2019. Effects of thermal hydrolysis on the metabolism of amino acids in sewage sludge in anaerobic digestion. Waste Manag. 88, 309–318. https://doi.org/10.1016/j.wasman.2019.03.060

Chen, T., Jin, Y., Liu, F., Meng, X., Li, H., Nie, Y., 2012. Effect of hydrothermal treatment on the levels of selected indigenous microbes in food waste. J. Environ. Manage. 106, 17–21. https://doi.org/10.1016/J.JENVMAN.2012.03.045

Chen, X., Xiang, X., Dai, R., Wang, Y., Ma, P., 2017. Effect of low temperature of thermal pretreatment on anaerobic digestion of textile dyeing sludge. Bioresour. Technol. 243, 426–432. https://doi.org/10.1016/j.biortech.2017.06.138

Cheng, J., Yue, L., Ding, L., Li, Y.Y., Ye, Q., Zhou, J., Cen, K., Lin, R., 2019. Improving fermentative hydrogen and methane production from an algal bloom through hydrothermal/steam acid pretreatment. Int. J. Hydrogen Energy 44, 5812–5820. https://doi.org/10.1016/J.IJHYDENE.2019.01.046

Choi, J.M., Han, S.K., Lee, C.Y., 2018. Enhancement of methane production in anaerobic digestion of sewage sludge by thermal hydrolysis pretreatment. Bioresour. Technol. 259, 207–213. https://doi.org/10.1016/j.biortech.2018.02.123

Chowdhury, B., Lin, L., Dhar, B.R., Islam, M.N., McCartney, D., Kumar, A., 2019. Enhanced biomethane recovery from fat, oil, and grease through co-digestion with food waste and addition of conductive materials. Chemosphere 236, 124362. https://doi.org/10.1016/j.chemosphere.2019.124362

Cole, M., Lindeque, P., Halsband, C., Galloway, T.S., 2011. Microplastics as contaminants in the marine environment: A review. Mar. Pollut. Bull. https://doi.org/10.1016/j.marpolbul.2011.09.025

Cox, K.D., Covernton, G.A., Davies, H.L., Dower, J.F., Juanes, F., Dudas, S.E., 2019. Human Consumption of Microplastics. Environ. Sci. Technol. https://doi.org/10.1021/acs.est.9b01517

Dai, H.H., Gao, J.F., Wang, Z.Q., Zhao, Y.F., Zhang, D., 2020a. Behavior of nitrogen, phosphorus and antibiotic resistance genes under polyvinyl chloride microplastics pressures in an aerobic granular sludge system. J. Clean. Prod. 256, 120402. https://doi.org/10.1016/J.JCLEPRO.2020.120402

Dai, H.H., Gao, J.F., Wang, Z.Q., Zhao, Y.F., Zhang, D., 2020b. Behavior of nitrogen, phosphorus and antibiotic resistance genes under polyvinyl chloride microplastics pressures in an aerobic granular sludge system. J. Clean. Prod. 256, 120402. https://doi.org/10.1016/j.jclepro.2020.120402

Dai, X., Li, X., Zhang, D., Chen, Y., Dai, L., 2016. Simultaneous enhancement of methane production and methane content in biogas from waste activated sludge and perennial ryegrass anaerobic co-digestion: The effects of pH and C/N ratio. Bioresour. Technol. https://doi.org/10.1016/j.biortech.2016.05.100

Das, K., Roychoudhury, A., 2014. Reactive oxygen species (ROS) and response of antioxidants as ROS-scavengers during environmental stress in plants. Front. Environ. Sci. 2, 53. https://doi.org/https://doi.org/10.3389/fenvs.2014.00053

Dasgupta, A., Chandel, M.K., 2019. Enhancement of biogas production from organic fraction of municipal solid waste using hydrothermal pretreatment. Bioresour. Technol. Reports 7, 100281.

Dastyar, W., Mirsoleimani Azizi, S.M., Meshref, M.N.A., Dhar, B.R., 2021a. Powdered activated carbon amendment in percolate tank enhances high-solids anaerobic digestion of organic fraction of municipal solid waste. Process Saf. Environ. Prot. 151, 63–70. https://doi.org/10.1016/J.PSEP.2021.04.033

Dastyar, W., Mohammad Mirsoleimani Azizi, S., Dhadwal, M., Ranjan Dhar, B., 2021b. High-solids anaerobic digestion of organic fraction of municipal solid waste: Effects of feedstock to inoculum ratio and percolate recirculation time. Bioresour. Technol. 337, 125335. https://doi.org/10.1016/J.BIORTECH.2021.125335

Devos, P., Haddad, M., Carrère, H., 2020. Thermal Hydrolysis of Municipal sludge: Finding the Temperature Sweet Spot: A Review. Waste and Biomass Valorization 1–19.

Dhar, B.R., Elbeshbishy, E., Hafez, H., Nakhla, G., Ray, M.B., 2013. Assessing the optimum SRT for anaerobic digester with sludge pretreatment for sulfide control, in: 86th Annual Water Environment Federation Technical Exhibition and Conference, WEFTEC 2013. https://doi.org/10.2175/193864713813685881

Dhar, B.R., Nakhla, G., Ray, M.B., 2012. Techno-economic evaluation of ultrasound and thermal pretreatments for enhanced anaerobic digestion of municipal waste activated sludge. Waste Manag. 32, 542–549. https://doi.org/10.1016/j.wasman.2011.10.007

Dilara Hatinoglu, M., Dilek Sanin, F., 2022. Fate and effects of polyethylene terephthalate (PET) microplastics during anaerobic digestion of alkaline-thermal pretreated sludge. Waste Manag. 153, 376–385. https://doi.org/10.1016/J.WASMAN.2022.09.016

Ding, H.H., Chang, S., Liu, Y., 2017. Biological hydrolysis pretreatment on secondary sludge: Enhancement of anaerobic digestion and mechanism study. Bioresour. Technol. 244, 989–995. https://doi.org/10.1016/j.biortech.2017.08.064

Dolfing, J., Mulder, J.W., 1985. Comparison of methane production rate and coenzyme F420 content of methanogenic consortia in anaerobic granular sludge. Appl. Environ. Microbiol.

https://doi.org/10.1128/aem.49.5.1142-1145.1985

Dong, H., Chen, Y., Wang, J., Zhang, Y., Zhang, P., Li, X., Zou, J., Zhou, A., 2021. Interactions of microplastics and antibiotic resistance genes and their effects on the aquaculture environments, Journal of Hazardous Materials. https://doi.org/10.1016/j.jhazmat.2020.123961

Dubois, M., Gilles, K.A., Hamilton, J.K., Rebers, P.A. t, Smith, F., 1956. Colorimetric method for determination of sugars and related substances. Anal. Chem. 28, 350–356.

Eckert, E.M., Di Cesare, A., Kettner, M.T., Arias-Andres, M., Fontaneto, D., Grossart, H.P., Corno, G., 2018. Microplastics increase impact of treated wastewater on freshwater microbial community. Environ. Pollut. 234, 495–502. https://doi.org/10.1016/j.envpol.2017.11.070

Eftaxias, A., Diamantis, V., Aivasidis, A., 2018. Anaerobic digestion of thermal pre-treated emulsified slaughterhouse wastes (TESW): Effect of trace element limitation on process efficiency and sludge metabolic properties. Waste Manag. 76, 357–363. https://doi.org/10.1016/j.wasman.2018.02.032

El Gnaoui, Y., Karouach, F., Bakraoui, M., Barz, M., El Bari, H., 2020. Mesophilic anaerobic digestion of food waste: Effect of thermal pretreatment on improvement of anaerobic digestion process. Energy Reports 6, 417–422.

Elbeshbishy, E., Dhar, B.R., Nakhla, G., Lee, H.-S., 2017. A critical review on inhibition of dark biohydrogen fermentation. Renew. Sustain. Energy Rev. 79. https://doi.org/10.1016/j.rser.2017.05.075

Elyasi, S., Amani, T., Dastyar, W., 2015. A comprehensive evaluation of parameters affecting treating high-strength compost leachate in anaerobic baffled reactor followed by electrocoagulation-flotation process. Water, Air, Soil Pollut. 226, 1–14.

Eskicioglu, C., Prorot, A., Marin, J., Droste, R.L., Kennedy, K.J., 2008. Synergetic pretreatment of sewage sludge by microwave irradiation in presence of H2O2 for enhanced anaerobic digestion. Water Res. 42, 4674–4682. https://doi.org/10.1016/j.watres.2008.08.010

Feng, L.J., Wang, J.J., Liu, S.C., Sun, X.D., Yuan, X.Z., Wang, S.G., 2018. Role of extracellular

polymeric substances in the acute inhibition of activated sludge by polystyrene nanoparticles. Environ. Pollut. 238, 859–865. https://doi.org/10.1016/J.ENVPOL.2018.03.101

Feng, Q., Song, Y.C., Kim, Dong Hyun, Kim, M.S., Kim, Dong Hoon, 2019. Influence of the temperature and hydraulic retention time in bioelectrochemical anaerobic digestion of sewage sludge. Int. J. Hydrogen Energy 44, 2170–2179. https://doi.org/10.1016/J.IJHYDENE.2018.09.055

Feng, Y., Duan, J.-L., Sun, X.-D., Ma, J.-Y., Wang, Q., Li, X.-Y., Tian, W.-X., Wang, S.-G., Yuan, X.-Z., 2020. Insights on the inhibition of anaerobic digestion performances under short-term exposure of metal-doped nanoplastics via Methanosarcina acetivorans. Environ. Pollut. https://doi.org/10.1016/j.envpol.2020.115755

Feng, Y., Feng, L.J., Liu, S.C., Duan, J.L., Zhang, Y.B., Li, S.C., Sun, X.D., Wang, S.G., Yuan, X.Z., 2018. Emerging investigator series: Inhibition and recovery of anaerobic granular sludge performance in response to short-term polystyrene nanoparticle exposure. Environ. Sci. Water Res. Technol. https://doi.org/10.1039/c8ew00535d

Ferreira, L.C., Souza, T.S.O., Fdz-Polanco, F., Pérez-Elvira, S.I., 2014. Thermal steam explosion pretreatment to enhance anaerobic biodegradability of the solid fraction of pig manure. Bioresour. Technol. 152, 393–398. https://doi.org/10.1016/J.BIORTECH.2013.11.050

Flemming, H.-C., Wingender, J., 2010. The biofilm matrix. Nat. Rev. Microbiol. 8, 623–633.

Fu, S.F., Ding, J.N., Zhang, Y., Li, Y.F., Zhu, R., Yuan, X.Z., Zou, H., 2018. Exposure to polystyrene nanoplastic leads to inhibition of anaerobic digestion system. Sci. Total Environ. 625, 64–70. https://doi.org/10.1016/j.scitotenv.2017.12.158

Galafassi, S., Nizzetto, L., Volta, P., 2019. Plastic sources: A survey across scientific and grey literature for their inventory and relative contribution to microplastics pollution in natural environments, with an emphasis on surface water. Sci. Total Environ. https://doi.org/10.1016/j.scitotenv.2019.07.305

Gao, J., Li, Z., Chen, H., 2023. Untangling the effect of solids content on thermal-alkali pre-treatment and anaerobic digestion of sludge. Sci. Total Environ. 855, 158720. https://doi.org/10.1016/J.SCITOTENV.2022.158720

García, J., García-Galán, M.J., Day, J.W., Boopathy, R., White, J.R., Wallace, S., Hunter, R.G., 2020. A review of emerging organic contaminants (EOCs), antibiotic resistant bacteria (ARB), and antibiotic resistance genes (ARGs) in the environment: Increasing removal with wetlands and reducing environmental impacts. Bioresour. Technol. https://doi.org/10.1016/j.biortech.2020.123228

Gies, E.A., LeNoble, J.L., Noël, M., Etemadifar, A., Bishay, F., Hall, E.R., Ross, P.S., 2018. Retention of microplastics in a major secondary wastewater treatment plant in Vancouver, Canada. Mar. Pollut. Bull. https://doi.org/10.1016/j.marpolbul.2018.06.006

Gong, L., Yang, X., Wang, Z., Zhou, J., You, X., 2019. Impact of hydrothermal pre-treatment on the anaerobic digestion of different solid–liquid ratio sludges and kinetic analysis. RSC Adv. 9, 19104–19113. https://doi.org/10.1039/C9RA01662G

Gonzalez, A., Hendriks, A.T.W.M., van Lier, J.B., de Kreuk, M., 2018. Pre-treatments to enhance the biodegradability of waste activated sludge: Elucidating the rate limiting step. Biotechnol. Adv. 36, 1434–1469. https://doi.org/10.1016/j.biotechadv.2018.06.001

Grube, M., Lin, J.G., Lee, P.H., Kokorevicha, S., 2006. Evaluation of sewage sludge-based compost by FT-IR spectroscopy. Geoderma 130, 324–333. https://doi.org/10.1016/j.geoderma.2005.02.005

Gunaseelan, V.N., 2004. Biochemical methane potential of fruits and vegetable solid waste feedstocks. Biomass and bioenergy 26, 389–399.

Guo, J., Peng, Y., Ni, B.-J., Han, X., Fan, L., Yuan, Z., 2015. Dissecting microbial community structure and methane-producing pathways of a full-scale anaerobic reactor digesting activated sludge from wastewater treatment by metagenomic sequencing. Microb. Cell Fact. 14, 33. https://doi.org/10.1186/s12934-015-0218-4

Guo, J.J., Huang, X.P., Xiang, L., Wang, Y.Z., Li, Y.W., Li, H., Cai, Q.Y., Mo, C.H., Wong, M.H., 2020. Source, migration and toxicology of microplastics in soil. Environ. Int. 137, 105263. https://doi.org/10.1016/J.ENVINT.2019.105263

Guo, N., Ma, X., Ren, S., Wang, S., Wang, Y., 2019. Mechanisms of metabolic performance enhancement during electrically assisted anaerobic treatment of chloramphenicol wastewater.

Water Res. https://doi.org/10.1016/j.watres.2019.03.032

Haffiez, N., Azizi, S.M.M., Zakaria, B.S., Dhar, B.R., 2022a. Propagation of antibiotic resistance genes during anaerobic digestion of thermally hydrolyzed sludge and their correlation with extracellular polymeric substances. Sci. Rep. 12, 1–13. https://doi.org/10.1038/s41598-022-10764-1

Haffiez, N., Chung, T.H., Zakaria, B.S., Shahidi, M., Mezbahuddin, S., Hai, F.I., Dhar, B.R., 2022b. A critical review of process parameters influencing the fate of antibiotic resistance genes in the anaerobic digestion of organic waste. Bioresour. Technol. 354, 127189. https://doi.org/10.1016/J.BIORTECH.2022.127189

Haffiez, N., Zakaria, B.S., Azizi, S.M.M., Dhar, B.R., 2023. Fate of intracellular, extracellular polymeric substances-associated, and cell-free antibiotic resistance genes in anaerobic digestion of thermally hydrolyzed sludge. Sci. Total Environ. 855, 158847. https://doi.org/https://doi.org/10.1016/j.scitotenv.2022.158847

Haug, R.T., Stuckey, D.C., Gossett, J.M., McCarty, P.L., 1978. Effect of thermal pretreatment on digestibility and dewaterability of organic sludges. J. (Water Pollut. Control Fed. 73–85.

He, D., Luo, Y., Lu, S., Liu, M., Song, Y., Lei, L., 2018. Microplastics in soils: Analytical methods, pollution characteristics and ecological risks. TrAC - Trends Anal. Chem. https://doi.org/10.1016/j.trac.2018.10.006

He, Z.W., Yang, W.J., Ren, Y.X., Jin, H.Y., Tang, C.C., Liu, W.Z., Yang, C.X., Zhou, A.J., Wang, A.J., 2021. Occurrence, effect, and fate of residual microplastics in anaerobic digestion of waste activated sludge: A state-of-the-art review. Bioresour. Technol. 331, 125035. https://doi.org/10.1016/J.BIORTECH.2021.125035

Heyer, R., Kohrs, F., Reichl, U., Benndorf, D., 2015. Metaproteomics of complex microbial communities in biogas plants. Microb. Biotechnol. https://doi.org/10.1111/1751-7915.12276

Horne, A.J., Lessner, D.J., 2013. Assessment of the oxidant tolerance of Methanosarcina acetivorans. FEMS Microbiol. Lett. https://doi.org/10.1111/1574-6968.12115

Hosseini Koupaie, E., Johnson, T., Eskicioglu, C., 2018. Comparison of different electricity-based

thermal pretreatment methods for enhanced bioenergy production from municipal sludge. Molecules 23, 2006.

Hwang, J., Choi, D., Han, S., Choi, J., Hong, J., 2019. An assessment of the toxicity of polypropylene microplastics in human derived cells. Sci. Total Environ. 684, 657–669. https://doi.org/10.1016/j.scitotenv.2019.05.071

Iranpour, R., Cox, H.H.J., Kearney, R.J., Clark, J.H., Pincince, a. B., Daigger, G.T., 2004. Regulations for biosolids land application in US and European Union. J. Residuals Sci. Technol.

Iyare, P.U., Ouki, S.K., Bond, T., 2020. Microplastics removal in wastewater treatment plants: a critical review. Environ. Sci. Water Res. Technol. 6, 2664–2675.

Jankowska, E., Sahu, A.K., Oleskowicz-Popiel, P., 2017. Biogas from microalgae: Review on microalgae's cultivation, harvesting and pretreatment for anaerobic digestion. Renew. Sustain. Energy Rev. https://doi.org/10.1016/j.rser.2016.11.045

Jenner, L.C., Rotchell, J.M., Bennett, R.T., Cowen, M., Tentzeris, V., Sadofsky, L.R., 2022. Detection of microplastics in human lung tissue using μFTIR spectroscopy. Sci. Total Environ. 831, 154907. https://doi.org/10.1016/J.SCITOTENV.2022.154907

Jeong, S.Y., Chang, S.W., Ngo, H.H., Guo, W., Nghiem, L.D., Banu, J.R., Jeon, B.H., Nguyen, D.D., 2019. Influence of thermal hydrolysis pretreatment on physicochemical properties and anaerobic biodegradability of waste activated sludge with different solids content. Waste Manag. 85, 214–221. https://doi.org/10.1016/j.wasman.2018.12.026

Jiang, Y., Dennehy, C., Lawlor, P.G., Hu, Z., McCabe, M., Cormican, P., Zhan, X., Gardiner, G.E., 2019. Exploring the roles of and interactions among microbes in dry co-digestion of food waste and pig manure using high-throughput 16S rRNA gene amplicon sequencing. Biotechnol. Biofuels 12, 1–16.

Jiao, Y., Cody, G.D., Harding, A.K., Wilmes, P., Schrenk, M., Wheeler, K.E., Banfield, J.F., Thelen, M.P., 2010. Characterization of extracellular polymeric substances from acidophilic microbial biofilms. Appl. Environ. Microbiol. 76, 2916–2922.

Jolliffe, I.T., 2002. Springer series in statistics. Princ. Compon. Anal. 29.

Jones, R.N., Ramsay, D.A., Keir, D.S., Dobriner, K., 1952. The intensities of carbonyl bands in the infrared spectra of Steroids1. J. Am. Chem. Soc. 74, 80–88.

Karakashev, D., Batstone, D.J., Angelidaki, I., 2005. Influence of environmental conditions on methanogenic compositions in anaerobic biogas reactors. Appl. Environ. Microbiol. 71, 331–8. https://doi.org/10.1128/AEM.71.1.331-338.2005

Kassem, N., Hockey, J., Lopez, C., Lardon, L., Angenent, L.T., Tester, J.W., 2020. Integrating anaerobic digestion, hydrothermal liquefaction, and biomethanation within a power-to-gas framework for dairy waste management and grid decarbonization: a techno-economic assessment. Sustain. Energy Fuels 4, 4644–4661.

Kavitha, S., Rajesh Banu, J., Subitha, G., Ushani, U., Yeom, I.T., 2016. Impact of thermo-chemo-sonic pretreatment in solubilizing waste activated sludge for biogas production: Energetic analysis and economic assessment. Bioresour. Technol. 219, 479–486. https://doi.org/10.1016/j.biortech.2016.07.115

Kibler, K.M., Reinhart, D., Hawkins, C., Motlagh, A.M., Wright, J., 2018. Food waste and the food-energy-water nexus: a review of food waste management alternatives. Waste Manag. 74, 52–62.

Kim, D., Lee, K., Park, K.Y., 2015. Enhancement of biogas production from anaerobic digestion of waste activated sludge by hydrothermal pre-treatment. Int. Biodeterior. Biodegrad. 101, 42–46. https://doi.org/10.1016/j.ibiod.2015.03.025

Kim, S.M., Dien, B.S., Singh, V., 2016. Promise of combined hydrothermal/chemical and mechanical refining for pretreatment of woody and herbaceous biomass. Biotechnol. Biofuels 9, 1–15.

Kor-Bicakci, G., Eskicioglu, C., 2019. Recent developments on thermal municipal sludge pretreatment technologies for enhanced anaerobic digestion. Renew. Sustain. Energy Rev. 110, 423–443. https://doi.org/10.1016/j.rser.2019.05.002

Kumar Biswal, B., Huang, H., Dai, J., Chen, G.H., Wu, D., 2020. Impact of low-thermal

pretreatment on physicochemical properties of saline waste activated sludge, hydrolysis of organics and methane yield in anaerobic digestion. Bioresour. Technol. 297, 122423. https://doi.org/10.1016/j.biortech.2019.122423

Lafratta, M., Thorpe, R.B., Ouki, S.K., Shana, A., Germain, E., Willcocks, M., Lee, J., 2020. Dynamic biogas production from anaerobic digestion of sewage sludge for on-demand electricity generation. Bioresour. Technol. https://doi.org/10.1016/j.biortech.2020.123415

Lambie, S.C., Kelly, W.J., Leahy, S.C., Li, D., Reilly, K., McAllister, T.A., Valle, E.R., Attwood, G.T., Altermann, E., 2015. The complete genome sequence of the rumen methanogen Methanosarcina barkeri CM1. Stand. Genomic Sci. 10, 1–8.

laqa Kakar, F., Koupaie, E.H., Razavi, A.S., Hafez, H., Elbeshbishy, E., 2020. Effect of hydrothermal pretreatment on volatile fatty acids production from thickened waste activated sludge. BioEnergy Res. 13, 591–604.

laqa Kakar, F., Koupaie, E.H., Razavi, A.S., Hafez, H., Elbeshbishy, E., Kakar, F. laqa, Koupaie, E.H., Razavi, A.S., Hafez, H., Elbeshbishy, E., 2019. Effect of Hydrothermal Pretreatment on Volatile Fatty Acids Production from Thickened Waste Activated Sludge. BioEnergy Res. 13, 1–14. https://doi.org/10.1007/s12155-019-10056-z

Le, N.T., Julcour-Lebigue, C., Barthe, L., Delmas, H., 2016. Optimisation of sludge pretreatment by low frequency sonication under pressure. J. Environ. Manage. 165, 206–212. https://doi.org/10.1016/j.jenvman.2015.09.015

Lehner, R., Weder, C., Petri-Fink, A., Rothen-Rutishauser, B., 2019. Emergence of Nanoplastic in the Environment and Possible Impact on Human Health. Environ. Sci. & Technol. 53, 1748–1765. https://doi.org/10.1021/acs.est.8b05512

Li, H., Li, C., Liu, W., Zou, S., 2012. Optimized alkaline pretreatment of sludge before anaerobic digestion. Bioresour. Technol. 123, 189–194. https://doi.org/10.1016/j.biortech.2012.08.017

Li, J., Zhang, K., Zhang, H., 2018. Adsorption of antibiotics on microplastics. Environ. Pollut. https://doi.org/10.1016/j.envpol.2018.02.050

Li, J., Liu, F., Yang, C., Zheng, S., Xiao, L., Li, Jinhua, Tu, C., Luo, Y., 2020. Inhibition effect of

polyvinyl chloride on ferrihydrite reduction and electrochemical activities of Geobacter metallireducens. J. Basic Microbiol. https://doi.org/10.1002/jobm.201900415

Li, L., Geng, S., Li, Z., Song, K., 2020. Effect of microplastic on anaerobic digestion of wasted activated sludge. Chemosphere 247, 125874. https://doi.org/10.1016/J.CHEMOSPHERE.2020.125874

Li, S., Cao, Y., Zhao, Z., Zhang, Y., 2019. Regulating secretion of extracellular polymeric substances through dosing magnetite and zerovalent iron nanoparticles to affect anaerobic digestion mode. ACS Sustain. Chem. Eng. 7, 9655–9662. https://doi.org/0.1021/acssuschemeng.9b01252

Li, Z., Chen, H., 2022. Elucidating the role of solids content in low-temperature thermal hydrolysis and anaerobic digestion of sewage sludge. Bioresour. Technol. 362, 127859. https://doi.org/10.1016/J.BIORTECH.2022.127859

Liang, Z., Li, W., Yang, S., Du, P., 2010. Extraction and structural characteristics of extracellular polymeric substances (EPS), pellets in autotrophic nitrifying biofilm and activated sludge. Chemosphere 81, 626–632.

Liao, B.Q., Allen, D.G., Droppo, I.G., Leppard, G.G., Liss, S.N., 2001. Surface properties of sludge and their role in bioflocculation and settleability. Water Res. 35, 339–350. https://doi.org/10.1016/S0043-1354(00)00277-3

Liao, Q., Guo, L., Ran, Y., Gao, M., She, Z., Zhao, Y., Liu, Y., 2018. Optimization of polyhydroxyalkanoates (PHA) synthesis with heat pretreated waste sludge. Waste Manag. 82, 15–25. https://doi.org/10.1016/j.wasman.2018.10.019

Liao, X., Li, H., Zhang, Y., Liu, C., Chen, Q., 2016. Accelerated high-solids anaerobic digestion of sewage sludge using low-temperature thermal pretreatment. Int. Biodeterior. Biodegrad. 106, 141–149. https://doi.org/10.1016/j.ibiod.2015.10.023

Limbach, L.K., Wick, P., Manser, P., Grass, R.N., Bruinink, A., Stark, W.J., 2007. Exposure of engineered nanoparticles to human lung epithelial cells: influence of chemical composition and catalytic activity on oxidative stress. Environ. Sci. Technol. 41, 4158–4163.

Liu, H., Shi, J., Xu, X., Zhan, X., Fu, B., Li, Y., 2017. Enhancement of sludge dewaterability with filamentous fungi Talaromyces flavus S1 by depletion of extracellular polymeric substances or mycelium entrapment. Bioresour. Technol. 245, 977–983. https://doi.org/10.1016/j.biortech.2017.08.185

Liu, H., Zhou, X., Ding, W., Zhang, Z., Nghiem, L.D., Sun, J., Wang, Q., 2019. Do Microplastics Affect Biological Wastewater Treatment Performance? Implications from Bacterial Activity Experiments. ACS Sustain. Chem. Eng. https://doi.org/10.1021/acssuschemeng.9b05960

Liu, He, Han, P., Liu, Hongbo, Zhou, G., Fu, B., Zheng, Z., 2018. Full-scale production of VFAs from sewage sludge by anaerobic alkaline fermentation to improve biological nutrients removal in domestic wastewater. Bioresour. Technol. 260, 105–114. https://doi.org/10.1016/j.biortech.2018.03.105

Liu, Jibao, Zheng, J., Zhang, J., Yu, D., Wei, Y., 2020a. The performance evaluation and kinetics response of advanced anaerobic digestion for sewage sludge under different SRT during semi-continuous operation. Bioresour. Technol. 308, 123239. https://doi.org/10.1016/j.biortech.2020.123239

Liu, Jibao, Zheng, J., Zhang, J., Yu, D., Wei, Y., 2020b. The performance evaluation and kinetics response of advanced anaerobic digestion for sewage sludge under different SRT during semi-continuous operation. Bioresour. Technol. 308, 123239. https://doi.org/10.1016/J.BIORTECH.2020.123239

Liu, Jianwei, Dong, L., Dai, Q., Liu, Y., Tang, X., Liu, Junxin, Xiao, B., 2020. Enhanced anaerobic digestion of sewage sludge by thermal or alkaline-thermal pretreatments: Influence of hydraulic retention time reduction. Int. J. Hydrogen Energy 45, 2655–2667. https://doi.org/10.1016/j.ijhydene.2019.11.198

Liu, W., Zhang, J., Liu, H., Guo, X., Zhang, X., Yao, X., Cao, Z., Zhang, T., 2021. A review of the removal of microplastics in global wastewater treatment plants: Characteristics and mechanisms. Environ. Int. 146, 106277. https://doi.org/10.1016/J.ENVINT.2020.106277

Liu, Xiaohui, Lee, C., Kim, J.Y., 2020. Thermal hydrolysis pre-treatment combined with anaerobic digestion for energy recovery from organic wastes. J. Mater. Cycles Waste Manag. 22, 1370–

1381.

Liu, X., Wang, W., Gao, X., Zhou, Y., Shen, R., 2012. Effect of thermal pretreatment on the physical and chemical properties of municipal biomass waste. Waste Manag. 32, 249–255. https://doi.org/10.1016/j.wasman.2011.09.027

Loow, Y.-L., Wu, T.Y., Jahim, J.M., Mohammad, A.W., Teoh, W.H., 2016. Typical conversion of lignocellulosic biomass into reducing sugars using dilute acid hydrolysis and alkaline pretreatment. Cellulose 23, 1491–1520.

Lu, D., Sun, F., Zhou, Y., 2018. Insights into anaerobic transformation of key dissolved organic matters produced by thermal hydrolysis sludge pretreatment. Bioresour. Technol. 266, 60–67. https://doi.org/10.1016/j.biortech.2018.06.059

Lu, Y., Zhang, Q., Wang, X., Zhou, X., Zhu, J., 2020. Effect of pH on volatile fatty acid production from anaerobic digestion of potato peel waste. Bioresour. Technol. https://doi.org/10.1016/j.biortech.2020.123851

Luo, J., Zhang, Q., Zhao, J., Wu, Y., Wu, L., Li, H., Tang, M., Sun, Y., Guo, W., Feng, Q., Cao, J., Wang, D., 2020. Potential influences of exogenous pollutants occurred in waste activated sludge on anaerobic digestion: A review. J. Hazard. Mater. 383, 121176. https://doi.org/10.1016/J.JHAZMAT.2019.121176

M. Hernandez, L., Yousefi, N., Tufenkji, N., 2017. Are There Nanoplastics in Your Personal Care Products? Environ. Sci. & Technol. Lett. 4, 280–285. https://doi.org/10.1021/acs.estlett.7b00187

Ma, Y., Wilson, C.A., Novak, J.T., Riffat, R., Aynur, S., Murthy, S., Pruden, A., 2011. Effect of various sludge digestion conditions on sulfonamide, macrolide, and tetracycline resistance genes and class I integrons. Environ. Sci. Technol. 45, 7855–7861. https://doi.org/110.1021/es200827t

Mahon, Anne Marie, O'Connell, B., Healy, M.G., O'Connor, I., Officer, R., Nash, R., Morrison, L., 2017. Microplastics in sewage sludge: effects of treatment. Environ. Sci. Technol. 51, 810–818. https://doi.org/https://doi.org/10.1021/acs.est.6b04048

Mahon, A. M., O'Connell, B., Healy, M.G., O'Connor, I., Officer, R., Nash, R., Morrison, L., 2017. Microplastics in sewage sludge: Effects of treatment. Environ. Sci. Technol. https://doi.org/10.1021/acs.est.6b04048

Mao, R., Lang, M., Yu, X., Wu, R., Yang, X., Guo, X., 2020. Aging mechanism of microplastics with UV irradiation and its effects on the adsorption of heavy metals. J. Hazard. Mater. https://doi.org/10.1016/j.jhazmat.2020.122515

Mariotti, F., Tomé, D., Mirand, P.P., 2008. Converting nitrogen into protein—beyond 6.25 and Jones' factors. Crit. Rev. Food Sci. Nutr. 48, 177–184.

Mason, S.A., Garneau, D., Sutton, R., Chu, Y., Ehmann, K., Barnes, J., Fink, P., Papazissimos, D., Rogers, D.L., 2016. Microplastic pollution is widely detected in US municipal wastewater treatment plant effluent. Environ. Pollut. https://doi.org/10.1016/j.envpol.2016.08.056

Meshref, M.N.A., Azizi, S.M.M., Dastyar, W., Maal-Bared, R., Dhar, B.R., 2021. Low-temperature thermal hydrolysis of sludge prior to anaerobic digestion: Principal component analysis (PCA) of experimental data. Data Br. 38, 107323. https://doi.org/10.1016/J.DIB.2021.107323

Miao, L., Wang, P., Hou, J., Yao, Y., Liu, Z., Liu, S., Li, T., 2019. Distinct community structure and microbial functions of biofilms colonizing microplastics. Sci. Total Environ. https://doi.org/10.1016/j.scitotenv.2018.09.378

Mirsoleimani Azizi, S.M., Haffiez, N., Zakaria, B., Dhar, B., n.d. Thermal Hydrolysis of Sludge Counteracts Polystyrene Nanoplastics-Induced Stress during Anaerobic Digestion. ACS ES&T Eng. 2, 1306–1315. https://doi.org/10.1021/acsestengg.1c00460

Mirsoleimani Azizi, S.M., Zakaria, B., Haffiez, N., Dhar, B., n.d. Sludge Thermal Hydrolysis for Mitigating Oxidative Stress of Polystyrene Nanoplastics in Anaerobic Digestion: Significance of the Solids Content. ACS Sustain. Chem. Eng. 11, 7253–7262. https://doi.org/10.1021/acssuschemeng.3c01349

Mohammad Mirsoleimani Azizi, S., Dastyar, W., Meshref, M.N.A., Maal-Bared, R., Ranjan Dhar, B., 2021a. Low-temperature thermal hydrolysis for anaerobic digestion facility in wastewater treatment plant with primary sludge fermentation. Chem. Eng. J. 130485.

https://doi.org/10.1016/j.cej.2021.130485

Mohammad Mirsoleimani Azizi, S., Hai, F.I., Lu, W., Al-Mamun, A., Ranjan Dhar, B., 2021b. A review of mechanisms underlying the impacts of (nano)microplastics on anaerobic digestion. Bioresour. Technol. 329, 124894. https://doi.org/10.1016/J.BIORTECH.2021.124894

Mohammad Mirsoleimani Azizi, S., Zakaria, B.S., Haffiez, N., Ranjan Dhar, B., 2023. Granular activated carbon remediates antibiotic resistance propagation and methanogenic inhibition induced by polystyrene nanoplastics in sludge anaerobic digestion. Bioresour. Technol. 377, 128938. https://doi.org/10.1016/J.BIORTECH.2023.128938

Moretto, G., Valentino, F., Pavan, P., Majone, M., Bolzonella, D., 2019. Optimization of urban waste fermentation for volatile fatty acids production. Waste Manag. 92, 21–29. https://doi.org/10.1016/j.wasman.2019.05.010

Morris, R., Schauer-Gimenez, A., Bhattad, U., Kearney, C., Struble, C.A., Zitomer, D., Maki, J.S., 2014. Methyl coenzyme M reductase (mcrA) gene abundance correlates with activity measurements of methanogenic H2/CO2-enriched anaerobic biomass. Microb. Biotechnol. 7, 77. https://doi.org/10.1111/1751-7915.12094

Mosallanejad, A., Taghvaei, H., Mirsoleimani-azizi, S.M., Mohammadi, A., Rahimpour, M.R., 2017. Plasma upgrading of 4methylanisole: A novel approach for hydrodeoxygenation of bio oil without using a hydrogen source. Chem. Eng. Res. Des. 121, 113–124. https://doi.org/10.1016/J.CHERD.2017.03.011

Mu, H., Chen, Y., 2011. Long-term effect of ZnO nanoparticles on waste activated sludge anaerobic digestion. Water Res. 45, 5612–5620. https://doi.org/10.1016/j.watres.2011.08.022

Mu, H., Zheng, X., Chen, Y., Chen, H., Liu, K., 2012. Response of anaerobic granular sludge to a shock load of zinc oxide nanoparticles during biological wastewater treatment. Environ. Sci. Technol. 46, 5997–6003. https://doi.org/10.1021/es300616a

Müller, J.A., 2001. Prospects and problems of sludge pre-treatment processes. Water Sci. Technol. 44, 121–128.

Munir, M.T., Mansouri, S.S., Udugama, I.A., Baroutian, S., Gernaey, K. V., Young, B.R., 2018.

Resource recovery from organic solid waste using hydrothermal processing: Opportunities and challenges. Renew. Sustain. Energy Rev. 96, 64–75. https://doi.org/10.1016/J.RSER.2018.07.039

Nazari, L., Yuan, Z., Santoro, D., Sarathy, S., Ho, D., Batstone, D., Xu, C. (Charles), Ray, M.B., 2017. Low-temperature thermal pre-treatment of municipal wastewater sludge: Process optimization and effects on solubilization and anaerobic degradation. Water Res. 113, 111–123. https://doi.org/https://doi.org/10.1016/j.watres.2016.11.055

Nel, A., Xia, T., Mädler, L., Li, N., 2006. Toxic potential of materials at the nanolevel. Science (80-.). 311, 622–627. https://doi.org/10.1126/science.1114397

Neumann, P., Barriga, F., Álvarez, C., González, Z., Vidal, G., 2018. Process performance assessment of advanced anaerobic digestion of sewage sludge including sequential ultrasound–thermal (55 °C) pre-treatment. Bioresour. Technol. 262, 42–51. https://doi.org/10.1016/J.BIORTECH.2018.03.057

Neyens, E., Baeyens, J., Creemers, C., 2003. Alkaline thermal sludge hydrolysis. J. Hazard. Mater. 97, 295–314. https://doi.org/10.1016/S0304-3894(02)00286-8

Neyens, E., Baeyens, J., Dewil, R., De Heyder, B., 2004. Advanced sludge treatment affects extracellular polymeric substances to improve activated sludge dewatering. J. Hazard. Mater. 106, 83–92. https://doi.org/10.1016/j.jhazmat.2003.11.014

Nges, I.A., Liu, J., 2010. Effects of solid retention time on anaerobic digestion of dewatered-sewage sludge in mesophilic and thermophilic conditions. Renew. Energy 35, 2200–2206. https://doi.org/10.1016/j.renene.2010.02.022

Ngo, P.L., Pramanik, B.K., Shah, K., Roychand, R., 2019. Pathway, classification and removal efficiency of microplastics in wastewater treatment plants. Environ. Pollut. 255, 113326. https://doi.org/10.1016/J.ENVPOL.2019.113326

Nguyen, D.D., Yoon, Y.S., Nguyen, N.D., Bach, Q.V., Bui, X.T., Chang, S.W., Le, H.S., Guo, W., Ngo, H.H., 2017. Enhanced efficiency for better wastewater sludge hydrolysis conversion through ultrasonic hydrolytic pretreatment. J. Taiwan Inst. Chem. Eng. 71, 244–252. https://doi.org/10.1016/j.jtice.2016.12.019

Nizzetto, L., Futter, M., Langaas, S., 2016. Are agricultural soils dumps for microplastics of urban origin?, Environmental Science and Technology. ACS Publications. https://doi.org/https://doi.org/10.1021/acs.est.6b04140

Nnadozie, C.F., Kumari, S., Bux, F., 2017. Status of pathogens, antibiotic resistance genes and antibiotic residues in wastewater treatment systems. Rev. Environ. Sci. Bio/Technology 16, 491–515.

Nuruddin, M., Hosur, M., Uddin, M.J., Baah, D., Jeelani, S., 2016. A novel approach for extracting cellulose nanofibers from lignocellulosic biomass by ball milling combined with chemical treatment. J. Appl. Polym. Sci. 133.

O'Connor, I.A., Golsteijn, L., Hendriks, A.J., 2016. Review of the partitioning of chemicals into different plastics: Consequences for the risk assessment of marine plastic debris. Mar. Pollut. Bull. 113, 17–24. https://doi.org/10.1016/J.MARPOLBUL.2016.07.021

Oliveira, J., Belchior, A., da Silva, V.D., Rotter, A., Petrovski, Ž., Almeida, P.L., Lourenço, N.D., Gaudêncio, S.P., 2020. Marine environmental plastic pollution: mitigation by microorganism degradation and recycling valorization. Front. Mar. Sci. 7.

Pagés-Díaz, J., Cerda Alvarado, A.O., Montalvo, S., Diaz-Robles, L., Curio, C.H., 2020. Anaerobic bio-methane potential of the liquors from hydrothermal carbonization of different lignocellulose biomasses. Renew. Energy 157, 182–189. https://doi.org/10.1016/J.RENENE.2020.05.025

Paik, P., Kar, K.K., 2006. Glass transition temperature of high molecular weight polystyrene: effect of particle size, bulk to micron to nano, in: NSTI-Nanotech. pp. 483–486.

Park, M., Kim, N., Lee, S., Yeon, S., Seo, J.H., Park, D., 2019. A study of solubilization of sewage sludge by hydrothermal treatment. J. Environ. Manage. 250, 109490. https://doi.org/10.1016/j.jenvman.2019.109490

Passaris, I., Van Gaelen, P., Cornelissen, R., Simoens, K., Grauwels, D., Vanhaecke, L., Springael, D., Smets, I., 2018. Cofactor F430 as a biomarker for methanogenic activity: application to an anaerobic bioreactor system. Appl. Microbiol. Biotechnol. https://doi.org/10.1007/s00253-017-8681-y

Pei, J., Yao, H., Wang, H., Ren, J., Yu, X., 2016. Comparison of ozone and thermal hydrolysis combined with anaerobic digestion for municipal and pharmaceutical waste sludge with tetracycline resistance genes. Water Res. 99, 122–128. https://doi.org/10.1016/j.watres.2016.04.058

Peng, L., Appels, L., Su, H., 2018. Combining microwave irradiation with sodium citrate addition improves the pre-treatment on anaerobic digestion of excess sewage sludge. J. Environ. Manage. 213, 271–278. https://doi.org/10.1016/j.jenvman.2018.02.053

Pereira de Albuquerque, F., Dhadwal, M., Dastyar, W., Mirsoleimani Azizi, S.M., Karidio, I., Zaman, H., Dhar, B.R., 2021. Fate of disposable face masks in high-solids anaerobic digestion: experimental observations and review of potential environmental implications. Case Stud. Chem. Environ. Eng. 100082. https://doi.org/10.1016/j.cscee.2021.100082

Pham, D.N., Clark, L., Li, M., 2021. Microplastics as hubs enriching antibiotic-resistant bacteria and pathogens in municipal activated sludge. J. Hazard. Mater. Lett. 2, 100014. https://doi.org/10.1016/j.hazl.2021.100014

Phan, H. V., Wickham, R., Xie, S., McDonald, J.A., Khan, S.J., Ngo, H.H., Guo, W., Nghiem, L.D., 2018. The fate of trace organic contaminants during anaerobic digestion of primary sludge: A pilot scale study. Bioresour. Technol. https://doi.org/10.1016/j.biortech.2018.02.040

Pilli, S., Yan, S., Tyagi, R.D., Surampalli, R.Y., 2015. Thermal pretreatment of sewage sludge to enhance anaerobic digestion: a review. Crit. Rev. Environ. Sci. Technol. 45, 669–702.

Prata, J.C., da Costa, J.P., Lopes, I., Duarte, A.C., Rocha-Santos, T., 2019. Effects of microplastics on microalgae populations: A critical review. Sci. Total Environ. https://doi.org/10.1016/j.scitotenv.2019.02.132

Pud, A., Ogurtsov, N., Korzhenko, A., Shapoval, G., 2003. Some aspects of preparation methods and properties of polyaniline blends and composites with organic polymers. Prog. Polym. Sci. 28, 1701–1753. https://doi.org/10.1016/J.PROGPOLYMSCI.2003.08.001

Qian, J., Han, Y., Guo, J., Zhang, J., Hou, Y., Song, Y., Lu, C., Li, H., 2021. Semi-starvation fluctuation driving rapid partial denitrification granular sludge cultivation in situ by

microorganism exudate metabolites feedbacks. Environ. Res. 196, 110938. https://doi.org/10.1016/J.ENVRES.2021.110938

Qin, R., Su, C., Liu, W., Tang, L., Li, X., Deng, X., Wang, A., Chen, Z., 2020. Effects of exposure to polyether sulfone microplastic on the nitrifying process and microbial community structure in aerobic granular sludge. Bioresour. Technol. https://doi.org/10.1016/j.biortech.2020.122827

Rajagopal, R., Massé, D.I., Singh, G., 2013. A critical review on inhibition of anaerobic digestion process by excess ammonia. Bioresour. Technol. https://doi.org/10.1016/j.biortech.2013.06.030

Rajesh Banu, J., Ushani, U., Rajkumar, M., Naresh Kumar, R., Parthiba Karthikeyan, O., 2017. Impact of mild alkali dosage on immobilized Exiguobacterium spp. mediated cost and energy efficient sludge disintegration. Bioresour. Technol. 245, 434–441. https://doi.org/10.1016/j.biortech.2017.08.216

Raso, J., Mañas, P., Pagán, R., Sala, F.J., 1999. Influence of different factors on the output power transferred into medium by ultrasound. Ultrason. Sonochem. 5, 157–162. https://doi.org/10.1016/S1350-4177(98)00042-X

Ray, P.D., Huang, B.W., Tsuji, Y., 2012. Reactive oxygen species (ROS) homeostasis and redox regulation in cellular signaling. Cell. Signal. 24, 981–990. https://doi.org/10.1016/J.CELLSIG.2012.01.008

Réveillé, V., Mansuy, L., Jardé, É., Garnier-Sillam, É., 2003. Characterisation of sewage sludge-derived organic matter: Lipids and humic acids. Org. Geochem. 34, 615–627. https://doi.org/10.1016/S0146-6380(02)00216-4

Rezaee, M., Gitipour, S., Sarrafzadeh, M.-H., 2020. Different pathways to integrate anaerobic digestion and thermochemical processes: moving toward the circular economy concept. Environ. Energy Econ. Res. 4, 57–67.

Riau, V., De la Rubia, M.Á., Pérez, M., 2010. Temperature-phased anaerobic digestion (TPAD) to obtain class A biosolids: A semi-continuous study. Bioresour. Technol. https://doi.org/10.1016/j.biortech.2009.11.101

Rolsky, C., Kelkar, V., Driver, E., Halden, R.U., 2020. Municipal sewage sludge as a source of microplastics in the environment. Curr. Opin. Environ. Sci. Heal. https://doi.org/10.1016/j.coesh.2019.12.001

Rouches, E., Herpoël-Gimbert, I., Steyer, J.P., Carrere, H., 2016. Improvement of anaerobic degradation by white-rot fungi pretreatment of lignocellulosic biomass: A review. Renew. Sustain. Energy Rev. 59, 179–198. https://doi.org/10.1016/J.RSER.2015.12.317

Rozzi, A., Remigi, E., 2004. Methods of assessing microbial activity and inhibition under anaerobic conditions: a literature review. Re/Views Environ. Sci. Bio/Technology 3, 93–115.

Ruan, D., Zhou, Z., Pang, H., Yao, J., Chen, G., Qiu, Z., 2019. Enhancing methane production of anaerobic sludge digestion by microaeration: Enzyme activity stimulation, semi-continuous reactor validation and microbial community analysis. Bioresour. Technol. https://doi.org/10.1016/j.biortech.2019.121643

Ruffino, B., Cerutti, A., Campo, G., Scibilia, G., Lorenzi, E., Zanetti, M., 2020. Thermophilic vs. mesophilic anaerobic digestion of waste activated sludge: Modelling and energy balance for its applicability at a full scale WWTP. Renew. Energy. https://doi.org/10.1016/j.renene.2020.04.068

Sáez-Plaza, P., Navas, M.J., Wybraniec, S., Michałowski, T., Asuero, A.G., 2013. An overview of the Kjeldahl method of nitrogen determination. Part II. Sample preparation, working scale, instrumental finish, and quality control. Crit. Rev. Anal. Chem. 43, 224–272.

Sahoo, K., Mani, S., 2019. Economic and environmental impacts of an integrated-state anaerobic digestion system to produce compressed natural gas from organic wastes and energy crops. Renew. Sustain. Energy Rev. 115, 109354. https://doi.org/10.1016/J.RSER.2019.109354

Samaras, V.G., Stasinakis, A.S., Thomaidis, N.S., Mamais, D., Lekkas, T.D., 2014. Fate of selected emerging micropollutants during mesophilic, thermophilic and temperature co-phased anaerobic digestion of sewage sludge. Bioresour. Technol. https://doi.org/10.1016/j.biortech.2014.03.154

Seeley, M.E., Song, B., Passie, R., Hale, R.C., 2020. Microplastics affect sedimentary microbial communities and nitrogen cycling. Nat. Commun. https://doi.org/10.1038/s41467-020-

16235-3

Senesi, N., D'Orazio, V., Ricca, G., 2003. Humic acids in the first generation of EUROSOILS. Geoderma 116, 325–344. https://doi.org/10.1016/S0016-7061(03)00107-1

Sheng, G.P., Yu, H.Q., Li, X.Y., 2010. Extracellular polymeric substances (EPS) of microbial aggregates in biological wastewater treatment systems: A review. Biotechnol. Adv. https://doi.org/10.1016/j.biotechadv.2010.08.001

Shi, J., Wu, D., Su, Y., Xie, B., 2020. (Nano)microplastics promote the propagation of antibiotic resistance genes in landfill leachate. Environ. Sci. Nano 7, 3536–3546. https://doi.org/10.1039/D0EN00511H

Siddiqui, K., 2013. Heuristics for sample size determination in multivariate statistical techniques. World Appl. Sci. J. 27, 285–287.

Silva, S.A., Cavaleiro, A.J., Pereira, M.A., Stams, A.J.M., Alves, M.M., Sousa, D.Z., 2014. Long-term acclimation of anaerobic sludges for high-rate methanogenesis from LCFA. Biomass and Bioenergy 67, 297–303. https://doi.org/10.1016/j.biombioe.2014.05.012

Song, B., Lin, R., Lam, C.H., Wu, H., Tsui, T.H., Yu, Y., 2021. Recent advances and challenges of inter-disciplinary biomass valorization by integrating hydrothermal and biological techniques. Renew. Sustain. Energy Rev. 135, 110370. https://doi.org/10.1016/J.RSER.2020.110370

Summers, S., Henry, T., Gutierrez, T., 2018. Agglomeration of nano- and microplastic particles in seawater by autochthonous and de novo-produced sources of exopolymeric substances. Mar. Pollut. Bull. 130, 258–267. https://doi.org/10.1016/J.MARPOLBUL.2018.03.039

Sun, C., Li, W., Chen, Z., Qin, W., Wen, X., 2019. Responses of antibiotics, antibiotic resistance genes, and mobile genetic elements in sewage sludge to thermal hydrolysis pre-treatment and various anaerobic digestion conditions. Environ. Int. 133, 105156. https://doi.org/10.1016/J.ENVINT.2019.105156

Sun, J., Dai, X., Wang, Q., van Loosdrecht, M.C.M., Ni, B.J., 2019. Microplastics in wastewater treatment plants: Detection, occurrence and removal. Water Res.

https://doi.org/10.1016/j.watres.2018.12.050

Sun, J., Guo, L., Li, Q., Zhao, Y., Gao, M., She, Z., Wang, G., 2016. Structural and functional properties of organic matters in extracellular polymeric substances (EPS) and dissolved organic matters (DOM) after heat pretreatment with waste sludge. Bioresour. Technol. 219, 614–623. https://doi.org/10.1016/j.biortech.2016.08.042

Sun, W., Gu, J., Wang, X., Qian, X., Peng, H., 2019. Solid-state anaerobic digestion facilitates the removal of antibiotic resistance genes and mobile genetic elements from cattle manure. Bioresour. Technol. 274, 287–295. https://doi.org/10.1016/J.BIORTECH.2018.09.013

Sun, Y., Luo, H., Iboleon, R., Wang, Z., 2022. Fate of antibiotic resistance genes and class 1 integrons during sludge treatment using pilot-scale anaerobic digestion with thermal hydrolysis pretreatment. Bioresour. Technol. 364, 128043. https://doi.org/10.1016/J.BIORTECH.2022.128043

Tang, J., Wu, Y., Esquivel-Elizondo, S., Sørensen, S.J., Rittmann, B.E., 2018. How microbial aggregates protect against nanoparticle toxicity. Trends Biotechnol. 36, 1171–1182.

Tian, T., Qiao, S., Li, X., Zhang, M., Zhou, J., 2017. Nano-graphene induced positive effects on methanogenesis in anaerobic digestion. Bioresour. Technol. https://doi.org/10.1016/j.biortech.2016.10.058

Tian, T., Qiao, S., Yu, C., Zhou, J., 2019. Effects of nano-sized MnO2 on methanogenic propionate and butyrate degradation in anaerobic digestion. J. Hazard. Mater. 364, 11–18. https://doi.org/10.1016/j.jhazmat.2018.09.081

Tong, J., Fang, P., Zhang, J., Wei, Y., Su, Y., Zhang, Y., 2019. Microbial community evolution and fate of antibiotic resistance genes during sludge treatment in two full-scale anaerobic digestion plants with thermal hydrolysis pretreatment. Bioresour. Technol. 288, 121575. https://doi.org/10.1016/j.biortech.2019.121575

Tong, J., Liu, J., Zheng, X., Zhang, J., Ni, X., Chen, M., Wei, Y., 2016. Fate of antibiotic resistance bacteria and genes during enhanced anaerobic digestion of sewage sludge by microwave pretreatment. Bioresour. Technol. 217, 37–43. https://doi.org/10.1016/j.biortech.2016.02.130

Tong, J., Lu, X.T., Zhang, J.Y., Sui, Q., Wang, R., Chen, M., Wei, Y., 2017. Occurrence of antibiotic resistance genes and mobile genetic elements in enterococci and genomic DNA during anaerobic digestion of pharmaceutical waste sludge with different pretreatments. Bioresour. Technol. 235, 316–324. https://doi.org/10.1016/j.biortech.2017.03.104

Tourinho, P.S., Ivar do Sul, J.A., Fillmann, G., 2010. Is marine debris ingestion still a problem for the coastal marine biota of southern Brazil? Mar. Pollut. Bull. 60, 396–401. https://doi.org/10.1016/J.MARPOLBUL.2009.10.013

Toutian, V., Barjenbruch, M., Loderer, C., Remy, C., 2021. Impact of process parameters of thermal alkaline pretreatment on biogas yield and dewaterability of waste activated sludge. Water Res. 202, 117465. https://doi.org/10.1016/J.WATRES.2021.117465

Toutian, V., Barjenbruch, M., Unger, T., Loderer, C., Remy, C., 2020. Effect of temperature on biogas yield increase and formation of refractory COD during thermal hydrolysis of waste activated sludge. Water Res. 171, 115383. https://doi.org/10.1016/j.watres.2019.115383

Val del Río, A., Morales, N., Isanta, E., Mosquera-Corral, A., Campos, J.L., Steyer, J.P., Carrère, H., 2011. Thermal pre-treatment of aerobic granular sludge: Impact on anaerobic biodegradability. Water Res. 45, 6011–6020. https://doi.org/10.1016/j.watres.2011.08.050

Villamil, J.A., Mohedano, A.F., Rodriguez, J.J., De la Rubia, M.A., 2019. Anaerobic co-digestion of the aqueous phase from hydrothermally treated waste activated sludge with primary sewage sludge. A kinetic study. J. Environ. Manage. 231, 726–733. https://doi.org/10.1016/j.jenvman.2018.10.031

Villamil, J.A., Mohedano, A.F., San Martín, J., Rodriguez, J.J., de la Rubia, M.A., 2020. Anaerobic co-digestion of the process water from waste activated sludge hydrothermally treated with primary sewage sludge. A new approach for sewage sludge management. Renew. Energy 146, 435–443. https://doi.org/10.1016/j.renene.2019.06.138

Vu, M.T., Noori, M.T., Min, B., 2020. Magnetite/zeolite nanocomposite-modified cathode for enhancing methane generation in microbial electrochemical systems. Chem. Eng. J. 393, 124613. https://doi.org/10.1016/j.cej.2020.124613

Wang, C., Zhao, J., Xing, B., 2021. Environmental source, fate, and toxicity of microplastics. J.

Hazard. Mater. https://doi.org/10.1016/j.jhazmat.2020.124357

Wang, D., Zhao, J., Zeng, G., Chen, Y., Bond, P.L., Li, X., 2015. How Does Poly(hydroxyalkanoate) Affect Methane Production from the Anaerobic Digestion of Waste-Activated Sludge? Environ. Sci. Technol. https://doi.org/10.1021/acs.est.5b03112

Wang, M., Li, R., Zhao, Q., 2019. Distribution and removal of antibiotic resistance genes during anaerobic sludge digestion with alkaline, thermal hydrolysis and ultrasonic pretreatments. Front. Environ. Sci. Eng. 13, 1–10.

Wang, T., Zhai, Y., Zhu, Y., Peng, C., Xu, B., Wang, Tao, Li, C., Zeng, G., 2017. Acetic acid and sodium hydroxide-aided hydrothermal carbonization of woody biomass for enhanced pelletization and fuel properties. Energy & fuels 31, 12200–12208.

Wang, X., Zhao, J., Yang, Q., Sun, J., Peng, C., Chen, F., Xu, Q., Wang, S., Wang, D., Li, X., Zeng, G., 2017. Evaluating the potential impact of hydrochar on the production of short-chain fatty acid from sludge anaerobic digestion. Bioresour. Technol. https://doi.org/10.1016/j.biortech.2017.07.051

Wang, Z., Gao, J., Dai, H., Zhao, Y., Li, D., Duan, W., Guo, Y., 2021. Microplastics affect the ammonia oxidation performance of aerobic granular sludge and enrich the intracellular and extracellular antibiotic resistance genes. J. Hazard. Mater. 409, 124981. https://doi.org/10.1016/j.jhazmat.2020.124981

Wei, W., Hao, Q., Chen, Z., Bao, T., Ni, B.J., 2020. Polystyrene nanoplastics reshape the anaerobic granular sludge for recovering methane from wastewater. Water Res. 182, 116041. https://doi.org/10.1016/j.watres.2020.116041

Wei, W., Huang, Q.-S., Sun, J., Wang, J.-Y., Wu, S.-L., Ni, B.-J., 2019a. Polyvinyl chloride microplastics affect methane production from the anaerobic digestion of waste activated sludge through leaching toxic bisphenol-A. Environ. Sci. Technol. 53, 2509–2517.

Wei, W., Huang, Q.-S.S., Sun, J., Dai, X., Ni, B.-J.J., 2019b. Revealing the mechanisms of polyethylene microplastics affecting anaerobic digestion of waste activated sludge. Environ. Sci. Technol. 53, 9604–9613. https://doi.org/10.1021/acs.est.9b02971

Wei, W., Huang, Q.S., Sun, J., Wang, J.Y., Wu, S.L., Ni, B.J., 2019c. Polyvinyl Chloride Microplastics Affect Methane Production from the Anaerobic Digestion of Waste Activated Sludge through Leaching Toxic Bisphenol-A. Environ. Sci. Technol. https://doi.org/10.1021/acs.est.8b07069

Wei, W., Zhang, Y.T., Huang, Q.S., Ni, B.J., 2019d. Polyethylene terephthalate microplastics affect hydrogen production from alkaline anaerobic fermentation of waste activated sludge through altering viability and activity of anaerobic microorganisms. Water Res. 163, 114881. https://doi.org/10.1016/j.watres.2019.114881

Wenjing, L., Chao, P., Lama, A., Xindi, F., Rong, Y., Dhar, B.R., 2019. Effect of pre-treatments on biological methane potential of dewatered sewage sludge under dry anaerobic digestion. Ultrason. Sonochem. 52. https://doi.org/10.1016/j.ultsonch.2018.11.022

Wilson, C.A., Novak, J.T., 2009. Hydrolysis of macromolecular components of primary and secondary wastewater sludge by thermal hydrolytic pretreatment. Water Res. 43, 4489–4498. https://doi.org/10.1016/j.watres.2009.07.022

Wright, M.S., Baker-Austin, C., Lindell, A.H., Stepanauskas, R., Stokes, H.W., McArthur, J.V., 2008. Influence of industrial contamination on mobile genetic elements: class 1 integron abundance and gene cassette structure in aquatic bacterial communities. ISME J. 2, 417–428. https://doi.org/10.1038/ismej.2008.8

Wu, Y., Cui, E., Zuo, Y., Cheng, W., Rensing, C., Chen, H., 2016. Influence of two-phase anaerobic digestion on fate of selected antibiotic resistance genes and class I integrons in municipal wastewater sludge. Bioresour. Technol. https://doi.org/10.1016/j.biortech.2016.03.086

Wu, Z., Nguyen, D., Lam, T.Y.C., Zhuang, H., Shrestha, S., Raskin, L., Khanal, S.K., Lee, P.H., 2021. Synergistic association between cytochrome bd-encoded Proteiniphilum and reactive oxygen species (ROS)-scavenging methanogens in microaerobic-anaerobic digestion of lignocellulosic biomass. Water Res. 190, 116721. https://doi.org/10.1016/j.watres.2020.116721

Xu, J., Sheng, G.P., Ma, Y., Wang, L.F., Yu, H.Q., 2013. Roles of extracellular polymeric

substances (EPS) in the migration and removal of sulfamethazine in activated sludge system. Water Res. 47, 5298–5306. https://doi.org/10.1016/j.watres.2013.06.009

Xu, Z., Bai, X., Ye, Z., 2021. Removal and generation of microplastics in wastewater treatment plants: A review. J. Clean. Prod. 291, 125982. https://doi.org/10.1016/J.JCLEPRO.2021.125982

Xue, Y., Liu, H., Chen, S., Dichtl, N., Dai, X., Li, N., 2015. Effects of thermal hydrolysis on organic matter solubilization and anaerobic digestion of high solid sludge. Chem. Eng. J. 264, 174–180. https://doi.org/10.1016/j.cej.2014.11.005

Yang, S., McDonald, J., Hai, F.I., Price, W.E., Khan, S.J., Nghiem, L.D., 2017. The fate of trace organic contaminants in sewage sludge during recuperative thickening anaerobic digestion. Bioresour. Technol. https://doi.org/10.1016/j.biortech.2017.02.020

Yang, X., Nie, J., Wang, D., Zhao, Z., Kobayashi, M., Adachi, Y., Shimizu, K., Lei, Z., Zhang, Z., 2019. Enhanced hydrolysis of waste activated sludge for methane production via anaerobic digestion under N2-nanobubble water addition. Sci. Total Environ. https://doi.org/10.1016/j.scitotenv.2019.07.330

Yenigün, O., Demirel, B., 2013. Ammonia inhibition in anaerobic digestion: A review. Process Biochem. https://doi.org/10.1016/j.procbio.2013.04.012

Yun, H., Liang, B., Ding, Y., Li, S., Wang, Z., Khan, A., Zhang, Peng, Zhang, Pengyun, Zhou, A., Wang, A., Li, X., 2021. Fate of antibiotic resistance genes during temperature-changed psychrophilic anaerobic digestion of municipal sludge. Water Res. 194, 116926. https://doi.org/10.1016/J.WATRES.2021.116926

Zakaria, B.S., Barua, S., Sharaf, A., Liu, Y., Dhar, B.R., 2018. Impact of antimicrobial silver nanoparticles on anode respiring bacteria in a microbial electrolysis cell. Chemosphere 213, 259–267. https://doi.org/10.1016/j.chemosphere.2018.09.060

Zakaria, B.S., Dhar, B.R., 2021. Characterization and significance of extracellular polymeric substances, reactive oxygen species, and extracellular electron transfer in methanogenic biocathode. Sci. Rep. 11, 1–13. https://doi.org/https://doi.org/10.1038/s41598-021-87118-w

Zakaria, B.S., Dhar, B.R., 2020. Changes in syntrophic microbial communities, EPS matrix, and gene-expression patterns in biofilm anode in response to silver nanoparticles exposure. Sci. Total Environ. 734, 139395. https://doi.org/10.1016/j.scitotenv.2020.139395

Zakaria, B.S., Dhar, B.R., 2019. Progress towards catalyzing electro-methanogenesis in anaerobic digestion process: Fundamentals, process optimization, design and scale-up considerations. Bioresour. Technol. https://doi.org/10.1016/j.biortech.2019.121738

Zang, Y., Yang, Y., Hu, Y., Ngo, H.H., Wang, X.C., Li, Y.Y., 2020. Zero-valent iron enhanced anaerobic digestion of pre-concentrated domestic wastewater for bioenergy recovery: Characteristics and mechanisms. Bioresour. Technol. 310, 123441. https://doi.org/10.1016/J.BIORTECH.2020.123441

Zettler, E.R., Mincer, T.J., Amaral-Zettler, L.A., 2013. Life in the "plastisphere": microbial communities on plastic marine debris. Environ. Sci. Technol. 47, 7137–7146. https://doi.org/10.1021/es401288x

Zhang, C., Su, H., Baeyens, J., Tan, T., 2014. Reviewing the anaerobic digestion of food waste for biogas production. Renew. Sustain. Energy Rev. 38, 383–392. https://doi.org/10.1016/j.rser.2014.05.038

Zhang, D., Feng, Y., Huang, H., Khunjar, W., Wang, Z.W., 2020. Recalcitrant dissolved organic nitrogen formation in thermal hydrolysis pretreatment of municipal sludge. Environ. Int. https://doi.org/10.1016/j.envint.2020.105629

Zhang, J., Liu, J., Lu, T., Shen, P., Zhong, H., Tong, J., Wei, Y., 2019. Fate of antibiotic resistance genes during anaerobic digestion of sewage sludge: Role of solids retention times in different configurations. Bioresour. Technol. https://doi.org/10.1016/j.biortech.2018.12.008

Zhang, J., Mao, F., Loh, K.C., Gin, K.Y.H., Dai, Y., Tong, Y.W., 2018. Evaluating the effects of activated carbon on methane generation and the fate of antibiotic resistant genes and class I integrons during anaerobic digestion of solid organic wastes. Bioresour. Technol. 249, 729–736. https://doi.org/10.1016/J.BIORTECH.2017.10.082

Zhang, J., Wang, S., Lang, S., Xian, P., Xie, T., 2016. Kinetics of combined thermal pretreatment and anaerobic digestion of waste activated sludge from sugar and pulp industry. Chem. Eng.

J. 295, 131–138. https://doi.org/10.1016/j.cej.2016.03.028

Zhang, J., Zhao, M., Li, C., Miao, H., Huang, Z., Dai, X., Ruan, W., 2020. Evaluation the impact of polystyrene micro and nanoplastics on the methane generation by anaerobic digestion. Ecotoxicol. Environ. Saf. 205, 111095. https://doi.org/10.1016/J.ECOENV.2020.111095

Zhang, Q., Fan, D., Pang, X., Zhu, W., Zhao, J., Xu, J., 2021. Effects of polyethylene microplastics on the fate of antibiotic resistance genes and microbial communities in anaerobic digestion of dairy wastes. J. Clean. Prod. 292, 125909. https://doi.org/10.1016/j.jclepro.2021.125909

Zhang, X., Chen, J., Li, J., 2020. The removal of microplastics in the wastewater treatment process and their potential impact on anaerobic digestion due to pollutants association. Chemosphere. https://doi.org/10.1016/j.chemosphere.2020.126360

Zhang, Y., Xu, S., Cui, M., Wong, J.W.C., 2019. Effects of different thermal pretreatments on the biodegradability and bioaccessibility of sewage sludge. Waste Manag. 94, 68–76. https://doi.org/10.1016/j.wasman.2019.05.047

Zhang, Z., Chen, Y., 2020. Effects of microplastics on wastewater and sewage sludge treatment and their removal: A review. Chem. Eng. J. 382, 122955. https://doi.org/10.1016/J.CEJ.2019.122955

Zhao, J., Hou, T., Zhang, Z., Shimizu, K., Lei, Z., Lee, D.J., 2020. Anaerobic co-digestion of hydrolysate from anaerobically digested sludge with raw waste activated sludge: Feasibility assessment of a new sewage sludge management strategy in the context of a local wastewater treatment plant. Bioresour. Technol. 314, 123748. https://doi.org/10.1016/j.biortech.2020.123748

Zhao, P., Chen, H., Ge, S., Yoshikawa, K., 2013. Effect of the hydrothermal pretreatment for the reduction of no emission from sewage sludge combustion. Appl. Energy 111, 199–205. https://doi.org/10.1016/j.apenergy.2013.05.029

Zheng, L., Zhang, Z., Tian, L., Zhang, L., Cheng, S., Li, Z., Cang, D., 2019. Mechanistic investigation of toxicological change in ZnO and TiO2 multi-nanomaterial systems during anaerobic digestion and the microorganism response. Biochem. Eng. J. 147, 62–71. https://doi.org/10.1016/j.bej.2019.03.017

Zhou, P., Meshref, M.N.A., Dhar, B.R., 2021. Optimization of thermal hydrolysis process for enhancing anaerobic digestion in a wastewater treatment plant with existing primary sludge fermentation. Bioresour. Technol. 321, 124498. https://doi.org/10.1016/j.biortech.2020.124498

Appendix A

Supplementary Information for Chapter 3

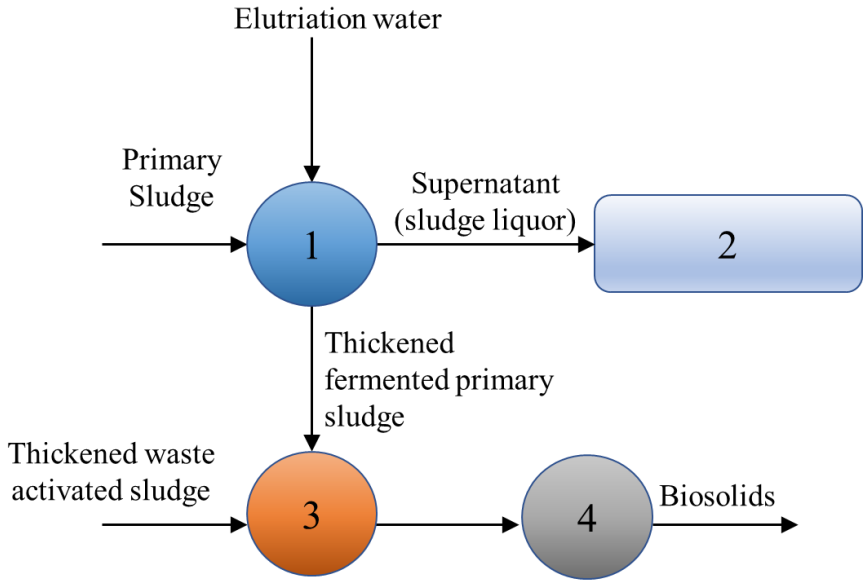

1. Fermenter/thickener
2. Biological nutrient removal process (anaerobic zone)
3. Blend tanks
4. Anaerobic digester

Figure A1. A simplified process flow diagram of sludge processing at the Gold Bar Wastewater Treatment Plant.

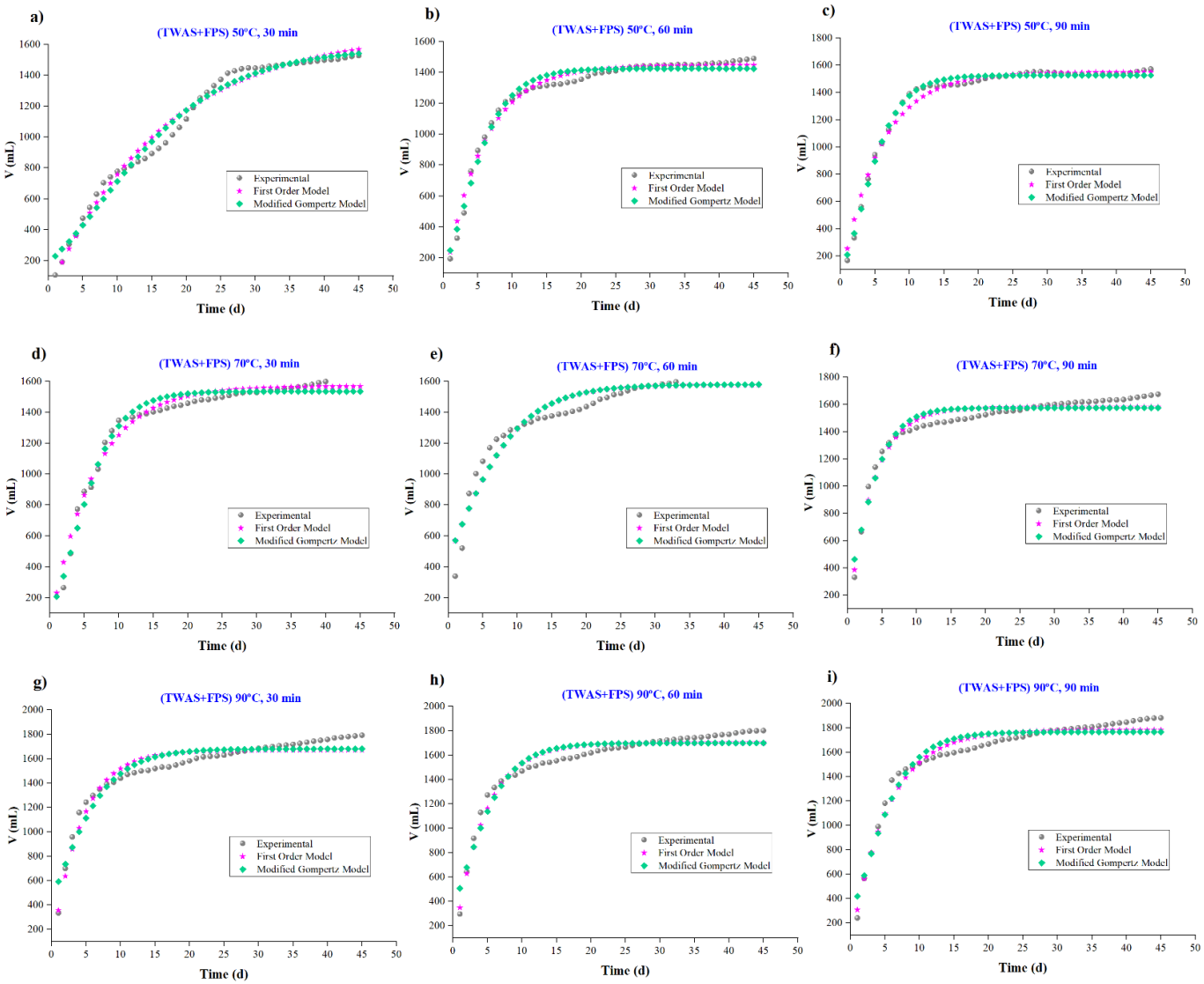

Figure A2. Experimental (grey) and predicted methane production for scheme-1; First order model (magenta) and the modified Gompertz model (green).

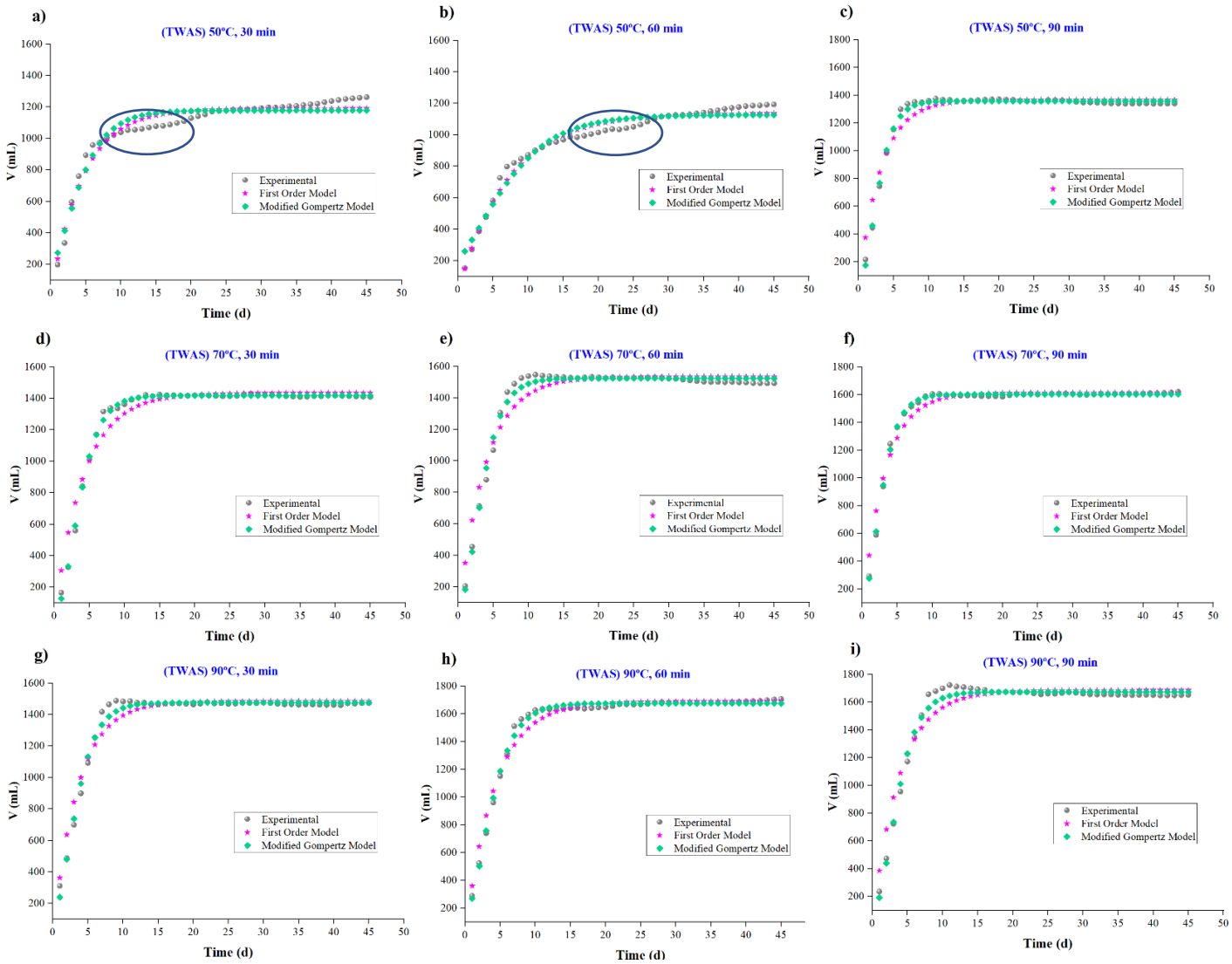

Figure A3. Experimental (grey) and predicted methane production for scheme-2; First order model (magenta) and the modified Gompertz model (green).

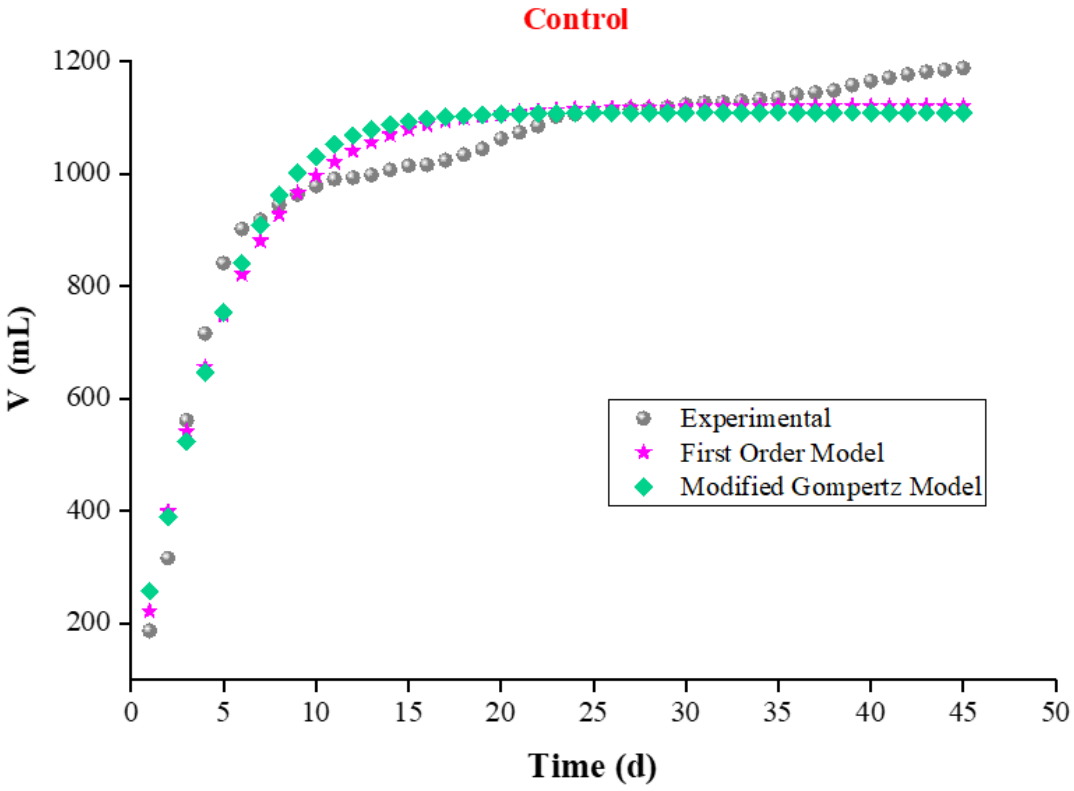

Figure A4. Experimental (grey) and predicted methane production for the control; First order model (magenta) and the modified Gompertz model (green).

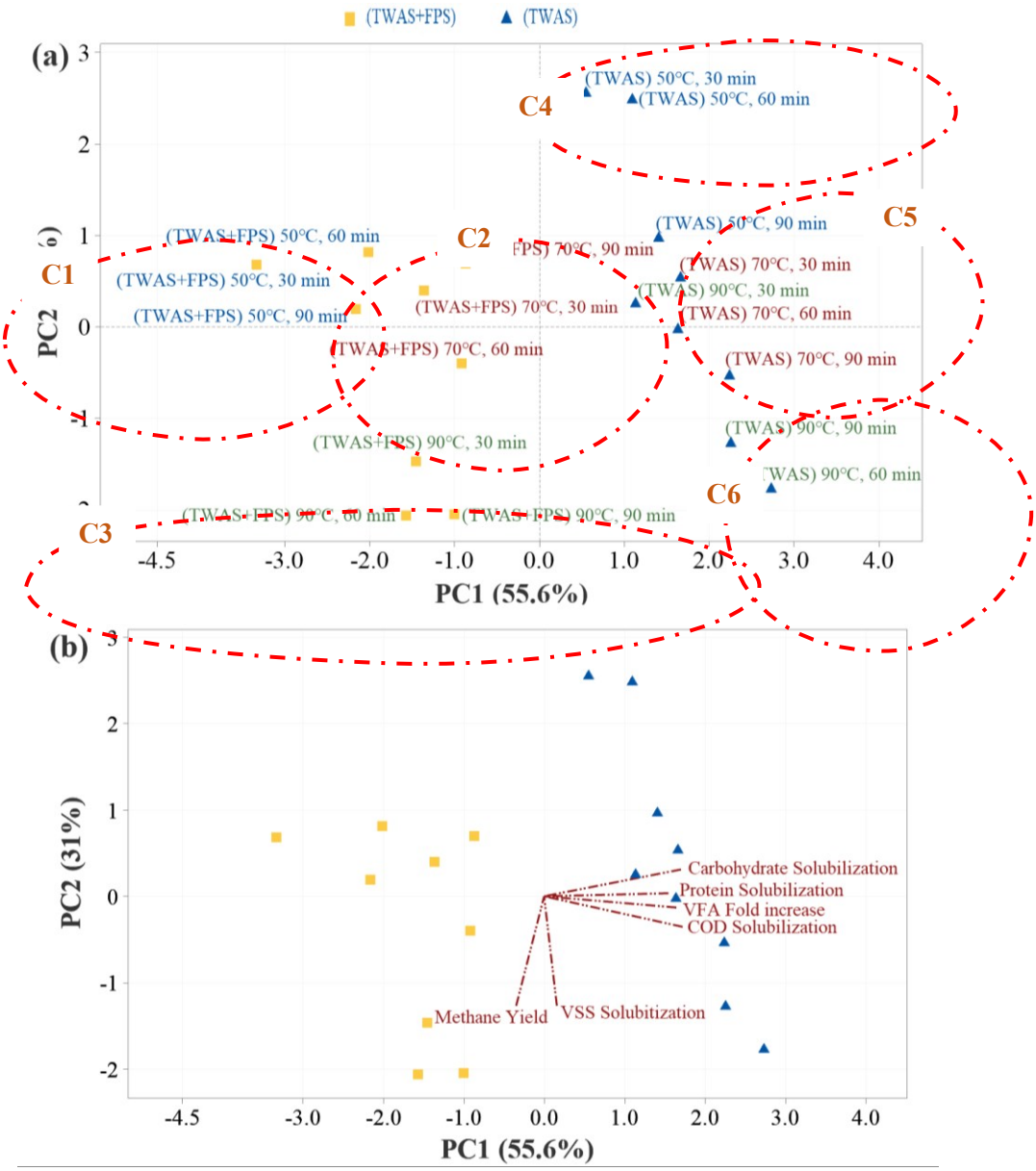

Figure A5. (a) Score plot for PCA analysis of all thermally hydrolysed sludge samples, PC 1 (55.6%) and PC 2 (31%), (b) Biplot and loading plot of PC1 and PC2 with project lines of all pretreated samples where sample loadings are represented as vectors radiating from the origin. Sample scores are indicated by symbols (according to each scheme), samples that are chemically similar will plot near to each other (clustered together), samples are color-coded by substrate source.

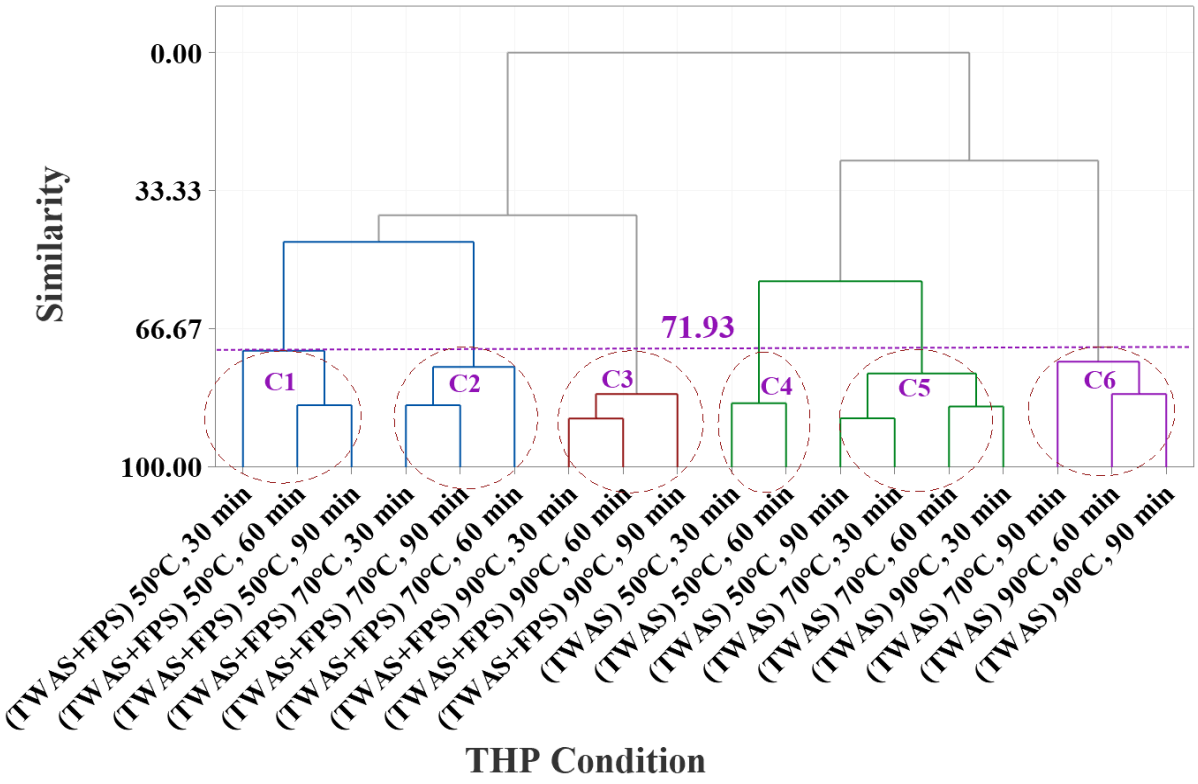

Figure A6. Dendrogram of the cluster analysis for solubilization metrics and methane yield based on THP conditions. At similarity level of 71.93; 6 main clusters were observed similar to PCA in Fig. S5: cluster 1 (TWAS+FPS samples at 50ºC and 30-60 min), cluster 2 (TWAS+FPS samples at 70ºC and 30-90 min); cluster 3 (TWAS+FPS samples at 90ºC and 30-90 min); cluster 4 (TWAS samples at 50ºC (30-60 min)); cluster 5 (TWAS samples at 50ºC (90 min); 70ºC (30-60 min), and 90ºC and 30 min); and cluster 6 (TWAS samples at 70ºC (30 min) and 90ºC (60-90 min)).

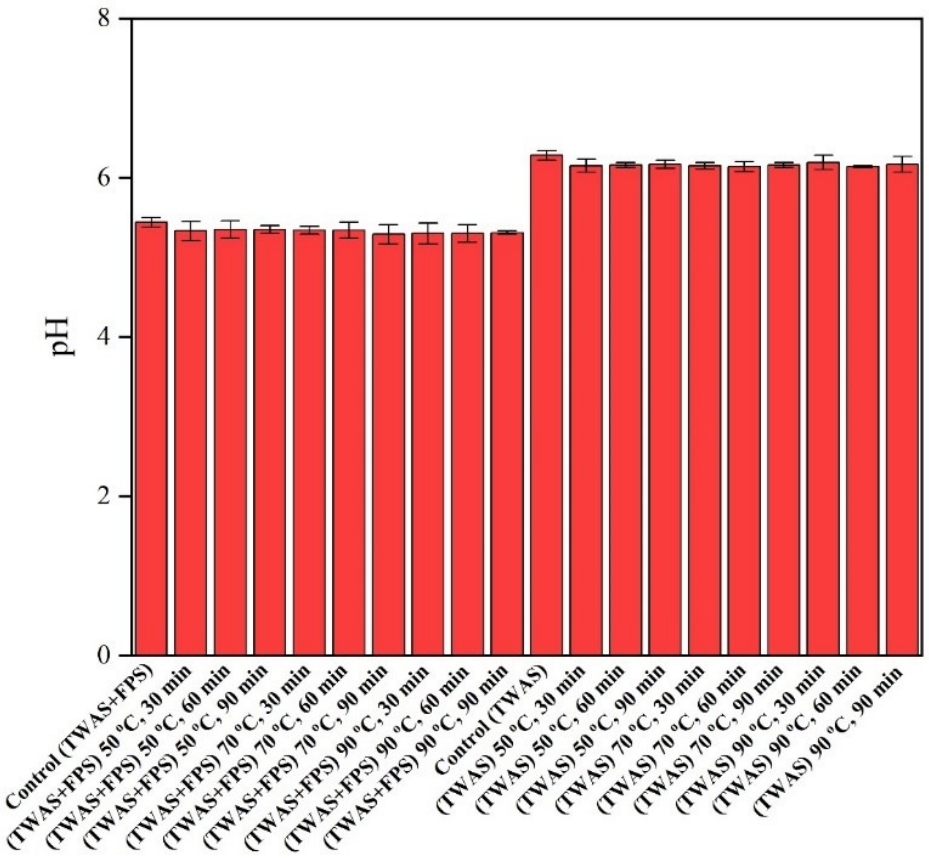

Figure A7. Effect of various pretreatment conditions on pH.

Appendix B

Supplementary Information for Chapter 4

Table B4. Characteristics of substrate and inoculum.

Parameters	**Inoculum**	**Substrate**		
	Digested sludge	**PS[a]**	**TWAS[b]**	**PS+TWAS[c]**
TSS (mg/L)	16,625± 125	33,875 ± 125	26,500 ± 250	30,188 ± 63
VSS (mg/L)	16,625 ± 1,250	30,500 ± 1,500	24,875 ± 375	30,188 ± 937
TCOD (mg/L)	24,188 ± 18	50,126 ± 750	39,385 ± 345	44,756± 210
SCOD (mg/L)	3,280 ± 97	5,152 ± 75	2,047 ± 51	3,600 ± 13
TVFA (mg COD/L)	125 ± 2	1,125 ± 13	103 ± 3	614 ± 4
TAN (mg/L)	1,244 ±57	79.45 ± 1.9	199 ± 1.5	139.2 ± 1.4
pH	7.50 ± 0.01	6.4 ± 0.01	6.6± 0.01	7.4 ± 0.04

[a] Primary sludge (PS).

[b] Thickened waste activated sludge (TWAS).

[c] Mixture of PS and TWAS (volume ratio of 1:1).

Text B1. EPS characterization

For characterization of EPS, sludge samples were washed three times using 0.1 MPBS, pH 7.4. The supernatant was then discarded after centrifugation at 3000 ×g for 15 min at 21ºC. For EPS extraction, the heating method was used according to the procedure detailed in the literature (Xu et al., 2013; Zakaria and Dhar, 2020). Briefly, the samples were washed twice with 0.9% NaCl (w/v), following by resuspension in 0.9% NaCl (w/v). Afterward, samples were incubated at 60ºC in a water bath for 30 min. Then, three times centrifugation at 20,000 ×g for 20 min at 4ºC was conducted. The supernatant was collected and then filtered using a 0.2 µm filter. The EPS was kept and stored at -20ºC for further analysis. Also, the pellets were collected to examine the interfering of intracellular components to EPS measurements due to cell lysis using the Glucose-6-Phosphate Dehydrogenase kit (Sigma-Aldrich, USA) according to the manufacture's protocol (Liang et al., 2010; Xu et al., 2013).

The carbohydrate content was determined using the modified phenol-sulfuric acid method (Dubois et al., 1956), using glucose as the standard. A mixture of 2 mL EPS and 5mL concentrated sulfuric acid was prepared. After mixing, 0.05 mL of 80 wt% phenol was added to the mixture. After 10 min at room temperature, the mixture was shaken and incubated at 30ºC for 20 min. Afterward, the samples were cooled down at room temperature. Then, the absorbance was read at 490 nm with a spectrophotometer (Model DR 3900, HACH, Germany) within 10 min for both standard and test samples (Jiao et al., 2010; Mohammad Mirsoleimani Azizi et al., 2021a). Pierce™ Modified Lowry Protein Assay Kit (Thermo Fisher, USA) was utilized to determine the protein contents of the EPS according to the manufacturer's instructions.

Text B2. Microscopic imaging

For TEM imaging, sludge samples were prepared according to the methods provided in the literature (Zakaria et al., 2018). Briefly, sludge samples were fixed for 24h in a 2.5% glutaraldehyde. Then, washed three times for 15 min in a phosphate buffer solution (0.1M, pH 7.4), post-fixed in 1% Osmium Tetroxide (Polysciences, USA) in a phosphate buffer solution (0.1M, pH 7.4) for 1 h, then washed by phosphate buffer solution (0.1M, pH 7.4) three times for 15 min each. Afterwards, the samples were dehydrated in graded series of ethanol (50%, 70%, 90% and three times 100% for 25 min each), infiltered with Spurr's Resin (Ethanol: Spurr Mixture, 1:1 for 3 h), then in 100% Spurr Resin overnight two times. Embedding was done by incubating in flat molds with fresh Spurr Resin for 24 h at 70ºC. Ultra-thin sections were obtained using a Reichert-Jung Ultracut E ultra-microtome (USA). Semi-thin sections were mounted on grid and stained with uranyl acetate and leadcitrate stain. Once the regions of interest were identified, ultra-thin sections were obtained and observed, and images were photo-graphed using a TEM (Philips-FEI, Morgagni 268, USA) equipped with a Gatan Orius CCD Camera.

For SEM imaging, samples were prepared according to the procedure provided in the literature (Braet et al., 1997; Zakaria et al., 2018) after slight modification. Samples were fixed in 3% glutaraldehyde for 24 h, then washed three times for 15 min in a PBS buffer solution (0.1M, pH 7.4). The samples were dehydrated in graded series of ethanol (50%, 70%, 90% and three times 100% for 20 min each), and finally immersed in mixture series of ethanol/hexamethyldisilazane (HMDS) of 25%, 50%, 75% and three times 100% for 20 min each, then dried in a desiccator. Then, samples were mounted on stubs and coated with carbon to be observed with Zeiss Sigma 300 VP-FESEM (Carl Zeiss, Cambridge, UK) at 10.0 KV. For each sample, microscopic imaging (both SEM and TEM) was performed at least four different locations and used for qualitative assessment of biofilms.

Text B3. Characterization of bacterial community

For genomic DNA extraction, the collected sludge samples were centrifuged to separate cell pellets. Then, the genomic DNA of the samples was extracted using PowerSoil® DNA Isolation Kit (MoBio Laboratories, Carlsbad, USA) according to the manufacturer's instructions. Afterwards, to measure the concentrations, quality, and integrity of the extracted DNA, NanoDrop spectrophotometer (2000C, Thermo Scientific, USA) was utilized. Extracted DNA samples were stored at -70ºC until Illumina Miseq Sequencing was performed and analyzed by RTL Genomics Laboratory (Lubbock, TX, USA). Universal bacterial primers 357Wf: CCTACGGGNGGCWGCAG and 785R: GACTACHVGGGTATCTAATCC were used to target 16S rRNA gene (Zakaria et al., 2018). Also, qPCR was performed to quantify cell copy numbers. qPCR mixtures were prepared in 25 µL reactions using QuantiFast SYBR® Green PCR Kit (Qiagen, CA) as the following: 2 µL of the DNA template, 12.5 µL 2x master mix, 2.5 µL forward and reverse specific primer, and 5.5 µL nuclease-free water. CFX 96 real-time PCR system with a C1000 Thermal Cycler (Bio-Rad, USA) was used with the following cycling conditions according to the QuantiFast SYBR® Green PCR Kit's protocol; PCR initial heat activation cycle at 95ºC for 5 min, 35 cycles at 95ºC for 10 sec and 60ºC for 30 sec, and finally, one cycle at 40ºC for 30 seconds. Triplicate reactions were run for all samples.

To analyze the microbial diversity, the nucleotide sequence reads were sorted out using a data analysis pipeline. Short sequences, noisy reads, and chimeric sequences were removed through a denoising step and chimera detection, respectively. Then each sample was run through the analysis pipeline to determine the taxonomic information for each constituent read. Bacteria taxonomy was assigned using the Quantitative Insights Into Microbial Ecology (QIIME 2) pipeline (https://qiime.org/, Bolyen et al., 2019). Raw data analysis methodology for sequencing (https://rtlgenomics.com/documents) was provided by the laboratory.

Table B2. List of primers used for the analysis of ARGs.

	Genes	Forward primer	Reverse primer
Tetracycline	***tet*A**	GCTACATCCTGCTTGCCTTC	CATAGATCGCCGTGAAGAGG
	***tet*B**	GGCAGGAAGAATAGCCACTAA	AGCGATCCCACCACCAG
	***tet*M**	ACAGAAAGCTTATTATATAAC	TGGCGTGTCTATGATGTTCAC
	***tet*X**	CAATAATTGGTGGTGGACCC	TTCTTACCTTGGACATCCCG
	***tet*W**	GAGAGCCTGCTATATGCCAGC	GGGCGTATCCACAATGTTAAC
	***tet*Q**	AGAATCTGCTGTTTGCCAGTG	CGGAGTGTCAATGATATTGCA
Sulfonamides	***sul*1**	CGCACCGGAAACATCGCTGCAC	TGAAGTTCCGCCGCAAGGCTCG
	***sul*2**	TCCGGTGGAGGCCGGTATCTGG	CGGGAATGCCATCTGCCTTGAG
MRG	***intl*1**	CCTCCCGCACGATGATC	TCCACGCATCGTCAGGC
	***intl*2**	GTTATTTTATTGCTGGGATTAGGC	TTTTACGCTGCTGTATGGTGC
Macrolide	***erm*B**	GATACCGTTTACGAAATTGG	GAATCGAGACTTGAGTGTGC
	***erm*C**	TTTGAAATCGGCTCAGGAAAA	ATGGTCTATTTCAATGGCAGTTACG
β-lactam	***bla*$_{TEM}$**	ATCAGCAATAAACCAGC	CCCCGAAGAACGTTTTC
	***bla*$_{OXA}$**	ATATCTCTACTGTTGCATCTCC	AAACCCTTCAAACCATCC
16srRNA	**16srRNA**	CCTACGGGNGGCWGCAG	GACTACHVGGGTATCTAATCC

Text B4. Impact of THP alone

The impact of THP (80 and 160ºC for 60 min) on COD solubilization, VSS reduction, NH_3, methane generation, and pH is provided in Table S3. The obtained results indicated that the THP positively affects COD solubilization, leading to 14.5 and 33.9% improvement in solubilization (compared to the control) after applying THP at 80 and 160ºC, respectively. Analogous to COD solubilization, 24.4 and 46.4% increase in VSS reduction was attained after exposure to at 80 and 160ºC, respectively. The ammonia content in the sludge also demonstrated an increasing trend and reached 219.4 and 398 mg/L by applying THP (80 and 160ºC for 60 min), which is significantly higher than control (139.1 mg/L). Regarding methane generation, exposure to THP improved methane generation (compared to the control) by 16% (80ºC) and 65% (160ºC). Also, the EPS composition was significantly affected by applying THP. For instance, the protein content reduced to 197 and 94 mg/g sludge after exposure to 80 and 160ºC, respectively, whereas the protein content for the initial sample was 306 mg/g sludge.

Table B3. The effects of THP alone (without PsNPs exposure).

	Raw sludge	Pretreated Sludge	
		THP-80°C	THP-160°C
TCOD (mg/L)	44,755	44,963	45,539
SCOD (mg/L)	3,599	10,087	18,864
COD solubilization (%)	-	14.4	33.9
TSS mg/L)	30,187	25,600	16,175
VSS (mg/L)	27,687	20,931	14,838
VSS removal (%)	-	24.4	46.4
EPS Polysaccharide (mg/g sludge)	187	173	93
EPS Proteins (mg/g sludge)	306	197	94
NH_3-N (mg/L)	139	219	398
pH	6.5	6.4	5.6
Increase in methane yield (%) [a]	-	16	21

[a] Compared to the control

Text B5. Kinetic analysis

The first-order kinetic and modified Gompertz were used, as illustrated in Eqs. (S1) and (S2) respectively (Jibao Liu et al., 2020a; Vu et al., 2020; Zhang et al., 2016), to evaluate methanogenesis kinetics from the BMP test experimental data:

$$V(t) = V_m\ (1 - e^{-kt}) \quad \text{(S1)}$$

$$V(t) = V_m \cdot \exp\left\{-\exp\left[1 + (\lambda - t)\ \frac{Re}{V_m}\right]\right\} \quad \text{(S2)}$$

Where, V(t) is the cumulative methane production at time t (mL), V_m is the experimental ultimate methane production potential (mL), k is the kinetic methanogenesis rate constant (d^{-1}), t is the cumulative time for the production of methane (days), e is a mathematical constant (2.718282), λ is the lag phase for methane production (days), and R is the maximum production rate of methane (mL/d) (Mohammad Mirsoleimani Azizi et al., 2021a). Non-linear regression analyses using Minitab 19 were performed to ensure generating the best model fit of the methane production and to estimate the values of the kinetic constants (k, λ, and R). Based on the measured methane production from the BMP tests, the initial estimated values were used in the model in the first iterations to minimize the standard error estimate and to attain the best fit values of kinetic parameters.

Table S4 shows methanogenesis rate constant (k) and maximum methane production (V_m) estimated with the first-order kinetic model. The differences between estimated V_m and experimentally measured total cumulative methane production were ≤5%. The highest V_m values were estimated at 50 µg/L (1,782 mL) and 80ºC-50 µg/L (1,998 mL). Nonetheless, all samples demonstrated slightly lower k values than the control. Notably, the results indicated that samples pretreated at 160ºC could not be modeled by a first-order kinetic model. Moreover, no specific trends were observed with increasing PsNPs concentration and applying pretreatment. For instance, at 50, 100, and 150 µg/L, k values were 0.15, 0.17, and 0.16 d^{-1} indicating no specific trends. Also, 80ºC-50 µg/L and 80ºC-100 µg/L demonstrated equal k values (0.19 d^{-1}) whereas it decreased to 0.14 d^{-1} for 80ºC-150 µg/L. The higher methane yields observed for pretreated samples than unpretreated could be attributed to higher methanogenesis rates.

Analogous to the first-order model, the differences between the experimental total cumulative methane production and estimated V_m with the modified Gompertz model were very marginal (see Table S4). Most of the samples showed negative λ, suggesting methane production started without any substantial lag phases. However, for those samples pretreated at 160ºC, a higher amount of λ was achieved, demonstrating a longer required time for commencing methane generation. This finding indicates that methanogens might slowly adopt some of the solubilized organics (refractory and/or inhibitory compounds) released during the THP of sewage sludge or additives released from PsNPs (Mohammad Mirsoleimani Azizi et al., 2021a). Also, the obtained R values were considerably higher than the control (132 mL/d) for 50 µg/L, 80ºC-50 µg/L, 100 µg/L, and 80ºC-100 µg/L indicating reduced lag phases and higher maximum methane production rates contributed to the higher methane yields.

Table *B*4. Kinetic parameters estimated with the first-order and modified Gompertz model.

Experimental conditions	First Order Model				Modified Gompertz Model						Experimental	Differences	
	Methanogenesis rate constant k (d^{-1})	Standard error of k	Estimated Maximum methane production V_m (mL)	Standard error of V_m	Maximum methane production V_m (mL)	Standard error of V_m	Maximum Methane Production Rate, R (mL/d)	Standard error for R	Lag phase, λ (d)	Standard error for λ	Measured maximum methane production Vm (mL)	First Order Model	Modified Gompertz Model
50 µg/L	0.15	0.005	1,782	15.54	1,735	19.06	149	9.92	-1.03	0.43	1,846	3.46%	6.02%
80ºC-50 µg/L	0.19	0.007	1,998	15.75	1,953	11.97	260	12.72	0.08	0.2	2,051	2.59%	4.77%
160ºC-50 µg/L	-	-	-	-	3,357	407	85	3.73	4.75	0.7	2,205	-	-53%
100 µg/L	0.17	0.005	1,295	9.63	1,264	11.38	135	7.66	-0.72	0.34	1,343	3.58%	5.89%
80ºC-100 µg/L	0.19	0.006	1,690	12.71	1,650	10.42	206	9.94	-0.04	0.21	1,728	2.20%	4.52%
160ºC-100 µg/L	-	-	-	-	3,147	442	75	3.00	5.58	0.72	1,960	-	-61%
150 µg/L	0.16	0.005	1,105	9.81	1,091	12.85	85	6.06	-1.97	0.53	1,157	4.50%	5.71%
80ºC-150 µg/L	0.14	0.003	1,388	0.003	1,356	13.34	106	6.03	-1.43	0.40	1,442	3.75%	5.97%
160ºC-150 µg/L	-	-	-	-	2,136	122	62	2.40	2.15	0.54	1,654	-	-29%
Control	0.2	0.007	1,548	12.10	1,547	15.40	132	9.55	-2.44	0.51	1,638	5.50%	5.55%

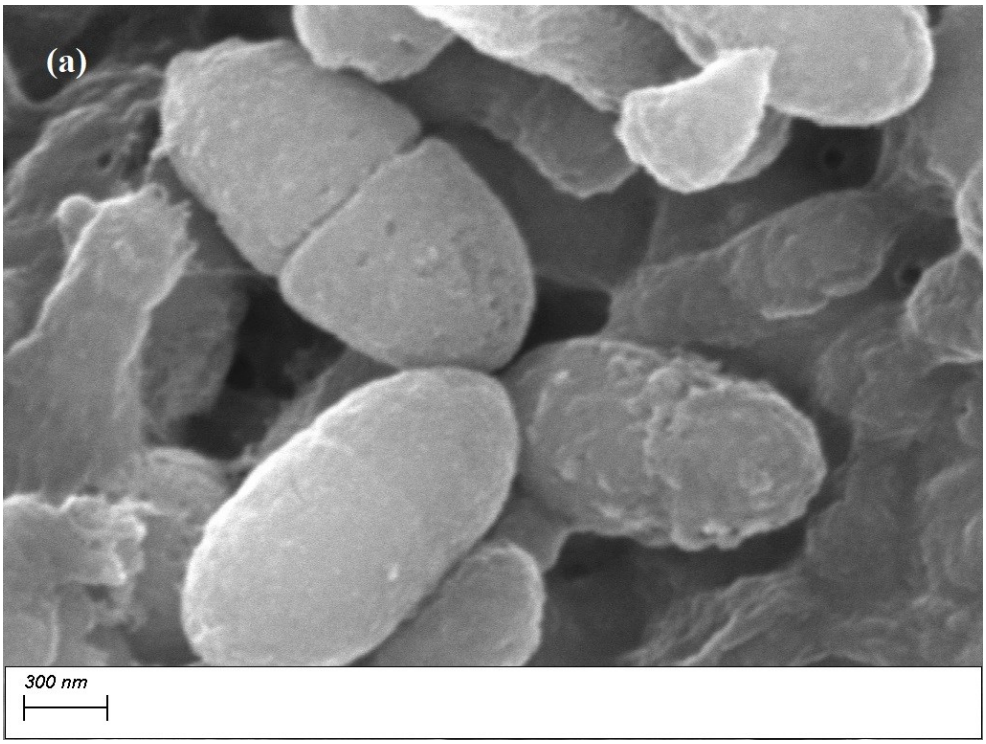
(a)
300 nm

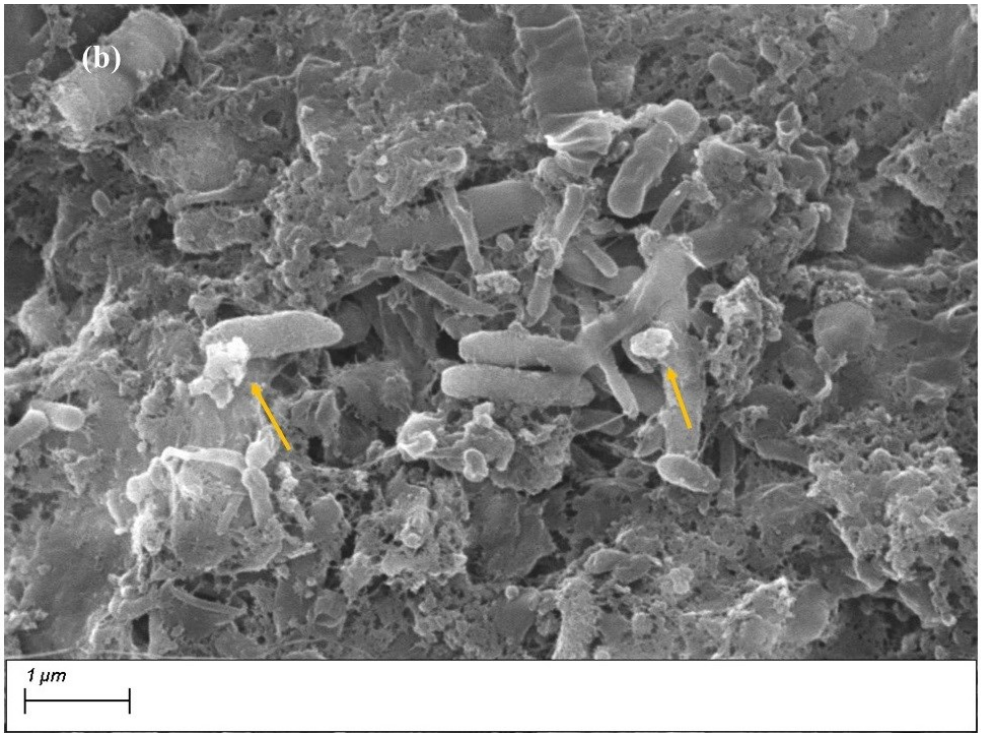
(b)
1 µm

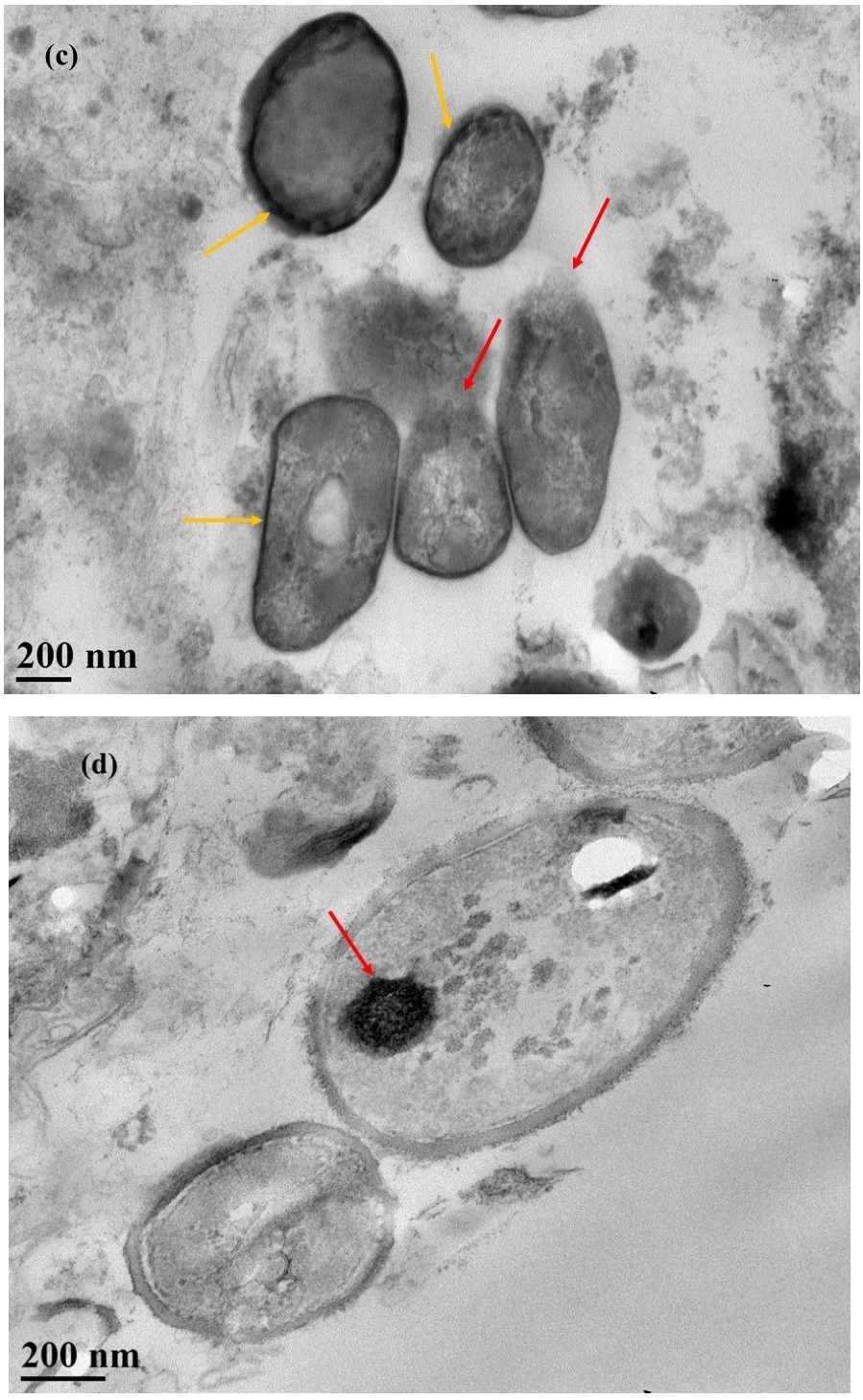

Figure B1. SEM visualization of sludge samples: (a) without PsNPs, (b) with PsNPs; and TEM visualization of samples (c-d) with PsNPs; Orange arrows indicate the protected cells by EPS, and red arrows indicate the penetration of PsNPs inside the cells and cell rupture.

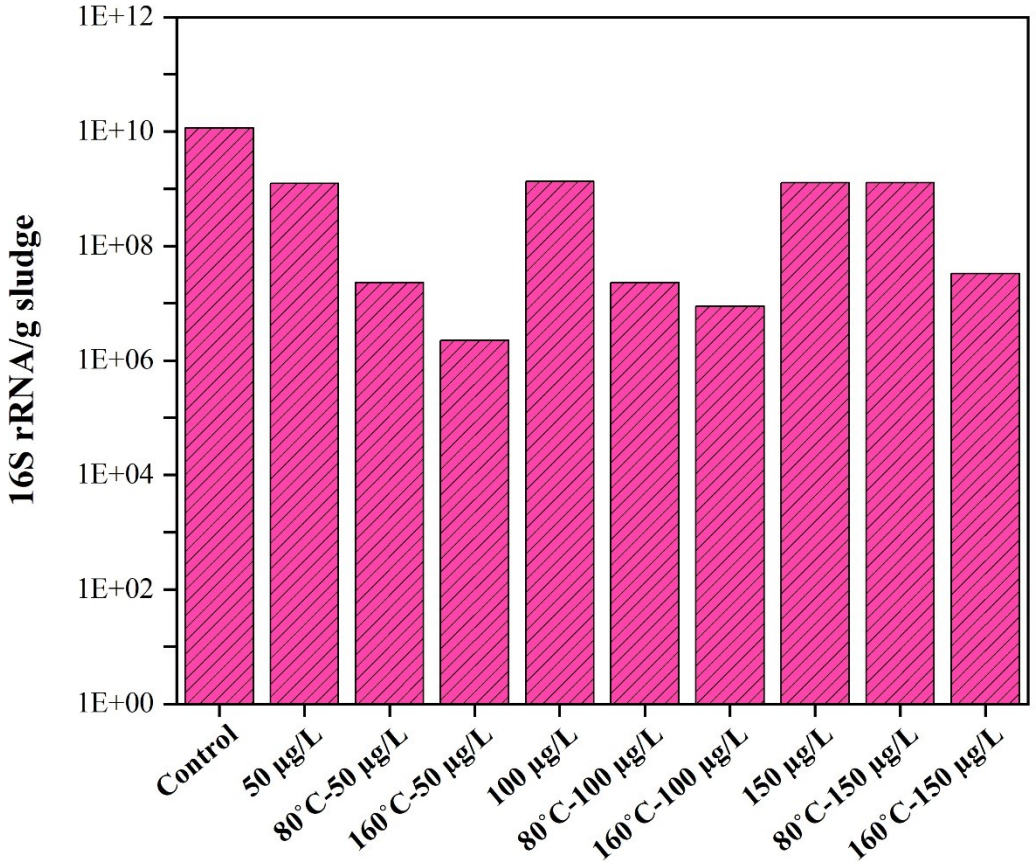

Figure B2. 16S rRNA gene copies under different experimental conditions.

Text B6. Microbial diversity

Alpha diversity indices were calculated to assess and compare the microbial diversity among different conditions (see Table S5). Compared to the control, all test conditions demonstrated a substantial increase in the species richness, indicated by high higher Chao1 and OTUs scores. However, 50 µg/L of PsNPs showed the highest scores, which were substantially higher than the control (Chao1: 35 vs. 304 and OTUs: 32 vs. 302). However, no significant difference in richness was observed among other samples. The highest Pielou's score was attained for 160ºC-50 µg/L (0.68). However, no significant difference in overall species evenness was found among the experimental reactors. Consequently, the Shannon index scores, which demonstrate both evenness and richness, were also higher in the experimental reactors than in the control. The highest Shannon index value among experimental reactors (5.33) was obtained in the 160ºC-50 µg/L. It was reported that a diverse microbial community can enhance microorganism tolerance against venomous nanoparticles (Tang et al., 2018; Zakaria and Dhar, 2020).

Table B5. Diversity and richness of microbial community under different experimental conditions.

Test conditions	Chao 1	Coverage	Pielou's evenness	OTUs	Shannon
Control	35	1	0.64	35	3.30
50 µg/L	304	1	0.64	302	5.31
80°C-50 µg/L	245	1	0.65	244	5.22
160°C-50 µg/L	229	1	0.68	229	5.33
100 µg/L	238	1	0.63	237	4.97
80°C-100 µg/L	233	1	0.64	232	5.02
160°C-100 µg/L	201	1	0.67	201	5.18
150 µg/L	281	1	0.64	279	5.27
80°C-150 µg/L	259	1	0.61	259	4.94
160°C-150 µg/L	218	1	0.60	218	5.28

Text B7. Microbial community at the phylum level

Fig. S3 shows the changes in microbial communities at the phylum level. The major phyla comprising the control reactor were WWE1 (31%), Chloroflexi (28%), Firmicutes (18%), Bacteroidetes (10%), and Spirochaetes (4%), comprising >90% of the communities. They were also dominant in the reactors fed with sludge exposed to PsNPs; the five most dominant phyla were WWE1 (19-35%), Chloroflexi (19-24%), Firmicutes (13-30%), Bacteroidetes (9-10%), and Spirochaetes (6-7%). WWE1 demonstrated considerable decrement in their relative abundance from 31% (control) to 19% for 160ºC-150 µg/L of PsNPs. Compared to the control, Chloroflexi abundance significantly decreased in response to THP and PsNPs. For instance, at 160ºC-50 µg/L, its abundance reduced to 17% from 28% in control. However, the phylum Firmicutes demonstrated a different behavior under different experimental conditions, and its abundance in six reactors decreased while abundances increased in the other three reactors. For example, in the reactor fed with sludge exposed to 50 µg/L of PsNPs, Firmicutes abundance slightly decreased from 18% (control) to 16%, while the abundance increased to 27% for 160ºC-50 µg/L of PsNPs. Interestingly, for THP at 160ºC (160ºC-100 µg/L and 160ºC-150 µg/L) similar trend was observed, and Firmicutes abundance enhanced to 28 and 30%, respectively. Notably, Chloroflexi, Firmicutes, and Bacteroidetes, which together constituted 56% of the total microbial community in control, are recognized as protein and polysaccharide degraders (Wei et al., 2020). After exposure to PsNPs at 50, 100, and 150 µg/L, the abundance of these phyla decreased. Thus, PsNPs exposure might reduce the sludge organics degradation in these reactors (Wei et al., 2020). However, the abundance of Proteobacteria, Synergistetes, and Spirochaetes, which represent a small portion of the microbial communities, enhanced after exposure to THP and PsNPs.

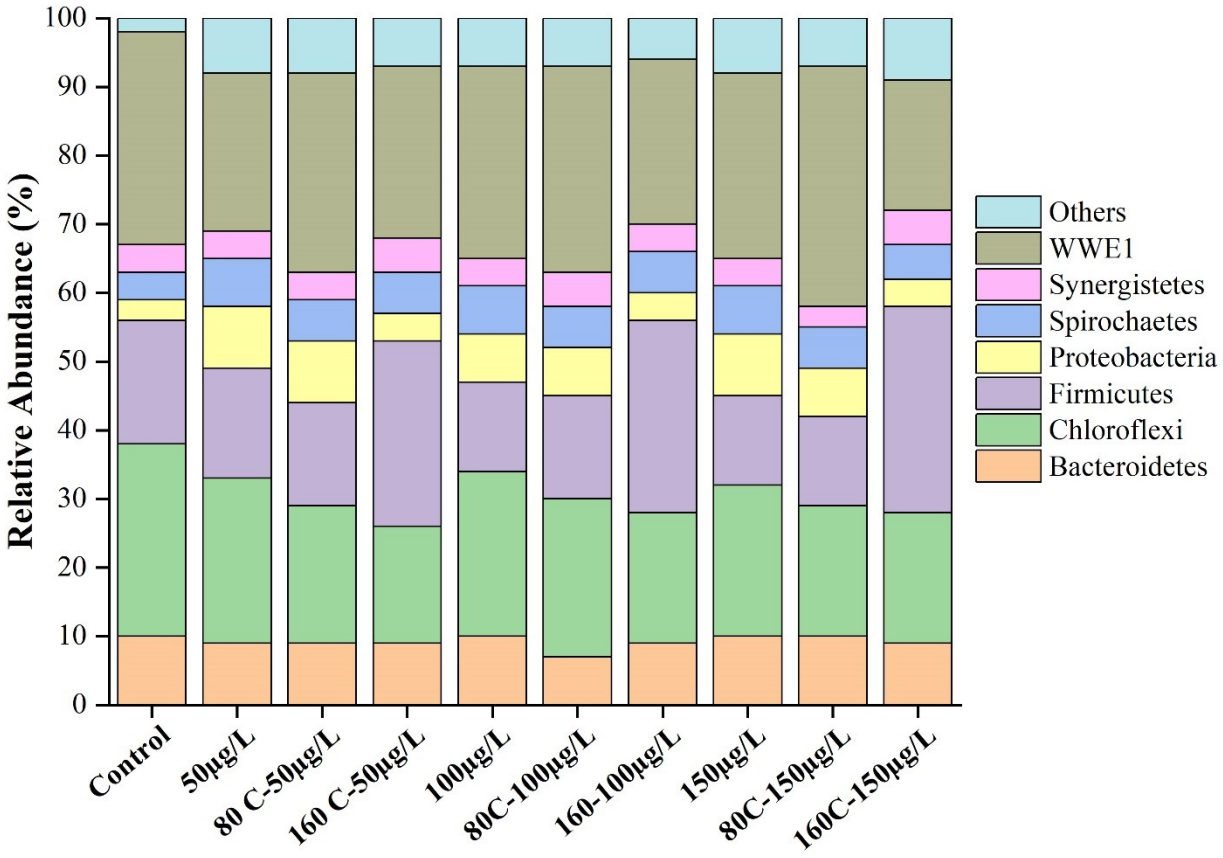

Figure B3. Relative abundance of bacterial communities at the phylum level.

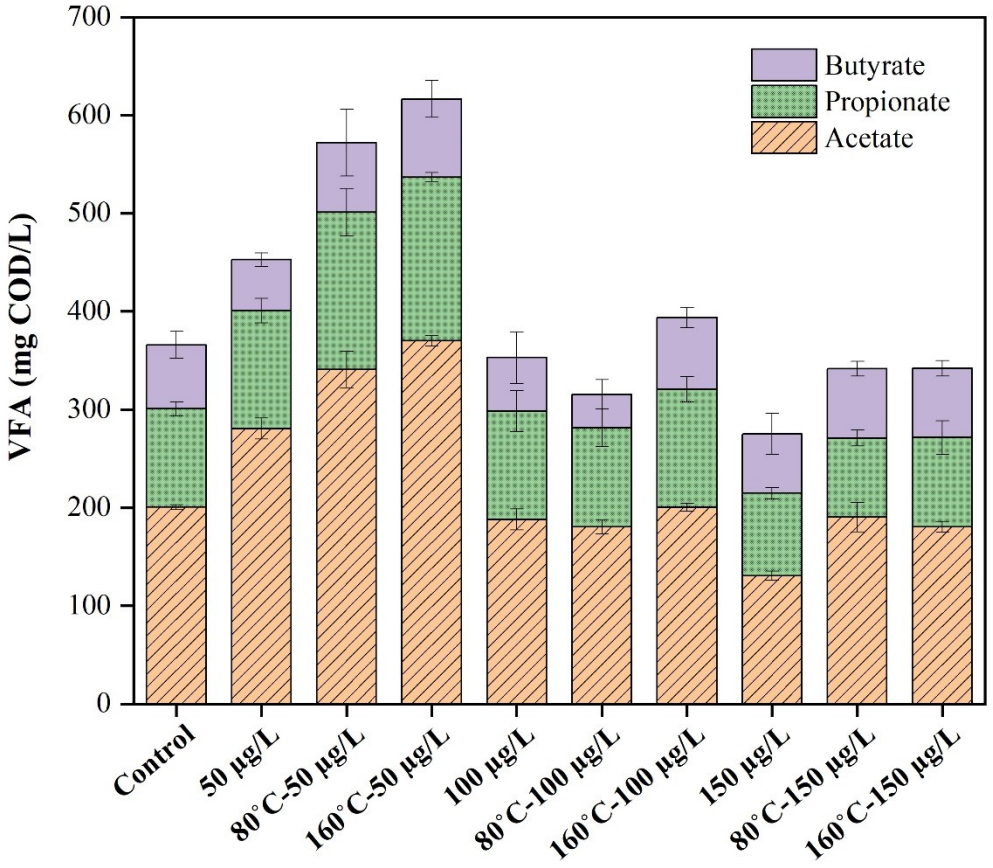

Figure B4. VFAs accumulation under different experimental conditions.

Appendix C

Supplementary Information for Chapter 5

Table C5. Characteristics of inoculum and substrate.

Parameters	**Inoculum (Digested sludge)**	**Substrate (Primary sludge)**
TSS (mg/L)	15,625 ± 125	32,675 ± 105
VSS (mg/L)	14,625 ± 129	28,526 ± 149
TCOD (mg/L)	23,064 ± 1061	52,215 ± 1,050
SCOD (mg/L)	4,664 ± 325	7,408 ± 97
TVFA (mg COD/L)	158 ± 0.5	899 ± 13
TAN (mg/L)	1,181 ± 67	80 ± 2.6
Alkalinity (mg/L)	6,655 ± 55	4,381 ± 29
pH	7.9 ± 0.01	6.8 ± 0.01

Table C2. Primers used for studying ARGs and 16S rRNA.

	Forward (5'-3')	**Reverse (5'-3')**
*tet*A	GCTACATCCTGCTTGCCTTC	CATAGATCGCCGTGAAGAGG
*tet*B	GGCAGGAAGAATAGCCACTAA	AGCGATCCCACCACCAG
*tet*W	GAGAGCCTGCTATATGCCAGC	GGGCGTATCCACAATGTTAAC
*tet*M	ACAGAAAGCTTATTATATAAC	TGGCGTGTCTATGATGTTCAC
*sul*1	CGCACCGGAAACATCGCTGCAC	TGAAGTTCCGCCGCAAGGCTCG
*sul*2	TCCGGTGGAGGCCGGTATCTGG	CGGGAATGCCATCTGCCTTGAG
*erm*B	GATACCGTTTACGAAATTGG	GAATCGAGACTTGAGTGTGC
bla_{TEM}	ATCAGCAATAAACCAGC	CCCCGAAGAACGTTTTC
*intl*1	CCTCCCGCACGATGATC	TCCACGCATCGTCAGGC
*intl*2	GTTATTTTATTGCTGGGATTAGGC	TTTTACGCTGCTGTATGGTGC
16S rRNA	CCTACGGGNGGCWGCAG	GACTACHVGGGTATCTAATCC

Table C3. The effects of THP alone (without PsNPs exposure).

	Pretreated Sludge		
	4%TS	8%TS	12%TS
TCOD (mg/L)	45,512	79,851	111,698
SCOD (mg/L)	18,951	36,987	45,213
COD solubilization (%)	33.4	32.1	36.3
VSS reduction (%)	22.6	26.4	35.2
EPS Polysaccharide (mg/g sludge)	200	210	232
EPS Proteins (mg/g sludge)	154	182	190
pH	6.4	6.6	6.5
Increase in methane yield (%) [a]	9.77	9.53	62.1

[a] Compared to the control

Table C4. Kinetic parameters estimated with the first-order and modified Gompertz model.

Experimental conditions	First Order Model				Modified Gompertz model				
	Methanogenesis rate constant k (d^{-1})	Standard error of k	Estimated Maximum methane production V_m *(mL/g COD)	Standard error of V_m	Maximum methane production V_m *(mL/g COD)	Maximum Methane Production Rate, R (mL/g COD/d)	Standard error for R	Lag phase, λ (d)	Standard error for λ
Control-4%TS	0.17	0.003	208.29	0	208.29	14.91	0.53	-2.82	0.31
Control-8%TS	0.11	0.002	193.86	0	193.86	9.34	0.22	-3.38	0.29
Control-12%TS	0.06	0.004	157.72	0	157.72	8.12	0.53	6.53	0.71
PsNPs-4%TS	0.08	0.005	195.41	0	195.41	11.66	0.23	-4.42	0.22
PsNPs-8%TS	0.05	0.003	190.8	0	190.8	7.73	0.39	2.16	0.68
PsNPs-12%TS	0.05	0.002	165.77	0	165.77	5.33	0.29	4.56	0.92
THP- PsNPs-4%TS	0.09	0.002	222.23	0	222.23	9.89	0.32	-3.11	0.42
THP- PsNPs-8%TS	0.06	0.002	241.61	0	241.61	8.38	0.49	5.61	0.88
THP- PsNPs-12%TS	0.07	0.002	240.43	0	240.43	8.76	0.36	5.54	0.59

* V_m values were fixed at the experimental total cumulative methane yields

Text C1. Kinetic analysis

The first-order kinetic and modified Gompertz were used, as illustrated in Eqs. (S1) and (S2), respectively (Jibao Liu et al., 2020a; Vu et al., 2020; Zhang et al., 2016), to evaluate methanogenesis kinetics from the BMP test experimental data:

$$V(t) = V_m\ (1 - e^{-kt}) \quad \text{(C1)}$$

$$V(t) = V_m \cdot \exp\left\{-\exp\left[1 + (\lambda - t)\ \frac{Re}{V_m}\right]\right\} \quad \text{(C2)}$$

Where V(t) is the cumulative methane production at time t (mL), V_m is the experimental ultimate methane production potential (mL), k is the kinetic methanogenesis rate constant (d^{-1}), and t is the cumulative time for the production of methane (days), e is a mathematical constant (2.718282), λ is the lag phase for methane production (days), and R is the maximum production rate of methane (mL/d) (Mohammad Mirsoleimani Azizi et al., 2021a). Non-linear regression analyses using Minitab 19 were performed to ensure generating the best model fit of the methane production and to estimate the values of the kinetic constants (k, λ, and R). Based on the measured methane production from the BMP tests, the initial estimated values were used in the model in the first iterations to minimize the standard error estimate and to attain the best fit values of kinetic parameters.

Table C4 shows the methanogenesis rate constant (k) and maximum methane production (V_m) estimated with the first-order kinetic model. Controls demonstrated higher k values compared to other samples. Among control samples, the obtained k values in Control-4%TS (0.17 d^{-1}) was remarkably higher than Control-8%TS (0.11 d^{-1}) and Control-12%TS (0.06 d^{-1}). After adding PsNPs, the methanogenesis rate significantly decreased (compared to the respective controls). However, no specific trends were observed with increasing TS% and applying pretreatment. For instance, in PsNPS-4%TS, PsNPs-8%TS, and PsNPs-12%TS, k values were 0.08, 0.05, and 0.05 d^{-1} indicating no specific trends. Also, THP-PsNPs-4%TS demonstrated k value of 0.09 d^{-1} whereas it decreased to 0.06 d^{-1} for THP-PsNPs-8%TS and then increased to 0.07 d^{-1} for THP-PsNPs-12%TS. Despite lower k values, THP enhanced methane production, suggesting that it took longer for THP samples to achieve the maximum methane production compared to the control.

Based on this, the modified Gompertz model was used to estimate lag phase times (λ) and maximum methane production rates (R).

Control-4%TS and Control-8%TS showed negative λ, suggesting methane production started without any substantial lag phases. However, for Control-12%TS, a higher amount of λ (6.53 d) was achieved, demonstrating a longer required time for commencing methane generation. This finding indicates that at higher TS%, a mass transfer limitation could affect methane production steps. However, in PsNPs-12%TS, the lag phase decreased to 4.56, which could be related to the disintegrating flocs and secretion of EPS. After applying THP, no specific trends were observed by increasing TS%. For instance, methane production immediately started for THP-PsNPs-4%TS, whereas the lag phase increased for THP-PsNPs-8%TS and THP-PsNPs-12%TS.

This finding indicates a more prolonged time required for microbial adoption to solubilized organics (often refractory and/or inhibitory compounds) released during the THP of sewage sludge or additives released from PsNPs (Mohammad Mirsoleimani Azizi et al., 2021a). Also, the obtained R values for controls were considerably higher than most of the samples. For instance, Control-12%TS resulted in 8.12 mL/g COD/d whereas it decreased to 5.33 mL/g COD/d for PsNPs-12%TS. However, THP increased this value to 8.76 mL/g COD/d.

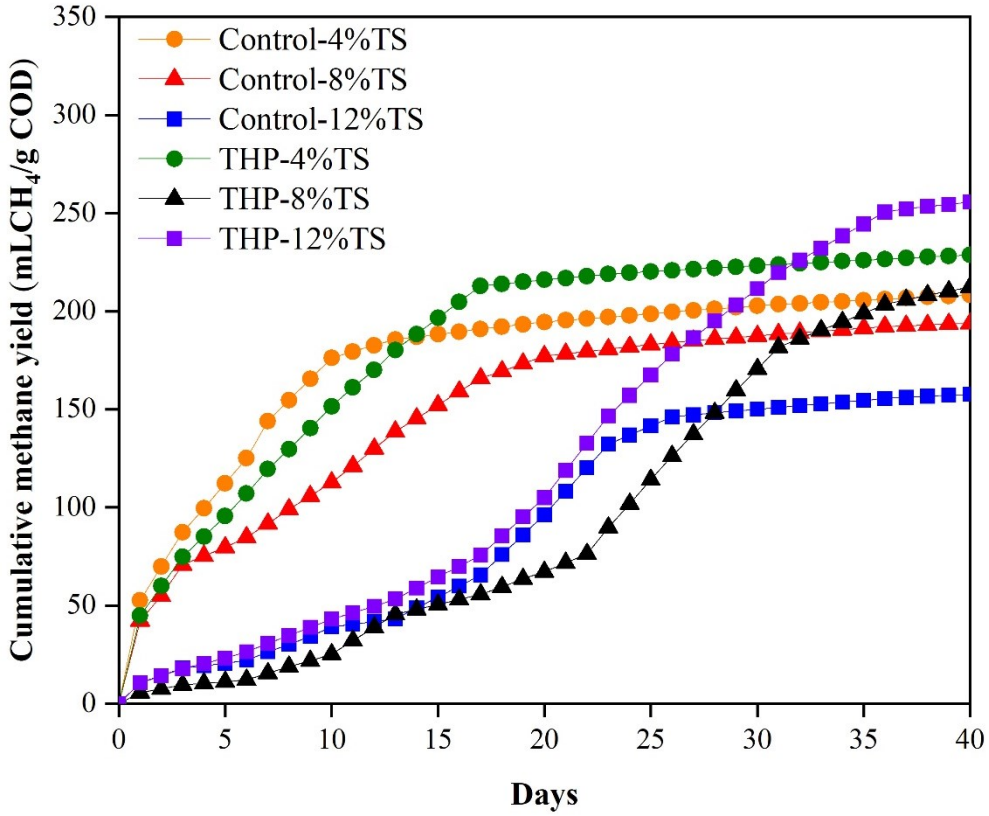

Figure C1. Cumulative methane yield for controls and THP samples.

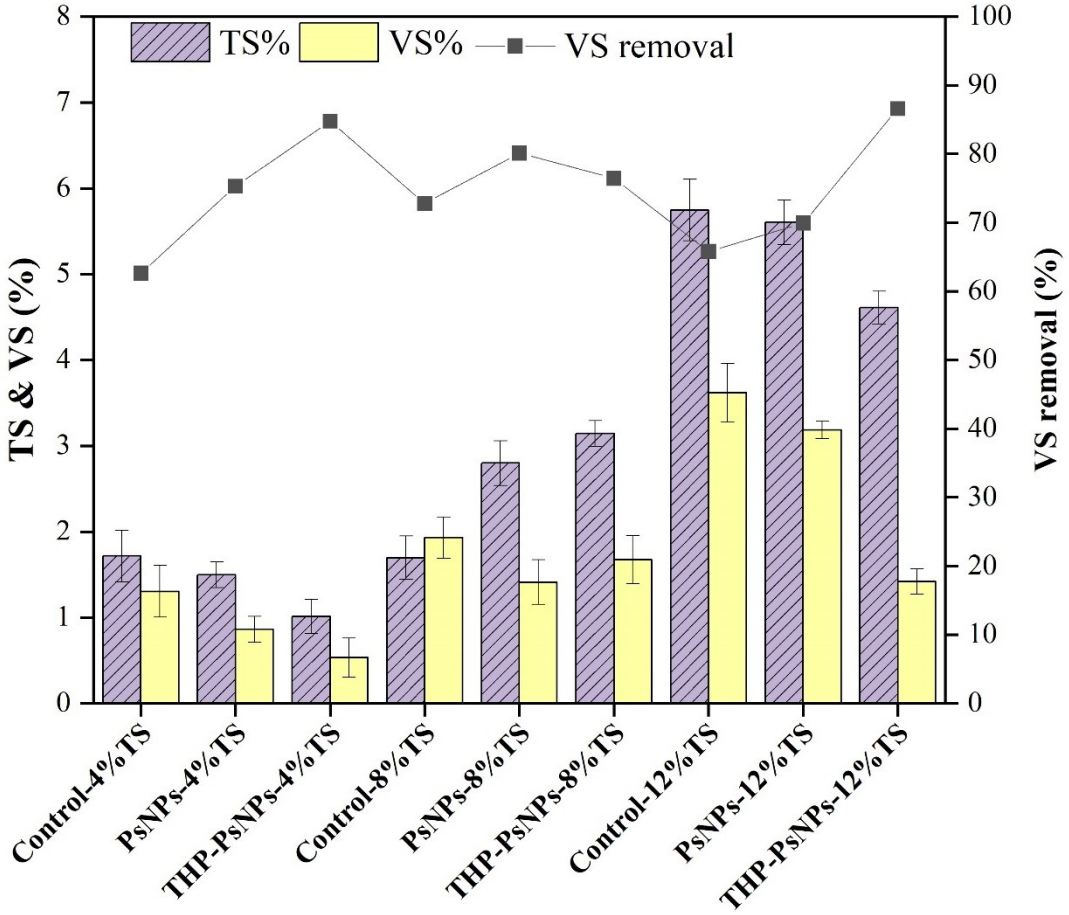

Figure C2. VS removal of the digestate samples under different experimental conditions.

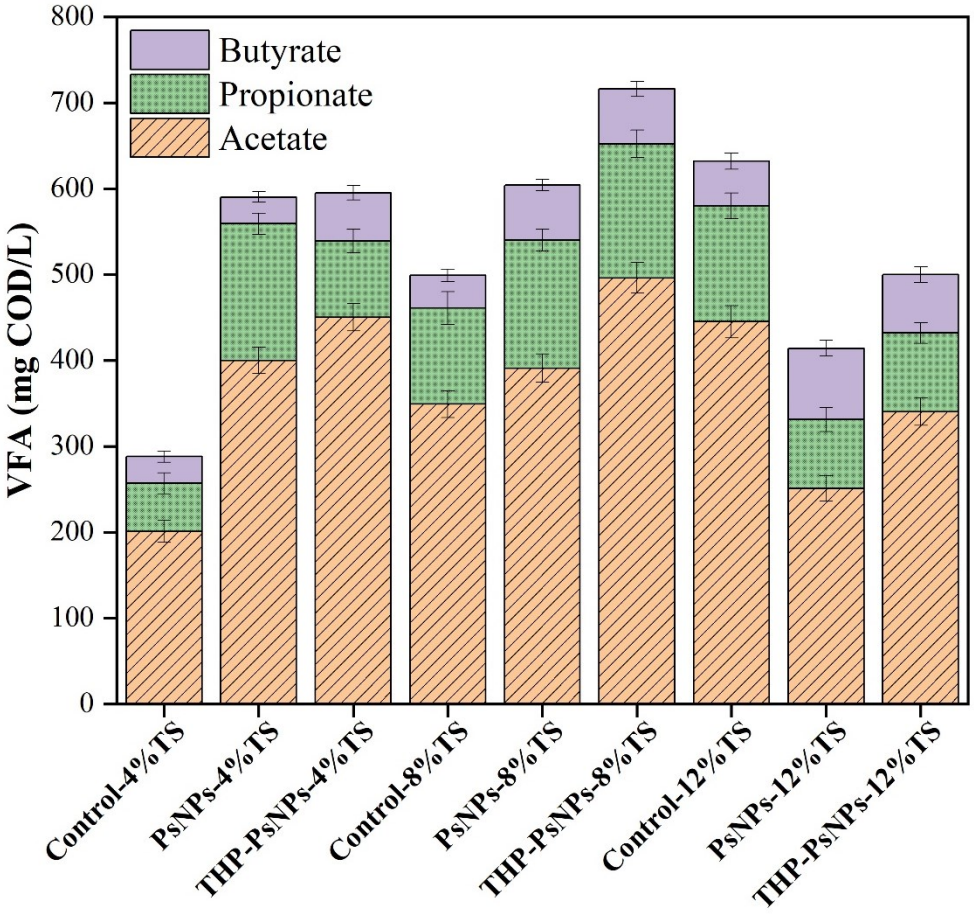

Figure C3. Accumulation of VFAs under different experimental conditions.

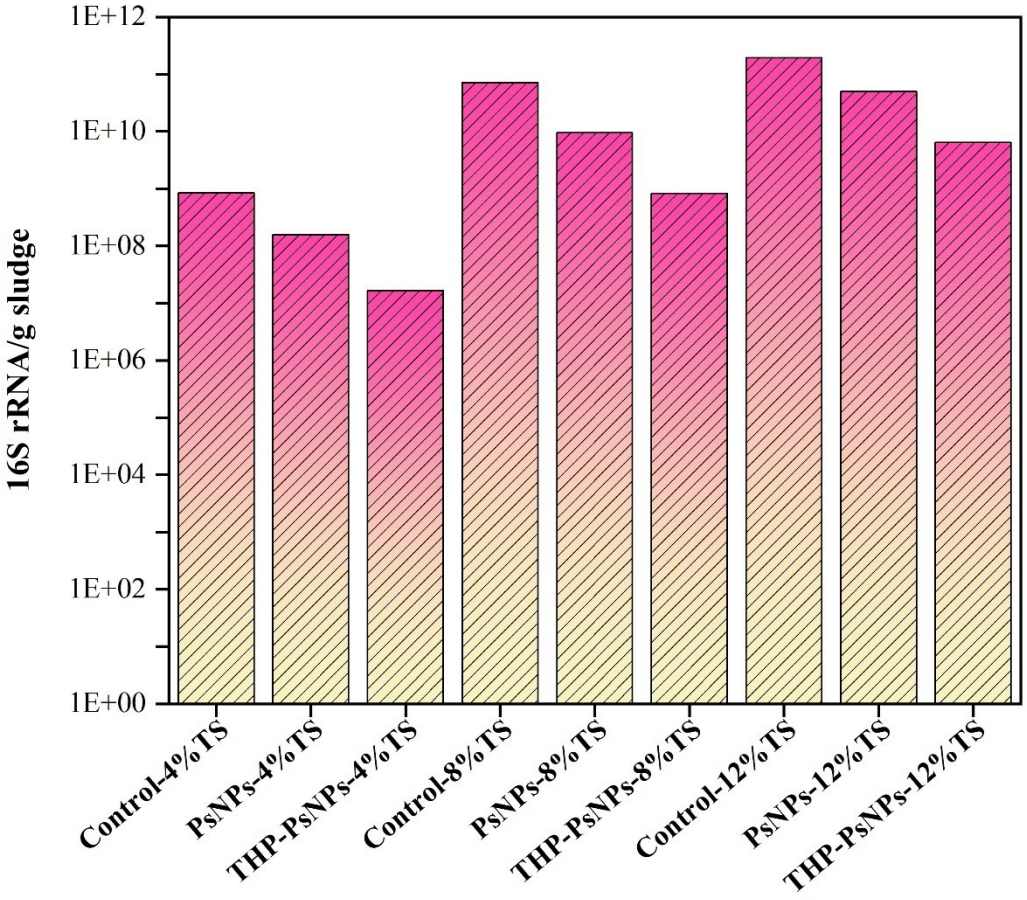

Figure C4. 16S rRNA gene copies under different experimental conditions. under different experimental conditions.

Appendix D

Supplementary Information for Chapter 6

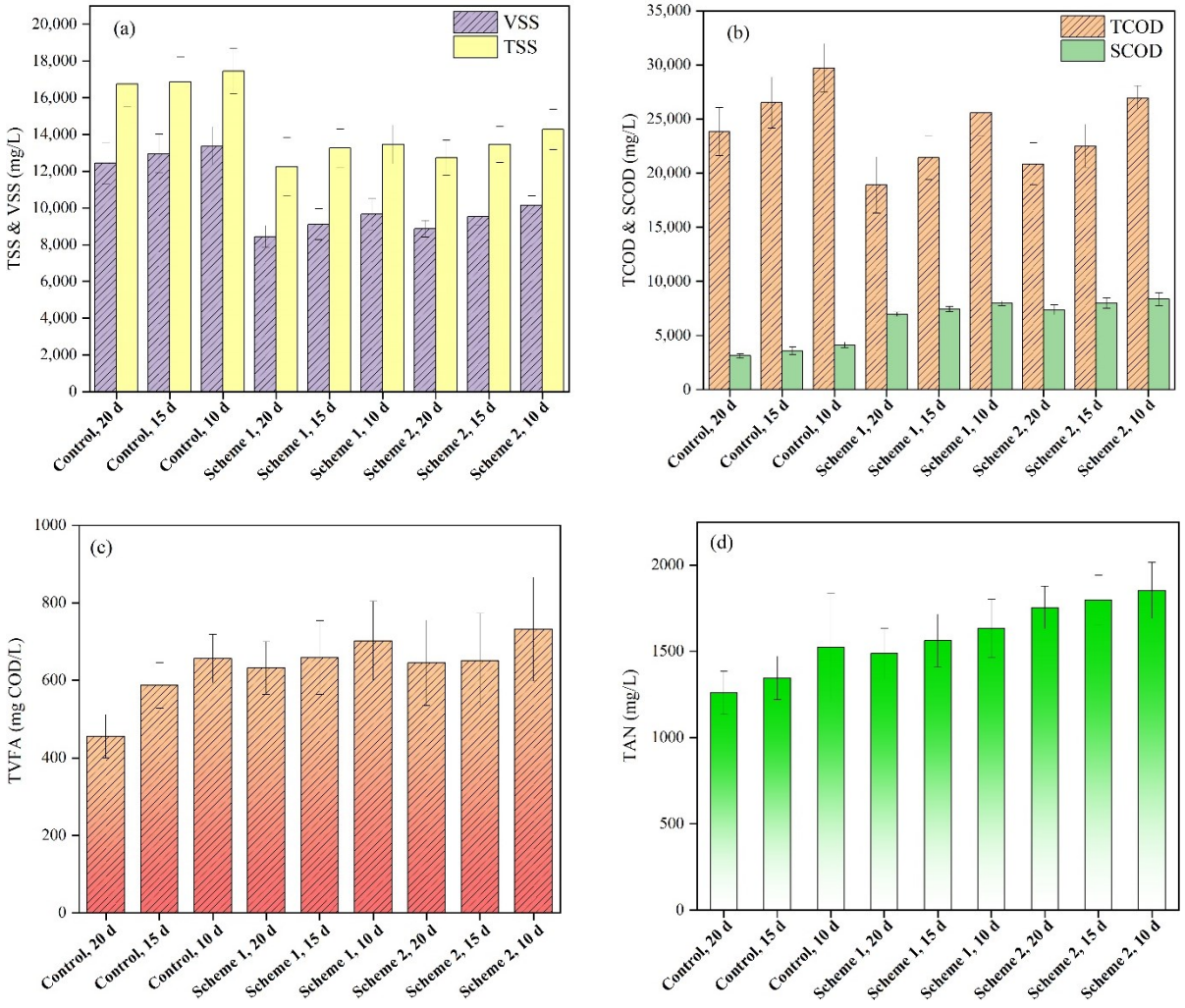

Figure D1. The effluent concentrations of organic matters under different operating conditions (a) TSS and VSS, (b) TCOD and SCOD, (c) TVFA, (d) TAN.

Table D1. COD balance under different experimental condition.

SRT (d)	Control	Scheme-1	Scheme-2
20	100	105	102
15	96	99	100
10	90	91	93

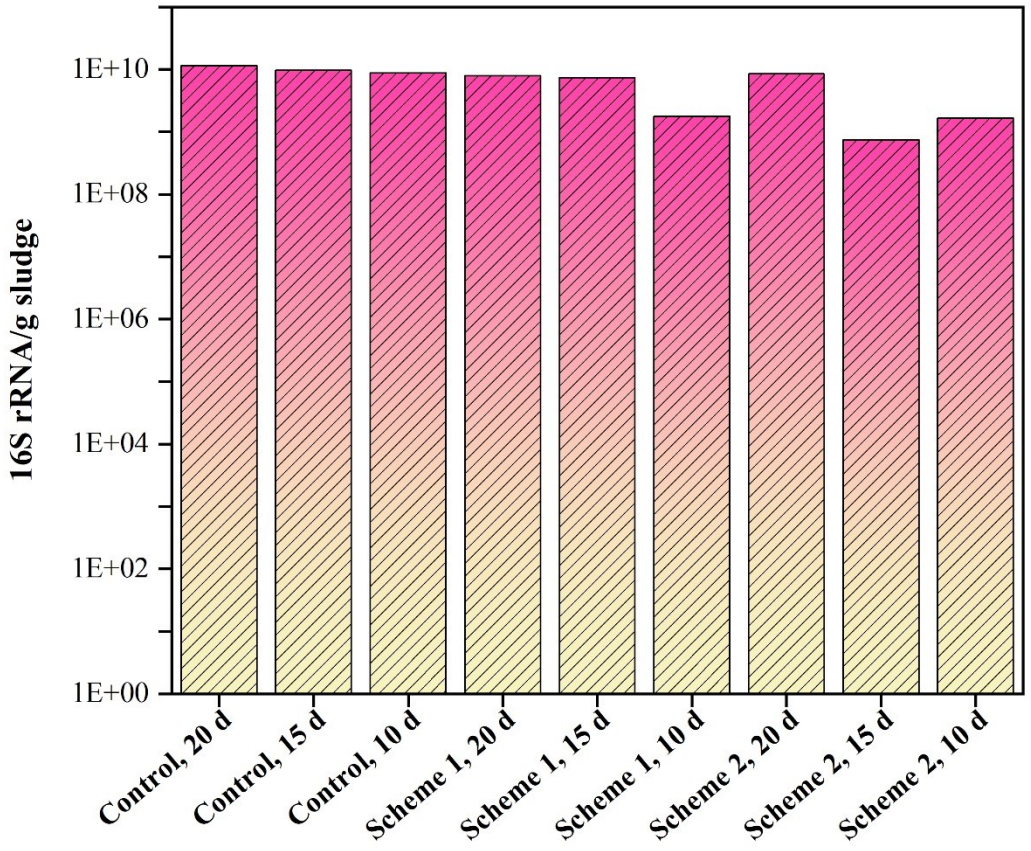

Figure D2.16S rRNA gene copies under different experimental conditions.

Appendix E

Supplementary Information for Chapter 7

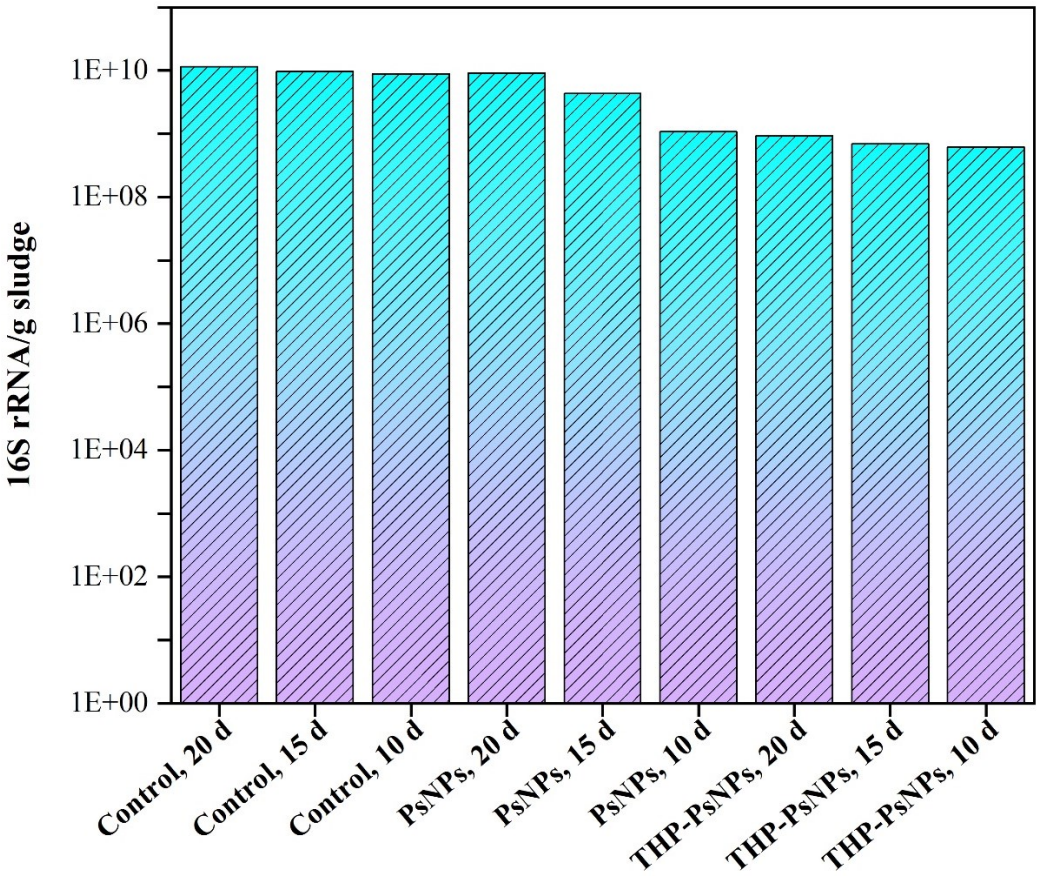

Figure E1.16S rRNA gene copies under different experimental conditions.

Table E1. Primers used for studying ARGs and 16S rRNA

	Forward (5'-3')	**Reverse (5'-3')**
*tet*A	GCTACATCCTGCTTGCCTTC	CATAGATCGCCGTGAAGAGG
*tet*B	GGCAGGAAGAATAGCCACTAA	AGCGATCCCACCACCAG
*tet*W	GAGAGCCTGCTATATGCCAGC	GGGCGTATCCACAATGTTAAC
*tet*M	ACAGAAAGCTTATTATATAAC	TGGCGTGTCTATGATGTTCAC
*sul*1	CGCACCGGAAACATCGCTGCAC	TGAAGTTCCGCCGCAAGGCTCG
*sul*2	TCCGGTGGAGGCCGGTATCTGG	CGGGAATGCCATCTGCCTTGAG
*erm*B	GATACCGTTTACGAAATTGG	GAATCGAGACTTGAGTGTGC
bla_{TEM}	ATCAGCAATAAACCAGC	CCCCGAAGAACGTTTTC
*intl*1	CCTCCCGCACGATGATC	TCCACGCATCGTCAGGC
*intl*2	GTTATTTTATTGCTGGGATTAGGC	TTTTACGCTGCTGTATGGTGC
16S rRNA	CCTACGGGNGGCWGCAG	GACTACHVGGGTATCTAATCC